The Impact of Decoherence and Dissipation on Cosmological Systems and on the Generation of Entanglement

Inaugural-Dissertation

zur

Erlangung des Doktorgrades

der Mathematisch-Naturwissenschaftlichen Fakultät

der Universität zu Köln

vorgelegt von

Friedemann Queißer

aus Radebeul

2010

Abstract

The physics of open quantum systems, and therefore the phenomenon of decoherence, has become important in many branches of research. Within this thesis, we investigate the system–environment interaction in the context of different problems. The influence of decoherence is ubiquitous and, due to the scale independence of quantum theory, not limited to microscopic systems.

One of the great open problems in theoretical physics is the appearance of a cosmological constant which differs by many orders of magnitude from the theoretical predicted value. In the first part of this thesis we will address this question within the framework of quantum mechanics. The considerations are based on a quantum mechanical model which explains the value of the cosmological constant without introducing extremely small numbers. Decoherence, based on the uncontrollable entanglement with the environment, can explain the localization of the vacuum energy to the classical observed value. The model mentioned above allows, in principle, the tunneling into a universe with a different vacuum energy. We investigate the modification of the tunneling rate due to dissipative effects which follow from the system–bath interaction.

Closely related to the cosmological constant problem and subject of the second part of this thesis is the spontaneous decay of a quantum field vacuum. Using a semiclassical approximation it is possible to investigate this process within the framework of the path integral formalism. We discuss the quantum–to–classical transition of the spontaneously nucleated vacuum bubbles. Furthermore, we investigate the dependence of the decay rate on the space-time backgrounds.

The third part of this thesis is dedicated to the interaction between quantum systems and their environment in a different context. We investigate the generation of entanglement between two systems which are interacting indirectly with each other through the coupling to a heat bath. The interaction–induced entanglement will be destroyed rapidly through decoherence and dissipation. We will show that it is possible to generate a significant amount of entanglement by imposing certain boundary conditions to the bath. Furthermore, the dependence of the entanglement generation on the spatial separation of the systems will be analyzed. Specifically we will examine the bathinduced entanglement of oscillators and spins.

Zusammenfassung

Die Physik offener Quantensysteme, und somit das Phänomen der Dekohärenz, hat eine bedeutende Rolle in vielen Bereichen der Forschung eingenommen. In der vorliegenden Arbeit wird die Wechselwirkung zwischen Systemen und ihrer Umgebung im Zusammenhang mit verschiedenen Fragestellungen untersucht. Der Einfluss von Dekohärenz ist allgegenwärtig und, aufgrund der Skalenunabhängigkeit der Quantenmechanik, nicht auf mikroskopische Systeme beschränkt.

Eines der großen Probleme innerhalb der theoretischen Physik ist das Auftreten einer kosmologischen Konstante beziehungsweise einer Vakuumenergie des Universums, die um viele Größenordnungen von dem vorhergesagten Wert abweicht. Im ersten Teil der vorliegenden Arbeit wollen wir uns dieser Fragestellung im Rahmen der Quantenmechanik zuwenden. Die Grundlage der Betrachtungen ist ein quantenmechanisches Modell, welches das Auftreten einer Vakuumenergie ohne Zuhilfenahme von unnatürlich kleinen Zahlen erklärt. Dekohärenz, basierend auf unkontrollierter Verschränkung mit der Umgebung, kann die Lokalisierung der Vakuumenergie auf den klassisch beobachteten Wert erklären. Das oben erwähnte quantenmechanische Modell erlaubt prinzipiell auch einen Tunnelprozess in ein Universum mit einer anderen Vakuumenergie. Wir untersuchen in diesem Kontext die Änderung der Tunnelwahrscheinlichkeit durch dissipative Effekte als Folge der Wechselwirkung zwischen System und Umgebung.

Eng verwandt mit dem Problem der kosmologischen Konstante ist der spontane Zerfall des Vakuums eines Quantenfeldes, welches Thema des zweiten Teils dieser Arbeit ist. Dieser Prozess wird oft innerhalb einer semiklassischen Näherung im Rahmen des Pfadintegralformalismus beschrieben. Anhand des Vakuumzerfalls wird mithilfe der Dekohärenz die Lokalisierung von entstehenden "Vakuumblasen" diskutiert. Weiterhin wird die Abhängigkeit der Zerfallsrate von verschiedenen Raumzeit–Hintergründen des Quantenfeldes beleuchtet.

Der dritte Teil dieser Arbeit widmet sich dem Einfluss der Wechselwirkung zwischen Quantensystemen und ihrer Umgebung in einem anderen Kontext. Untersucht wird hier die Erzeugung von Verschränkung zweier Systeme, die nicht direkt miteinander gekoppelt sind, aber indirekt über ein thermisches Bad wechselwirken. Die Verschränkung, welche die indirekte Wechselwirkung induziert, wird jedoch durch Dissipation und Dekohärenz schnell wieder zerstört. Es wird jedoch gezeigt, dass signifikant viel Verschränkung erzeugt werden kann, wenn das Bad gewissen Randbedingungen unterworfen wird. Insbesondere wird analysiert, wie sich der räumliche Abstand der Systeme auf die Erzeugung von Verschränkung auswirkt. Konkret wird die badinduzierte Verschränkung von Harmonischen Oszillatoren und Spins untersucht.

Contents

1 Introduction

The physics of open quantum systems is a very active area of research in theoretical and experimental physics. Every realistic physical system is in effect an open one since its interaction with environmental degrees is unavoidable. In certain cases, when the system is sufficiently shielded from the environment, the approximation of a closed system is viable. However, the only closed system in nature is the universe as a whole. A feature of open quantum systems are their non–unitary behavior. From the quantum mechanics of closed systems we know that, due to unitarity, every time evolution can be inverted. Stating differently, it is always possible to obtain the initial state of a system by applying a suitable unitary transformation. For an open system there does not exist, in general, a unitary transformation which inverts the time evolution.

In order to analyze open quantum systems one considers the unitary evolution of the system and "the rest of the universe" which contains all environmental degrees of freedom. Tracing over everything, but the system degrees of freedom, leads to the reduced dynamics of the open system. This contains a unitary part, describing the free evolution of the system, and a non–unitary part due to the system–environment interaction.

An important phenomenon, which is widely studied within the context of open quantum systems, is decoherence. It has been first introduced in 1970 by Zeh [1] who pointed out, that realistic macroscopic systems are never closed and interact strongly with their environment. This would explain, according to Zeh, the fragility of macroscopic quantum states through a "dynamical decoupling" of wave–function components. It took another decade until the decoherence program, including the quantum–to–classical transition, was formalized by Zurek [2, 3]. However, it is remarkable that this aspect of open quantum systems has not been investigated in the early days of quantum mechanics. Joos called it an "historical accident" that the implications of decoherence on fundamental problems had been overlooked so long [4]. Although the absence quantum of aspects on macroscopic scales had been noted very early, its connection to the system–environment interaction was not realized. We will introduce the concept of decoherence and related formal aspects in chapter 2.

Since quantum mechanics, and therefore decoherence, is believed to be viable on all scales, it can be applied to cosmological systems, for example dark energy. The

extremely small magnitude of the universe's vacuum energy is still an open problem. Before we address this issue in the context of quantum mechanics, we will give an incomplete review on standard cosmology in chapter 3. Special focus lies on different attempts to describe and explain dark energy. A possible quantum mechanism for the generation of a small cosmological constant will be introduced in chapter 4. Since one observes a classical cosmological constant, we investigate aspects of the quantum–to–classical due to interaction with environmental degrees of freedom.

It is well-known that the cosmological constant can be mimicked by a scalar field, see chapter 3. Therefore the vacuum energy of a scalar field is strongly related to the issue of dark energy. During the last years, it has been discussed whether our universe is only a small part of a huge cosmological landscape [5]. If it is true that the vacuum energy of the universe is determined by a scalar field, it might be possible that this field is trapped in a local minima of the landscape. However, due to quantum tunneling, the field can evolve into another minimal of the potential. This "decay of the vacuum" corresponds to the nucleation and rapid expansion of a finite size "new vacuum" bubble within a sea of "old vacuum". We will investigate the influence of decoherence and nontrivial geometrical backgrounds on this process, also know as "false vacuum decay" [6, 7], in chapter 5.

In the last part of this thesis, chapter 6, we address aspects of system–environment interaction in a different context: the generation of entanglement between remote quantum systems. Controllable entanglement of quantum systems, for example photons or ions, is necessary for the application of certain quantum algorithms. Entangled states of remote quantum systems are extremely fragile and sensitive to decoherence. During the last years, several authors proposed that it should be possible to generate entanglement via a bath–mediated interaction [8, 9]. The systems become entangled with each other through an indirect interaction, i.e. a coupling to the same thermal bath. After introducing different measures for entanglement in section 6.2, we will investigate the generation of bath mediated entanglement of oscillators and spins in sections 6.3 and 6.4. We will focus on the distance dependence of the bath–mediated entanglement generation and discuss under which circumstances this is a viable mechanism.

In the following we set the constants $\hbar$, c and k_B equal to one.

2 Decoherence

2.1 Collapse and Entanglement

According to many textbooks on quantum mechanics the measurement process requires a "collapse of the wave function"(see e.g. [10–13]). This dynamical process, which was introduced by Heisenberg [14], breaks the unitary time evolution which is given by the Schrödinger equation. Nevertheless, it remains unclear when transition from the unitary time-evolution to the *non-unitary* time evolution takes place.

Since the measurement process is crucial for the interpretation of quantum mechanics, we will discuss it here using the example of a double slit experiment with electrons.

Consider electrons passing through a plate with two slits and hitting a screen which is placed parallel behind the plate. The density distribution of the striking electrons on the screen exhibits an interference pattern, independent of whether the electrons pass the plate individually or in a bunch. The quantum mechanical state of an electron in a double slit experiment is given by

$$|\Psi\rangle = \frac{1}{\sqrt{2}}(|\psi_L\rangle + |\psi_R\rangle)\,, \tag{2.1}$$

where $|\psi_R\rangle$ and $|\psi_L\rangle$ represent the partial waves passing from the right and left slit to the screen, respectively. Measuring the position of the electron at one of the slits will destroy the interference pattern as soon as we find the particle to be present at one of the slits. According to Bohr there exists the *principle of complementarity* between waves and particles [15]; depending on the experiment one observes either interferences or acquires knowledge of the electron's path. This principle was also subject of a debate between Einstein and Bohr in 1927 [16] that involved the double-slit experiment. Einstein argued, that it should be possible to measure the direction of the recoil of the screen when the particle is striking. Bohr claimed that obtaining any which-path information leads to a disturbance of the system and the interference pattern vanishes, the wave function $|\Psi\rangle$ collapses on either of the states $|\psi_R\rangle$ and $|\psi_L\rangle$.

However, this either–or distinction is not correct. It is possible in certain situations to gain *some* information about the path of the electron without disturbing the interference pattern completely [17, 18] which is in conflict with the complementarity

between waves and particles. To discuss this feature, the description in terms of a collapse of the wave function is no longer suitable. Instead, we will assume that both, system and measurement apparatus, are evolving unitarily. We will treat the measurement apparatus and the system quantum-mechanically and use the so-called von Neumann scheme and the concept of entanglement. This stands in contrast to the Copenhagen interpretation which includes the indispensability of *classical* concepts for the measurement process [19, 20].

Regarding the double slit experiment, the inclusion of the detector system into the quantum-mechanical treatment can be achieved as follows [21]. One places behind each slit a detector which is initially in the state $|\text{ready}\rangle$. By covering the left slit and placing the particle source directly behind the right slit, such that the particle will pass through the latter, the electron is prepared in the state $|\psi_R\rangle$. The detector behind the right slit will trigger and the composite system of particle *and* detector will evolve according to

$$|\psi_R\rangle |\text{ready}\rangle \rightarrow |\psi_R\rangle |R\rangle . \tag{2.2}$$

In an analogous way it is also possible to cover the right slit such that the time evolution reads

$$|\psi_L\rangle |\text{ready}\rangle \rightarrow |\psi_R\rangle |L\rangle . \tag{2.3}$$

Due to the linearity of the Schrödinger equation, we may also consider the time evolution of a superposition,

$$\frac{1}{\sqrt{2}}(|\psi_R\rangle + |\psi_L\rangle) |\text{ready}\rangle \rightarrow \frac{1}{\sqrt{2}}(|\psi_R\rangle |R\rangle + |\psi_L\rangle |L\rangle) . \tag{2.4}$$

This is the *von Neumann* measurement scheme which involves the superposition principle and the linearity of the Schrödinger equation [22]. The composite system is determined by a pure state with all available information of electron and detector,

$$|\Psi\rangle\langle\Psi| = \frac{1}{2} (|\psi_R\rangle |R\rangle + |\psi_L\rangle |L\rangle) (\langle\psi_R| \langle R| + \langle\psi_L| \langle L|) . \tag{2.5}$$

Since we are interested only in information about the electron, we trace out all degrees of freedom concerning the detector. We find the *reduced* density matrix for the electron to read

$$\begin{aligned} \rho_{\text{electron}} &\equiv \text{tr}_{\text{detector}} |\Psi\rangle\langle\Psi| \tag{2.6} \\ &= \frac{1}{2} [|\psi_R\rangle\langle\psi_R| + |\psi_L\rangle\langle\psi_L| + |\psi_R\rangle\langle\psi_L|\langle L|R\rangle + |\psi_L\rangle\langle\psi_R|\langle R|L\rangle] . \end{aligned}$$

As we see, the interference pattern is only destroyed when the detector states are orthogonal. In this case, the detectors are perfectly able to distinguish whether the

particle moved through the right and left slit, respectively. When they are unable to resolve the path, the interference pattern is not destroyed. In general, there can be a finite overlap of the detector states, i.e. $0 < |\langle R|L \rangle| < 1$, such that the interference pattern is only partially destroyed.

Note that even in the case of perfect measurement, $\langle R|L \rangle = 0$, no collapse into a partial wave is assumed. The global superposition (2.4) still exists, but it is inaccessible to an observer by means of *local* observations.

The example considered above is a special case of an *ideal* measurement process, which is determined through an interaction of von Neumann's form, i.e.

$$H_{\text{int}} = \sum_n |n\rangle\langle n| \otimes A_n \,, \tag{2.7}$$

where $|n\rangle$ denote the state vectors of the system under consideration, and the operators A_n are acting only on a macroscopic measurement apparatus. Furthermore, the operators A_n have to be chosen such that the overlap between different apparatus states $|\Phi_n(t)\rangle$ originating from the same initial detector state $|\Phi_{\text{in}}\rangle$ is negligible for sufficiently large times, i.e. $\langle \Phi_m(t)|\Phi_n(t)\rangle \approx \delta_{mn}$. The interaction (2.7) has the characteristic to leave the state vectors of the system unperturbed. In other words, any backreaction of the apparatus onto the system is neglected.

An initial product state containing a superposition of different system state vectors $|n\rangle$ and the initial apparatus state $|\Phi_{\text{in}}\rangle$ will evolve into an entangled state,

$$\left(\sum_n c_n|n\rangle \right) |\Phi_{\text{in}}\rangle \rightarrow \sum_n c_n|n\rangle \, |\Phi_n(t)\rangle \,, \tag{2.8}$$

which is obviously a generalization of the situation considered in (2.4).

An observer will not have access to the global state but only to a local subsystem, given by the reduced system density matrix that is obtained by tracing out the apparatus states,

$$\rho_{\text{sys}} = \sum_{n,m} c_m^* c_n |n\rangle\langle m| \rightarrow \sum_{n,m} c_m^* c_n \langle \Phi_m|\Phi_n\rangle |n\rangle\langle m| \,. \tag{2.9}$$

If the apparatus states are orthogonal to each other, i.e. $\langle \Phi_m|\Phi_n\rangle = \delta_{nm}$, the system matrix becomes diagonal,

$$\rho_{\text{sys}} \rightarrow \sum_n |c_n|^2 |n\rangle\langle n| \,. \tag{2.10}$$

All interference terms are destroyed locally in the basis defined by the interaction (2.7). The phase relations are inaccessible for an observer by means of *local* observations.

In the context of a system–environment interaction, equation (2.8) is the formal description of the *decoherence* process (see section 2.2). In realistic scenarios, the environmental states $|\Phi_n(t)\rangle$ will be approximately orthogonal which leads to a reduced density matrix of the form (2.10). However, this does not imply a collapse of the system's wave function to a specific state, say $|n\rangle$, as in the standard interpretation of quantum mechanics. In contrast, all physical outcomes are in principle possible and no specific state is singled out. Thus, the determination of a *definite* outcome of the measurement process remains unsolved within the concept of decoherence and leads to the "many-worlds interpretation" which is subject of section 2.3. In principle, it is always possible to enlarge the system so as to include system *and* apparatus and thus recover the coherences.

It is important to remark that the diagonal form of the density matrix (2.10) does not represent a proper mixture. A proper mixture describes a situation, where the system is in either of the states $|n\rangle$, whereas the pure state (2.8) involves superpositions between different $|n\rangle$. The formal similarity of the reduced density matrix (2.10) with a proper mixture originates from the non-unitary trace operation with respect to the apparatus. Since all phase relations can in principle be obtained by enlarging the system, this cannot be compared with a situation finding the system in one of the states $|n\rangle$.

2.2 Decoherence and Environment

Based on the universality of quantum mechanics and and the superposition principle, the decoherence program was first initiated by Zeh in [1] (see also [20]). It can be considered as the solution to the following difficulty that arises when the measurement apparatus is treated quantum–mechanically. According to the entangled system–apparatus state (2.4) that can be seen as special case of (2.8), superpositions of different "pointer positions" $|\Phi_n(t)\rangle$ are generally possible. However, a Geiger counter being in a superposition of $|$"an atomic decay has been detected"$\rangle$ and $|$"no atomic decay has been detected"$\rangle$ has never been observed. Zeh noted, that the treatment of system and apparatus as closed system is unrealistic and the interaction between the macroscopic measurement device and its environment has to be taken into account [1]. This environment, e.g. photons, air molecules etc., is usually considered to be extremely large and practically inaccessible to a local observer. To state it more explicitly, we assume the environment to be initially in the state $|E_0\rangle$. Schrödinger's equation generates the time evolution into an entangled state, i.e.

$$\left(\sum_n c_n|n\rangle|\Phi_n\rangle\right)|E_0\rangle \rightarrow \sum_n c_n|n\rangle|\Phi_n(t)\rangle|E_n(t)\rangle. \tag{2.11}$$

Orthogonality of the environmental states, which is valid under realistic conditions, leads to the reduced density matrix which contains all available information of a local observer,

$$\rho_{\mathrm{red}} = \sum_n |c_n|^2 |n\rangle\langle n| \otimes |\Phi_n(t)\rangle\langle\Phi_n(t)|\,. \qquad (2.12)$$

In the context of the entangled system–apparatus state (2.8), the states $|\Phi_n(t)\rangle$ have to be interpreted as "remainder of the universe" including the measurement apparatus [1]. The special case of non-orthogonal apparatus states (see equation (2.6)) is only valid, if system and apparatus are shielded from the environment.

Furthermore, the decoherence program can also be applied *without* referring to a measurement device, e.g. a detector. This leads naturally to an explanation for the *quantum–to–classical transition* [23–25]. Due to the ubiquitous interaction of physical systems with its environment, e.g. scattering of photons and airmolecules, every object experiences a continuous monitoring process. On macroscopic scales, decoherence is very efficient and information about the phase relations on an object are delocalized in the environment on very short time scales.

2.3 Pointer Basis and Everett Interpretation

Associated with the quantum measurement, being described in terms of entanglement of system and apparatus, is the preferred basis problem. From the state (2.8), the measured observable is not uniquely defined since it is possible to find for any choice of system states $\{|n\rangle\}$ the corresponding apparatus states $\{|\Phi_n\rangle\}$. The decoherence program can be used to define a suitable pointer basis [26], this is also known as *Environment–induced superselection of a preferred basis.* Zurek suggested that the preferred pointer basis "contains a reliable record of the state of the system $\mathcal{S}$" [2]. In other words, demanding that the system–apparatus correlations $|n\rangle|\Phi_n\rangle$ are not disturbed by the interaction with the environment, singles out a basis $\{|\Phi_n\rangle\}$ which satisfies a dynamical *stability criterion* [27]. Mathematically, one demands that the Hamiltonian describing the apparatus–environment interaction commutes (at least in a good approximation) with the projectors $|\Phi_n\rangle\langle\Phi_n|$.

In the context of system–environment interaction, that is without referring to an explicit measurement apparatus, different cases of the emergence of a pointer basis are distinguished. If the dynamics is dominated by the system–environment interaction, the pointer states are eigenstates of the interaction Hamiltonian. Typical system–environment interactions are scattering processes which are described through Newton's or Coulomb's force law. Since gravitational and electrodynamic interactions depend on the distance, the pointer states are position eigenstates [2, 3]. When the internal dynamics of the system is dominating, the environment will only be able

to monitor constants of motion and the pointer states are energy eigenstates of the system Hamiltonian [28]. For the intermediate case, the pointer states are localized in phase space [29].

This superselection of a preferred basis is also used to solve the preferred–basis problem in the relative state interpretations of quantum mechanics. The most prominent example is the Everett interpretation [30]. Everett abandoned the special role of the observer that is part of the Copenhagen interpretation and assumed the existence of a state $|\Psi\rangle$ representing the universe which is evolving according to the Schrödinger equation. Every term in the superposition of the state $|\Psi\rangle$ at the completion of the measurement corresponds to a physical state which can be understood to be relative to the other part of the total state. To state it more explicitly, every term of the superposition represents a physical state which is realized in a certain "Everett branch". This relative-state formalism was the motivation for the "many-worlds interpretation" of DeWitt [31] and Deutsch [32]. The superselection of a preferred basis using the concept of decoherence can be used to define stable Everett branches [33].

For an extensive review of decoherence and the interpretation of quantum mechanics, see [34]

2.4 Localization

An important application of the decoherence process is the localization of macroscopic objects due to the ubiquitous interaction with their environment. Starting from the quantum mechanics of isolated systems, it is not obvious that macroscopic objects are found in spatial localized states. As an example, for the author of this thesis it is not possible to be in a superposition of two different locations, say Cologne and Dresden. Does this mean that the superposition principle does not apply to "classical objects"? And where is the borderline between quantum mechanics and classical mechanics?

This problem was already the subject of a debate between Born and Einstein. The former stated that the solution lies in the limit of large masses (Born, November 26, 1954),

"[...] Aber nun muss ich mir doch die Freiheit nehmen zu behaupten, dass Deine Behandlung des Beispiels (ein zwischen zwei Wänden hin und her prallender Ball) nicht das beweist, was Du behauptest: nämlich dass die wellenmechanische Lösung im Grenzfall makroskopischer Dimensionen nicht in die klassische Bewegung übergeht. Das liegt nur daran, dass Du – verzeih mir die Frechheit – eine unrichtige, der Frage nicht angemessene Lösung des Problems gewählt hast. Macht man es gemäß den Vorschriften, so erhält man eine Lösung, die im Grenzfalle (Masse $\rightarrow \infty$)

genau in die klassische deterministische Bewegung übergeht –obwohl sie natürlich für endliche (große) Werte der Masse immer nur statistische Aussagen mit riesiger Wahrscheinlichkeit produziert. Wenn man einen Ablauf beschreiben will, muss man die zeitabhängige Schrödinger-Gleichung

$$-\frac{\hbar^2}{2m}\frac{\partial^2 \psi}{\partial x^2} = i\hbar\frac{\partial \psi}{\partial t} \qquad (2.13)$$

benutzen, und nicht, wie Du es tust, den speziellen Fall, dass ψ proportional $e^{i\omega t}$ ist ($\hbar\omega = E$), betrachten; denn dieser entspricht scharfer Energie, also unbestimmtem Orte [...] $\psi(x,0)$ ist der willkürliche Anfangszustand. Diesen muss man so wählen, dass er ausdrückt: Zur Zeit $t = 0$ ist der Ball nahe am Punkt x mit ungefähr der Geschwindigkeit v. Also muss $\psi(x,0)$ überall Null sein außer in einem kleinen Intervall um die Stelle x_0 [...] Dann kommt sicher heraus (man kann es qualitativ ohne Rechnung einsehen), dass das Wellenbündel $\psi(x,t)$ hin und her prallt genau wie ein Teilchen, wobei es ein bisschen verwaschener wird. Aber diese Ungenauigkeiten werden für $m \to \infty$ verschwindend klein [...]"

In a reply to this letter, Einstein points out that the superposition principle allows also states that cannot be called "classical",

"[...] Zunächst muss ich sagen, dass Dein Standpunkt mich überrascht hat. Ich dachte nämlich, dass angenäherte Übereinstimmung mit der klassischen Mechanik stets dann zu erwarten sei, wenn die in Betracht kommenden de Broglie-Wellen-längen klein sind gegenüber den sonstigen relevanten räumlichen Abmessungen. Ich sehe aber, dass Du die klassische Mechanik nur mit solchen ψ-Funktionen in Beziehung bringen willst, die bezüglich Koordinaten und Impulsen "eng" sind. Wenn man es so auffasst, dann kommt man aber zu der Ansicht, dass weitaus die meisten quantentheoretisch denkbaren Vorgänge von Makrosystemen keinen Anspruch darauf machen dürfen, durch die Makro-Mechanik annähernd beschreibbar zu sein. Dann müss te man sich z. B. sehr wundern, wenn ein Stern oder eine Fliege, die man zum ersten Mal sieht, so etwas wie quasi-lokalisiert erscheinen.

Wenn man sich nun aber trotzdem auf Deinen Standpunkt stellt, so muss man wenigstens verlangen, dass ein System, welches zu einer gewissen Zeit "quasi-lokalisiert" ist, es gemäß der Schrödinger-Gleichung auch *bleiben* muss. Dies ist eine rein mathematische Frage, und Du erwartest, dass die Rechnung diese Erwartung bestätigen werde. Dies scheint mir aber ausgeschlossen zu sein [...]"

The solution to this problem starts with the observation that macroscopic objects are constantly interacting with the environment which adopts the role of a measurement apparatus. Since the environment is very large, the exact knowledge of the

state describing the composite system of the macroscopic object and environment is generally not possible. For a local observer who has only access to some degrees of freedom of the macroscopic object, say position and momentum, the interference terms which are present in the composite state are unobservable. The process of decoherence depends crucially on the number of degrees of freedom present in the environment. A single photon scattering at the macroscopic object is not able to resolve the distance between two possible positions, i.e. the wavelength of the photon is larger than the distance. However, a huge amount of scattering photons makes the decoherence process very efficient [35].

Ignoring any recoil, one finds the reduced density matrix ρ of a macroscopic object to be [21, 24]

$$\langle x|\rho(t)|x'\rangle = \rho(x, x', t) = \rho(x, x', 0)\exp\left(-\Lambda t(x - x')^2\right), \tag{2.14}$$

where $|x\rangle$ are the position eigenstates of the object and Λ is the localization rate determining the "efficiency" of the decoherence process. Λ depends linearly on the incoming flux of the scattering particles which emphasizes the role of the amount of "measuring events". We see from (2.14) that phase relations between different position eigenstates of the macroscopic object are exponentially suppressed. The pointer states coincide in (exponentially) good approximation with the position eigenstates. As can be seen from (2.14), interferences are *dynamically* suppressed, which corresponds to the dynamical choice of pointer states that are determined through the interaction.

2.5 Observation of Decoherence

The process of decoherence on mesoscopic objects was observed in different setups. Here we want to mention only some of the experimental breakthroughs. For an extensive discussion see e.g. [21]

In 1996, Brune and collaborators [36] were able to create a mesoscopic state of radiation fields and watched the destruction of this superposition by decoherence. A rubidium atom is prepared in a superposition of two Rydberg states and traverses a cavity which contains a coherent state. Due to the experimental setup, the atom and the coherent state become entangled in such a way, that the field is finally in a superposition of different states after measuring the atomic state. It was possible to observe the decay of the field superposition due to decoherence.

This was the first time, that a mesoscopic "Schrödinger kitten" was generated and decoherence was observed in a controlled way.

Later on, the effect of decoherence has been observed in experiments involving a superposition of C_{70} molecules [37] and in various setups involving superconducting quantum interference devices (SQUID's) [38].

2.6 Decoherence in Quantum Field Theory

The process of decoherence is universal and can also be applied in field theoretic settings. Kiefer [39] considered measurements of electromagnetic fields by charges in the context of scalar QED where the magnetic field is measured through a scalar field which could describe charged pions, for example.

Furthermore, decoherence was applied in order to understand the classicality of space-time. The scheme of the canonical formalism of quantization applying to general relativity leads to the "timeless" Wheeler-DeWitt equation,

$$H_{\mathrm{grav}}\psi = 0, \tag{2.15}$$

which is unfortunately only solvable using various approximation schemes and symmetry reductions [40]. However, it has been shown that the classicality of space-time, i.e. the scale factor of the universe, can be understood through interaction with light degrees of freedom such as density perturbations in the early universe [41].

2 Decoherence

3 Cosmological Models

Before we apply the concept of decoherence to a cosmological issue in section 4, we give a short overview about some basic facts concerning the standard model of cosmology. For detailed introductions, see [42–45].

Einstein included in 1917 a cosmological constant Λ in the field equations of general relativity. The motivation was the incorporation of Mach's principle into the theory of general relativity. Mach's principle states that it is useless to define any motion with respect to an absolute space, meaningful is only the motion with respect to all objects in the universe. Einstein wanted to incorporate Mach's principle on cosmological scales such that space-time vanishes if the universe does not contain any matter. This can be achieved using the field equations with cosmological constant,

$$R_{\mu\nu} - \frac{1}{2}g_{\mu\nu}R - \Lambda g_{\mu\nu} = 8\pi G T_{\mu\nu} \,, \tag{3.1}$$

where $R_{\mu\nu}$ denotes the Ricci tensor, $g_{\mu\nu}$ are the metric coefficients, $T_{\mu\nu}$ is the energy momentum tensor, and G is the gravitational constant. Here and in the following we use for the metric the sign convention $(+, -, -, -,)$.

A positive cosmological constant allows a static and closed universe since it acts as repulsive "force" counterbalancing the attractive force of matter. The mass of this universe is directly related to its volume such that the universe disappears if the mass vanishes. According to Mach, it was only meaningful to define a motion of an object against a material background. Nonetheless, in the static Einstein universe without matter there is no background which could be used as a reference frame.

Slipher observed in the 1920s a redshift of the light from distant galaxies, which can be explained by the Doppler effect if the galaxies are departing from each other. In 1922, Friedmann constructed a matter dominated model for the expanding universe without cosmological constant, which led finally Einstein to abandon the idea of a cosmological constant.

3.1 Friedmann-Robertson-Walker Universe

Assuming spatial homogeneity and isotropy of the universe, one finds the Friedmann-Robertson-Walker line element

$$ds^2 = dt^2 - a^2 \left(\frac{dr^2}{1 - kr^2} + r^2 d\theta^2 + r^2 \sin^2 \theta^2 d\phi^2 \right) \,, \tag{3.2}$$

where $a(t)$ denotes the scale factor of the universe and $k \in (1, 0, -1)$ is the spatial curvature for a closed, flat or open universe, respectively. If the energy momentum tensor describes a perfect fluid with density ρ and pressure P, Einstein's equations reduce to two coupled ordinary equations, the Friedmann equations. The first differential equation involved only first derivatives of the scale factor,

$$H^2 = \frac{8\pi G \rho}{3} + \frac{\Lambda}{3} - \frac{k}{a^2} \tag{3.3}$$

where the Hubble parameter is defined as $H = \dot{a}/a$. The second differential equation for the scale factor is the acceleration equation,

$$\frac{\ddot{a}}{a} = -\frac{4\pi G}{3}(\rho + 3P) + \frac{\Lambda}{3} . \tag{3.4}$$

Equation (3.3) can be rewritten in the form

$$\frac{1}{2}\dot{a}^2 + V(a) = -\frac{k}{2} \tag{3.5}$$

with a potential for the scale factor,

$$V(a) = -\frac{4\pi G}{3}\rho a^2 - \frac{\Lambda}{6}a^2 . \tag{3.6}$$

The right hand side of equation (3.5) can be interpreted as total energy of a particle with coordinate a moving in a potential $V(a)$.

From (3.5) one can easily derive the static Einstein universe. For simplicity we assume pressureless matter with the energy density $\rho = \rho_{\mathrm{mat}}(a_0/a)^3$, where a_0 denotes the present scale factor and ρ_{mat} is the present matter density. The potential has a maximum for

$$a = \left(\frac{4\pi G \rho_{\mathrm{mat}} a_0^3}{\Lambda} \right)^{1/3} . \tag{3.7}$$

Since the scale factor is constant, we have $a = a_0$ which leads to the critical cosmological constant, $\Lambda = \Lambda_{\mathrm{crit}} = 4\pi G \rho_{\mathrm{mat}}$. Using energy conservation, i.e. equation (3.5), we find $\Lambda_{\mathrm{crit}} = 1/a_0^2$.

However, this solution is unstable since small perturbations would lead to an expansion or an collaps of the universe. Furthermore, the Einstein static universe contradicts with the observations suggesting an expanding universe.

Although there are various models with nonvanishing spatial curvature [42], we will focus on spatially flat universes, since the model investigated in chapter 4 is defined with vanishing spatial curvature.

The critical density of the universe is defined by

$$\rho_{\text{crit}} = \frac{3H_0^2}{8\pi G}\,,\tag{3.8}$$

where H_0 is the current value of the Hubble parameter. Defining the density parameters for the different matter components at the present epoch to be $\Omega_i \equiv \rho_i(a_0)/\rho_{\text{crit}}$, one can recast equation (3.3) into the form

$$\frac{H^2}{H_0^2} = \frac{\Omega_{\text{rad}}}{a^4} + \frac{\Omega_{\text{mat}}}{a^3} + \Omega_\Lambda\,.\tag{3.9}$$

In a spatially flat universe, the density parameters add up to one, i.e. $\sum_i \Omega_i = 1$. Neglecting the contribution from radiation, i.e. $\Omega_{\text{rad}} = 0$, one obtains for $\Omega_{\text{mat}} + \Omega_\Lambda = 1$ the exact analytical solution

$$a(t) \propto \left(\sinh \frac{3}{2}\sqrt{\frac{\Lambda}{3}}t\right)^{2/3}.\tag{3.10}$$

This solution interpolates between a matter dominated epoch for $\sqrt{\Lambda}t \ll 1$ and an exponential expansion for $\sqrt{\Lambda}t \gg 1$.

An approximate exponential increase of the scale factor is obtained if the cosmological constant dominates the energy content of the universe, which is obviously the case for $\Omega_\Lambda \neq 0$ at late times as can be deduced from equation (3.9). If $\Omega_{\text{mat}} = \Omega_{\text{rad}} = 0$, we obtain from (3.9) an exact exponential increase of the scale factor, which is assumed to be the case during the period of inflation in the early universe [46]. The corresponding geometry is the de Sitter space, which is defined through the hyperplane

$$-X_1^2 + X_2^2 + X_3^2 + X_4^2 + X_5^2 = H^{-2}\tag{3.11}$$

in a five-dimensional auxiliary space. The solution with $k = 0$ is given by the flat spatial sections of de Sitter space, whereas solutions of (3.9) for nonvanishing spatial curvature, i.e. $k = \pm 1$, correspond to closed and open spatial sections of de Sitter space, respectively. The explicit coordinates of these geometries, which will be important in section (5), and further considerations concerning de Sitter geometry are given in [47, 48].

3.2 Models for Dark Energy

Since observations hint to the existence of a cosmological constant respectively dark energy (see [49]), there have been various attempts for theoretical explanations. The

ad hoc introduction of the parameter Λ in the field equations of general relativity (see equation (3.1)) does not offer a deeper understanding of its origin.

Zeldovich proposed that the cosmological constant may be the vacuum energy of a scalar field. Unfortunately this is a divergent quantity. For a single scalar field ϕ with mass m in Minkowski space, one obtains the energy momentum tensor

$$T_{ij} = \phi_{,i}\phi_{,j} - \frac{1}{2}\eta_{ij}\phi_{,k}\phi^{,k} + \frac{1}{2}m^2\phi^2\eta_{ij}\,, \tag{3.12}$$

where η_{ij} denotes the Minkowski metric. Quantization of the scalar field according to

$$\phi = \frac{1}{\sqrt{2L^3\sqrt{k^2+m^2}}}\sum_{\mathbf{k}}\left(a_{\mathbf{k}}e^{-i\sqrt{k^2+m^2}t+i\mathbf{kx}} + h.c.\right) \tag{3.13}$$

leads to the vacuum expectation values

$$\langle 0|T_{0i}|0\rangle = 0\,, \tag{3.14}$$

and

$$\langle 0|T_{00}|0\rangle = -\langle 0|T_{ii}|0\rangle = \frac{1}{2}\sum_{\mathbf{k}}\omega_{\mathbf{k}} = \frac{L^3}{4\pi^2}\int_0^\infty dk k^2\sqrt{k^2+m^2}\,, \tag{3.15}$$

where L^3 is the quantization volume. Although the energy momentum tensor is formally equal to the introduction of a cosmological constant, the expression (3.15) is problematic since it contains an ultraviolet divergence.

In standard quantum field theory, this causes no problems since usually one is interested in energy *differences*, allowing a redefinition of the zero point energy. In contrast, the field equations (3.1) are sensitive to the absolute value of energy contained in all forms of matter. A naive cutoff at the Planck scale does not solve the problem since the cosmological constant would be $\Lambda_{\text{Planck}} \sim 10^{76}\text{GeV}^4$, in strong disagreement with the observed value $\Lambda_{\text{Obs}} \sim 10^{-47}\text{GeV}^4$. This strong discrepancy is known as the cosmological-constant problem.

In order to obtain a realistic value for Λ, various approaches have been investigated. Dolgov proposed a decaying cosmological constant due to a non-minimal coupling to the scalar curvature [50–52]. The generation of a small cosmological constant from inflationary particle production was pushed forward by Sahni and Habib [53].

Many attempts have been made to explain dark energy using a minimally coupled and spatially homogeneous scalar field ϕ. The energy density and the pressure are given by

$$\rho_\phi = \frac{1}{2}\dot{\phi}^2 + V(\phi)\,, \tag{3.16}$$

$$P_\phi = \frac{1}{2}\dot{\phi}^2 - V(\phi)\,, \tag{3.17}$$

which leads for $\dot{\phi}^2 \ll V(\phi)$ to an approximate equation of state $\rho \approx -P$ which resembles the equation of state of a cosmological constant. If the universe contains only a scalar field and pressureless matter, we find from the Friedmann equations (3.3) and (3.4) with $k = \Lambda = 0$

$$4\pi G a^2 H^2 \left(\frac{d\phi}{da}\right)^2 = -aH\frac{dH}{da} - \frac{3}{2}\Omega_{\text{mat}}H_0^2 \left(\frac{a_0}{a}\right)^3 . \tag{3.18}$$

Since the left hand side of equation (3.18) is always positive, we have

$$-aH\frac{dH}{da} \geq \frac{3}{2}\Omega_{\text{mat}}H_0^2 \left(\frac{a_0}{a}\right)^3 , \tag{3.19}$$

which is nothing else but the weak energy condition for a dark energy term.

Depending on the shape of the potential, different scenarios have been discussed in the literature. Simple potentials, e.g. $V(\phi) = m^2\phi^2/2$, cause fine tuning problems: the relative values of matter and field densities have to be adjusted to high accuracy, in order to be approximately equal at the present epoch.

Choosing the scalar field potential [54]

$$V(\phi) = \frac{k}{\phi^\alpha} , \quad k, \alpha > 0 , \tag{3.20}$$

one finds that the background energy density ρ_{B} of radiation or matter is related to the energy density of the scalar field according to

$$\frac{\rho_\phi}{\rho_{\text{B}}} \propto t^{\frac{4}{2+\alpha}} . \tag{3.21}$$

Thus the scalar field density dominates at late times even if it was subdominant at early times .

For an overview on various scalar field models, see [42] and references therein.

Beside the scalar field models of Λ, also hydrodynamic models are discussed in the literature [55–57]. Within these models one describes the Λ-term with a phenomenological equation of state, $P = P(\rho)$. In the case of a cosmological constant, the equation of state reads $P = w\rho$ with the equation of state parameter $w = -1$. WMAP seven-year data limits on the equation of state parameter are $w = -1.12^{0.42}_{-0.43}$. Using in addition results from the Sloan Digital Sky Survey Data, one finds $w = -0.980 \pm 0.053$ [49].

3.3 Anthropic Considerations

As we pointed out in the last section, the discrepancy between the observed value of a cosmological constant and a naively predicted one is extremely large. Nevertheless,

it might be the case that the small value of Λ is accidental and results from the initial conditions in the universe. As example, it is obvious that the distance between the earth and the sun is not a fundamental length that can be derived from a theory. This length is rather accidental and could in principle be different. However, most of the possible distances would not be suitable for the evolution of life.

If our universe is part of a large multiverse in which the cosmological constant adopts all possible values, one might apply anthropic ideas. Weinberg showed in 1987 that the formation of galaxies is only possible if

$$\rho_\Lambda < \frac{500\rho_{\mathrm{mat}}(t_R)(\delta_{\mathrm{mat}}(t_R))^3}{729} \, , \tag{3.22}$$

where δ_{mat} is a typical density perturbation and t_R is the time of recombination [58]. This estimate reduces the difference between theoretical prediction of the cosmological constant and the observed value by 120 orders of magnitude.

We do not know whether we live in a probable universe, since the distribution of vacua in a hypothetical cosmological landscape is unknown and all attempts to derive a distribution rely on various assumptions [59].

During the last years the occurrence of a *string landscape* with as much as 10^{500} possible vacuum states brought new aspects into the discussion [60–64]. The arising of the landscape can be understood as follows. One considers the ten–dimensional space-time of string theory to be of the form $M^{3,1} \times X$, where $M^{3,1}$ represents our space-time and the manifold X is chosen to be small and compact. This compactification scheme introduces a high amount of ambiguity, since the choice of X is far from being unique. The continuous degeneracy of consistent ten–dimensional background are labeled by so–called *moduli* which appear as massless scalar fields in four dimensions. Since nobody ever observed those fields it is necessary to generate a potential such that the moduli become massive. This is done via flux compactification [62, 65, 66] where one assumes non–zero background values of the field strengths of the gauge fields appearing in the theory. Varying the background fluxes leads to an ensemble of moduli potentials. The set of all possible four–dimensional constructions is called string landscape.

Note that the idea of multiverses in cosmology have to be distinguished from multiverses arising in the Everett-interpretation (see chapter 2). The latter refers to possible outcomes of quantum decisions whereas the cosmological landscape is a complicated potential landscape arising from the huge amount of possible compactifations of extra dimensions in string theory.

3.4 Observational Hints to a Nonvanishing Cosmological Constant

Several independent observations hint to a cosmological constant greater than zero. In order to come to this conclusion, results from WMAP data have to be combined with high redshift supernova observations and models for structure formation.

The current value of the Hubble constant is according to WMAP seven-year data $H_0 \approx (71 \pm 2.5) \text{km/sec/Mpc}$ [49] and the age of the universe is $t_0 = (13.75 \pm 0.13) \text{Gyr}$, which would be in conflict with the age of the oldest stars unless the universe is flat and Λ–dominated with a total energy density $\Omega_{\text{mat}} + \Omega_\Lambda \simeq 1$. In an open matter dominated universe for instance, some globular clusters would be older than the age of the universe unless the Hubble parameter is very small, $H_0 < 45 \text{km/sec/Mpc}$.

Observations of the large scale structure of the universe favor a universe with a low matter density [67, 68]. Parameters in these models agree with $\Omega_{\text{mat}} \approx 0.3$ and $\Omega_\Lambda \approx 0.7$.

Supernovae of type Ia can be used as standard candles in cosmology since dispersion in their luminosity is very small and the width of the supernova lightcurve is strongly correlated with its intrinsic luminosity. These standard candles have been used to determine the value of H_0 and the joint probability distribution of Ω_{mat} and Ω_Λ which gives in combination with CMB results a peak of the likelihood near $\Omega_{\text{mat}} + \Omega_\Lambda = 1$ [69, 70].

3 Cosmological Models

4 Cosmological Constant from Decoherence?

Many attempts have been made to investigate the vacuum energy contribution Λ on a more fundamental basis (see section 3.2), however, its origin is still unknown and one of the biggest issues in cosmology. In particular, Λ could in general be time-dependent, although it seems that all data are consistent with the state parameter $w = -1$ [49].

An interesting idea to explain a small positive cosmological constant was put forward by Yokoyama [71]. He assumed that, perhaps due to some unknown symmetry, the exact ground state of the universe is characterized by a vanishing vacuum energy, that is, a vanishing cosmological constant. This part of the cosmological-constant problem thus remains unsolved by his proposal. The observed small deviation from zero arises, according to [71], from the fact that the universe is not in its ground state. More concretely, Yokoyama considers a double-well potential as a model for the dark energy. This is motivated by recent ideas in string theory where a 'landscape' of many (perhaps as many as 10^{500}) local minima of a complicated potential is discussed, see the short discussion in section 3.3. The simplest approximation to accommodate these ideas is to start from a double-well potential, which is a well studied example in quantum theory, and then to extend the discussion to the presence of many minima.

The ground state for a double-well potential is extended (delocalized) over both minima. In contrast to this, a state localized in one of the minima is a superposition of the eigenstates; in the simplest case, it is a superposition of the ground and the first excited state. The effective energy of such localized states is bigger than the ground-state energy and is thus positive in our case. If the wall between the wells is not too small, the values for this positive energy are tiny because they differ from the ground-state energy only by a small tunneling factor proportional to $\exp(-S_0)$, where S_0 is the instanton action. The reason for the observed small positive cosmological constant could thus lie in the fact that the universe is in a localized state being concentrated near one of the minima of the potential. An extension of Yokoyama's work to the case of many wells (taking into account ideas from string theory) was suggested in [72]. However, the authors consider the ground state of our universe to be a superposition of all accessible vacuum states. Due to the unavoidable interaction between the configuration of the universe and environmental degrees of freedom, for

example standard model fields or thermal excitations, this seems to be a doubtful assumption.

As long as the universe stays in a localized state, the effective equation of state would be $p \approx -\rho$. There exists, however, a certain probability that the universe can tunnel into another localized state. The question then arises how big the time scale and the tunneling rate are which should obey all known observational constraints [49]. In the following we shall elaborate on this idea in two respects. First, it has to be justified why the universe is not in its ground state in the first place, but in a localized state. The key concept for addressing this problem is decoherence [21, 25]. It has been pointed out in section (2) that decoherence is used in quantum mechanics in order to understand the emergence of classical properties, for example, the spatial localization of a particle which is originally in a superposition of localized states.

The case closest to our cosmological situation is the emergence of molecular structure ([25], section 3.2.4). Chiral molecules such as sugar can be described by a double-well potential. While their energy eigenstates are delocalized over both minima, their chiral (parity-violating) states are localized in the two minima. Except for small molecules, these systems are usually found in their localized states. The reason is the ubiquitous interaction with environmental degrees of freedom such as air molecules and photons which 'fix' the molecular structure and thus lead to chiral states; this is decoherence. A similar mechanism is invoked here to justify that the universe is in a state with small positive Λ.

Our second elaboration is a direct consequence of the first problem. If additional 'decohering' degrees of freedom are present, they will have an effect on the tunneling rate. One may expect that they will in general *reduce* this rate, so that tunneling will become less likely [73]. We shall thus discuss both the pure tunneling rate of the isolated system as well as its modification by the environment. These considerations should be relevant, too, for the inflationary stage of the early universe, which was also dominated by an (effective) cosmological constant. We shall discuss both the case of two minima and of many minima.

We start in section 4.1 with a brief introduction on tunneling in quantum mechanics and quantum field theory, mainly following the treatment given in [74]. Then we will give short review of Yokoyama's proposal in section 4.2. In the subsequent section 4.3, we will present our model in detail. The reduced density matrix describing the cosmological constant will be considered in section 4.4. Modifications of the tunneling rate due to system-environment interaction are subject of section 4.5, aspects of decoherence in a cosmological landscape are discussed in section 4.6.

4.1 Tunneling in Quantum Theory

Tunneling is a purely quantum mechanical phenomenon and cannot be understood in classical terms [74]. It describes the barrier penetration of particles being trapped in a local minima of a potential. Classically, the particle would not have enough energy to overcome the barrier. In contrast, the quantum mechanical description of a particle relies on a wave function that is non-vanishing within the potential barrier.

Consider the Hamiltonian of a particle moving in a one-dimensional potential,

$$H = \frac{p^2}{2} + V(x) \,. \tag{4.1}$$

According to Feynman, the transition amplitude of the particle moving from x_i to x_f is

$$\langle x_f | e^{-iHt/\hbar} | x_i \rangle = N \int Dx \, e^{iS/\hbar} \,, \tag{4.2}$$

where we reintroduced Planck's constant $\hbar$ explicitly and N is a normalization constant. The euclidean version of (4.2) can be obtained by the analytical continuation of the time $t \to -it_E$, and reads

$$\langle x_f | e^{-HT/\hbar} | x_i \rangle = N \int Dx \, e^{-S_E/\hbar} \,, \tag{4.3}$$

where T is the euclidean time within the particle state changes from $|x_i\rangle$ to $|x_f\rangle$. The euclidean action, given by

$$S_E = \int_{-T/2}^{T/2} dt_E \left[\frac{1}{2} \left(\frac{dx}{dt_E} \right)^2 + V(x) \right] \tag{4.4}$$

determines the motion of a particle in a potential $-V$.

Formula (4.3) is often used for obtaining the tunneling amplitude of the particle, the motivation shall be given in section 4.1.2. The left hand side of equation (4.3) can be evaluated in a set of energy eigenstates of the Hamiltonian,

$$H|n\rangle = E_n|n\rangle, \tag{4.5}$$

and therefore

$$\langle x_f | e^{-HT/\hbar} | x_i \rangle = \sum_n e^{-E_n T/\hbar} \langle x_f | n \rangle \langle n | x_i \rangle \,. \tag{4.6}$$

The leading term of this expression in the large T limit is determined by the lowest energy eigenstate and the corresponding wave-function. The big advantage of the

path integral formulation is, that the right hand side of (4.3) can be evaluated in the semi-classical limit, i.e. for small $\hbar$. Expanding up to first order in $\hbar$, we have

$$N \int Dx e^{-S_E/\hbar} = A \exp(-S_E/\hbar) , \qquad (4.7)$$

where S_E is the classical Euclidean action and the prefactor A is determined by the second variation of the action.

4.1.1 The Harmonic Oscillator

To start with, we consider the harmonic oscillator with frequency ω. The path integral has to be evaluated along all possible trajectories $x(t_E)$ with $x(-T/2) = x_i$ and $x(T/2) = x_f$. We separate the function $x(t_E)$ in a classical trajectory $\bar{x}$ and a sum of real and orthonormal functions $x_n(t_E)$ that are vanishing at the boundaries,

$$x(t_E) = \bar{x}(t_E) + \sum_n c_n x_n(t_E) , \qquad (4.8)$$

with

$$\int_{-T/2}^{T/2} dt_E x_n(t_E) x_m(t_E) = \delta_{nm} . \qquad (4.9)$$

A simple example is the case $x_i = x_f = 0$. The classical action vanishes since $\bar{x} = 0$ and we are left with contributions from the second variation of the action,

$$
\begin{aligned}
\langle 0|e^{-HT/\hbar}|0\rangle &= N \prod_k \int dc_k (2\pi\hbar)^{-1/2} \exp\left(-\frac{1}{\hbar} \sum_n \left(-\frac{d^2}{dt_E^2} + \omega^2 \right) c_n^2 \right) \\
&= N \left[\text{Det}\left(-\frac{d^2}{dt_E^2} + \omega^2 \right) \right]^{-1/2} , \qquad (4.10)
\end{aligned}
$$

where the orthonormality of the x_n has been used. For large T, we find with an appropriate normalization

$$N \left[\text{Det}\left(-\frac{d^2}{dt_E^2} + \omega^2 \right) \right]^{-1/2} = \left(\frac{\omega}{\pi\hbar} \right)^{1/2} e^{-\omega T/2} , \qquad (4.11)$$

from which we deduce the ground state energy,

$$E_0 = \frac{1}{2}\omega\hbar . \qquad (4.12)$$

4.1.2 The Double Well

Now we investigate the tunneling process in an even potential, $V(x) = V(-x)$, with two local minima and their corresponding position eigenstates $|x_+\rangle$ and $|x_-\rangle$. In the following we will compute the transition amplitudes

$$\langle x_+|e^{-HT/\hbar}|x_+\rangle = \langle x_-|e^{-HT/\hbar}|x_-\rangle \tag{4.13}$$

and

$$\langle x_+|e^{-HT/\hbar}|x_-\rangle = \langle x_-|e^{-HT/\hbar}|x_+\rangle \,. \tag{4.14}$$

In contrast to the simple harmonic oscillator, the classical solutions to the equations of motion for vanishing energy are nontrivial. Varying the action (4.4), we find the differential equation

$$-\frac{d^2\bar{x}}{dt_E^2} + V'(\bar{x}) = 0, \tag{4.15}$$

which has for vanishing energy the solution

$$\bar{x}(t) = \int_0^t dt_E \sqrt{2V} + x_{+/-}. \tag{4.16}$$

The corresponding classical euclidean action reads

$$S_E = \int dt_E \left(\left(\frac{d\bar{x}}{dt_E}\right)^2 + V(\bar{x}) \right) = \int_{x_-}^{x_+} d\bar{x}\sqrt{2V} \,. \tag{4.17}$$

Thus, the expression for the tunneling rate, $\Gamma \propto \exp(-S_E)$, coincides with the usual amplitude for transmission through a potential barrier that can be obtained by solving the Schrödinger equation explicitly [74]. The euclidean path integral formalism has the advantage that it can be generalized to field theoretical settings.

The classical solutions going from x_- to x_+ are called "instantons", because they are similar to particle–like solutions of classical field theories. Whereas particle–like solutions like solitons are structures in space, the instanton solutions are structures in time (see p. 271 in [74]).

In order to compute the amplitudes (4.2) and (4.3) one has to sum over all configurations starting at $x_{+/-}$ and ending at $x_{+/-}$. The instanton solutions are centered around times $t_1, ..., t_n$, where

$$T/2 > t_1 > ... > t_n > -T/2 \,. \tag{4.18}$$

Furthermore, one is assuming that the instantons are widely separated. In other words, the time scale of the transition from x_- to x_+ has to be much smaller than T.

For n instantons, the formula (4.11) is corrected due to the transitions between x_- and x_+,

$$\left(\frac{\omega}{\pi\hbar}\right)^{1/2} e^{-\omega T/2} \rightarrow \left(\frac{\omega}{\pi\hbar}\right)^{1/2} e^{-\omega T/2} K^n , \qquad (4.19)$$

with $\omega^2 = V''(x_{+/-})$ and K is defined such that the right hand side of (4.19) gives the correct answer for a single instanton, i.e. $n = 1$.

The instantons are centered at times t_i which fulfill the relation (4.18). By integrating over all possible centers we obtain the factor

$$\int_{-T/2}^{T/2} dt_1 \int_{t_1}^{T/2} dt_2 ... \int_{t_{n-1}}^{T/2} dt_n = \frac{T^n}{n!} . \qquad (4.20)$$

All together this leads to the transition amplitudes

$$
\begin{aligned}
\langle x_+ | e^{-HT/\hbar} | x_+ \rangle &= \langle x_- | e^{-HT/\hbar} | x_- \rangle \qquad (4.21)\\
&= \left(\frac{\omega}{\pi\hbar}\right)^{1/2} e^{-\omega T/2} \sum_{n=0}^{\infty} \frac{(KTe^{-S_E/\hbar})^{2n}}{(2n)!} \\
&= \left(\frac{\omega}{\pi\hbar}\right)^{1/2} e^{-\omega T/2} \frac{1}{2} \left[\exp(KTe^{-S_0/\hbar}) + \exp(-KTe^{S_0/\hbar}) \right]
\end{aligned}
$$

and

$$
\begin{aligned}
\langle x_+ | e^{-HT/\hbar} | x_- \rangle &= \langle x_- | e^{-HT/\hbar} | x_+ \rangle \qquad (4.22)\\
&= \left(\frac{\omega}{\pi\hbar}\right)^{1/2} e^{-\omega T/2} \sum_{n=0}^{\infty} \frac{(KTe^{-S_E/\hbar})^{2n+1}}{(2n+1)!} \\
&= \left(\frac{\omega}{\pi\hbar}\right)^{1/2} e^{-\omega T/2} \frac{1}{2} \left[\exp(KTe^{-S_0/\hbar}) - \exp(-KTe^{S_0/\hbar}) \right] .
\end{aligned}
$$

From these expressions, we can deduce the two lowest eigenfunctions of the Hamiltonian, $|0\rangle = (|x_+\rangle + |x_-\rangle)/\sqrt{2}$ and $|1\rangle = (|x_+\rangle - |x_-\rangle)/\sqrt{2}$ with the energy eigenvalues $E_0 = \hbar\omega/2 - \hbar K \exp(-S_0/\hbar)$ and $E_1 = \hbar\omega/2 + \hbar K \exp(-S_0/\hbar)$, respectively. These are the usual odd and even combinations of localized harmonic oscillator states. The degeneracy is broken by the exponential small tunnel splitting, $\exp(-S_E/\hbar)$.

The correction K is given according to Callan and Coleman [75] by the ratio of two functional determinants,

$$K = \left(\frac{S_E}{2\pi\hbar}\right)^{1/2} \left| \frac{\text{Det}(-d^2/dt_E^2 + \omega^2)}{\text{Det}'(-d^2/dt_E^2 + V''(\bar{x}))} \right|^{1/2} , \qquad (4.23)$$

where the prime indicates that the zero eigenvalue has been omitted. Otherwise the evaluation of the determinant would lead to an infinity, i.e. the integral over the

expansion coefficient c_1 which corresponds to the eigenfunction with zero eigenvalue, x_1, is not bounded. This eigenfunction appears due to the time translational invariance and can be obtained by differentiating the equation of motion (4.15) with respect to time. It reads explicitly

$$x_1(t_E) = S_E^{-1/2} \frac{d\bar{x}}{dt_E} \, , \tag{4.24}$$

where the normalization is obtained through equation (4.17) and the normalization (4.9). Comparing the changes of x induced by a small change of the instanton center t_1,

$$dx = \frac{d\bar{x}}{dt_1} dt_1, \tag{4.25}$$

and the change induced by a variation of the expansion coefficient, c_1,

$$dx = x_1 dc_1, \tag{4.26}$$

one finds

$$\left(\frac{1}{2\pi\hbar} \right)^{1/2} dc_1 = \left(\frac{S_E}{2\pi\hbar} \right)^{1/2} dt_1 \, . \tag{4.27}$$

This explains the inclusion of a factor $(S_E/2\pi\hbar)^{1/2}$ instead of the zero eigenvalue in equation (4.23).

In the following sections, we set $\hbar = 1$ again.

4.2 Yokoyama's Proposal

Before describing our model in detail, we will give a short review on Yokoyama's proposal [71]. He considered an abstract field theory with two localized vacuum states, $|+\rangle$ and $|-\rangle$. The transition is classical forbidden, but quantum mechanically, there exists an instanton solution describing the tunneling from $|+\rangle$ to $|-\rangle$ and vice versa. It follows that the true ground state, $|S\rangle$, is given by the symmetric superposition

$$|S\rangle = \frac{|+\rangle + |-\rangle}{\sqrt{2}} \, . \tag{4.28}$$

The local energy density of both $|+\rangle$ and $|-\rangle$ is given by ρ_0, whereas the energy density of the ground state, ρ, can be obtained by summing over all instanton

configurations. Yokoyama considers the probability amplitude for the system to remain in the ground state,

$$\langle S|e^{-HT}|S\rangle =: \exp(-\mathcal{V}T\rho)\,, \tag{4.29}$$

where H is the (time independent) Hamiltonian of the system. The volume $\mathcal{V}$ is the spatial region, in which the quantum field is defined. From section (4.1) we know that the tunneling amplitude is determined by the instanton action S_E. In order to evaluate (4.29), the expressions

$$\langle +|e^{-HT}|+\rangle = \langle -|e^{-HT}|-\rangle \tag{4.30}$$

and

$$\langle +|e^{-HT}|-\rangle = \langle +|e^{-HT}|-\rangle \tag{4.31}$$

have to be obtained. If the field rested in a potential with only one local minima, one would find only the contributions from the second variation of the classical action since the classical action vanishes. Generalizing (4.11), one finds

$$N\mathrm{Det}(-\partial_{t_E}^2 - \nabla^2)^{-1/2} \propto e^{-\rho_0 \mathcal{V}T}\,, \tag{4.32}$$

where $\rho_0 \mathcal{V}$ is the sum of the ground state energies of all harmonic oscillators within the quantization volume $\mathcal{V}$. Again, the instantons and anti-instantons correct the formula such that we have

$$N\mathrm{Det}(-\partial_{t_E}^2 - \nabla^2)^{-1/2} \propto (\mathcal{V}K)^n e^{-\rho_0 \mathcal{V}T}\,, \tag{4.33}$$

where K is given by a ratio of functional determinants similar to (4.23). We integrate again over the centers of the locations of the instantons and find a factor $T^n/n!$ as in equation (4.20). Now we have to sum up all instanton configurations,

$$\langle +|e^{-HT}|+\rangle = e^{-\rho_0 \mathcal{V}T} \sum_{n=0}^{\infty} \frac{\left(KT\mathcal{V}e^{-S_0}\right)^{2n}}{(2n)!} \tag{4.34}$$

and

$$\langle +|e^{-HT}|-\rangle = e^{-\rho_0 \mathcal{V}T} \sum_{n=0}^{\infty} \frac{\left(KT\mathcal{V}e^{-S_0}\right)^{2n+1}}{(2n+1)!}\,. \tag{4.35}$$

From (4.34) and (4.35), Yokoyama's result can be derived,

$$\langle S|e^{-HT}|S\rangle = \exp\left(-\mathcal{V}T\left(\rho_0 - Ke^{-S_0}\right)\right)\,. \tag{4.36}$$

The energy density ρ is supposed to vanish according to some unknown symmetry, i.e.

$$\rho = 0 = \rho_0 - Ke^{-S_0}.\tag{4.37}$$

Since the energy density of a localized vacuum state ρ_0 equals the dark energy density of our universe, one has with (4.37) a natural explanation for its smallness, i.e. $\rho_0 = 10^{-120} M_{\text{Planck}}^4$. One can account for this small value without introducing small numbers since from (4.37) follows $S_0 = 120 \ln 10 + \ln(K/M_{\text{Planck}}^4)$. The requirement that the universe is too young to be relaxed into the ground state $|S\rangle$ leads with the tunneling rate per unit volume, $\Gamma = Ke^{-2S_0}$, and the current Hubble parameter, $H_0 = \sqrt{\rho_0/(3M_{\text{Planck}}^2)}$, to the condition

$$\Gamma/H_0^4 \approx 9M_{\text{Planck}}^4/K \leq 1.\tag{4.38}$$

4.3 The Model

In this section we will incorporate Yokoyama's idea in an explicit model, explaining in addition the localization of the Λ-term.

The vacuum energy is mimicked by a scalar field ϕ in a quartic potential with two quasi-localized minima; this we shall call our 'system'. Furthermore, we consider a scalar field environment, which will influence our system. The system and the environment are supposed to evolve in a flat FRW-background with the line element

$$ds^2 = g_{\mu\nu}^{\text{B}} dx^\mu dx^\nu = dt^2 - a^2(t)(dx^2 + dy^2 + dz^2).\tag{4.39}$$

We assume here for later convenience that the scale factor, a, has the dimension of a length, while x, y, and z are dimensionless. The action of system and environment then reads

$$S = \int d^4x \sqrt{-g^{\text{B}}}\left(\mathcal{L}_{\text{sys}} + \mathcal{L}_{\text{env}} + \mathcal{L}_{\text{int}}\right),\tag{4.40}$$

where g^{B} is the determinant of the metric $g_{\mu\nu}^{\text{B}}$ and $\mathcal{L}_{\text{sys}}$, $\mathcal{L}_{\text{env}}$ and $\mathcal{L}_{\text{int}}$ denote the Lagrangian of the system, environment and interaction, respectively. The spatially homogeneous scalar field describing the vacuum energy is given by

$$\mathcal{L}_{\text{sys}} = \frac{1}{2}\dot{\phi}^2 - V(\phi).\tag{4.41}$$

The Lagrangian of the environment, $\mathcal{L}_{\text{env}}$, reads in the case of the scalar field environment

$$\mathcal{L}_{\text{env},\sigma} = \frac{1}{2}\partial_\mu\sigma\partial^\mu\sigma.\tag{4.42}$$

The interaction between the system and environment has to be suited to distinguish different values of the scalar field ϕ. In quantum mechanical settings usually one choses *bilinear* interactions, see for instance the Caldeira-Leggett model [73, 76] or the Spin-Boson model described in section 5.3 of [21]. However, the field ϕ is assumed to be spatially *homogeneous*. Therefore, a bilinear term in the action which is of the form $\int d^3x\sigma(\mathbf{x},t)\phi(t)$ would give no interesting dynamics, since only a single Fourier component of the scalar field σ, the one with vanishing momenta, interacts with the system field. We consider instead the *tri-linear* interaction

$$\mathcal{L}_{\text{int},\sigma} = -g_S\sigma^2\phi \tag{4.43}$$

for the scalar field environment. Here, the coupling constants g_S has to be chosen such that the product $g_S\phi$ is positive, but otherwise arbitrary. This requirement assures that the corresponding Hamiltonians are bounded from below and the theory is stable.

The terms can formally be derived from an expansion of the determinant $\sqrt{-g}$ into the scalar and tensor modes. Therefore, we consider the FRW line element with scalar and tensor perturbations [77],

$$ds^2 = (1+2\psi_1)dt^2 - a^2((1-2\psi_2)\delta_{ij} + h_{ij})dx^idx^j \,, \tag{4.44}$$

where $\psi_{1/2}$ are scalar perturbations and h_{ij} are tensor modes. In the transverse and traceless gauge, there are only two independent tensor modes, $h_{23} = h_{32}$ and $h_{22} = -h_{33}$. If there is a linear term in the potential of the system field ϕ, we have

$$\int d^3x\sqrt{-g}\phi \approx \tag{4.45}$$

$$\int d^3x\sqrt{-g^B}\left(1 + \psi_1 - 3\psi_2 - 2\psi_1^2 + \frac{3}{2}(\psi_1 - \psi_2)^2 - \frac{1}{2}h_{22}^2 - \frac{1}{2}h_{23}^2\right)\phi \,.$$

Discarding the terms linear in ψ_1 and ψ_2 for the reason mentioned above, we are left with tri-linear interactions of the form (4.43).

4.4 The Reduced Density Matrix

The Hamiltonian which can be derived from (4.40) reads in momentum representation

$$H_{\phi,\sigma} = \int dp^3\left(\frac{1}{2a^3}\tilde{\Pi}(\mathbf{p})\tilde{\Pi}(-\mathbf{p}) + \frac{a}{2}p^2\tilde{\sigma}(\mathbf{p})\tilde{\sigma}(-\mathbf{p})\right. \tag{4.46}$$

$$\left. +g_Sa^3\phi\tilde{\sigma}(\mathbf{p})\tilde{\sigma}(-\mathbf{p})\right) + H_\phi \,,$$

where we defined

$$\sigma(\mathbf{x}) = \frac{1}{(2\pi)^{3/2}} \int d^3p \; \tilde{\sigma}_{ab}(\mathbf{p})e^{i\mathbf{x}\mathbf{p}} \,, \tag{4.47}$$

$$\Pi(\mathbf{x}) = \frac{1}{(2\pi)^{3/2}} \int d^3p \; \tilde{\Pi}(\mathbf{p})e^{i\mathbf{x}\mathbf{p}} \,. \tag{4.48}$$

Note that $\mathbf{p}$ is dimensionless and the scalar field ϕ is spatially homogeneous, i.e. $\phi(\mathbf{x},t) = \phi(t)$.

In the following we simplify the part of the Hamiltonian describing the system. We shall assume that the dynamics of the system is dominated by the two lowest energy eigenvalues of the double-well potential, that is, we assume that their difference is much smaller than the energy gaps within a single well. It is then possible to reduce the system to an effective two-state system,

$$H_\phi = \begin{pmatrix} E_+ & \Delta \\ \Delta & E_- \end{pmatrix} \,, \tag{4.49}$$

where E_+ and E_- are the energy levels of the localized minima, and Δ is the tunneling matrix element. The reduction of system to an effective two-state system leads to the interaction

$$H_{\text{int},\sigma} = g_S a^3(t) \begin{pmatrix} \phi_+ & 0 \\ 0 & \phi_- \end{pmatrix} \int d^3p \; \sigma(\mathbf{p})\sigma(-\mathbf{p}) \,, \tag{4.50}$$

where the environment can only distinguish between the two different minima of the potential, ϕ_+ and ϕ_-.

All together, our model resembles a spin–boson model [78], although the coupling in the standard situation is taken to be linear in the environmental fields. It is well known that situations with a double-well potential can often be described by an effective two-state system [21, 25]. Spin–boson models describe the interaction of a central system with its environment, when the system is effectively acting as two-level system.

With this simplification at hand it is possible to calculate the reduced density matrix of the two-state system. We assume that the initial state is a product of a system and an environmental state, $|\Psi\rangle_{\text{sys}} \otimes |\Psi\rangle_{\text{env}}$. The time evolution will then generate an entanglement between them. This evolution is governed by the functional Schrödinger equation

$$i|\dot{\Psi}\rangle = H_{\phi,\sigma}|\Psi\rangle \,. \tag{4.51}$$

Setting $\Delta = 0$ in (4.49), it is possible to solve the Schrödinger equation exactly. We assume the state of system and environment to be of Gaussian form [79] and make the ansatz

$$|\Psi\rangle = \begin{pmatrix} \alpha N_+(t) \exp\left(-\frac{1}{2}\int d^3p \; \sigma(\mathbf{p})\Omega_+(\phi,p,t)\sigma(-\mathbf{p}) - iE_+t\right) \\ \beta N_-(t) \exp\left(-\frac{1}{2}\int d^3p \; \sigma(\mathbf{p})\Omega_-(\phi,p,t)\sigma(-\mathbf{p}) - iE_-t\right) \end{pmatrix} \,, \tag{4.52}$$

where $\Omega_{+/-}(p,t)$ and $N_{+/-}(t)$ are time-dependent functions to be determined from the Schrödinger equation, α and β are constants with $|\alpha|^2 + |\beta|^2 = 1$. With the above ansatz one obtains the following Riccati-type equations, cf. [39],

$$-i\dot{\Omega}_{+/-}(p,t) = -\frac{(\Omega_{+/-}(p,t))^2}{a^3} + p^2 a + g_S a^3 \phi_{+/-} \tag{4.53}$$

and

$$\frac{1}{2a^3}\mathrm{Tr}\Omega_{+/-}(p,t) = i\frac{\dot{N}_{+/-}}{N_{+/-}} \,. \tag{4.54}$$

These equations can be solved by the ansatz

$$\Omega_{+/-}(p,t) = -ia^3 \frac{\dot{u}_{+/-}(p)}{u_{+/-}(p)} \,. \tag{4.55}$$

Switching to conformal time defined by $a\,d\eta = dt$, we obtain

$$(p^2 + 2g_S \phi_{+/-} a^2)u_{+/-}(p,\eta) + \frac{2a'}{a}u'_{+/-}(p,\eta) + u''_{+/-}(p,\eta) = 0\,. \tag{4.56}$$

The density matrix for system and environment is given by the pure state

$$\rho(t) = |\Psi\rangle\langle\Psi| \tag{4.57}$$

from which the reduced density matrix shall be obtained by integrating out the environmental scalar field,

$$\rho(t)_{\mathrm{sys}} = \mathrm{Tr}_{\mathrm{env}}|\Psi\rangle\langle\Psi|\,. \tag{4.58}$$

In position representation, this reads

$$\rho_{ij} = \int D\sigma \Psi_i^*[\sigma]\Psi_j[\sigma]\,, \tag{4.59}$$

where i,j run over the values $+$ and $-$, and $\Psi \equiv (\Psi_+, \Psi_-)^{\mathrm{T}}$. Since we neglected dissipation by setting $\Delta = 0$, the diagonal elements of the reduced density matrix remain unchanged, that is, one has

$$\begin{aligned} \rho_{++}(t) &= |\alpha|^2 |N_+(t)|^2 \int D\sigma \exp\left[-\int d^3 p \sigma(\mathbf{p})\Re\Omega_+(t)\sigma(-\mathbf{p})\right] \\ &= |\alpha|^2 = \rho_{++}(0) \end{aligned} \tag{4.60}$$

as well as $\rho_{--}(t) = \rho_{--}(0)$. The probabilities of finding the system in state 1 or 2 are thus unchanged by the environment; this corresponds to a quantum-nondemolition (or ideal) measurement [21, 25].

The non-diagonal elements can be calculated as follows,

$$
\begin{aligned}
\rho_{+-}(t) &= \rho_{-+}^*(t) = \alpha\beta^* N_+ \left(N_-\right)^* \times \\
&\quad \int D\sigma \exp\left(-\frac{1}{2}\int d^3p \left(\Omega_+ + \Omega_-^*\right) - i(E_+ - E_-)t\right) \\
&= \alpha\beta^* \frac{\det^{1/4}(\Re\Omega_+)\det^{1/4}(\Re\Omega_-)}{\det^{1/2}\left(\left(\Omega_+ + \Omega_-^*\right)/2\right)} \times \\
&\quad \times \exp\left(-i\int^t dt' \frac{1}{2a^3}\mathrm{Tr}(\Re\Omega_+ - \Re\Omega_-) - i(E_+ - E_-)t\right). \quad (4.61)
\end{aligned}
$$

The functions $\Omega_{+/-}$ depend on the small parameter $a^2\gamma/p^2$ for sub-Hubble modes and γ/H^2 for super-Hubble modes, where $\gamma = 2g_S\phi_{+/-}$. (For notational convenience we suppress the indices $+$ and $-$ on γ.) Expanding up to second order in γ, we have

$$
\begin{aligned}
\Omega_{+/-}(\gamma) &\approx \left.\Omega_{+/-}\right|_{\gamma=0} + \left.\frac{d}{d\gamma}\Omega_{+/-}\right|_{\gamma=0}\gamma + \frac{1}{2}\left.\frac{d^2}{d\gamma^2}\Omega_{+/-}\right|_{\gamma=0}\gamma^2 \\
&=: \Omega + \Omega'\gamma + \frac{1}{2}\Omega''\gamma^2. \quad (4.62)
\end{aligned}
$$

The approximate expression for the non-diagonal elements then reads

$$
\rho_{+-}(t) = \rho_{+-}(0)\exp\left(-\frac{g_S^2(\phi_+ - \phi_-)^2}{4}\mathrm{Tr}\left(\frac{(\Re\Omega')^2 + (\Im\Omega')^2}{(\Re\Omega)^2}\right) - i\varphi_{+-}\right) \quad (4.63)
$$

with $\rho_{+-}(0) = \alpha\beta^*$ and

$$
\begin{aligned}
\varphi_{+-} &= \mathrm{Tr}\left(\frac{\Im\Omega'}{\Re\Omega}\frac{g_S(\phi_+ - \phi_-)}{2} + \left(\frac{\Im\Omega''}{\Re\Omega} - \frac{\Im\Omega'\Re\Omega'}{(\Re\Omega)^2}\right)\frac{g_S^2(\phi_+^2 - \phi_-^2)}{2}\right) \\
&\quad + \int^t dt' \frac{1}{2a^3}\mathrm{Tr}(\Re\Omega_+ - \Re\Omega_-) + (E_+ - E_-)t. \quad (4.64)
\end{aligned}
$$

In the following we want to discuss the explicit form of the decoherence factor. To begin with, we consider the impact of the sub-Hubble modes on the system. Within a WKB-approximation, which is adequate for $p^2 \gg a''/a$, the solutions to the differential equation (4.53) reads

$$
u_{+/-}(k, \eta) = \frac{A}{a}\exp\left(i\int^\eta d\eta'\omega_{+/-}(\eta')\right), \quad (4.65)
$$

where

$$
\omega_{+/-}(\eta) = \left(k^2 + 2g_S\phi_{+/-}a^2 - \frac{a''}{a}\right)^{1/2}. \quad (4.66)
$$

4 Cosmological Constant from Decoherence?

We have chosen an instantaneous vacuum in the infinite past, also known as Bunch–Davies vacuum [80]. This is possible since the interaction vanishes for $a \to 0$ when the modes are far inside the horizon. The trace of the real part of the exponent in (4.63) reads

$$
\mathrm{Tr} \left(\frac{(\Re \Omega')^2 + (\Im \Omega')^2}{(\Re \Omega)^2} \right) = \frac{\pi a^4 V}{(2\pi)^3} \int_{k_{\min}}^{\infty} dk \frac{k^2}{\left(k^2 - \frac{a''}{a} \right)^2}
$$

$$
= \frac{\pi a^4 V}{2(2\pi)^3} \left(\frac{k_{\min}}{k_{\min}^2 - \frac{a''}{a}} + \frac{1}{2} \sqrt{\frac{a}{a''}} \ln \left(\frac{k_{\min} + \sqrt{\frac{a''}{a}}}{k_{\min} - \sqrt{\frac{a''}{a}}} \right) \right) . \tag{4.67}
$$

The WKB-approximation holds for modes far inside the horizon $k_{\min} > \sqrt{a''/a}$, in the case of a constant Hubble rate we have $k_{\min} > \sqrt{2} H a$.

To discuss the explicit form of the decoherence rate for super-Hubble modes we shall restrict ourselves to the de Sitter case $H = \mathrm{const}$. It is not possible to take WKB solutions, since the time evolution is highly non-adiabatic for super-Hubble modes. The solution for equation (4.56) is given by

$$
u_{+/-}(p, \eta) = \frac{H \sqrt{\pi}}{2} \left(\frac{\eta}{p} \right)^{3/2} \mathcal{H}^{(1)}_{\sqrt{9/4 - 2g_S \phi_{+/-}/H^2}}(p\eta) , \tag{4.68}
$$

where $\mathcal{H}^{(1)}$ denotes a Hankel function. This expression is equal to the usual Bunch–Davies vacuum for $g_S = 0$:

$$
u_{g_S=0}(p, \eta) = -\frac{H\eta}{\sqrt{2} p^2} \left(1 + \frac{i}{p\eta} \right) e^{ip\eta} . \tag{4.69}
$$

In this example it is easy to obtain the effect of particle creation on the decoherence factor. Using a Gaussian state and the expression (4.69), it is easy to show that for $g = 0$ we have

$$
\Omega(p, t) = \frac{p^2 a^2}{p - iaH} . \tag{4.70}
$$

Using (4.70) and the approximation of (4.68) for $p\eta \to 0$,

$$
u_{+/-}(p, \eta) \propto \left(\frac{\eta}{p} \right)^{3/2} \left(\frac{p\eta}{2} \right)^{-\sqrt{9/4 - 2g_S \phi_{+/-}/H^2}} , \tag{4.71}
$$

we obtain for the impact of super-Hubble modes on the system

$$
\mathrm{Tr} \left(\frac{(\Re \Omega')^2 + (\Im \Omega')^2}{(\Re \Omega)^2} \right) = \frac{4\pi V a^2}{9(2\pi)^3 H^2} \int_{p_{\min}}^{p_{\max}} dp \left(1 + \frac{2aH}{p} \right)^2
$$

$$
= \frac{4\pi V a^2}{9(2\pi)^3 H^2} \left[p_{\max} - p_{\min} - \left(\frac{2a^2 H^2}{p_{\max}} - \frac{2a^2 H^2}{p_{\min}} \right) - \left(\frac{a^4 H^4}{3p_{\max}^3} - \frac{a^4 H^4}{3p_{\min}^3} \right) \right] . \tag{4.72}
$$

This result for the trace depends on the minimal and maximal values for the dimensionless wave number. For the super-Hubble modes, we take for the minimal wavelength the Hubble scale, so $p_{\max} = 2\pi aH$. For the maximal wavelength, a reasonable value is given by the scale factor itself, so $p_{\min} = 2\pi$. Evaluating the trace using these numbers and inserting the result into (4.63), we find for the absolute value of the non-diagonal element of the density matrix,

$$|\rho_{+-}(t)| = |\rho_{+-}(0)| \exp\left(-\frac{g_S^2 a^2 V(\phi_+ - \phi_-)^2}{72\pi^2 H^2}\left[\frac{(aH)^4}{24\pi^3} + \mathcal{O}(aH)^2\right]\right). \quad (4.73)$$

We recognize explicitly that this non-diagonal element becomes smaller for increasing aH, that is, decoherence becomes efficient and the field is localized in one of the wells.

Evaluating the density matrix (4.67) for the sub-Hubble modes, we obtain with $k_{\min} = 2\pi Ha$,

$$|\rho_{+-}(t)| = |\rho_{+-}(0)| \exp\left(-\frac{g_S^2 a^3 VC(\phi_+ - \phi_-)^2}{64\pi^2 H}\right), \quad (4.74)$$

where $C \approx 0.3296$. Taking the ratio of the widths of the two Gaussians (4.73) and (4.74), we obtain

$$\frac{(\Delta\phi)^2_{\text{super}}}{(\Delta\phi)^2_{\text{sub}}} \approx \frac{8.9\pi^3}{(aH)^3}, \quad (4.75)$$

which goes to zero for $aH \to \infty$, that is, the super-Hubble modes are much more efficient in the localization of ϕ than the sub-Hubble modes.

4.5 Modification of the Tunneling Rate

In this section we investigate the influence of the system–environment interaction on the tunneling rate. Before we discuss this in detail, we shall recall some basic facts on tunneling in quantum mechanical settings under the influence of environmental degrees of freedom. An important generic model is the Caldeira–Leggett model that has been considered in [73]. The authors consider the tunneling of a macroscopic variable out of a metastable state. The bilinear interaction with an environment, modeled by a set of harmonic oscillators, changes the decay rate. Since the environmental degrees of freedom appear only linearly and quadratically in the action, they can be integrated out. The authors derive an effective euclidean action for the

macroscopic variable,

$$S_{\text{eff}}[q] \;=\; \int_0^T dt_E \left(\frac{1}{2} M \dot{q}^2 + V(q) \right) \tag{4.76}$$

$$+ \frac{\eta}{4\pi} \int_{-\infty}^{\infty} dt_E \int_0^T dt'_E \frac{(q(t_E) - q(t'_E))^2}{(t_E - t'_E)^2} \;, \tag{4.77}$$

where M is the mass of the macroscopic variable, q denotes the position variable and η is a friction coefficient greater than zero. Due to the interaction with environmental degrees of freedom, the effective action (4.76) is *nonlocal* in time, resulting in an equation of motion with a nonlocal friction term,

$$M\ddot{q} = \frac{\partial V}{\partial \bar{q}} + \frac{\eta}{\pi} \int_{-\infty}^{\infty} dt'_E \frac{\bar{q}(t_E) - \bar{q}(t'_E)}{(t_E - t'_E)^2} \;. \tag{4.78}$$

Since the modified decay rate is given at lowest order by $\exp(-S_{\text{eff}}[\bar{q}])$, the system–bath interaction *reduces* the tunneling probability because the nonlocal correction term in (4.76) is always positive.

4.5.1 Minkowski Background

In contrast to [73] we investigate tunneling in a potential which is bounded from below. Therefore the field may tunnel between both localized vacua, whereas a decaying particle as in [73] will not tunnel to the metastable state from outside. Before we discuss this in detail, we want to recall some basic facts about tunneling in field theory. We shall first address the case of a Minkowski background and then turn to the exanding Universe.

According to [74], the transition probabililty of a system given by a scalar field Lagrangian is of the form

$$\langle \phi_- | e^{-HT} | \phi_+ \rangle = N \int D\phi\, e^{-S_{E,\phi}} \tag{4.79}$$

which can be approximated to first order in $\hbar$ according to

$$\Gamma_0 = A \exp(-S_{E,\phi}) \;, \tag{4.80}$$

where $S_{E,\phi}$ is the classical Euclidean action of the scalar field evaluated along the tunneling trajectory of ϕ; the prefactor A can be determined by the second variation of the action.

According to the classical equations of motion, the field ϕ adopts for most of the time the value ϕ_+ of the false vacuum and approaches the value ϕ_- of the true

vacuum after a short transition time. The terms "false vacuum" and "true vacuum" may be misleading, since they denote the classical minima of the potential (with ϕ_+ representing here the higher minimum), in contrast to the true quantum mechanical vacuum which is a superposition of ϕ_+ and ϕ_-.

The tunneling time T between the two vacuum states is assumed to be large compared to the characteristic instanton transition time $1/\omega$. We thus consider situations in which the various tunneling processes from one minimum to the other can be considered separately. This classical picture of separated transitions can only by justified by decoherence since the superposition principle is universally valid and thus holds also for widely separated jumps.

Assuming spherical symmetry, the transition between the localized vacuum states can be described by the growth of a bubble that is nucleating spontaneously at a radius R_0. For a more extensive discussion of nucleating vacuum bubbles, see section 5.

Starting from (4.40) and switching to euclidean time $t \to -it_E$ we find the euclidean action

$$S_E = S_{E,\phi} + \int dx^3 dt_E \sigma(\mathbf{x}, t) \left(-\frac{1}{2} \left(\frac{d^2}{dt_E^2} + \nabla^2 \right) + g_S \phi(t_E) \right) \sigma(\mathbf{x}, t) . \quad (4.81)$$

Integrating out the environmental field σ leads to the formal expression

$$\Gamma = \Gamma_0 N \int D\sigma(\mathbf{x}, t) \exp(-S_E) = \sqrt{\frac{\text{Det}(-d^2/dt_E^2 - \nabla^2)}{\text{Det}(-d^2/dt_E^2 - \nabla^2 + 2g_S \phi(t_E))}} \Gamma_0 . \quad (4.82)$$

The normalization N was chosen such that the expression simplifies to the bare tunneling amplitude for $g_S = 0$, i.e. $\Gamma|_{g_S=0} = \Gamma_0$. Solving the nonlocal equations of motion given by the variation of

$$S_{E,\text{eff}} = S_{E,\phi} - \frac{1}{2} \text{Tr} \ln(-d^2/dt_E^2 - \nabla^2 + 2g_S \phi) \quad (4.83)$$

and evaluating the effective action along the tunneling trajectory of ϕ would give the exact modification of the tunneling amplitude. In order to simplify the calculations, we will neglect the backreactions of the environment on the trajectory of $\phi(t_E)$. Thus, we assume that $\phi(t_E)$ can be obtained roughly by solving the unperturbed equations of motion, and we are left with a computation of a functional determinant.

In order to compute the functional determinant we have to solve the eigenvalue equation

$$\left(-\frac{d^2}{dt_E^2} - \triangle + 2g_s \phi(t_E) \right) \psi = \lambda \psi . \quad (4.84)$$

4 Cosmological Constant from Decoherence?

Since the nucleation of the bubble is spherical symmetric, it is appropriate to use the Laplacian in spherical coordinates. Making the ansatz $\psi = \phi_{ln}(r)Y_{lm}(\theta,\phi)u(t_E)$, we find for the eigenvalue equation of the radial component

$$\left(-\frac{1}{r^2}\frac{\partial}{\partial r}r^2\frac{\partial}{\partial r} + \frac{l(l+1)}{r^2}\right)\phi_{ln}(r) = \kappa_{nm}\phi_{ln}(r)\,. \quad (4.85)$$

A natural boundary condition would be $\phi_{ln}(R_0) = 0$, i.e. the eigenfunctions are vanishing at the boundary of the bubble. Equation (4.85) is solved by the spherical Bessel functions, i.e. $\phi_{ln}(r) \propto j_l(\kappa_{ln}r)$. The eigenvalues κ_{ln} are the n-th root of j_l divided by R_0. We thus have

$$\text{Det}(-\Box_E + 2g_s\phi(t_E)) = \prod_{n,l=0}^{\infty} (2l+1)\text{Det}_{nl}\left(-\frac{d^2}{dt_E^2} + \kappa_{ln}^2 + 2g_s\phi(t_E)\right)\,, \quad (4.86)$$

Where the degeneracy of the eigenvalues was taken into account with a factor $2l+1$.

Since the eigenvalues of the spherical Bessel functions are not explicitely known, we simplify the problem by assuming periodic boundary conditions in a volume L^3 with $L = \mathcal{O}(R_0)$. For the spatial part of the euclidean D'Alembert operator we choose periodic boundary conditions with a length L. The functional determinant involved in (4.82) separates into a product of functional determinants labeled with the mode number n:

$$\text{Det}\left(-\frac{d^2}{dt_E^2} - \nabla^2 + 2g_S\phi(t_E)\right) = \prod_{n=0}^{\infty} d_n\text{Det}_n\left(-\frac{d^2}{dt_E^2} + \frac{4\pi^2 n^2}{L^2} + 2g_S\phi(t_E)\right)\,, \quad (4.87)$$

where d_n is the degeneracy of the mode number n which is in three dimensions roughly equal to $4\pi n^2$ for large n. This expression is divergent for two reasons. Firstly, for each fixed mode number n the determinant is an infinite product of eigenvalues, which is in general infinite. Secondly, due to the infinite number of modes the situation becomes even worse.

In order to regularize the expression (4.87) we choose the ζ-function regularization method presented in [81]. A short summary of this method is given in the appendix. For any second-order differential operator $\mathcal{D}$ we can write

$$(\text{Det}\mathcal{D})^{1/2} = \exp\left(-\frac{1}{2}\zeta'(0) - \frac{1}{2}\zeta(0)\ln\mu^2\right)\,, \quad (4.88)$$

where $\zeta(s)$ is a generalized zeta function,

$$\zeta(s) = \sum_{\lambda}\frac{1}{\lambda^s}\,, \quad (4.89)$$

involving all eigenvalues λ of the differential operator. The parameter μ appearing in (4.88) is a renormalization parameter with dimension of a mass. According to [81], the ζ-function reads

$$\zeta(s) = \frac{\sin(\pi s)}{\pi} \int_0^\infty \frac{dM^2}{M^{2s}} \frac{d^2}{dM^2} I(M^2, s) \tag{4.90}$$

with

$$I(M^2, s) = \sum_{n=1}^\infty \frac{1}{n^{2s}} \ln u(M^2 n^2, t_E). \tag{4.91}$$

The integral (4.90) converges for some $s > 0$, since $I(M^2, s)$ increases with finite polynomial order $\propto M^k$, and can be analytically continued to $s = 0$ [81]. The functions $u(-\lambda, t_E)$ are the eigenfunctions of the differential operator under consideration. The eigenvalue equation corresponding to (4.87) reads for fixed n

$$\left(-\frac{d^2}{dt_E^2} + \frac{4\pi^2 n^2}{L^2} + 2g_S\phi(t_E) \right) u(-\lambda, t_E) = \lambda\, u(-\lambda, t_E). \tag{4.92}$$

Note that the differential operator is always positive definite since $g_S\phi(t_E) > 0$.

In general two independent boundary conditions are needed in order to determine the eigenvalues of (4.92) uniquely. We assume that the mode functions have a root at nucleation time T_0, i.e. $u(-\lambda, T_0) = 0$ [81]. This time is usually in the order of or equal to the nucleation radius R_0 [6]. The second boundary condition is given by the normalization, see below. Since the employed regularization method discards one of the two independent solutions of equation (4.92) (see appendix for a detailed discussion), the eigenfunctions are uniquely determined by a normalization condition.

The leading term of the uniform WKB-solution of (4.92) reads

$$
\begin{aligned}
u(-\lambda, t_E) &= \left(\frac{4\pi^2 n^2}{L^2} + 2g_S\phi(t_E) - \lambda \right)^{-1/4} \\
&\quad \times \exp\left[\int_{t_{E,0}}^{t_E} dt'_E \left(\frac{4\pi^2 n^2}{L^2} + 2g_S\phi(t'_E) - \lambda \right)^{1/2} \right],
\end{aligned} \tag{4.93}
$$

where the choice of $t_{E,0}$ determines the normalization of $u(-\lambda, t_E)$. We assume that the scalar field ϕ is in the true vacuum at some large positive time t_E, i.e. $\phi(t_E) = \phi_-$ and fix the normalization such that

$$
\begin{aligned}
u(-\lambda, t_E) &= \left(\frac{4\pi^2 n^2}{L^2} + 2g_S\phi_- - \lambda \right)^{-1/4} \\
&\quad \times \exp\left[-\left(\frac{4\pi^2 n^2}{L^2} + 2g_S\phi_- - \lambda \right)^{1/2} t_E \right].
\end{aligned} \tag{4.94}
$$

4 Cosmological Constant from Decoherence?

Since the normalization of $u(-\lambda, t_E)$ enters the function $I(M^2, s)$ only logarithmically, a different normalization will not alter the results significantly.

Including the approximate degeneracy of $4\pi n^2$ we find for large t_E

$$I(M^2, s) \;=\; \sum_{n=1}^{\infty} \frac{4\pi n^2}{n^{2s}} \left[-\frac{1}{4} \ln \left(\frac{4\pi^2 n^2}{L^2} + 2g_S\phi(t_E) + M^2 n^2 \right) \right.$$
$$\left. + \left(\frac{4\pi^2 n^2}{L^2} + 2g_S\phi(t_E) + M^2 n^2 \right)^{1/2} t_E \right], \qquad (4.95)$$

where we assumed that $\phi(t_E)$ is approximately constant for large t_E. For $M^2 \to 0$ we define

$$I(0, s) \equiv \sum_{n=1}^{\infty} \frac{f(n)}{n^{2s}} \qquad (4.96)$$

with

$$f(n) = -2\pi n^2 \ln n + g(n) \qquad (4.97)$$

and

$$g(n) \;=\; -\pi n^2 \ln \left(\frac{4\pi^2}{L^2} + \frac{2g_S\phi(t_E)}{n^2} \right)$$
$$+ 4\pi n^2 \left(\frac{4\pi^2 n^2}{L^2} + 2g_S\phi(t_E) \right)^{1/2} t_E. \qquad (4.98)$$

The function $I(0, s)$ can be evaluated using the Abel-Plana-formula [81, 82]

$$I(0, s) \;=\; -\sum_{n=1}^{\infty} \frac{2\pi n^2 \ln n}{n^{2s}} + \int_0^1 dn\, g(n) + \int_1^{\infty} dn\, \frac{g(n)}{n^{2s}}$$
$$+ i \int_0^{\infty} dy\, \frac{g(iy) - g(-iy)}{e^{2\pi y} - 1} - \frac{1}{2} g(0) + \mathcal{O}(s). \qquad (4.99)$$

The sum on the right hand side of (4.99) will not affect the ζ-function since it gives an M-independent term of $I(M^2, s)$. We retained in (4.99) the regularizing factor $1/n^{2s}$ only in the sum and the second integral since the remaining terms are finite for $s \to 0$. The splitting of the integral at $x = 1$ is made for convenience and does not affect the end result. In order to regularize the remaining integral we have to integrate by parts several times. For this purpose we change the integration variable to $x = 1/n$ and define the function

$$\phi(x) = x^3 g(1/x), \qquad (4.100)$$

which is analytic at $x = 0$. Integrating by parts, the divergent integral in (4.99) leads to

$$\int_1^\infty dn \frac{g(n)}{n^{2s}} = \sum_{k=0}^4 \frac{(-1)^k}{(2s-4)\cdot ... \cdot (2s-4+k)} x^{2s-4+k} \phi^{(k)}(x) \Big|_0^1$$
$$- \frac{1}{(2s-4)\cdot ... \cdot 2s} \int_0^1 dx x^{2s} \phi^{(5)}(x). \qquad (4.101)$$

We keep only the boundary terms at $x = 0$ which are finite for the subsequent application of the limits $s \to 0$ and $x \to 0$. The divergent boundary terms are regularized with the parameter s. In other words, one keeps the parameter s sufficiently large and takes the limit $x \to 0$ such that the divergences are vanishing.

The function $I(0, s)$ can be expanded around $s = 0$ according to

$$I(0, s) = \frac{I^{\text{pole}}(0)}{s} + I^{\text{R}}(0) + \mathcal{O}(s). \qquad (4.102)$$

The term of the regularized quantity (4.101) which is proportional to $1/s$ in the limit $s \to 0$ reads

$$I^{\text{pole}}(0) = \frac{1}{48} \frac{d^4 \phi(x)}{dx^4} \Big|_{x=0}. \qquad (4.103)$$

The part of (4.99) which is regular in the limit $s \to 0$ is given by

$$I^{\text{R}}(0) = \frac{25}{288} \frac{d^4 \phi(x)}{dx^4} \Big|_{x=0} - \frac{1}{24} \int_0^\infty dx \ln x \frac{d^5 \phi(x)}{dx^5}$$
$$+ i \int_0^\infty dy \frac{g(iy) - g(-iy)}{e^{2\pi y} - 1} - \frac{1}{2} g(0) - \sum_{n=1}^\infty \frac{2\pi n^2 \ln n}{n^{2s}}. \qquad (4.104)$$

The expression (4.103) and the second integral in (4.104) result from the convergent integral remaining after the repeated integration by parts. A factor x^{2s}/s in this integral can be expanded according to $x^{2s}/s = 1/s + 2 \ln x + \mathcal{O}(s)$ which leads to the aforementioned terms.

The first term in (4.104) results from the finite contributions of the boundary terms where the limit $x \to 0$ and $s \to 0$ can be interchanged. We find the explicit expressions

$$I^{\text{pole}}(0) = -\frac{g_S^2 L^3 t_E \phi^2(t_E)}{8\pi^2}, \qquad (4.105)$$

and

$$
\begin{aligned}
I^R(0) &= \frac{g_S L^3 \phi(t_E)}{24\pi^2}\left[2\sqrt{2\pi g_S \phi(t_E)} + g_S \phi(t_E) t_E\left(14 + 3\ln\left(\frac{L^2 g_S \phi(t_E)}{2^3 \pi^2}\right)\right)\right] \\
&\quad -\frac{25}{48}\frac{g_S^2 L^3 \phi^2(t_E) t_E}{\pi^2} - 2\Re\left\{i\pi \int_0^{\frac{L}{\pi}\sqrt{\frac{g_S\phi(t_E)}{2}}} \frac{y^2}{e^{2\pi y}-1}\ln\left(1 - \frac{L^2 g_S \phi(t_E)}{2\pi^2 y^2}\right)\right\} \\
&\quad +8\pi \int_{\frac{L}{\pi}\sqrt{\frac{g_S\phi(t_E)}{2}}}^{\infty} dy\, \frac{y^2\left(\frac{4\pi^2 y^2}{L^2} - 2g_S\phi(t_E)\right)^{1/2} t_E}{e^{2\pi y}-1} - \sum_{n=1}^{\infty}\frac{2\pi n^2 \ln n}{n^{2s}}\,.
\end{aligned}
\tag{4.106}
$$

Furthermore we need the pole part of $I(M^2, 0)$ for $M \neq 0$. Equation (4.103) holds also for arbitrary M if we replace $4\pi^2/L^2 \to 4\pi^2/L^2 + M^2$ in the definition of $g(n)$. More directly we may expand $I(M^2, s)$ for large n and use the fact that the Riemannian ζ_R-function has a pole at $s = 1$, i.e.

$$
\zeta_R(2s + 1) = \frac{1}{2s} + \mathcal{O}(s^0)\,.
\tag{4.107}
$$

We find

$$
I^{\text{pole}}(M^2) = -\frac{g_S^2 \pi t_E \phi^2(t_E)}{\left(\frac{4\pi^2}{L^2} + M^2\right)^{3/2}}\,.
\tag{4.108}
$$

In the limit $M \to \infty$ we find the regular part of $I_R(M^2, 0)$ to be

$$
I^R(M^2 \to \infty) = -\sum_{n=1}^{\infty}\frac{2\pi n^2 \ln n}{n^{2s}}\,.
\tag{4.109}
$$

This sum appears also in $I(0, s)$ and will therefore not affect $\zeta(0)$ and $\zeta'(0)$. The logarithmic contribution of $I(M^2, 0)$ vanishes since $\zeta_R(-2) = 0$.

Using (4.88) and equation (9.21) from the Appendix, we can compute the modified tunneling amplitude from $I(M^2, s)$. Expanding (4.106) up to the first order in g_S and using the normalization defined through (4.94), we find the modified tunneling amplitude to read

$$
\Gamma = \Gamma_0 \exp\left(-\frac{g_S \phi(t_E) L^2}{8\pi} + \frac{g_S L t_E \phi(t_E)}{12}\right)\,.
\tag{4.110}
$$

This result can be stated more explicitly with a given shape of the function $\phi(t_E)$, i.e.

$$
\phi(t_E) = \frac{\phi_- - \phi_+}{2}\tanh(\omega t_E) + \frac{\phi_- + \phi_+}{2}
\tag{4.111}
$$

with the characteristic time scale of the instanton, $1/\omega$. Considering the limit of large Euclidean nucleation time T_0, i.e. $T_0 \gg 1/\omega$, we find

$$\Gamma \approx \Gamma_0 \exp\left(-\frac{g_S \phi_- L^2}{8\pi} + \frac{g_S \phi_- L T_0}{12}\right). \tag{4.112}$$

Note that the exponent in (4.112) is positive if $L \approx T_0 \approx R_0$. In the case that $T_0 \gg L$, the contribution resulting from sub-exponential terms of the WKB-expansion can be neglected, i.e.

$$\Gamma(T_0 \gg L) \approx \Gamma_0 \exp\left(\frac{g_S \phi_- L T_0}{12}\right). \tag{4.113}$$

This result deserves some explanation. Since the interaction term (4.43) is quadratic in the environmental field, it has a positive mean, i.e. $\langle \sigma^2 \rangle > 0$. Thus, the effect introduced by the interaction increases with the quantization length L. Because the product $g_S \phi$ is demanded to be positive in order to render the theory stable, the interaction *enhances* the tunneling amplitude.

At the beginning of this section we stated, that Caldeira and Leggett found a suppression of the tunneling amplitude due to dissipative effects of the environment [73]. Their model involves a spectral density with a cutoff frequency Ω_c. This would correspond to a *finite* number of environmental degrees of freedom. How would our results be changed if we had considered an environment out of N harmonic oscillators instead a field with infinitely many degrees of freedom? Expanding the expression (4.95) to lowest nonvanishing order in g_S leads to a g_S-independent sum, which is canceled by the normalization in (4.82), and a term linear in g_S, involving the sum

$$\sum_{n=1}^{N} n = \frac{N}{2}(N+1). \tag{4.114}$$

Obviously the expression (4.114) is always greater than zero, which finally would lead to a *suppression* of the tunneling amplitude.

In contrast, an infinite number of environmental degrees of freedom has to be regularized. We chose a regularization method which is based on the analytically continuation of a generalized ζ_R-function. These regularization method flips the sign,

$$\sum_{n=1}^{\infty} \frac{n}{n^{2s}} = -\frac{1}{12} + \mathcal{O}(s), \tag{4.115}$$

which leads to the positive sign in (4.112) and therefore to an *enhancing* of the tunneling amplitude.

Regularization methods involving generalized ζ-functions have been applied in various branches of quantum field theory. One of the most famous result where the regularization method has predictive power is the Casimir effect [83]. It was shown by Casimir [84] that two uncharged perfectly conducting plates attract each other. The corresponding force per unit area reads (with factors of $\hbar$ and c restored)

$$F = -\frac{\hbar c \pi^2}{240 a^4} \,, \tag{4.116}$$

where a denotes the distance between the plates. The force depends in general crucially on the geometry determining the boundary conditions of the field and can both be repulsive and attractive. In order to regularize the infinite mode sums appearing in the expressions determining the Casimir force, one usually uses a regularization based on the Riemannian ζ-function [83].

The boundary conditions defining the eigenvalues of the determinant (4.82) lead to an enhancing of the tunneling amplitude. Modifications of the boundary conditions could alter the results significantly.

Physically we interpret the enhancing of the tunneling amplitude in the following way. Due to boundary conditions defining the functional determinant, there are *fewer* environmental modes than there would be without the boundary conditions and thus *less* decoherence.

4.5.2 FRW Universe

In a Friedmann universe with scale factor a, the eigenvalue equation (4.92) changes to

$$\left(-\frac{d^2}{dt_E^2} - \frac{3\dot{a}}{a}\frac{d}{dt_E} + \frac{4\pi^2 n^2}{L^2 a^2} + 2g_S\phi(t_E) \right) u(-\lambda, t_E) = \lambda\, u(-\lambda, t_E)\,. \tag{4.117}$$

With the ansatz $u(-\lambda, t_E) = \varphi_1(-\lambda, t_E)\varphi_2(t_E)$ and an appropriate choice for $\varphi_2(t_E)$, we eliminate the first derivative in (4.117),

$$\left(-\frac{d^2}{dt_E^2} + \frac{4\pi^2 n^2}{L^2 a^2} + \frac{9\dot{a}^2}{4a^2} + 2g_S\varphi(t_E) + \frac{3}{2}\frac{d}{dt_E}\left(\frac{\dot{a}}{a}\right) \right) \varphi_1(-\lambda, t_E) =$$
$$= \lambda\, \varphi_1(-\lambda, t_E)\,. \tag{4.118}$$

The scale factor is in general a complex function of the euclidean time t_E leading to complex eigenvalues of the differential operator. Assuming that no eigenvalues lie on the negative real axis, we can still apply the regularization method. The functional determinant related to (4.118) is obtained by substituting

$$L^2 \rightarrow L^2 a^2 \tag{4.119}$$

and

$$2g_S\phi(t_E) \rightarrow 2g_S\phi(t_E) + \frac{9\dot{a}^2}{4a^2} + \frac{3}{2}\frac{d}{dt_E}\left(\frac{\dot{a}}{a}\right) . \tag{4.120}$$

We restrict ourselves to the flat de Sitter space with $\dot{a}/a = -iH = const.$ with a small Hubble parameter, i.e. $T_0, L \ll 1/H$ and $H \ll \omega$. Using equation (4.95), we find a correction term of order $g_S H^2$,

$$\begin{aligned}
\Gamma &= \Gamma_0 \exp\left[\frac{g_S L\phi_- T_0}{12} - \frac{g_S L^2\phi_-}{8\pi} \right.\\
&\left. -g_S H^2\phi_-\left(\frac{LT_0^3}{72} - \frac{3L^4}{128\pi} - \frac{9L^3 T_0}{32\pi^2}\left(1 - \ln\left(\frac{4\pi}{L}\right)\right)\right)\right], \quad (4.121)
\end{aligned}$$

where we omitted terms that can be neglected for large T_0. In order to discuss the
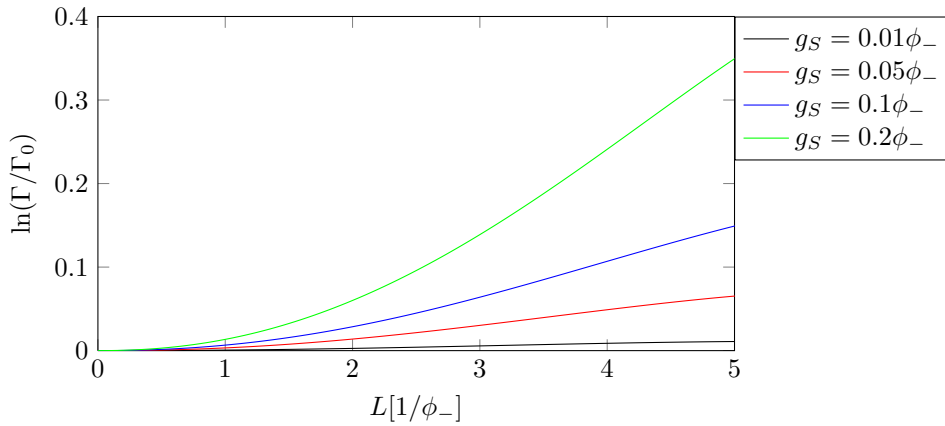
Figure 4.1: We set $L = T_0$ and show the change of modified tunneling rate with increasing L for different couplings g_s.

result quantitatively we depict in fig. 4.1 the dependence of $\ln(\Gamma/\Gamma_0)$ on the length L which is roughly the size of the nucleating vacuum bubble. The Hubble parameter has been set to zero and we evaluated $\ln(\Gamma/\Gamma_0)$, using the expressions (4.106) and (4.108). Obviously, the correction term of the nucleation rate increases with L and the coupling g_S. In fig. 4.2 we depict the correction term of the exponent in (4.121) for small values of the Hubble parameter, i.e. $L, T_0 \ll 1/H$. The finite Hubble horizon diminishes the exponent for small L and T_0.
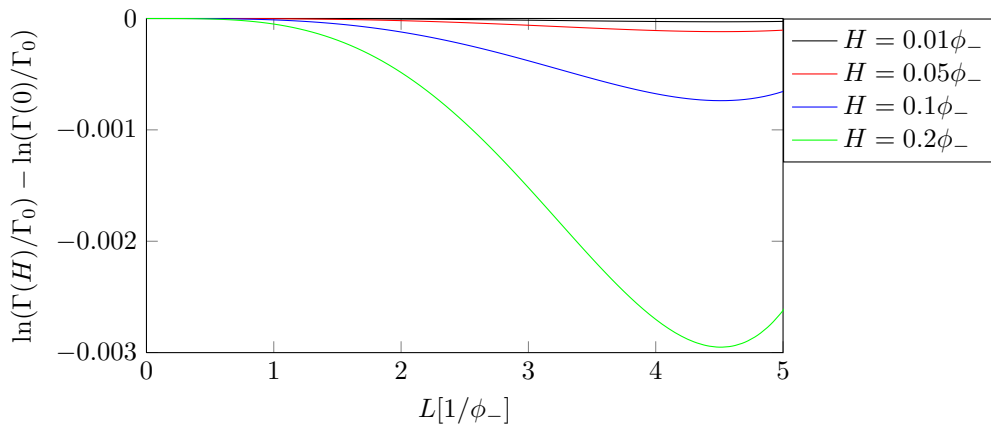
Figure 4.2: We set $L = T_0$ and show the change of modified tunneling rate with increasing L for different Hubble parameters H. The coupling was chosen to be $g_S = 0.1\,\Phi_-$.

4.6 Cosmic Landscape

The cosmic landscape motivated by string theory [60, 85] has been discussed in various publications. Usually one considers Coleman–de Luccia tunneling [6, 7, 86–88] between a huge amount of vacua and discusses various solutions of ad hoc rate equations. Under certain circumstances, a continuum limit of the rate equations can be derived [89].

According to Coleman and de Luccia [7], the probability for a field to tunnel from a local minima i to a local minima j is given by

$$\Gamma_{i \to j} = e^{-S(\phi) + S(\phi_i)}, \tag{4.122}$$

where $S(\phi)$ is the Euclidean action for the tunneling trajectory, and $S(\phi_i)$ is the euclidean action for the initial configuration $\phi = \phi_i$. Coleman and de Luccia incorporated gravitational effects by including the Ricci scalar into the action.

Furthermore, finite temperature effects have been considered in [90] based on Hawking–Moss tunneling [91, 92], i.e. a homogeneous tunneling of the universe occuring everywhere at the same time. The solution of Hawking and Moss does not interpolate between the field configurations; the tunneling rate reads

$$\Gamma_{i \to j} = e^{-S(\phi_{\text{top}}) + S(\phi_i)}, \tag{4.123}$$

where ϕ_{top} denotes the field value corresponding to the top of the potential barrier between the local minima, ϕ_i and ϕ_j.

Tye proposed rapid tunneling assuming that resonance tunneling is dominant in the landscape [93, 94] (see also [95] for a critic based on standard QFT). In

the following we want to extend our model discussed in the preceding sections to multilevel systems in order to see under what circumstances an ad hoc rate equation can be formulated.

One can, for example, generalize the Hamiltonian (4.49) and the interaction (4.50) in the following way:

$$H_\phi \;=\; H_{\text{diag}} + H_\Delta = \text{diag}(\omega_1, ..., \omega_n) + \sum_{i \neq j} \Delta_{ij} |i\rangle \langle j| \,, \qquad (4.124)$$

$$H_{\text{int}} \;=\; g_S a^3(t) \text{diag}(S_{11}, ..., S_{nn}) \int d^3p \, \sigma(p)\sigma(-p) \,. \qquad (4.125)$$

The interpretation is as follows: The numbers ω_i denote the different local vacua of a cosmic landscape and the Δ_{ij} are tunneling matrix elements which can be computed in WKB-approximation. The pointer states S_{ii} distinguish the different vacua, which is an obvious generalization of measuring the left and the right well in the double-well systems discussed above.

Since the tunneling matrix elements are usually exponentially small, the short time dynamics (short with respect to the tunneling times Δ_{ij}^{-1}) is determined by the decoherence rates. The off-diagonal elements of the density matrix read

$$\rho_{ij}(t) = \rho_{ij}(0) \exp\left(-\frac{g_S^2 (S_{ii} - S_{jj})^2}{4} \text{Tr}\left(\frac{(\Re \Omega'^S)^2 + (\Im \Omega'^S)^2}{(\Re \Omega^S)^2} \right) - i\varphi_{ij} \right) \,. \quad (4.126)$$

One can conclude from this expression that the suppression of interference terms depends crucially on the distance between different minima in the landscape.

Neglecting possible degeneracies and assuming that the typical decoherence rate is much larger than the tunneling rate, the system dynamics is determined by the equations [21]

$$\dot{\rho}_{ii}(t) = - \int_0^t ds [H_\Delta(t), [H_\Delta(s), \rho(s)]]_{ii} \,. \qquad (4.127)$$

Applying a Markov approximation one obtains

$$\dot{\rho}_{ii}(t) = \lambda \sum_{k \neq i} |\Delta_{ik}|^2 (\rho_{kk} - \rho_{ii}) \,, \qquad (4.128)$$

where λ is chosen such that the coarse graining in time is not too small and the approximation is valid.

There exists another generalization of the model where the tunneling between different vacua may, in fact, be *mediated* by the environment. This is described by setting $\Delta_{ij} = 0$ and $S_{ij} \neq 0, i \neq j$ in the above Hamiltonian. Indirect coupling between metastable states is a well-known phenomena in glasses, see, for example, [96].

4 Cosmological Constant from Decoherence?

In the following we will derive the master equations for the environment-mediated tunneling. The interaction Hamiltonian in the interaction picture has the form

$$H_{\text{int}}^I(t) = g_S a^3(t) \sum_{ij} e^{i(\omega_i - \omega_j)} S_{ij} |i\rangle\langle j| \int d^3p \, \sigma(\mathbf{p}, t)\sigma(-\mathbf{p}, t). \tag{4.129}$$

Restricting ourselves to flat de Sitter space, the operators $\sigma(\mathbf{p}, t)$ are given by

$$\sigma(\mathbf{p}, t) = f_p(t) a_{\mathbf{p}} e^{i\mathbf{px}} + h.c. \tag{4.130}$$

with [80]

$$f_p(t) = \sqrt{\frac{V}{(2\pi)^3}} \frac{1}{\sqrt{2p^3}} \left(\frac{p}{a(t)} + iH\right) e^{i\frac{p}{a(t)H}}. \tag{4.131}$$

Applying the Redfield approximation [21], we find for the system density matrix

$$\dot{\rho}_S^I(t) = -\text{Tr}_B \int_0^t ds [H_{\text{int}}^I(t), [H_{\text{int}}^I(s), \rho_S^I(t)\rho_B]]. \tag{4.132}$$

In the limit of vanishing temperature, the bath density matrix is just $\rho_B = |0\rangle\langle 0|$. The coefficients of the density matrix satisfy the system of differential equations [97],

$$\dot{\rho}_{ji}^I = \delta_{ji} \sum_{k \neq i} \rho_{kk}^I (w_{kiik}^+ + w_{kiik}^-) - \rho_{ji}^I \left[\sum_l (w_{jllj}^+ + w_{illi}^-) - w_{iijj}^+ - w_{iijj}^- \right] \tag{4.133}$$

with the correlation functions

$$\begin{aligned} w_{klmn}^+(t) &= g_S^2 \int_0^t ds \, e^{i(\omega_k - \omega_l)(s-t)} S_{kl} S_{mn} a^3(t) a^3(s) \\ &\times \int d^3p \int d^3q \langle \sigma(\mathbf{p}, s)\sigma(-\mathbf{p}, s)\sigma(\mathbf{q}, t)\sigma(-\mathbf{q}, t)\rangle \end{aligned} \tag{4.134}$$

and

$$\begin{aligned} w_{mnkl}^-(t) &= g_S^2 \int_0^t ds \, e^{i(\omega_k - \omega_l)(s-t)} S_{kl} S_{mn} a^3(t) a^3(s) \\ &\times \int d^3p \int d^3q \langle \sigma(\mathbf{p}, t)\sigma(-\mathbf{p}, t)\sigma(\mathbf{q}, s)\sigma(-\mathbf{q}, s)\rangle. \end{aligned} \tag{4.135}$$

In deriving equation (4.133), several approximations have been performed: the Born approximation, which states that the total density matrix can be written approximately as a tensor product of the bath density matrix and the system density

matrix, and the rotating wave approximation which is valid when the intrinsic time scale of the system is much larger than the relaxation time of the open system. Since the correlation functions are not homogeneous in time due to the scale factor, the master equation is not Markovian.

The rates in (4.133) are not necessarily exponentially small and may therefore dominate the dynamics of the string landscape. The transition probabilities between the vacua are symmetric, since we assume that the environment is described by a Gaussian wave function rather than an ensemble of states. On the other hand, the tunneling rates in the Pauli equations (4.133) are not symmetric and jumping to lower energy levels is more probable than jumping to higher energy levels depending on the bath temperature. It would be interesting how the situation changes if the Gaussian is replaced by a (micro)canonical ensemble.

Evaluating the correlation functions we find

$$
\begin{aligned}
w^+_{klmn}(t) &= g_S^2 \int_0^t ds\, e^{i(\omega_k - \omega_l)(s-t)} S_{kl} S_{mn} a^3(t) a^3(s) \\
&\times \frac{(2\pi)^3}{V} \int d^3k \left(2(f_k(t) f_k^*(s))^2 + \frac{V}{(2\pi)^3} \int d^3p |f_k(t)|^2 |f_p(s)|^2 \right)
\end{aligned}
\tag{4.136}
$$

and

$$
\begin{aligned}
w^-_{mnkl}(t) &= g_S^2 \int_0^t ds\, e^{i(\omega_k - \omega_l)(s-t)} S_{kl} S_{mn} a^3(t) a^3(s) \\
&\times \frac{(2\pi)^3}{V} \int d^3k \left(2(f_k(s) f_k^*(t))^2 + \frac{V}{(2\pi)^3} \int d^3p |f_k(s)|^2 |f_p(t)|^2 \right) .
\end{aligned}
\tag{4.137}
$$

The dominating contributions in the correlators (4.136) and (4.137) are given by infrared contributions $k < Ha$, since the phases in the integrands are oscillating rapidly if $k > Ha$. Neglecting the second term in the bracket of (4.136) respectively (4.137) and applying the approximation $e^{ik/Ha} \approx 1$ leads to

$$
\begin{aligned}
w^+_{klmn}(t) &= g_S^2 \int_0^t ds\, e^{i(\omega_k - \omega_l)(s-t)} S_{kl} S_{mn} a^3(t) a^3(s) \\
&\times \frac{2V}{(2\pi)^3} \int d^3k \frac{1}{(2k^3)^2} \left(\frac{k}{a(t)} + iH \right)^2 \left(\frac{k}{a(s)} - iH \right)^2
\end{aligned}
\tag{4.138}
$$

and an analogous expression for $w^-_{mnkl}(t)$. The evolution equation for the off-diagonal elements reads in the Schrödinger picture

$$
\dot{\rho}^{\mathrm{Sch}}_{ij} = -(\Gamma_{ij} - i(\omega_i - \omega_j)) \rho^{\mathrm{Sch}}_{ij}
\tag{4.139}
$$

with

$$
\Gamma_{ij} = \Re \left(\sum_l (w^+_{jllj} + w^-_{illi}) - w^+_{iijj} - w^-_{iijj} \right) .
\tag{4.140}
$$

4 Cosmological Constant from Decoherence?

The imaginary part of the correlation function has been absorbed in the frequencies ω_i. For $S_{ij} = S_{ii}\delta_{ij}$ we obtain for $a(t) \gg a(0)$

$$\Gamma_{ij} \approx g_S^2 (S_{ii} - S_{jj})^2 \frac{VH^3 a^6(t)}{9(2\pi)^2} \left(\frac{1}{k_{\min}^3} - \frac{1}{k_{\max}^3} \right) \tag{4.141}$$

where $k_{\min}$ is an infrared cutoff and $k_{\max} \sim Ha$. Solving equation (4.126) using the rates (4.141) gives for large times

$$
\begin{aligned}
|\rho_{ij}(t)| &= \rho_{ij}(0) \exp\left(-g_s^2 \int_{t_0}^t dt' \Gamma_{ij}(t') \right) \\
&\approx \exp\left(-\frac{(S_{ii} - S_{jj})^2}{4} \frac{Va^6 H^2}{56\pi^2} \left(\frac{1}{k_{\min}^3} - \frac{1}{k_{\max}^3} \right) \right).
\end{aligned} \tag{4.142}
$$

This result can be compared with the off-diagonal element (4.63). Using the dominant contribution of the exponent, given by equation (4.72), we find

$$|\rho_\pm(t)| = \rho_\pm(0) \exp\left(-g_s^2 \frac{(\phi_+ - \phi_-)^2}{4} \frac{Va^6 H^2}{56\pi^2} \left(\frac{1}{p_{\min}^3} - \frac{1}{p_{\max}^3} \right) \right). \tag{4.143}$$

The transition between the different localized vacuum states is given by the rate equation

$$\dot{\rho}_{ii}^{\mathrm{Sch}} = -2 \sum_{k \neq i} (\Re w_{ikki}^+ \rho_{ii}^{\mathrm{Sch}} - \Re w_{kiik}^+ \rho_{kk}^{\mathrm{Sch}}). \tag{4.144}$$

For $a(t) \gg a(0)$ we find

$$\Re w_{kiik}^+ = \Re w_{ikki}^+ = \frac{g_S^2 |S_{ik}|^2 Va^6(t)}{(2\pi)^2} \frac{H^5}{9H^2 + (\omega_i - \omega_k)^2} \left(\frac{1}{k_{\min}^3} - \frac{1}{k_{\max}^3} \right). \tag{4.145}$$

Depending on the physical situation whether a bath-induced coupling between different vacua or whether the tunneling dominates, equation (4.144) or (4.128) describes the evolution of the cosmic landscape.

The evolution is described by n coupled ordinary differential equations and can obviously not be solved for $n \sim 10^{500}$ vacua; therefore, further assumptions and approximations are necessary in order to obtain some physical insight.

The approximation of Markov equations via Fokker–Planck equations is, for example, described in [98] and can always be applied if there is some small expansion parameter, for example, the ratio of the jumps between different vacua and the size of the tunneling landscape. The large number of vacua motivates the transition from discrete values $\rho_{ii}(t)$ to a function $\rho_x(t)$ where x is a continuous coordinate in a smooth cosmic landscape. When the landscape is one-dimensional one might

consider the following scenario: There is a probability to go to the left and to the right which is described by functions $\alpha(x')$ and $\beta(x')$ when the observer is located at a position x'. These functions are the continuum limit next-neighbour transitions rates in equation (4.128),

$$\lambda|\Delta_{i,i+1}|^2 = \beta_i \rightarrow \beta(x),$$
$$\lambda|\Delta_{i,i-1}|^2 = \alpha_i \rightarrow \alpha(x) \,, \tag{4.146}$$

respectively equation (4.144),

$$2\Re w^+_{i,i+1,i+1,i} = \beta_i \rightarrow \beta(x),$$
$$2\Re w^+_{i,i-1,i-1,i} = \alpha_i \rightarrow \alpha(x) \,. \tag{4.147}$$

The probability that there is a local minimum in the potential between x and $x + dx$ is $\Omega\gamma(x)dx$, where Ω denotes the size of the cosmic landscape. Therefore, we take into account the tunneling rates and the distance to "nearest neighbours" of local vacua.

The transition from the sum in (4.144) to a continuous description can be understood as follows:

$$\begin{aligned}
\sum_k w^+_{kiik}\rho_{kk} \;\; =: \;\; & \sum_k w(i,k)\rho(k) \\
= \;\; & \int dx(\delta(x - k_1) + ... + \delta(x - k_n))w(i,x)\rho(x) \\
\approx \;\; & \int dx \int dk f(x - k)w(i,x)\rho(x) \\
= \;\; & \int dx\gamma(x)w(i,x)\rho(x) \,. \tag{4.148}
\end{aligned}$$

Following the treatment of [98] and assuming detailed balance,

$$\beta(x')\gamma(x)\rho(x')_{\text{stat}} = \alpha(x')\gamma(x')\rho(x)_{\text{stat}} \,, \tag{4.149}$$

where $\rho(x)_{\text{stat}}$ is some stationary distribution, the Fokker–Planck equation of diffusion type holds:

$$\frac{\partial\rho(x,t)}{\partial t} = \frac{2}{\Omega}\frac{\partial}{\partial x}\frac{1}{\gamma(x)}\frac{\partial}{\partial x}\frac{\rho(x,t)}{\rho_{\text{stat}}(x)} \,. \tag{4.150}$$

This equation describes diffusion in an inhomogeneous medium, since the rates do not prefer a special direction in the cosmic landscape, that is, the dynamics is a random walk in an inhomogeneous medium. The drift term in equation (4.150) is

due to inhomogeneities in the cosmic landscape and vanishes for $\gamma(x) = \text{const}$. In the following we will rescale the time such that the factor $2/\Omega$ is absorbed.

If the pure tunneling given by (4.128) dominates and $\gamma(x) = \lambda\Delta^2$, where Δ is a typical tunneling rate, we obtain the usual solution for the diffusion equation,

$$\rho(x,t) = \frac{1}{\sqrt{\pi\lambda\Delta^2 t}} \exp\left(-\frac{x^2}{\lambda\Delta^2 t}\right) . \tag{4.151}$$

If the dynamics is environment-induced and given by (4.144), the diffusion depends on the scale factor. For a scalar-field environment and assuming $a(t) = \exp(Ht)$, the result is approximately given by

$$\rho(x,t) = \sqrt{\frac{H}{\pi D(a^6 - 1)}} \exp\left(-\frac{Hx^2}{D(a^6 - 1)}\right) , \tag{4.152}$$

with

$$D = \frac{g_{\text{s}}^2 L^3 S^2}{H^2} , \tag{4.153}$$

where S denotes a typical transition element S_{ik} in the interaction (4.125). The width of the distibution (4.152) increases faster than the width of (4.151) due to the exponentially increasing scale factor a. Therefore the diffusion process may become faster if the system environment interaction dominates the dynamics in the landscape. This is, of course, only possible if the cosmic landscape and its environment exchange enough energy to lift the scalar field from one local minima to another.

4.7 Conclusions

Based on a model which gives an explanation of the small cosmological constant within the framework of quantum theory, we studied the influence of the environment. Within this model, a scalar field which mimics dark energy can tunnel between two local minima. We showed how decoherence can justify the localization in a well and the (local) disappearance of superpositions. Furthermore, the model was generalized by taking into account an arbitrary number of local minima. Through decoherence it was possible to derive effective rate equations which are similar to the Pauli equations in quantum electrodynamics [97]. From these rate equations it is possible to derive Fokker–Planck equations in the continuum limit. A realistic scenario enabling the calculation of the observed value can only be presented after a definite cosmic landscape for the potential has been retrieved from a fundamental theory.

Furthermore, the change of the tunneling rate due to dissipative effects has been discussed. Using a renormalization method for functional determinants we have derived, in contrast to the findings of Caldeira and Leggett [73] in a quantum mechanical setting, an increase of the tunneling rate.

5 Influence of Nontrivial Backgrounds and Decoherence on Vacuum Decay

We present solutions of vacuum decay in non-Minkowski space-times. In the case of de Sitter space-time we find a decay rate that can be recovered in some limit from earlier publications and derive explicit expressions of the trajectories of the nucleating bubbles. In contrast to the manifest $O(4)$–invariant setting of [7], our considerations rely on an $O(3)$–invariant setting which allows the investigation of tunneling in FRW–universes with power-law scale factors. In addition, we discuss the vacuum decay in Schwarzschild-de Sitter and Reissner-Nordström space-times. In the case of Minkowski space-time we include an interaction with environmental degrees of freedom and analyze the effects of decoherence and dissipation as well as the quantum-to-classical transition of the nucleating bubble.

5.1 Introduction

The decay of metastable vacuum states has been of great interest for several decades. Since the literature addressing this topic is enormous, we want to mention only some of the important results that have been found.

In the context of field theory, vacuum decay was first described using a semiclassical approach in [6, 75, 99]; later on, gravitational effects on and of vacuum decay have been studied in [7, 100–102]. The influence of finite temperature on vacuum decay has been addressed in [103].

Based on quantum tunneling, important cosmological models were proposed, for example eternal inflation [104, 105], the Hartle-Hawking-instanton [106, 107] or the Hawking-Moss instanton [108]. The quantum creation of topological defects, e.g. strings and branes in a fixed space-time, have been discussed in [109, 110].

In the last years, several authors have suggested that string theory in four dimensions might have as many as 10^{500} different vacua [111, 112]. All these vacua considered in string theory are local minima of a very complicated potential, resulting from the huge amount of possible compactifications of the ten-dimensional, respectively eleven-dimensional theory, to four dimensions. In this context the tunneling

between different local minima is of great importance.

Many of the findings concerning quantum tunneling are based on the high symmetries of Minkowski and de Sitter space-time. Coleman considered tunneling of scalar fields in a Minkowski background [6] and in a closed de Sitter universe [7]. In both cases, the $O(4)$-symmetry after Wick rotation was used explicitly.

Here we want to generalize results of vacuum decay in curved backgrounds to various $O(3)$-symmetric settings. Although the chosen background is determined by Einstein's equation, we neglect the backreaction of the (time-dependent) vacuum energy distribution on the curvature scalar.

The decay of metastable vacua is usually treated in the instanton picture which is of great success [74]. One assumes that the scalar field is initially located in a false vacuum ϕ_f and tunnels through a barrier into the true vacuum ϕ_t. In order to make the problem tractable, the field theoretical problem is reduced to a quantum mechanical problem by means of symmetry considerations. Both vacua denote classical minima of the potential and have to be distinguished from the quantum mechanical ground state, which is given by the symmetric superposition of ϕ_f and ϕ_t. One may ask under what circumstances it is allowed to ignore quantum mechanical superpositions by considering only localized, i.e. "classical", vacuum states. Analogous to this situation would be the localization of chiral molecules in left-handed or right-handed states, although under certain circumstances, a superposition between both can be observed [21, 25]. The localization of quantum states can only be justified with the influence of a system-environment interaction; therefore one aim of this paper will be to investigate the influence of decoherence on vacuum tunneling.

This chapter is organized as follows. In Section 5.2 we summarize known results of vacuum decay. We then turn in Section 5.3 to vacuum decay in fixed backgrounds. The influence of decoherence on tunneling and the decay rate will be discussed in section 5.4.

5.2 Vacuum Decay in Minkowski Space

The starting point is a scalar field theory

$$S_\phi = \int d^4x \left(\frac{1}{2} \partial_\mu \phi \partial^\mu \phi - V(\phi) \right), \tag{5.1}$$

where the potential $V(\phi)$ is assumed to have two local minima. The difference between the energy densities in the localized vacua is denoted by ϵ.

The Euclidean version of Feynman's path integral describing the transition from ϕ_f to ϕ_t reads [74]

$$\langle \phi_t | e^{-HT} | \phi_f \rangle = N \int D\phi \, e^{-S_\phi}, \tag{5.2}$$

where $T = it$ denotes the euclidean time, H is the Hamiltonian corresponding to the action (5.1) and N is the normalization of the path integral. The right hand side of equation (5.2) can be evaluated in the semiclassical limit. It follows, that the tunneling rate at lowest order is given by $\Gamma = A \exp(-2\Im(S))$, where S denotes the classical tunneling action and A includes the one-loop corrections [6].

Initially the field is constant in space, adopting the value ϕ_f. This situation is quantum mechanically unstable since the field can tunnel through the barrier. Due to the nucleation process, spatial regions with the field value ϕ_t are created spontaneously within the initial configuration.

Assuming $O(4)$-invariance of the tunneling solution, the field theoretical problem reduces to a quantum mechanical problem with a single degree of freedom ϕ depending on the four-dimensional radius ρ. The effective particle moves in a potential $-V(\phi)$ from the false vacuum ϕ_f to the true vacuum ϕ_t.

Following Coleman [6], the simplified euclidean action following from (5.1) reads

$$\Im(S) = -\frac{\pi^2}{4}\rho^4\epsilon + \pi^2\rho^3 S_1 \,. \tag{5.3}$$

The first term in (5.3) is a volume term originating from the field ϕ staying near ϕ_f until a very large "time" ρ. The second term arises from the transition of the particle from ϕ_f to ϕ_t around the "time" ρ where the soliton action S_1 depends on the concrete shape of the potential. In order to end up with a finite tunneling action, we demand that $V(\phi_f) = 0$. If $V(\phi_f) \neq 0$, we consider $S_\phi - S_{\phi_f}$.

The action (5.3) is minimized for $\rho = R_0 = 3S_1/\epsilon$ which leads to the famous result [6]

$$\Im(S) = \frac{27\pi^2 S_1^4}{4\epsilon^3} \,. \tag{5.4}$$

This specific tunneling action is valid in the so-called thin-wall approximation, meaning that the transition time between the vacua is small compared to the nucleation radius R_0. Analytic continuation to Minkowski time leads to the conclusion that the true vacuum bubble will expand almost instantly at the speed of light, since

$$R(t) = \sqrt{R_0^2 + t^2} \,. \tag{5.5}$$

It is possible to derive this result without referring explicitly to the $O(4)$-invariance of the problem after Wick rotation. Assuming spherical symmetry of the expanding vacuum bubble, the action consists of a volume term involving the difference between false and true vacuum and an integral over the two-dimensional surface of the sphere.

Using Minkowski time, the action reads [113]

$$
\begin{aligned}
S_R &= \int dt \left(\int_{|\mathbf{x}| \leq R} d^3 x \sqrt{-\eta}\epsilon - \int_{|\mathbf{x}|=R} d^2 x \sqrt{-\gamma}\sigma \right) \\
&= \int dt \left(\frac{4\pi R^3 \epsilon}{3} - 4\pi\sigma R^2 \sqrt{1 - \dot{R}^2} \right) ,
\end{aligned}
\tag{5.6}
$$

where η is the determinant of the Minkowski-metric and γ is the determinant of the induced metric on the surface of the sphere. The relative minus sign in the action (5.6) is due to the energy conservation of the system: The difference of the energies in the nucleating region has to be balanced by the negative energy of the surface of the sphere. This allows the interpretation of σ as surface tension. The solution of the classical equations of motion coincides with (5.5) after the substitution $\sigma \to S_1$.

In contrast to (5.3), the action (5.6) can be generalized in a straightforward manner to problems without $O(4)$-symmetry.

5.3 Tunneling in nontrivial Backgrounds

The geometry of space-time is determined by Einstein's equations involving the Ricci tensor and the energy momentum tensor. Although any change of the matter distribution will have an impact on the geometry [7], we will ignore this backreaction and consider the background to be fixed. Therefore we will discard any changes in the Einstein-Hilbert action due to the tunneling process. The effective action determining the dynamics of the scalar field is a straightforward generalization of (5.6) and reads (see also [109])

$$
S_R = \int dt \left(\int_{|\mathbf{x}| \leq R} d^3 x \sqrt{-g}\epsilon - \int_{|\xi|=R} d^2 \xi \sqrt{-\gamma}\sigma \right) .
\tag{5.7}
$$

Here we have denoted the determinant of an arbitrary metric $g_{\mu\nu}$ by g, and γ is the determinant of the induced metric

$$
\gamma_{ab} = g_{\mu\nu} \frac{\partial x^\mu}{\partial \xi^a} \frac{\partial x^\nu}{\partial \xi^b} ,
\tag{5.8}
$$

where the $x^\mu(\xi)$ parametrize the space-time manifold on the sphere using two coordinates ξ^a.

In the case of a Friedmann-Robertson-Walker universe with the line element

$$
ds^2 = a^2(y)(dy^2 - dx^2 - f^2(x)d\Omega^2) ,
\tag{5.9}
$$

the action (5.7) adopts the form

$$S_{x,FRW} = \int dy \left(4\pi\epsilon a^4(y) \int_0^{x(y)} dx' f^2(x') \right.$$
$$\left. -4\pi\sigma a^3(y) f^2(x) \sqrt{1 - \dot{x}^2(y)} \right). \tag{5.10}$$

The conformal time is denoted with y and the function f is given by $x, \sin(x)$ and $\sinh(x)$ for flat, closed and open universes, respectively. The coordinate of the bubble is given by the dimensionless function $x(y)$ and $\dot{x}$ denotes the derivative with respect to y.

For a given $a(y)$ it seems hopeless to find an analytic solution to the highly nonlinear equation of motion for $x(y)$. Therefore we will solve the inverse problem: given a radius function $x(y)$, we obtain solutions for a scale factor $a(y)$, among them solutions for physically reasonable cases.

The equation of motion resulting from (5.10) reads

$$\frac{d}{dy} \left(\sigma a^3 x^2 \frac{\dot{x}}{\sqrt{1 - \dot{x}^2}} \right) = \epsilon a^4 x^2 - 2\sigma a^3 x \sqrt{1 - \dot{x}^2}. \tag{5.11}$$

In order to find solutions for the differential equation (5.11), we assume the relation

$$\sqrt{1 - \dot{x}^2} = g(y)\dot{x}, \tag{5.12}$$

where $g(y)$ is chosen such that $g(y)\dot{x}$ is positive but otherwise arbitrary. From here it follows that

$$\frac{\dot{a}}{a} - \frac{\dot{g}}{3g} - \frac{ga}{R_0} + \frac{2}{3}\frac{\partial_x f(x)}{f(x)\dot{x}} = 0. \tag{5.13}$$

Equation (5.13) has the general solution

$$a(y) = \frac{\left(\frac{g(y)}{g(y_0)} \right)^{1/3} e^{-F(y)}}{C - \frac{1}{R_0} \int_{y_0}^y dy' \left(\frac{g(y')}{g(y_0)} \right)^{1/3} g(y') e^{-F(y')}}, \tag{5.14}$$

with

$$F(y) = \frac{2}{3} \int_{y_0}^y dy' \frac{\partial_x f(x)}{f(x)\dot{x}}. \tag{5.15}$$

The radius function reads

$$x(y) = \int_{\tilde{y}_0}^y dy' \frac{1}{\sqrt{1 + g^2(y')}}. \tag{5.16}$$

Although the solution for arbitrary functions x is thereby given in principle, the scale factor a, given by (5.14), will have an awkward form in general. The problem now is to find suitable functions g and x in order to obtain reasonable scale factors $a(y)$.

5.3.1 De Sitter Space

De Sitter space is of great importance for the understanding of the early universe and maybe also for the future, since cosmological data suggest that our universe is dominated by dark energy with an equation of state close to a cosmological constant [114].

De Sitter space is defined as a four-dimensional hyperboloid,

$$- X_0^2 + X_1^2 + X_2^2 + X_3^2 + X_4^2 = H^{-2} \,, \tag{5.17}$$

where H denotes the Hubble parameter and X_i are the coordinates in an auxiliary five-dimensional space. It is possible to choose a flat, closed or open spatial slicing of the de Sitter space leading to three different choices of coordinates. In order to distinguish the conformal times of the different coordinate patches, we denote them with z, y and w in case of the flat, closed and open spatial slicings, respectively.

The flat spatial sections of de Sitter space are defined as [47]

$$X_0 = \frac{1}{2H}\left(-\frac{1}{z} + z - \frac{x^2}{z}\right) \,, \tag{5.18}$$

$$X_1 = \frac{1}{2H}\left(-\frac{1}{z} - z + \frac{x^2}{z}\right) \,, \tag{5.19}$$

$$X_2 = -\frac{x_1}{Hz} \,, \tag{5.20}$$

$$X_3 = -\frac{x_2}{Hz} \,, \tag{5.21}$$

$$X_4 = -\frac{x_3}{Hz} \,, \tag{5.22}$$

with $x_1^2 + x_2^2 + x_3^2 = x^2$ and the conformal time z running from $-\infty$ to 0. The line element reads

$$ds^2 = a^2(z)(dz^2 - dx^2 - x^2 d\Omega^2) \tag{5.23}$$

with

$$a(z) = -\frac{1}{Hz} \,. \tag{5.24}$$

Using the equations (5.14) and (5.16) and the ansatz $g = \alpha/(z + \text{constant})$, we find

$$x(z) = \sqrt{\alpha^2 + \left(z + \frac{\alpha}{R_0 H}\right)^2} \,, \tag{5.25}$$

where the integration constant α is greater than zero.

In order to shrink the radius function (5.25) to zero, one has to continue z analytically to the complex plane, i.e. $z = -\alpha/(R_0 H) + iT$, with T running from α to 0. In order to determine the tunneling rate Γ, the action (5.10) has to be evaluated along the trajectory of x given by the analytic continuation. We find the expression

$$\Im(S) = \frac{\pi^2 \epsilon}{3H^4} \frac{\left(1 - \sqrt{1 + R_0^2 H^2}\right)^2}{\sqrt{1 + R_0^2 H^2}}, \tag{5.26}$$

which is independent of α and coincides with the result already found by Parke [115] in the limit $\kappa \to 0$ leaving $\kappa(U_f - U_t)$ constant. The result was also found by Simon *et al.* [116]. In the limit $H \to 0$, equation (5.26) coincides with (5.4). In the limit $\epsilon \to 0$, one obtains $\Im(S) = \pi^2 \sigma / H^3$, which is the result for the nucleation of a domain wall separating two degenerate vacua found by Basu *et al.* [109].

The physical bubble radius is

$$R_{\text{phys}} = ax = -\frac{\sqrt{\alpha^2 + \left(z + \frac{\alpha}{R_0 H}\right)^2}}{Hz}, \tag{5.27}$$

and the radius at nucleation, $R_{\text{nucl,flat}} = R_0$, is independent of α. Since the action is invariant under the rescaling $z \to \alpha z$ and $x \to \alpha x$, it is possible to eliminate α. This explains why (5.26) does not depend on this parameter.

Now we may transform this result to the closed spatial sections of de Sitter space-time, which are parametrized by [47]

$$X_0 = \frac{\sin(y)}{H \cos(y)}, \tag{5.28}$$

$$X_1 = \frac{1}{H \cos(y)} \cos(\chi), \tag{5.29}$$

$$X_2 = \frac{1}{H \cos(y)} \sin(\chi) \cos(\Theta), \tag{5.30}$$

$$X_3 = \frac{1}{H \cos(y)} \sin(\chi) \sin(\Theta) \cos(\phi), \tag{5.31}$$

$$X_4 = \frac{1}{H \cos(y)} \sin(\chi) \sin(\Theta) \sin(\phi). \tag{5.32}$$

The line element reads

$$ds^2 = a^2(y)(dy^2 - d\chi^2 - \sin^2(\chi)d\Omega^2) \tag{5.33}$$

with

$$a(y) = \frac{1}{H \cos(y)}, \quad y \in \left(-\frac{\pi}{2}, \frac{\pi}{2}\right). \tag{5.34}$$

Transforming the solution (5.25) to a closed de Sitter universe and using (5.14), we obtain the physical radius

$$
\begin{aligned}
R_{\text{phys}} &= a \sin(\chi) \\
&= \frac{1}{H \cos(y)} \sqrt{1 - \left(\frac{1 - A^2}{1 + A^2} \right)^2 \sin^2(y - y_0)}
\end{aligned}
\tag{5.35}
$$

with

$$
A = \alpha \sqrt{1 + \frac{1}{R_0^2 H^2}}, \quad \alpha > 0,
\tag{5.36}
$$

and

$$
y_0 = \pm \arcsin \left(\frac{2}{R_0 H} \frac{A}{1 - A^2} \right).
\tag{5.37}
$$

The solution with positive y_0 has a minimum in the contracting branch of the closed de Sitter universe at

$$
y_{\text{min}} = - \arccos \frac{\left(1 + \frac{1}{R_0^2 H^2} \right)^2 A}{\sqrt{A^2 + \frac{1}{4 R_0^2 H^2} (1 + 6 A^2 + A^4)}}
\tag{5.38}
$$

with the minimal radius

$$
R_{\text{min}} = \frac{R_0}{\sqrt{1 + R_0^2 H^2}}.
\tag{5.39}
$$

The solution with negative y_0 has the minimum value R_{min} in the expanding branch at $-y_{\text{min}}$. In contrast to the flat de Sitter solution, the nucleation radius depends on H and α. We have

$$
R_{\text{nucl,closed}} = R_0 \frac{1 - A^2}{1 + A^2}
\tag{5.40}
$$

at the nucleation time

$$
y_{\text{nucl}} = \arccos \left(\frac{2}{R_0 H} \frac{A}{1 - A^2} \right)
\tag{5.41}
$$

for the solution with the minimum in the expanding branch. The corresponding solution with the minimum in the contracting branch adopts the value (5.40) at the nucleation time $-y_{\text{nucl}}$. For this solution, it is possible that the physical nucleation

radius is *larger* than the physical radius at subsequent times (see fig. 5.1). The nucleation radius is determined by the requirement that the *comoving* radius adopts a minimum value for some real nucleation time. Subsequently, one chooses the analytical continuation to complex time such that comoving bubble radius shrinks to zero.

The value of A is constrained by the condition that y_0 given by (5.37) has to be real. From this condition and equation (5.39), we conclude that the nucleation radius is constrained by the relation

$$R_{\mathrm{min}} \leq R_{\mathrm{nucl,closed}} \leq R_{\mathrm{nucl,flat}} \,. \tag{5.42}$$

In order to shrink the bubble to zero we use complex time $y = y_{\mathrm{nucl}} + iU$, with U running from $\mathrm{arcosh}\frac{1+A^2}{1-A^2}$ to 0.
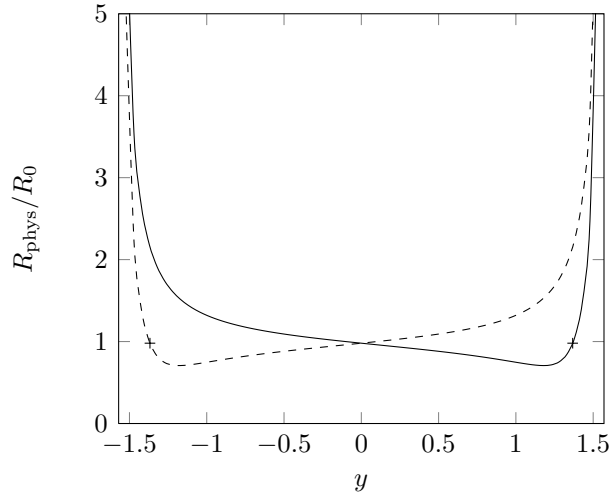
Figure 5.1: Choosing a slicing of de Sitter space with positive curvature, we find for the same values of R_0H and α two different solutions that can be obtained from each other by reflection with respect to the R_{closed}/R_0-axis. The marks on the curves label the nucleation radius and the nucleation time defined by $R_{\mathrm{phys}}(y_{\mathrm{nucl}}) = R_{\mathrm{nucl,closed}}$.

A third possibility is the spatially open slicing of de Sitter space using the coordinates [47]

$$X_0 = -\frac{\cosh(\psi)}{H\sinh(w)}\,, \tag{5.43}$$

$$X_1 = -\frac{\cosh(w)}{H\sinh(w)}\,, \tag{5.44}$$

$$X_2 = -\frac{1}{H\sinh(w)}\sinh(\psi)\cos(\Theta_2)\,, \tag{5.45}$$

$$X_3 = -\frac{1}{H\sinh(w)}\sinh(\psi)\sin(\Theta_2)\cos(\Theta_3)\,, \tag{5.46}$$

$$X_4 = -\frac{1}{H\sinh(w)}\sinh(\psi)\sin(\Theta_2)\sin(\Theta_3)\,, \tag{5.47}$$

and the scale factor

$$a(w) = -\frac{1}{H\sinh(w)}\,, \quad w \in (-\infty, 0)\,. \tag{5.48}$$

Transforming into these coordinates and using (5.14), we find

$$
\begin{aligned}
R_{\text{phys}} &= a\sinh(\psi) \\
&= -\frac{1}{H\sinh(w)}\sqrt{\left(\frac{1+A^2}{1-A^2}\right)^2\cosh^2(w+w_0)-1} \tag{5.49}
\end{aligned}
$$

with

$$w_0 = \operatorname{arsinh}\left(\frac{2}{R_0 H}\frac{A}{1+A^2}\right) > 0\,. \tag{5.50}$$

The bubble is nucleating at the radius

$$R_{\text{nucl,open}} = R_0\frac{1+A^2}{1-A^2} \tag{5.51}$$

and the time

$$w_{\text{nucl,open}} = -w_0\,. \tag{5.52}$$

Obviously, the size of the nucleation radius is constrained by

$$R_{\text{nucl,open}} \geq R_{\text{nucl,flat}}\,. \tag{5.53}$$

The analytic continuation of the time is $w = w_{\text{nucl}} + iV$, and V runs from $\arccos \frac{1-A^2}{1+A^2}$ to 0.

The tunneling rate for the flat, closed and open slicing is determined by the same expression (5.26) which can be concluded directly from the coordinate–invariant approach of [7]. However, it turns out that only the imaginary part of the finite instanton action (5.14) is coordinate independent since it obeys an $O(3)$–symmetry and is not generally covariant. The physical size of the nucleating bubble depends on the coordinate patches, as can be seen from equations (5.40) and (5.51). For the flat slicing of de Sitter space, the nucleation radius is independent of the nucleation time due to the manifest scale invariance of the action (5.10). In contrast, the nucleation radius for the closed and open slicing of de Sitter space depends explicitly on the integration constant α which enters the expressions of the nucleation times (5.41) and (5.52). This reflects the loss of scale invariance.

5.3.2 Power-Law Expansion in a spatially flat Universe

Since the action (5.10) is only $O(3)$–symmetric, it is also possible to find analytical solutions for a power-law scale factor if one restricts to the case $\epsilon = 0$, that is, two degenerate vacua.

In order to obtain the de Sitter universe as a limit for $n \to \infty$, we choose the scale factor of the form

$$a(t) = \frac{1}{H} \left(1 + \frac{Ht}{n} \right)^n , \tag{5.54}$$

where t is the cosmological time. Changing the parametrization from t to conformal time z, the scale factor reads

$$a(z) = \frac{1}{H} \left(-\frac{n-1}{n} z \right)^{-\frac{n}{n-1}} . \tag{5.55}$$

Unfortunately it is not possible to obtain an analytic expression for $x(z)$ such that the scale factor is exactly of the form given by equation (5.55). We will merely find a scale factor which coincides with the expression (5.55) for small z, i.e. large cosmological times t.

In order to obtain a power law behavior one has to choose the radius function

$$x(z) = \sqrt{\alpha^2 + \frac{2n-2}{2n+1} z^2} , \tag{5.56}$$

which coincides for $\epsilon \to 0$ and $n \to \infty$ with the result (5.25). The scale factor then reads

$$a(z) = \frac{1}{H} \left(-\frac{n-1}{n} z \right)^{-\frac{n}{n-1}} \left(1 + \frac{6(n-1)}{(2n+1)^2} \frac{z^2}{\alpha^2} \right)^{1/6} , \tag{5.57}$$

which has the expression (5.55) as limit for $z \to 0$.

Using this result we can calculate the tunneling amplitude via the instanton action. In order to increase the bubble radius from 0 to α, the conformal time has to run from $i\alpha\sqrt{(2n+1)/(2n-2)}$ to 0.

We find for the imaginary part of the action (5.10)

$$
\begin{aligned}
\Im(S) \;=\; & \sigma\alpha^3\pi^{3/2}\left(\frac{n-1}{n}\alpha H\right)^{-\frac{3n}{n-1}}\left(\frac{2(n-1)}{2n+1}\right)^{\frac{4n-1}{2(n-1)}} \times \\
& \times\frac{n-1}{n-4}\sin\left(\frac{\pi(2n+1)}{2(n-1)}\right)\frac{\Gamma\left(-\frac{1}{n-1}\right)}{\Gamma\left(\frac{1}{2}-\frac{1}{n-1}\right)} \xrightarrow{n\to\infty} \frac{\pi^2\sigma}{H^3}\,.
\end{aligned} \tag{5.58}
$$

For $n \to 1$, the expression oscillates rapidly, which means that the WKB approximation breaks down. This is due to the conformal-time parametrization of the scale factor. Note that the tunneling rate depends here on the size α of the bubble; the scale invariance is established only for $n \to \infty$.

5.3.3 Bubble Expansion without Tunneling

The nucleation of a vacuum bubble has so far been described through an increase of the radius from zero to R_{nucl} using analytical continuation of the time. One may ask whether it is possible to find solutions of (5.11) where no analytical continuation is necessary for the increase of the vacuum bubble from zero. This can be achieved by choosing the scale factor such that the tunneling barrier vanishes.

We consider a flat FRW-universe and

$$
g(y) = \tan(y)\,, \tag{5.59}
$$

giving the radius function for the bubble to be

$$
x(y) = \sin(y)\,. \tag{5.60}
$$

Using equation (5.14) we find

$$
a(y) = \frac{R_0|\cot(y)|^{1/3}}{3|\cos(y)|^{1/3}F_{21}\left(\frac{1}{6},\frac{1}{6},\frac{7}{6},\cos^2(y)\right)+C}\,, \tag{5.61}
$$

where F_{21} is a hypergeometric function and C is a constant greater than or equal to zero (see fig. 5.2). If the integration constant is chosen to be zero, the radius of the vacuum bubble increases from zero at $y = 0$, given that the scale factor is infinitely large at $y = 0$.
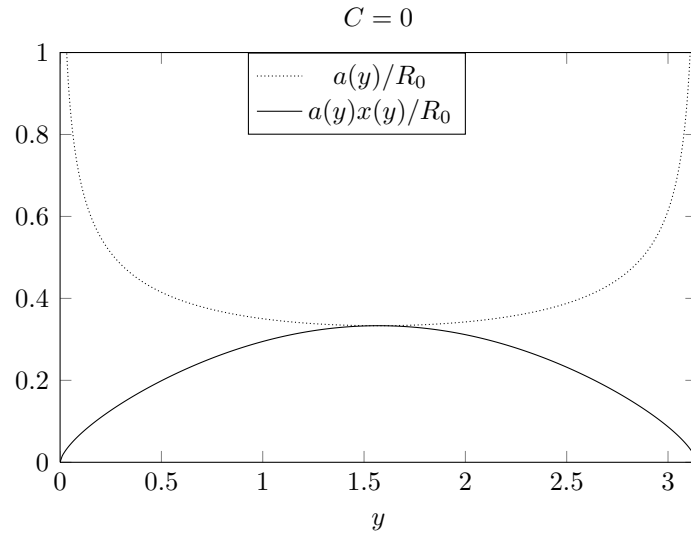
Figure 5.2: The physical bubble radius and the scale factor are plotted as functions of the conformal time, the constant of integration was chosen to be $C = 0$. This solution allows only an increase of the radius from zero if the scale factor is infinitely large at $y = 0$.
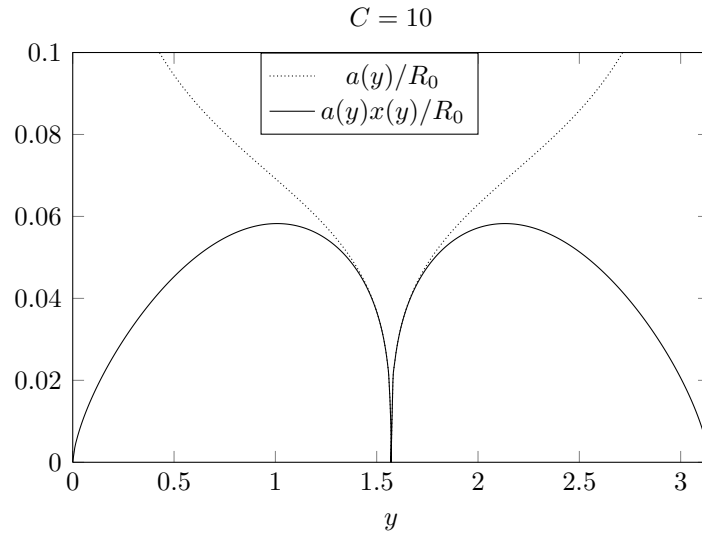
Figure 5.3: The physical bubble radius and the scale factor are plotted as functions of the conformal time, the constant of integration was chosen to be $C = 10$. The scale factor and the bubble radius increase from zero starting at $y = \pi/2$.

Choosing any $C > 0$, we find that the scale factor and the bubble radius grow from zero starting at $y = \pi/2$. Afterwards, the scale factor becomes infinitely large at $y = \pi$ whereas the bubble radius decreases to zero at $y = \pi$ after adopting some maximum value (see fig. 5.3). Due to the symmetry of the solution, there is also a branch where the bubble radius starts at zero for an infinite scale factor and decreases to zero again at $y = \pi/2$. Therefore we have obtained solutions that allow an expansion of a true vacuum bubble without a previous tunneling process.

5.3.4 Static Space-times

Solutions for vacuum decay in an $O(3)$-symmetric background with an explicit timelike Killing symmetry are easy to obtain if the center of the vacuum bubble coincides with the fixed point of the rotation symmetry.

The line element of a static space-time has the form

$$ds^2 = f(r)dt^2 - f^{-1}(r)dr^2 - r^2 d\Omega^2 \,, \tag{5.62}$$

where f is some function which depends only on r. From equation (5.7) we find

$$S = \frac{4\pi}{3}\epsilon R_0^4 \int dy\, x^2 \left(x - \sqrt{f - f^{-1}\dot{x}^2} \right) , \tag{5.63}$$

where we have introduced the dimensionless radius function $x = R/R_0$ and the dimensionless time $y = t/R_0$. From conservation of energy which is due to the timelike Killing symmetry, we find the first-order differential equation

$$\dot{x} = f\sqrt{1 - \frac{f}{x^2}} \,. \tag{5.64}$$

Whether it is possible to find a solution of the form $x = x(y)$ depends on the function f. The imaginary part of the tunneling action is given by

$$\Im(S) = \frac{4\pi}{3} R_0^4 \int_{x_1}^{x_2} dx x^2 f^{-1} \sqrt{f - x^2} \,, \tag{5.65}$$

where x_1 and x_2 are given by the two positive roots of $f - x^2$. These roots are exactly the turning points of the tunneling trajectory through an effective particle potential. Since this cannot be seen from (5.63) directly due to the non-standard form of the action, we will switch to the Hamiltonian formalism.

In order to get rid of the square root in the action we parametrize the action with an affine parameter λ, [117]

$$S = \frac{4\pi}{3}\epsilon R_0^4 \int d\lambda\, x^2 \left(x\frac{dy}{d\lambda} - \sqrt{f\left(\frac{dy}{d\lambda}\right)^2 - f^{-1}\left(\frac{dx}{d\lambda}\right)^2} \right). \tag{5.66}$$

Introducing an auxiliary variable ν leads to an action classically equivalent to (5.63):

$$\tilde{S} = \frac{4\pi}{3}\epsilon R_0^4 \int d\lambda\, x^2 \left(x\frac{dy}{d\lambda} - \frac{f(dy/d\lambda)^2 - f^{-1}(dx/d\lambda)^2}{2\nu} - \frac{\nu}{2} \right). \qquad (5.67)$$

The corresponding Hamiltonian constraint reads

$$H = \frac{3}{8\pi\epsilon R_0^4}\left(\frac{fP_x^2}{x^2} - \frac{1}{fx^2}\left(P_y - \frac{4\pi}{3}\epsilon R_0^4 x^3 \right)^2 + \left(\frac{4\pi}{3}\epsilon R_0^4 \right)^2 x^2 \right) \approx 0\,. \quad (5.68)$$

This gives rise to the potential of an effective particle potential

$$V(x) = \frac{2\pi}{3}\epsilon R_0^4 x^2 f^{-1}(f - x^2)\,. \qquad (5.69)$$

Using this potential we are able to interpret the results easily. Due to the timelike Killing vector field we have a conserved energy which constrains the Hamiltonian to zero. If the potential is greater than zero, the particle has to tunnel through the barrier. If $V(x) < 0$ for all x, the particle will leave the false vacua without tunneling.

We now consider two concrete cases: the Schwarzschild-de Sitter and the Reissner-Nordström space-times. For the Schwarzschild-de Sitter space-time we have

$$f(x) = 1 - \frac{2M}{R_0 x} - H^2 R_0^2 x^2\,. \qquad (5.70)$$

From this follows that the particle has to tunnel between

$$x_1 = \frac{2}{\sqrt{3(1 + R_0^2 H^2)}} \cos\left(\frac{1}{3}\arccos\left(\beta\right) - \frac{2\pi}{3} \right) \qquad (5.71)$$

and

$$x_2 = \frac{2}{\sqrt{3(1 + R_0^2 H^2)}} \cos\left(\frac{1}{3}\arccos\left(\beta\right) \right) \qquad (5.72)$$

with

$$\beta = -\frac{\sqrt{27}M}{R_0}\sqrt{1 + R_0^2 H^2}\,. \qquad (5.73)$$

The tunneling always occurs between the two horizons of Schwarzschild-de Sitter space. The trajectories of the bubble shell after tunneling are plotted in fig. 5.4 for different parameters. We see that close to the outer horizon the velocity decreases to zero.

Furthermore, the imaginary part of the tunneling action decreases for increasing black hole mass, since the barrier is lowered for increasing M. In fig. 5.5 the imaginary part of the action is plotted for different values of M and H. The barrier vanishes completely for

$$M > \frac{R_0}{\sqrt{27(1 + R_0^2 H^2)}} \,. \tag{5.74}$$
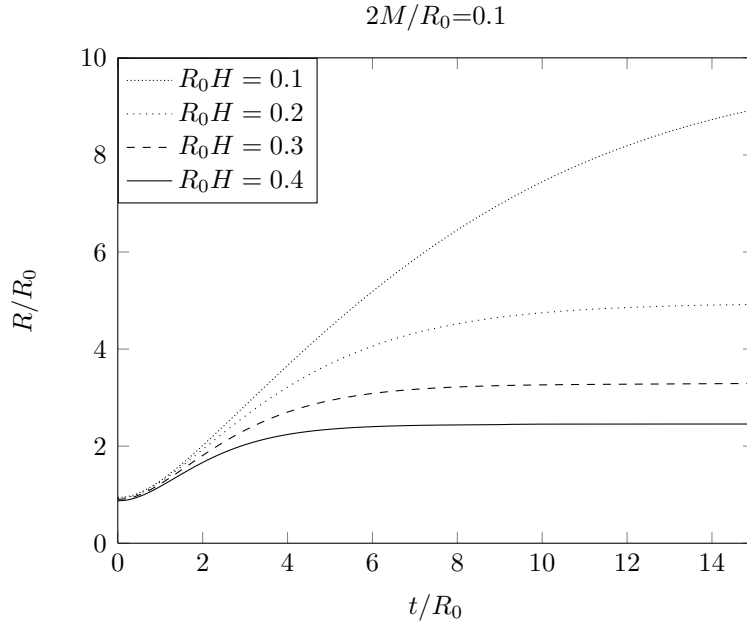
Figure 5.4: Schwarzschild-de Sitter space-time: The vacuum bubbles nucleating at a radius larger than the inner horizon of the Schwarzschild-de-Sitter-space-time reach the outer horizon in the limit of infinite times.

Our second example is the Reissner-Nordström-space-time defined by

$$f(x) = 1 - \frac{2M}{R_0 x} + \frac{Q^2}{R_0^2 x^2} \,. \tag{5.75}$$

If $|Q| < M$ holds, the line element describes a black hole with charge, if $|Q| > M$, the space-time describes a naked singularity. In the following we want to discard the latter case.
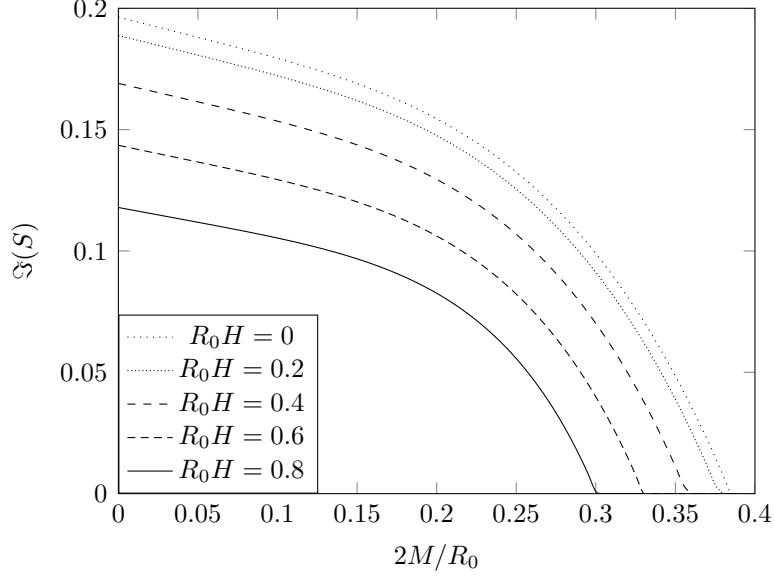
Figure 5.5: Schwarzschild-de Sitter space-time: The imaginary part of the tunneling action decreases with growing black hole mass M.

For $|Q| < M$, tunneling between x_1 and x_2 occurs only if $f - x^2$ has three positive roots. If there is only a single positive root of $f - x^2$, we find that a tunneling solution exists only behind the inner horizon and is not visible for an observer outside. Under the restrictions that $|Q| < M$ and that three positive roots exist, we find after some algebra

$$Q^2 < M^2 < \frac{R_0^2}{54}\left(1 + 36\frac{Q^2}{R_0^2} + \left(1 - 12\frac{Q^2}{R_0^2}\right)^{3/2}\right), \tag{5.76}$$

which implies $Q^2 < R_0^2/16$. The turning points of the potential are given by

$$
\begin{aligned}
x_{1/2} =\ & \sqrt{\frac{1}{6}\left(1 + \Re\left(\frac{\Delta}{2}\right)^{1/3}\right)} \\
& \pm \sqrt{\frac{1}{3} - \frac{1}{6}\Re\left(\frac{\Delta}{2}\right)^{1/3} - \frac{M}{R_0}\sqrt{\frac{3}{2}}\left(1 + \Re\left(\frac{\Delta}{2}\right)^{1/3}\right)^{-1/2}}
\end{aligned}
\tag{5.77}
$$

71

with

$$
\begin{aligned}
\Delta \;=\;& -2 - 72\frac{Q^2}{R_0^2} + 108\frac{M^2}{R_0^2} \\
& + i\sqrt{4\left(1 - 12\frac{Q^2}{R_0^2}\right)^3 - \left(2 + 72\frac{Q^2}{R_0^2} - 108\frac{M^2}{R_0^2}\right)^2}\,.
\end{aligned} \tag{5.78}
$$

In fig. 5.6 we plot the classical trajectory of the bubble after tunneling. The imaginary part of the action for different values of M and Q is depicted in fig. 5.7.
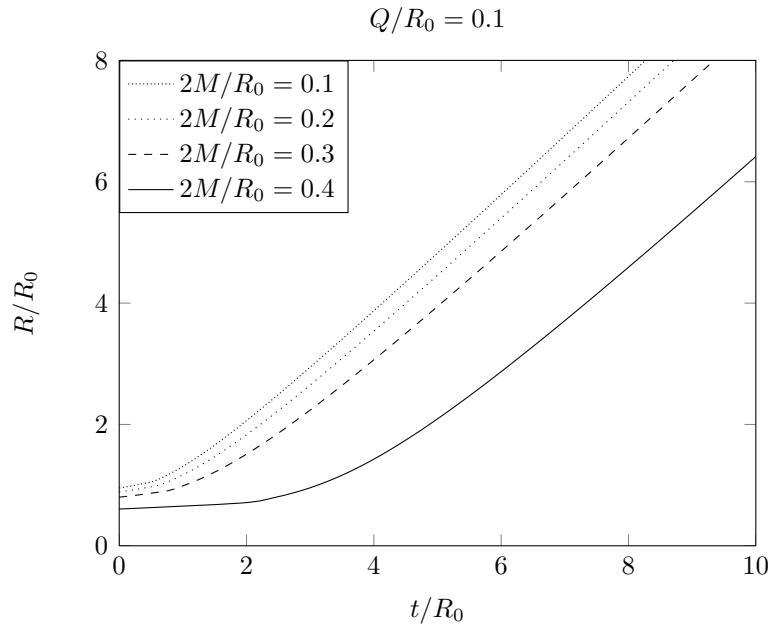
Figure 5.6: Reissner-Nordström space-time: The expansion of the vacuum bubbles starting at a nucleation radius larger than the outer horizon is growing to infinity.

Figure 5.7: Reissner-Nordström space-time: The imaginary part of the tunneling action decreases with growing black hole mass M. Since we do not consider naked singularities, we discard the values for $\Im(S)$ if $|Q| > M$.

5.4 Interaction with external Degrees of Freedom

5.4.1 The System-Environment Interaction

In the preceding sections, we have considered the scalar field ϕ to be an isolated system. Furthermore, the field was not represented by infinitely many degrees of freedom but rather a *single* quantum–mechanical variable R. In the semiclassical picture, the variable R moves along a tunneling trajectory through the barrier before it expands after nucleation. However, a more general field configuration could consist out of superpositions of vacuum bubbles with different radii R. Thus, the classical appearance of the vacuum bubble after nucleation cannot be deduced from here, since superpositions are in principle possible for arbitrary large vacuum bubbles. Here we will show how the localization of the field can be understood through the process of decoherence. More explicitly, we consider an interaction of the quantum mechanical variable R field with environmental degrees of freedom in the spirit of [118, 119]. We assume for the environmental modes the quadratic action

$$S_{\text{bath}} = \frac{1}{2} \int dt \int d^3x \left(\partial_\mu \psi \partial^\mu \psi - m^2 \psi^2 \right) , \tag{5.79}$$

where the mass m is a free parameter. The field ψ represents internal degrees of freedom of the field ϕ that have been neglected in the simplified description so far, or vacuum fluctuations of other fields.

For the interaction between the fluctuations ψ and the bounce field ϕ we choose

$$S_{\text{int}} = \int dt \int d^3x g\phi\psi \,. \tag{5.80}$$

This can be written as

$$
\begin{aligned}
S_{\text{int}} &= g \int d^4x \phi\psi \\
&= g \int d^4x \phi_f \psi - g \int dt \int_{|\mathbf{x}|<R} d^3x (\phi_f - \phi_t)\psi \,,
\end{aligned}
\tag{5.81}
$$

where we have neglected the small transition region between ϕ_f and ϕ_t. After Fourier transforming the environmental scalar field, the interaction reads

$$
\begin{aligned}
S_{\text{int}} &= g(\phi_t - \phi_f) \int dt \int_{|\mathbf{x}|<R} d^3x \sum_{\mathbf{k}} e^{i\mathbf{k}\mathbf{r}} \psi_{\mathbf{k}} \\
&= g(\phi_t - \phi_f) \int dt \sum_{\mathbf{k}} \frac{4\pi}{k^3} \left(\sin(kR) - kR\cos(kR) \right) \psi_{\mathbf{k}} \,,
\end{aligned}
\tag{5.82}
$$

where we have neglected the constant first term in the second line of equation (5.81). The radius R will be interpreted as a quantum variable like in the action (5.6). The interaction between R and ψ grows with kR, that is, modes with short wavelengths are able to resolve the vacuum bubble better than modes with longer wavelength, as expected.

5.4.2 Effective Two-state System

The simplest approximation for the description of a tunneling process between two a "false" vacua and a "true" vacua is a two–level system. As noted by Lee and Weinberg [86], the decay of the true vacuum is possible when thermal excitations or gravitational effects are taken into account. In general, superpositions of the local vacuum states cannot be neglected, if the tunneling rate is of the same order of magnitude as the decoherence rate, that is, the time scales of vacuum bubble localization and the tunneling process is of the same order. In this case, the instanton picture considering well–localized tunneling trajectories of the field, might be misleading.

We approximate the system and the environment by the Hamiltonian

$$
\begin{aligned}
H_{\text{total}} \;=\; & \begin{pmatrix} \frac{4\pi}{3} R_0^3 V(\phi_f) & \Gamma \\ \Gamma & \frac{4\pi}{3} R_0^3 V(\phi_t) \end{pmatrix} \\
& + \frac{1}{2} \int d^3x \left(\Pi_\psi^2 + (\nabla\psi)^2 + m^2\psi^2 \right) \\
& - g \begin{pmatrix} \phi_f & 0 \\ 0 & \phi_t \end{pmatrix} \int_{|\mathbf{x}|<R_0} d^3x \, \psi \,.
\end{aligned}
\tag{5.83}
$$

The first term in equation (5.83) describes the transition between the states "A bubble of radius R_0 has energy density $V(\phi_f)$" and "A bubble of radius R_0 has energy density $V(\phi_t)$" . The second term of equation (5.83) is the bath Hamiltonian, and the last term describes the environment measuring the system to be located at ϕ_f respectively ϕ_t.

The master equation for the reduced density matrix in the Schrödinger picture reads in the Redfield approximation [21]

$$
\begin{aligned}
\dot\rho_S(t) \;=\; & -i[H_0, \rho_S] \\
& - \mathrm{tr}_B \int_0^t ds [H_{\text{int}}, [H_{\text{int}}(s-t), \rho_S(t) \otimes \rho_B]]
\end{aligned}
\tag{5.84}
$$

with

$$
\begin{aligned}
H_{\text{int}} \;=\; & -4\pi g \begin{pmatrix} \phi_f & 0 \\ 0 & \phi_t \end{pmatrix} \sum_{\mathbf{k}} \int_0^{R_0} dr \, \frac{r}{k} \sin(kr)\psi_{\mathbf{k}} \\
\equiv \; & \sum_{\mathbf{k}} M_{\mathbf{k}}(R_0)\psi_{\mathbf{k}} \,.
\end{aligned}
\tag{5.85}
$$

The reduced density matrix ρ_S contains all available information about the effective two-state system.

Ignoring the free dynamics of the density matrix, equation (5.84) becomes

$$
\begin{aligned}
\dot\rho_S \;=\; & -\int_0^t ds \sum_{\mathbf{k}} A_{\mathrm{k}}(t-s)[M_{\mathbf{k}}(R_0), [M_{\mathbf{k}}(R_0), \rho_S]] \\
& + i \int_0^t ds \sum_{\mathbf{k}} B_{\mathrm{k}}(t-s)[M_{\mathbf{k}}(R_0), \{M_{\mathbf{k}}(R_0), \rho_S\}] \,.
\end{aligned}
\tag{5.86}
$$

The functions A_k and B_k are defined by

$$
\begin{aligned}
\langle \hat\psi_{\mathbf{k}} \hat\psi_{\mathbf{k}}(s-t) \rangle \;=\; & \frac{1}{2\mathcal{V}k}[\cos(k(t-s)) - i\sin(k(t-s))] \\
\equiv \; & A_k(t-s) - iB_k(t-s) \,,
\end{aligned}
\tag{5.87}
$$

where $\mathcal{V}$ denotes the quantization volume. We have restricted ourselves here to vanishing temperature. The second line of (5.86) contains a contribution to the unitary dynamics and will be ignored from here. Using this approximation we integrate equation (5.86) and find that the off-diagonal elements of the density matrix decay according to

$$\rho_{S,01}(t) = \rho_{S,01}(0)e^{-4g^2(\phi_f - \phi_t)^2 R_0^6 h(R_0, t)} \tag{5.88}$$

with

$$
\begin{aligned}
h(R_0, t) &= \frac{13t^2}{180R_0^2} + \frac{t^4}{720R_0^4} + \ln t\left(\frac{t^4}{48R_0^4} - \frac{t^6}{1440R_0^6}\right) \\
&\quad + \ln\left|\frac{t + 2R_0}{t - 2R_0}\right|\left(\frac{t}{15R_0} - \frac{t^3}{36R_0^3}\right) \\
&\quad + \ln\left|t^2 - 4R_0^2\right|\left(\frac{1}{18} - \frac{t^4}{96R_0^4} + \frac{t^6}{2880R_0^6}\right).
\end{aligned}
\tag{5.89}
$$

For times $t \lesssim R_0$ we find for the decoherence rate

$$\Gamma_{\text{dec}} \equiv \frac{\dot{\rho}_{S,01}}{\rho_{S,01}} \approx -g^2(\phi_f - \phi_t)^2 R_0^4 t, \tag{5.90}$$

which has to be compared with the transition frequency given by the difference between ground state and first excited state. In the case of degenerate vacua this is frequently given by the tunneling rate Γ. We see that $\Gamma > \Gamma_{\text{dec}}$ is in general possible for sufficiently small times. In cases when the nucleation radius is small or when the local minima of the potential are very close to each other, interference effects between different vacuum configurations are not necessarily negligible. Therefore we state that there could be regions in the cosmic landscape which should be treated quantum mechanically. The pure rate-equation approach which is frequently used is then doubtful.

For large $t \gg R_0$, the off-diagonal elements decay polynomially according to

$$
\begin{aligned}
\rho_{S,01}(t) &= \rho_{S,01}(0) \times \\
&\quad \times \exp\left[-\frac{4g^2}{9}(\phi_f - \phi_t)^2 R_0^6 \left(\frac{7}{4} + \ln\left(\frac{t}{2R_0}\right)\right)\right].
\end{aligned}
\tag{5.91}
$$

The result (5.91) can be compared with the suppression of interference in a well-known system, the dissipationless spin-boson model (see for example [120]). Using the ohmic spectral density by $J(\omega) = \omega \exp(\omega/\Omega)$, the decoherence rate in this model is given by

$$\Gamma(t) = -\lambda\frac{1}{2}\ln(1 + \Omega^2 t^2) - \lambda\ln\left(\frac{\sinh(t\pi T)}{t\pi T}\right), \tag{5.92}$$

where T denotes the temperature, λ the coupling strength, and Ω the frequency cutoff. The second term is due to the thermal contributions of the bath modes and is roughly equal to $-\lambda t\pi T$ for $t \gg 1/T$. Since we consider in our model only the case of vanishing temperature, the thermal contributions vanish and we are left with the vacuum fluctuations. Therefore we obtain only a logarithmic dependence of Γ_{dec} which is similar in the spin-boson model where one obtains for large times $\Gamma(t) \approx -\lambda \ln(\Omega t)$ in the limit $T \to 0$.

5.4.3 Localization of the growing Vacuum Bubble

The reduction of the scalar field tunneling process to a two–state system is a drastic simplification, since the scalar field has infinitely many degrees of freedom. However, this simplification is valid, if one is only interested in superpositions of a true vacuum bubble of vanishing size with a true vacuum bubble of size R_0. In the following, we apply the decoherence program on superpositions of vacuum bubbles with arbitrary radii R. This is appropriate in order to describe the quantum–to–classical transition of the expanding vacuum bubble. The possibility of a tunneling process back to the false vacuum will be discarded here.

Macroscopic objects, i.e. dust particles, are observed in well–localized states in contrast to microscopic particles that are often found in energy eigenstates. The localization can be explained with the interaction of the macroscopic object with the environment; the phase relations of different states are delocalized through continuous measurement [25]. A local observer has no access to the interference terms; this information can only be obtained through an exact knowledge of the environmental system which is in general not possible.

In order to quantize the system given by the action (5.6), we reparametrize the action analogously to (5.66) and obtain

$$S_R = \int d\lambda \left(\frac{4\pi R^3 \epsilon}{3} \dot{t} - 4\pi R^2 \sigma \sqrt{\dot{t}^2 - \dot{R}^2} \right) , \qquad (5.93)$$

which is classically equivalent to

$$\tilde{S}_R = \int d\lambda \left[\frac{4\pi R^3 \epsilon}{3} \dot{t} - 2\pi R^2 \sigma \left(\frac{\dot{t}^2 - \dot{R}^2}{\nu} + \nu \right) \right] . \qquad (5.94)$$

Since the kinetic term is quadratic in $\dot{R}$, we proceed with the canonical quantization procedure. After reparametrizing (5.79) and (5.80) in a similar way we obtain the

following canonical momenta:

$$P_R = \frac{4\pi R^2 \sigma}{\nu} \dot{R} \,, \tag{5.95}$$

$$P_t = 4\pi R^2 \left(\frac{R\epsilon}{3} - \frac{\sigma t}{\nu} \right) \tag{5.96}$$

$$- \sum_{\mathbf{k}} \left(\frac{1}{2t^2} \dot{\psi}_{\mathbf{k}} \dot{\psi}_{-\mathbf{k}} + \frac{1}{2}(k^2 + m^2)\psi_{\mathbf{k}}\psi_{-\mathbf{k}} \right.$$

$$\left. - g(\phi_t - \phi_f) \int_{|\mathbf{x}|<R} d^3 x e^{i\mathbf{k}\mathbf{x}} \psi_{\mathbf{k}} \right) \,,$$

$$P_{\psi_{\mathbf{k}}} = \frac{\dot{\psi}_{-\mathbf{k}}}{t} \,. \tag{5.97}$$

The constraint Hamiltonian reads

$$H = \frac{\nu}{8\pi R^2 \sigma} \left\{ 16\pi^2 R^4 \sigma^2 + P_R^2 \right. \tag{5.98}$$

$$- \left(P_t - \frac{4\pi R^3 \epsilon}{3} + \sum_{\mathbf{k}} \left[\frac{1}{2}(k^2 + m^2)\psi_{\mathbf{k}}\psi_{-\mathbf{k}} \right. \right.$$

$$\left. \left. + \frac{1}{2} P_{\psi_{\mathbf{k}}} P_{\psi_{-\mathbf{k}}} - g(\phi_t - \phi_f) \int_R d^3 x e^{i\mathbf{k}\mathbf{x}} \psi_{\mathbf{k}} \right] \right)^2 \right\} \approx 0 \,.$$

Since the quantization of the constraint equation (5.98) does not lead to a differential equation of Schrödinger type, we consider the square root of the constraint equation ignoring factor-ordering problems. We then find

$$i\partial_t |\Psi\rangle = \left(\sqrt{16\pi^2 \hat{R}^4 \sigma^2 + \hat{P}_R^2} - \frac{4\pi \hat{R}^3 \epsilon}{3} + \sum_{\mathbf{k}} \left[\frac{1}{2} \hat{P}_{\psi_{\mathbf{k}}} \hat{P}_{\psi_{-\mathbf{k}}} + \frac{1}{2}(k^2 + m^2)\hat{\psi}_{\mathbf{k}}\hat{\psi}_{-\mathbf{k}} \right. \right.$$

$$\left. \left. - g(\phi_t - \phi_f) \int_{|\mathbf{x}|<\hat{R}} d^3 x e^{i\mathbf{k}\mathbf{x}} \psi_{\mathbf{k}} \right] \right) |\Psi\rangle \,, \tag{5.99}$$

where the substitution $P_t \to -i\partial/\partial_t$ was performed. Except for the appearance of a square root, the Hamiltonian is of standard form. In order to simplify the problem further, we assume that the momentum P_R dominates over the quartic term for large R. This can be justified with the classical equations of motion: the radius R grows proportionally to t, but P_R grows proportionally to t^3. With this approximation, which is valid for $t \gg R_0$, we discard all the factor ordering problems. The system Hamiltonian simplifies to

$$H_0 \approx |P_R| - \frac{4\pi \hat{R}^3 \epsilon}{3} \,, \tag{5.100}$$

and the corresponding Heisenberg equations of motion have the solutions

$$
\begin{aligned}
\hat{R}^H(t) &= \hat{R}_0 \pm |t|\,, & (5.101)\\
\hat{P}_R^H(t) &= \hat{P}_R(0) + \frac{4\pi\epsilon}{3}\left((\hat{R}_0 \pm |t|)^3 - \hat{R}_0^3\right). & (5.102)
\end{aligned}
$$

Since we are interested in the localization of the growing vacuum bubbles, we restrict ourselves to the positive signs in equations (5.101) and (5.102). The interaction now reads

$$
\begin{aligned}
H_{\mathrm{int}} &= -4\pi g(\phi_t - \phi_f) \sum_{\mathbf{k}} \int_0^{\hat{R}} dr \frac{r}{k}\sin(kr)\psi_{\mathbf{k}} \\
&\equiv -\sum_{\mathbf{k}} f_k(\hat{R})\psi_{\mathbf{k}}\,, & (5.103)
\end{aligned}
$$

where the radius is not fixed, in contrast to the interaction (5.85). Using equations (5.84) and (5.87) we find the master equation

$$
\begin{aligned}
\dot{\rho}_S &= -i\left[H_0, \rho_S\right] & (5.104)\\
&\quad +i\int_0^t ds \sum_{\mathbf{k}} B_{\mathbf{k}}(t-s)[f_k(\hat{R}), \{f_k(\hat{R}+|t-s|), \rho_S\}] \\
&\quad -\int_0^t ds \sum_{\mathbf{k}} A_{\mathbf{k}}(t-s)[f_k(\hat{R}), [f_k(\hat{R}+|t-s|), \rho_S]]\,.
\end{aligned}
$$

Since we are only interested in decoherence, we drop the unitary part as well as the terms describing dissipation in equation (5.104). In order to obtain an estimate for the decoherence factor, we calculate the k-dependent correlators in (5.104) in the

position basis, i.e.

$$
\begin{aligned}
C(R, R', t) &\equiv \int_0^t ds \sum_{\mathbf{k}} A_k(t-s) f_k(R) f_k(R' + |t-s|) \\
&= \frac{g^2(\phi_t - \phi_f)^2}{120} \Big\{ Rt(63R^2R' + 53R'^3 + 48R^2t + 74R'^2t \\
&\quad + 52R't^2 + 16t^3) \\
&\quad + \frac{1}{8} \left[(R-R')^2 \ln(R-R')^2 + (R+R')^2 \ln(R+R')^2 \right] \\
&\quad \times (12R^3 - 14RR'^2 + 120RR't + 80Rt^2) \\
&\quad + \frac{1}{8} \left[(R-R')^2 \ln(R-R')^2 - (R+R')^2 \ln(R+R')^2 \right] \\
&\quad \times (9R^2R' + 60R^2t - 7R'^3 + 60R'^2t + 40R't^2) \\
&\quad - \frac{1}{8} \Big[(R-R'-2t)^3 \ln(R-R'-2t)^2 \\
&\quad + (R+R'+2t)^3 \ln(R+R'+2t)^2 \Big] \times \\
&\quad \times (12R^2 + 7R'^2 + 18R't + 8t^2) \\
&\quad - \frac{1}{8} \Big[(R-R'-2t)^3 \ln(R-R'-2t)^2 \\
&\quad - (R+R'+2t)^3 \ln(R+R'+2t)^2 \Big] (21RR' + 12Rt) \Big\} . \quad (5.105)
\end{aligned}
$$

Using this result it is possible to integrate the master equation (5.84),

$$
\begin{aligned}
\rho(R, R', t) &= \rho(R, R', 0) \exp \Big\{ - \int_0^t ds \big[C(R, R, s) \\
&\quad - C(R, R', s) - C(R', R, s) + C(R', R', s) \big] \Big\} . \quad (5.106)
\end{aligned}
$$

In the limit $t \ll |R - R'|$ we find

$$
\begin{aligned}
\rho(R, R', t) &= \rho(R, R', 0) \exp \Big[- \frac{g^2(\phi_t - \phi_f)^2}{8} (R - R')^2 t^2 \\
&\quad \times \Big\{ 4(R^2 + RR' + R'^2) + (R+R')^2 \ln \frac{(R+R')^2}{(R-R')^2} \Big\} \Big] , \quad (5.107)
\end{aligned}
$$

whereas for times $t \gg R, R'$ the non-unitary part of the density matrix is approxi-

mately given by

$$
\begin{aligned}
\rho(R, R', t) &\approx \rho(R, R', 0) \left| \frac{t^2(R + R' + 2t)^2}{((R - R')^2 - 4t^2)(R + t)(R' + t)} \right|^{-\frac{1}{45} g^2(\phi_t - \phi_f)^2 t^6} \\
&\approx \rho(R, R', 0) \exp \left[-\frac{g^2}{90} (\phi_t - \phi_f)^2 t^4 (R - R')^2 \right] .
\end{aligned} \tag{5.108}
$$

Compared to (5.91), the suppression of the off-diagonal elements increases strongly with time, since the vacuum bubble expands. The decoherence process is sensitive on the size of the vacuum bubble, that is, it is more efficient for larger than for smaller ones. In contrast to (5.85), the interaction (5.103) does not assume a fixed size of the vacuum bubbles.

5.4.4 Modified Tunneling Rate due to Environmental Degrees of Freedom

Caldeira and Leggett showed in [73, 76] that the decay rate of a metastable state is modified due to the interaction with the environment.

To obtain the modified tunneling amplitude one has to evaluate the path integral over all $\psi_\mathbf{k}$ and normalize the resulting expression such that the impact of the interaction vanishes if g tends to zero. Since the interaction (5.80) is bilinear, this will reduce to a ratio of two functional integrals which will be evaluated semiclassically. It is important to include a renormalization term in order to ensure, that the system cannot lower its potential energy by moving in the $\psi_\mathbf{k}$–directions of the configuration space [73]. After switching to imaginary time $T = -it$ we find the euclidean action

$$
S_\mathrm{E} = S_\mathrm{E,R} + S_\mathrm{E,bath} + S_\mathrm{E,int} + S_\mathrm{E,ren} \tag{5.109}
$$

with

$$
\begin{aligned}
S_\mathrm{E,R} &= -\int_0^{T_0} dT \left(\frac{4\pi\epsilon}{3} R^3 - 4\pi\sigma R^2 \sqrt{1 + \dot{R}^2} \right) , \\
S_\mathrm{E,bath} &= \int_0^{T_0} dT \sum_\mathbf{k} \frac{\mathcal{V}}{2} \left(\dot{\psi}_\mathbf{k} \dot{\psi}_{-\mathbf{k}} + (k^2 + m^2) \psi_\mathbf{k} \psi_{-\mathbf{k}} \right) , \\
S_\mathrm{E,int} &= -\int_0^{T_0} dT \sum_\mathbf{k} f_k(R) \psi_\mathbf{k} , \\
S_\mathrm{E,ren} &= \int_0^{T_0} dT \sum_\mathbf{k} \frac{f_k^2(R)}{2\mathcal{V}(k^2 + m^2)} ,
\end{aligned} \tag{5.110}
$$

where $f(R)$ was defined in equation (5.103) and $\mathcal{V}$ denotes again the quantization volume of the environmental modes. The euclidean time at which the bubble radius

vanishes is denoted with T_0 and coincides with R_0 in the limit of vanishing system-environment interaction. The ratio of the functional integrals can be evaluated exactly since the action is quadratic in the $\psi_{\mathbf{k}}$'s (see [121]). We find

$$\frac{\int \Pi_{\mathbf{k}} \mathcal{D}\psi_{\mathbf{k}} \exp(-S_{\mathrm{E}})}{\int \Pi_{\mathbf{k}} \mathcal{D}\psi_{\mathbf{k}} \exp(-S_{\mathrm{E}}(g=0))} = \exp(-S_{\mathrm{eff}}) \tag{5.111}$$

with

$$\begin{aligned} S_{\mathrm{eff}} &= S_{\mathrm{E,R}} + S_{\mathrm{E,ren}} \\ &\quad - \int_0^{T_0} dT \int_0^{T_0} dT' \sum_{\mathbf{k}} \frac{f_k(R)f_k(R')}{4\mathcal{V}\sqrt{k^2+m^2}} \frac{\cosh\left(\sqrt{k^2+m^2}\left(|T-T'|-\frac{T_0}{2}\right)\right)}{\sinh\left(\sqrt{k^2+m^2}\frac{T_0}{2}\right)}, \end{aligned} \tag{5.112}$$

with $R' = R(T')$. The expression (5.112) can be simplified by the definition $R(T + T_0) \equiv R(T)$, that is, we have

$$S_{\mathrm{eff}} = S_{\mathrm{E,R}} + \int_{-\infty}^{\infty} dT' \int_0^{T_0} dT \sum_{\mathbf{k}} \frac{e^{-\sqrt{k^2+m^2}|T-T'|}}{8\mathcal{V}\sqrt{k^2+m^2}}(f_k(R) - f_k(R'))^2 . \tag{5.113}$$

From this expression we deduce that the interaction with environmental degrees of freedom leads to a suppression of the tunneling amplitude (see [73]). Varying the effective action, we find the equations of motion to be

$$\begin{aligned} \frac{d}{dT}\left(\frac{4\pi\sigma R^2\dot{R}}{\sqrt{1+\dot{R}^2}}\right) &= -4\pi\epsilon R^2 + 8\pi\sigma R\sqrt{1+\dot{R}^2} \\ &\quad + \int_{-\infty}^{\infty} dT' \sum_{\mathbf{k}} \frac{e^{-\sqrt{k^2+m^2}|T-T'|}}{2\mathcal{V}\sqrt{k^2+m^2}} \partial_R f_k(R)(f_k(R) - f_k(R')) \end{aligned} \tag{5.114}$$

The term in the second line is a nonlocal friction term. We can state this result more explicitly, if we consider the limit $m = 0$ and expand $\partial_R f_k(R)(f_k(R) - f_k(R'))$ up to lowest order in k. Since contributions for large k are exponentially suppressed for $T \neq T'$, this approximation will not alter the integrand significantly. Thus, we find a friction term which is of a similar form as in [73],

$$\begin{aligned} \frac{1}{R^2}\frac{d}{dT}\left(\frac{4\pi\sigma R^2\dot{R}}{\sqrt{1+\dot{R}^2}}\right) &= -4\pi\epsilon + \frac{8\pi\sigma}{R}\sqrt{1+\dot{R}^2} \\ &\quad + \frac{4g^2}{3}(\phi_t - \phi_f)^2 \int_{-\infty}^{\infty} dT' \frac{R^3 - R'^3}{(T-T')^2}, \end{aligned} \tag{5.115}$$

where the integral has to be interpreted as its principal value.

Although in general one would have to solve equation (5.114) or (5.115) in order to find the numerical value of the instanton action, here we neglect the back reaction of the environment on the bubble and set $T_0 = R_0$. Substituting

$$\sum_{\mathbf{k}} \to \frac{\mathcal{V}}{(2\pi)^3} \int d^3 k \qquad (5.116)$$

and evaluating the integrals numerically, we find for $m = 0$ the correction to the imaginary part of the euclidean classical action (5.6) to be

$$S_{\text{eff}} - S_{\text{E,R}} \approx 0.088 g^2 (\phi_t - \phi_f)^2 R_0^6 . \qquad (5.117)$$

The correction for arbitrary m is plotted in fig. (5.8). Since the nonlocal terms as well as the renormalization term in the action (5.112) decrease with growing m, we find that the suppression of the tunneling process for large masses is weaker than it is for small masses.
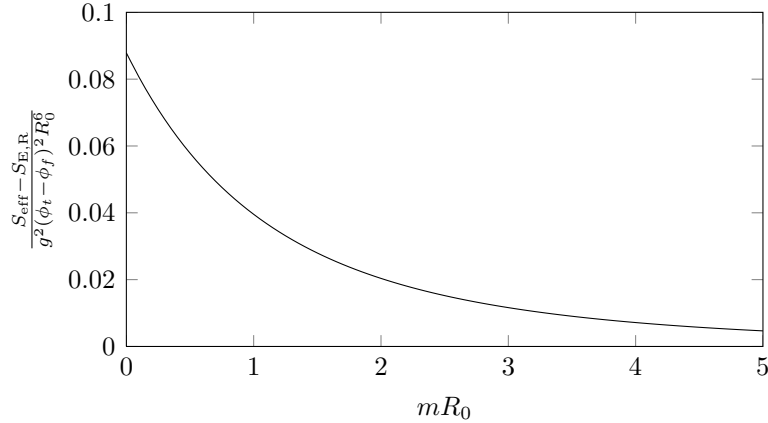
Figure 5.8: The system–environment interaction decreases with growing mass of the environmental field.

5.4.5 One-loop Corrections

So far we investigated a bilinear interaction between a quantum mechanical variable and an environmental field. In leading order WKB–expansion, the decay rate is suppressed due to dissipative effects. Here, we want to investigate corrections to the ground state energy from higher order WKB–approximation that contribute to the

decay probability. Expressing the action (5.109) in terms of the fields ϕ and ψ, we have

$$S_{\mathrm{E,R}} = S_{\mathrm{E},\phi} + S_{\mathrm{E,bath}} + S_{\mathrm{E,int}} + S_{\mathrm{E,ren}} \tag{5.118}$$

with

$$S_{\mathrm{E},\phi} = \int d^4x \left(\frac{1}{2}(\partial_\mu \phi)^2 + V(\phi) \right) \tag{5.119}$$

$$S_{\mathrm{E,bath}} = \frac{1}{2} \int d^4x (\partial_\mu \psi)^2 \tag{5.120}$$

$$S_{\mathrm{E,int}} = -g \int d^4x \phi\psi \tag{5.121}$$

$$S_{\mathrm{E,ren}} = -\frac{g^2}{2} \int d^4x \phi \Delta^{-1}\phi \,, \tag{5.122}$$

where we chose $m = 0$. The renormalization term (5.122) is similar to (5.110) and prevents the theory from becoming unstable due to the bilinear interaction. If this term were not present, the potential energy would become arbitrarily negative solely due to the measuring process of the field ϕ through the field ψ.

For $g = 0$ we know that the scalar field ϕ has an $O(4)$–invariant solution. Since the counterterm breaks this symmetry explicitly, the action (5.118) obeys only $O(3)$–invariance. The effective action for the scalar field ϕ is found by substituting

$$f_k(R) \to g\mathcal{V}\phi_{\pm\mathbf{k}} \tag{5.123}$$

in equation (5.113), where

$$\phi_{\mathbf{k}} = \frac{1}{\mathcal{V}} \int d^3x \phi(\mathbf{x},T) e^{-i\mathbf{kx}} \,. \tag{5.124}$$

We find

$$\begin{aligned}
S_{\mathrm{eff}} &= S_{\mathrm{E},\phi} + g^2\mathcal{V} \int dT' \int dT \sum_{\mathbf{k}} \frac{e^{-k|T-T'|}}{8k} \times \\
&\quad \times \left[\phi_{\mathbf{k}}(T) - \phi_{-\mathbf{k}}(T') \right] \left[\phi_{-\mathbf{k}}(T) - \phi_{\mathbf{k}}(T') \right]
\end{aligned} \tag{5.125}$$

and therefore

$$\begin{aligned}
S_{\mathrm{eff}} &= S_{\mathrm{E},\phi} + \frac{g^2}{(4\pi)^2} \int dT \int dT' \int dx^3 \int dy^3 \times \\
&\quad \times \left(\frac{\phi(|\mathbf{x}|,T)\phi(|\mathbf{y}|,T)}{|\mathbf{x}-\mathbf{y}|^2 + |T-T'|^2} - \frac{\phi(|\mathbf{x}|,T')\phi(|\mathbf{y}|,T)}{|\mathbf{x}+\mathbf{y}|^2 + |T-T'|^2} \right) ,
\end{aligned} \tag{5.126}$$

where we assumed $O(3)$–invariance of the field ϕ. The bounce goes from the false vacuum at time minus infinity to the false vacuum at time plus infinity

$$\lim_{T\to\pm\infty} \phi(|\mathbf{x}|, T) = \phi_f \tag{5.127}$$

and can be described in the thin wall approximation with a variable R, which was used in the preceding sections. R separates the true vacuum ϕ_t from the false vacuum ϕ_f. The corrected decay rate reads now

$$\Gamma = \frac{S_{\text{eff}}^2}{4\pi^2} \left| \frac{\text{Det}(\delta^2 \tilde{S}_{\text{eff}}/\delta\phi^2)}{\text{Det}'(\delta^2 S_{\text{eff}}/\delta\phi^2)} \right|^{1/2} \exp(-S_{\text{eff}}), \tag{5.128}$$

where the prime denotes, that the zero eigenvalues have been omitted and $\tilde{S}_{\text{eff}}$ is the action S_{eff} with $V(\phi)$ replaced by $V''(\phi_f)\phi^2/2$. We know from [74], that the second variation of S_{eff} has a negative eigenvalue for $g = 0$ which can be shown also for $g \neq 0$. We imbed the classical solution of the field equations $\bar{\phi}$ into a one–parameter family of functions

$$\phi_\lambda = \bar{\phi}(|\mathbf{x}|/\lambda, T/\lambda), \tag{5.129}$$

then we find

$$\begin{aligned} S_{\text{eff}}(\phi_\lambda) &= \lambda^2 \frac{1}{2} \int d^4x (\partial_\mu \bar{\phi})^2 + \lambda^4 \int d^4x V(\bar{\phi}) \\ &+ \lambda^6 \Lambda(\bar{\phi}), \end{aligned} \tag{5.130}$$

where the definition of Λ becomes obvious from equation (5.126). S_{eff} has to be stationary at $\lambda = 1$, since $\bar{\phi}$ is a solution of the equations of motion. With $dS_{\text{eff}}(\phi_\lambda)/d\lambda|_{\lambda=1} = 0$ we deduce

$$S_{\text{eff}}(\bar{\phi}) = \frac{1}{4} \int d^4x (\partial_\mu \bar{\phi})^2 - \frac{\Lambda(\bar{\phi})}{2} \tag{5.131}$$

and

$$\left. \frac{d^2 S_{\text{eff}}(\phi_\lambda)}{d\lambda^2} \right|_{\lambda=1} = -2 \int d^4x (\partial_\mu \bar{\phi})^2 + 12\Lambda(\bar{\phi}) \tag{5.132}$$

From (5.131) we know, that the effective action for the bounce is positive for $g = 0$ as well as for sufficient small g; and from (5.132) we know, that the second variation of S_{eff} has at least one negative eigenvalue under the same conditions. In order to

show that this is true for arbitrary g, we combine the embedding (5.129) and the expression (5.131) to

$$S_{\text{eff}}(\phi_\lambda) = \lambda^2 \frac{1}{4} \int d^4x (\partial_\mu \bar{\phi})^2 + \lambda^6 \frac{\Lambda(\bar{\phi})}{2} \,. \tag{5.133}$$

Varying with respect to λ leads to

$$S_{\text{eff}}(\bar{\phi}) = \frac{1}{6} \int d^4x (\partial_\mu \bar{\phi})^2 > 0 \,, \tag{5.134}$$

that is, the action is always positive though the potential is somewhere negative. For the second variation we deduce

$$\left. \frac{d^2 S_{\text{eff}}(\phi_\lambda)}{d\lambda^2} \right|_{\lambda=1} = -2 \int d^4x (\partial_\mu \bar{\phi})^2 < 0 \,, \tag{5.135}$$

that is, the second variation of the action has at least one negative eigenvalue for arbitrary g. Assuming that there is exactly one negative eigenvalue, we have a small imaginary contribution to the ground state energy which is exactly the decay probability per unit time.

5.5 Conclusions

We have discussed in various settings the behavior of vacuum tunneling in curved backgrounds. In particular the solutions concerning de Sitter space should be important for the investigation of the cosmic landscape.

Furthermore we included environmental degrees of freedom in order to investigate the quantum–to–classical transition. Using decoherence one may also justify the suppression of interferences of bounces in multibounce–configurations that are used in the dilute gas approximation. An analog situation would be the alpha–decay. The state vector is a superposition of different partial waves that are decohering due to the interaction between emitted particle and environment. If the decoherence process is weak, that is, for sufficiently small nucleation radii or small system-environment couplings, the intuitive picture of a particle moving along a tunneling trajectory might be misleading. We have chosen the interaction between system and environment to be linear in the environmental degrees of freedom, an assumption which has been applied to various models that can be described by a macroscopic variable [76]. The motivation behind this linear coupling is, that every single environmental degree of freedom is only weakly perturbed by the system. This does not mean that the effect on the system is weak, since infinitely many degrees of freedom are involved.

The specific form how the macroscopic variable enters the interaction was derived from a generic bilinear and locally Lorentz-invariant interaction between system field

and environmental field. In contrast to the treatment of decoherence in quantum mechanical models, we did not need to assume a particular form of the spectral density.

An aspect for future research addressing the tunneling in curved backgrounds could be the inclusion of one–loop corrections to the decay rate in a more explicit way than the formal functional determinants considered in [75].

6 Entanglement Generation via a Bosonic Heat Bath

The results presented in the following part of this thesis have been achieved in collaboration with Thomas Zell and Rochus Klesse.

6.1 Motivation

6.1.1 Entanglement as a Resource

In the preceding sections it has been stressed that entanglement between a system with a finite number of degrees of freedom and a reservoir with infinitely many degrees of freedom leads to a localization of the system variables. The central point of the process of decoherence is the *uncontrollable* entanglement between system and environment. In the following we want to investigate the generation of *controllable* entanglement which can be of use for quantum computing and quantum information processing.

It is well known that certain computational problems can be solved faster than with traditional algorithms by employing "quantum logic". Using Grover's algorithm [122] it is possible to find an item in a unsorted database with N entries in $\mathcal{O}(\sqrt{N})$ steps. Another prominent example is Shor's algorithm [123] for factoring an n-bit integer number using $\mathcal{O}(n^2)$ operations. In contrast, the best known classical algorithm, the so–called *number field sieve*, requires roughly $\exp(n^{1/3})$ operations. In other words, for some problems, quantum algorithms are exponentially faster than classical algorithms. As a proof of principle, Shor's algorithm has already been implemented on a quantum computer for factorizing the number 15 [124]. The key ingredient of Shor's quantum algorithm is the *quantum Fourier transformation* that is defined analogously to the discrete Fourier transformation. Due to the superposition principle it is possible to compute the quantum Fourier transformation of a state vector within a time that grows only polynomially with n, whereas the computing time of classical algorithms such as the *Fast Fourier Transform* grows as 2^n. For an overview of quantum algorithms, see e.g. [125].

Quantum cryptography allows secure information transmission [126], i.e. an eavesdropper cannot elicit any information from the transmitted quantum particles

without disturbing the information in such a way that the legitimate users notice his intervention. This secure information transmission has already been used for bank transfers [127].

Another interesting aspect is quantum teleportation of an unknown quantum state that can be implemented if two users are presharing a Bell state [128]. The original state is destroyed, otherwise teleportation would violate the no cloning theorem [129]. We want to state this example explicitly. Suppose two physicists, Alice and Bob, share the state of two perfectly entangled spins $|\psi\rangle = (|0\rangle_A|0\rangle_B + |1\rangle_A|1\rangle_B)/\sqrt{2}$, where 0 denotes "spin down" and 1 denotes "spin up" and the index denotes the owner of the component. The state which is in the possession of Alice and has to be teleported to Bob is of the form $|\phi\rangle = \alpha|0\rangle_A + \beta|1\rangle_A$. Alice applies to their qubits a so–called CNot gate, that is a unitary operation defined by $|\gamma\rangle|\delta\rangle \to |\gamma\rangle|\gamma \oplus \delta\rangle$, where $\oplus$ is the addition modulo 2. She then sends her first bit through an Hadamard gate defined by $|0\rangle \to (|0\rangle + |1\rangle)/\sqrt{2}$ and $|0\rangle \to (|0\rangle - |1\rangle)/\sqrt{2}$. Thus we have

$$|\psi\rangle|\phi\rangle \quad \longrightarrow \quad \frac{1}{2}\Bigg[|0\rangle_A|0\rangle_A(\alpha|0\rangle_B + \beta|1\rangle_B) + |0\rangle_A|1\rangle_A(\alpha|1\rangle_B + \beta|0\rangle_B)$$
$$+ |1\rangle_A|0\rangle_A(\alpha|0\rangle_B - \beta|1\rangle_B) + |1\rangle_A|1\rangle_A(\alpha|1\rangle_B - \beta|0\rangle_B)\Bigg] . (6.1)$$

Depending on Alice's measurements ($|0\rangle_A|0\rangle_A$, $|0\rangle_A|1\rangle_A$, $|1\rangle_A|0\rangle_A$ or $|1\rangle_A|1\rangle_A$), Bob will measure the corresponding outcome. Of course, in order to know the state in which he is, Alice has to tell Bob her measurement result. This prevents quantum teleportation from transmitting information faster than light. If Bob knows his quantum, he can apply the appropriate quantum gate in order to obtain Alice's state $|\phi\rangle = \alpha|0\rangle_A + \beta|1\rangle_A$.

6.1.2 Controllable vs. Uncontrollable Entanglement

The example discussed in the previous section did not involve any environmental degrees of freedom, which is obviously an idealization. Generally speaking, it is a difficult task to generate controllable entanglement between microscopic systems, e.g. spins, especially when they are spatially separated. On the one hand, the systems have to interact with each other in order to become entangled. On the other hand, they have to be shielded in order to avoid uncontrollable entanglement with the environment which leads to a localization of the systems.

In sections 4.4 and 5.4, we have seen explicitly that the efficiency of decoherence processes with respect to a system is determined by the distinguishability of different system states. For example, the localization rate of a macroscopic particle due to scattering processes depends on the distance in configuration space (see section 2.4), the localization rate of the effective two-state system which was discussed in section

4.4 depends on the separation of the local minima, and the off-diagonal elements of the reduced density matrix for the vacuum bubble discussed in section 5.4 decrease exponentially with increasing difference of the radii configurations of the bubbles.

During the last years, several authors have promoted that it should be possible to entangle systems that are coupled to the same heat bath and do not interact directly with each other [8, 9, 130, 131]. In other words, the interaction which generates the entanglement is solely determined by the coupling to a common environment. Entanglement between two two–level systems has been investigated in [8, 9, 130, 132–134], whereas entanglement of harmonic oscillators was the subject of discussion in [135–140].

Braun showed in [8] that the system-bath interaction leads to perfect entanglement of two qubits occupying the same position. He considered two spins with degenerate energy levels, and the heat bath was modeled by a collection of harmonic oscillators interacting bilinearly with the spins. The composite system can be solved exactly since it resembles a *dissipationless* two–spin boson model (see [78] for a review on the spin–boson model). Braun's theoretical model relies on two idealizing assumptions that cannot be met in general: since any eigendynamics of the spins is neglected (i.e. the energy levels are degenerate), the system does not exchange energy with the environment. Furthermore the spins are not spatially separated and no environmental mode with a finite wavelength is able to resolve the distance between the spins. However, Braun's results confirm that entanglement generation via a common heat bath might indeed be possible.

The author generalized the model in [130] where he investigated the entanglement generation of two spins that are coupled to the heat bath at different positions. Braun showed that the first maximum of entanglement appears after a period of time that scales with the third power of the spatial separation. For sufficiently large times, almost perfect entanglement can be generated, whereas for infinitely large times the entanglement vanishes. Dissipative effects are discarded in this generalized model as well.

This result is counterintuitive. Although both spins are strongly entangled with the bath (which should lead to a localization of the spin states), they are only weakly entangled with an individual bath mode. In other words, if the entanglement between a spin and N environmental degrees of freedom of the bath is of order γ, the entanglement with an individual bath mode should be of order γ/N. The generation of significant entanglement between the low–dimensional remote systems in the presence of infinitely many environmental modes is therefore doubtful. One may ask whether the findings of Braun rely on the disregard of dissipation. In the following we will pursue the study of dissipative effects on bath mediated entanglement of two remote systems.

This chapter is organized as follows. In section 6.2 we present different measures of

entanglement for bipartite systems. The generation of entanglement for two remote harmonic oscillators is discussed in 6.3 and a system involving two spins is the subject of section 6.4.

6.2 Entanglement Measures

Given a quantum state of a multi-partite system, it is in general very difficult to decide whether the subsystems are entangled with each other or not. Since we are interested in the entanglement of a bipartite system, we will restrict the discussion of entanglement measures to this case. For an extensive review of quantum entanglement, see [141].

Any bipartite *pure state* $|\Psi_{12}\rangle \in H_{12} = H_1 \otimes H_2$ is called *entangled* if and only if it cannot be written as a product of two vectors contained within the Hilbert spaces of the subsystems:

$$|\Psi_{12}\rangle = |\psi_1\rangle|\psi_2\rangle. \tag{6.2}$$

Expressed in terms of an orthonormal product basis $\{|e_1^i\rangle \otimes |e_2^i\rangle\}$, the state vectors reads

$$|\Psi_{12}\rangle = \sum_{i,j} A_{ij}|e_1^i\rangle \otimes |e_2^i\rangle. \tag{6.3}$$

The state is a product if and only if the matrix A_{ij} has a rank equal to 1.

Due to decoherence phenomena it is in practice impossible to prepare systems in pure states and one has to deal with *mixed states*. In those cases, it is generally much more difficult to define viable entanglement measures. It is useful to have a notion for *separable* states, i.e. unentangled configurations. Any bipartite state $\rho_{12} \in H_{12}$ is separable if and and only if it can be written as a convex combination of product states [142]:

$$\rho_{12} = \sum_i p_i \rho_1^i \otimes \rho_2^i, \tag{6.4}$$

where $\rho_1 \in H_1$ and $\rho_2 \in H_2$ are density matrices defined on the Hilbert spaces of the subsystems. The coefficients p_i are greater or equal to zero and add up to 1. Mixed states which cannot be written as a convex combination of product states are entangled.

6.2.1 The Positive Partial Transpose (PPT) Criterion

A strong criterion for identifying separable states has been proposed by Peres and Horodecki [143, 144]. It states that a bipartite mixed state is separable if the partially

transposed density matrix is a density operator. Expressing this statement in a fixed product basis, we say that the matrix

$$\langle m|\langle \mu|\rho_{12}^{T_2}|n\rangle|\nu\rangle \equiv \langle m|\langle \nu|\rho_{12}|n\rangle|\mu\rangle \tag{6.5}$$

has to be positive definite in order for ρ_{12} to be a separable state. This statement is independent of the chosen basis $\{|m\rangle, |n\rangle\}$. If the partial $\rho_{12}^{T_2}$ is positive definite, the density matrix can be written in the form (6.4). This condition is necessary and sufficient, if and only if $d_1 d_2 \leq 6$, where d_1 and d_2 are the dimensions of the systems [144]. In other words, for larger dimensions there can be entangled states whose partial transposed density matrix is positive definite.

6.2.2 Entanglement Measures for Spins and Oscillators

Vidal and Werner [145] used the Peres–Horodecki criterion to define entanglement measures. The first one is the *negativity*,

$$\mathcal{N}(\rho) \equiv \frac{||\rho_{12}^{T_2}||_1 - 1}{2} \tag{6.6}$$

which is equal to the absolute value of the sum of negative eigenvalues of the partial transposed density matrix $\rho_{12}^{T_2}$. In (6.6) we used the trace norm $||..||_1$. The negativity measures the partially transposed state's deviation from positive definiteness.

The second measure defined in [145] is the *logarithmic negativity*

$$\mathcal{E}(\rho) = \log_2 ||\rho_{12}^{T_2}||_1 \,. \tag{6.7}$$

Both measures do not increase under local operations and classical communication. In addition, the logarithmic negativity is an additive quantity.

The measures are useful in the context of information transfer based on nonlocal correlations [128]. Vidal and Werner showed that the negativity bounds the extent to which the state ρ_{12} can be used to perform quantum teleportation. The logarithmic negativity is an upper bound for the distillable entanglement contained in ρ_{12}, which is the amount of "almost" pure state entanglement that can be distilled from $\rho_{12}^{\otimes N}$, $N \to \infty$.

Although the measures are easy to compute for a system of two spins, they are clearly not viable for a bipartite system of harmonic oscillators with which we are dealing in section (6.3).

However, it is possible to derive from the Peres–Horodecki criterion a measure in the case of *Gaussian* oscillator states [146, 147]. This can be achieved by considering the covariance matrix which defines the Gaussian state up to a shift of the canonical variables. Since the covariance matrix can be defined for n oscillators, we will

consider this general case in the following. We start with the definition of the vector $R = (Q_1, ...Q_n, P_1, ..., P_n)$, where Q_i and P_i are the canonical variables of n harmonic oscillators which are chosen to be dimensionless. Gaussian states are uniquely defined by their first two moments which read

$$m_{1,i} = \text{Tr}(R_i \rho_{12}) \tag{6.8}$$

and

$$m_{2,ij} = \text{Tr}(R_i R_j \rho_{12}) \,. \tag{6.9}$$

The first moments, $m_{1,i}$, can always be eliminated by an appropriate shift of the canonical variables and will be set to zero in the following. Decomposing the second moments into commutators and anticommutators we have

$$
\begin{aligned}
\text{Tr}(R_i R_j \rho_{12}) &= \frac{1}{2}\text{Tr}(\{R_i, R_j\}\rho_{12}) + \frac{i}{2}\text{Tr}([R_i, R_j]\rho_{12}) \tag{6.10}\\
&= \frac{1}{2}\mathbf{Cov}_{ij} + \frac{i}{2}\sigma_{ij} \,, \tag{6.11}
\end{aligned}
$$

where the covariance matrix $\mathbf{Cov}$ is defined as the symmetric part of the second moments. The matrix σ is state-independent and given through the commutation relations of the canonical variables. For a single mode system, the covariance matrix reads

$$\mathbf{Cov} = \begin{pmatrix} 2\langle q^2 \rangle & \langle\{q,p\}\rangle \\ \langle\{q,p\}\rangle & 2\langle p^2 \rangle, \end{pmatrix} \tag{6.12}$$

which has to satisfy an uncertainty inequality, i.e.

$$\text{Det } \mathbf{Cov} = 4\langle q^2 \rangle\langle p^2 \rangle - \langle\{q,p\}\rangle^2 \geq 1 \,. \tag{6.13}$$

This $\text{Sp}(2, \mathbb{R})$–invariant condition is nothing else but the usual uncertainty inequality for hermitian operators. It follows from the Cauchy–Schwarz inequality for complex Hilbert spaces,

$$\text{Tr}(pq\rho)\text{Tr}(qp\rho) = \text{Tr}(\sqrt{\rho}pq\sqrt{\rho})\text{Tr}(\sqrt{\rho}qp\sqrt{\rho}) \leq \text{Tr}(p^2\rho)\text{Tr}(q^2\rho) \,, \tag{6.14}$$

where we used explicitly the positivity of the density matrix in order to write $\rho = \sqrt{\rho}\sqrt{\rho}$. Decomposing the product qp into a symmetric and antisymmetric part, the left hand side of (6.14) can be rewritten as

$$\text{Tr}(pq\rho)\text{Tr}(qp\rho) = \frac{1}{4}(\text{Tr}\{q,p\})^2 + \frac{1}{4} \,. \tag{6.15}$$

From this relation, together with (6.14), follows the uncertainty relation (6.13).

We turn again to the n–mode system. Unitary transformations generated by quadratic Hamiltonians act as symplectic transformations on the vector R [148],

$$U^\dagger R U = S R \,, \tag{6.16}$$

where $S \in \mathrm{Sp}(2n, \mathbb{R})$. For the second moments we find

$$
\begin{aligned}
\frac{1}{2}\mathbf{Cov}' + \frac{i}{2}\sigma' &\equiv \mathrm{Tr}(U^\dagger R R^T U \rho) \\
&= \mathrm{Tr}(S R R^T S^T \rho) \\
&= S\left(\frac{\mathbf{Cov}}{2} + \frac{i}{2}\sigma\right) S^T \\
&= S\,\frac{\mathbf{Cov}}{2}\,S^T + \frac{i}{2}\sigma \,,
\end{aligned}
\tag{6.17}
$$

where we used the invariance of σ under symplectic transformations in the last step.

It is obvious that, if a system defined through $\mathbf{Cov}$ is physically realizable, then so is $\mathbf{Cov}'$, since the uncertainty relation (6.13) is not affected by the symplectic transformation (6.17). The invertibility of S implies the inverse statement as well.

Furthermore it is guaranteed by Williamson's theorem [149, 150] that, for any symmetric positive $2n \times 2n$ matrix $\mathbf{Cov}$, there exists a symplectic S form such that

$$S\,\mathbf{Cov}\,S^T = \mathrm{diag}(\lambda_1, ..., \lambda_n, \lambda_1, ..., \lambda_n) \equiv \mathbf{Cov}_{\mathrm{diag}} \,. \tag{6.18}$$

This theorem implies, together with (6.13), that

$$\lambda_i \geq 1 \,, \quad i = 1, ..., n \,. \tag{6.19}$$

Note that, in general, a symplectic transformation is not a similarity transformation, therefore the eigenvalues of $\mathbf{Cov}$ and $\mathbf{Cov}'$ are different. However, the symplectic matrix acts on $\mathbf{Cov}\,\sigma$ as a similarity transformation. From equation (6.18) follows

$$\mathbf{Cov}_{\mathrm{diag}}\sigma = S\,\mathbf{Cov}\,S^T\sigma = S\,\mathbf{Cov}\,S^T\sigma S S^{-1} = S\,\mathbf{Cov}\,\sigma S^{-1} \,, \tag{6.20}$$

where we used, again, the invariance of σ under symplectic transformations. Since $\mathbf{Cov}_{\mathrm{diag}}\sigma$ takes an off-diagonal form, we consider the diagonal matrix

$$(\mathbf{Cov}_{\mathrm{diag}}\sigma)^2 = -\mathrm{diag}(\lambda_1^2, ..., \lambda_n^2, \lambda_1^2, ..., \lambda_n^2) \,. \tag{6.21}$$

In order to decide whether a state given by a covariance matrix is physically realizable, the eigenvalues of $-(\mathbf{Cov}\,\sigma)^2$ have to be greater than 1, since this matrix is related to $\mathbf{Cov}_{\mathrm{diag}}$ through a similarity transformation.

Now we are able to derive a measure for entanglement in the case of *two* harmonic oscillators. We consider the Wigner representation of the bipartite density matrix

$$W(Q_1, Q_2, P_1, P_2) = \tag{6.22}$$
$$= \frac{1}{(2\pi)^2} \int dQ'_1 dQ'_2 \left\langle Q_1 - \frac{Q'_1}{2}, Q_2 - \frac{Q'_2}{2} \middle| \rho \middle| Q_1 + \frac{Q'_1}{2}, Q_2 + \frac{Q'_2}{2} \right\rangle e^{iQ'_1 P_1 + iQ'_2 P_2}.$$

It follows, that the partial transpose operation on system 2 equals an inversion of the variable, $P_2 \to -P_2$. This corresponds to a "local time reversal" with respect to system 2,

$$R \to T_2 R, \quad T_2 = \text{diag}(1, 1, 1, -1). \tag{6.23}$$

The expectation value for the covariance matrix changes according to

$$\mathbf{Cov} \to T_2 \, \mathbf{Cov} \, T_2. \tag{6.24}$$

In order to represent a physically realizable state, the eigenvalues of the "local time–reversed" covariance matrix have to be greater than one. In contrast, if there are eigenvalues smaller than one, the original Gaussian state, defined through the covariance matrix $\mathbf{Cov}$, is *not* separable. This allows us to define an entanglement measure for a system of oscillators. Let λ_1 and λ_2 be the symplectic spectrum of the "locally time-reversed" covariance matrix of a Gaussian state. Then

$$\mathcal{E} = -\sum_{i=1}^{2} \log_2 \min(1, \lambda_i) \tag{6.25}$$

is the logarithmic negativity for the system of two oscillators.

Although the Peres criterion provides a useful entanglement measure for two qubits, we will use, in section (6.4), the *concurrence* which has been proven by Wootters to be a valid entanglement measure for two qubits [151]. It relies on the *entanglement of formation* which is defined as follows [152]. Given a density matrix ρ_{12} of a bipartite system, consider all pure–state decompositions of ρ_{12}, i.e. all ensembles of states $|\psi_i\rangle$ with probabilities p_i, such that

$$\rho_{12} = \sum_i p_i |\psi_i\rangle\langle\psi_i|. \tag{6.26}$$

For each pure state $|\psi\rangle\langle\psi|$, the entanglement E_N is defined as the von Neumann entropy of the respective subsystems,

$$E(\psi) = -\text{Tr}(\rho_1 \log_2 \rho_1) = -\text{Tr}(\rho_2 \log_2 \rho_2), \tag{6.27}$$

where $\rho_1 = \text{Tr}_2|\psi\rangle\langle\psi|$ and $\rho_2 = \text{Tr}_1|\psi\rangle\langle\psi|$. The entanglement of formation of the mixed state ρ_{12} is defined as the average entanglement of the pure states of the decomposition, minimized over all decompositions of ρ,

$$E(\rho) = \min \sum_i p_i E(\psi_i). \tag{6.28}$$

Wootters showed that in the case of two spins, (6.28) is equal to the expression

$$F(\mathcal{C}) = h\left(\frac{1 + \sqrt{1 - C^2}}{2}\right), \tag{6.29}$$

$$h(x) = -x \log_2 x - (1 - x) \log_2(1 - x) \tag{6.30}$$

with the concurrence

$$\mathcal{C} = \max\left\{0, \lambda_1 - \lambda_2 - \lambda_3 - \lambda_4\right\}. \tag{6.31}$$

The λ_i are the eigenvalues, in decreasing order, of the Hermitian matrix $R = \sqrt{\sqrt{\rho_{\text{sys}}}\tilde{\rho}_{\text{sys}}\sqrt{\rho_{\text{sys}}}}$ and

$$\tilde{\rho}_{\text{sys}} = (\sigma_y \otimes \sigma_y)\, \rho_{\text{sys}}^*\, (\sigma_y \otimes \sigma_y). \tag{6.32}$$

The star denotes complex conjugation and the matrix σ_y reads

$$\sigma_y = i|0\rangle\langle 1| - i|1\rangle\langle 0| \tag{6.33}$$

in the σ_z-eigenbasis. Since the function F is monotonically increasing from 0 to 1 as the concurrence goes from 0 to 1, the latter can be chosen as a viable measure of entanglement.

6.3 Entanglement of Harmonic Oscillators via a Common Heat Bath

6.3.1 The Exact Model

Since the dissipative two–spin boson model is not exactly solvable, we will focus here on a system of two harmonic oscillators coupled to a heat bath. One may argue that, for low temperatures, the oscillators resemble spins in a good approximation if only the two lowest levels are significantly populated [153]. To begin with, we derive the quantum mechanical setup from a generalization of a field theoretical model which was first analyzed by Unruh and Zurek in [29]. Although the solution of the model can be given explicitly in an integral representation, the analytical

expressions cannot be easily interpreted. Thomas Zell evaluated the integrals by applying numerical methods, see [154, 155]. In sections 6.3.2 and 6.3.3 we will discuss an analytic approximation of the model which is valid under certain restrictions.

The field theoretical model is given by two harmonic oscillators interacting with a massless scalar field. The Lagrangian has the form

$$
\begin{aligned}
L \;=\; & \frac{1}{2} \sum_{i=1,2} \left(\dot{Q}_i^2 - \Omega_0^2 Q_i^2 \right) + \frac{1}{2} \int d^3x \left(\dot{\phi}^2 - (\nabla\phi)^2 \right) \\
+ \; & g \int d^3x \dot{\phi}(\mathbf{x}) \left(\delta\left(\mathbf{x} - \frac{\mathbf{r}}{2}\right) Q_1 + \delta\left(\mathbf{x} + \frac{\mathbf{r}}{2}\right) Q_2 \right) .
\end{aligned}
\tag{6.34}
$$

The oscillators with canonical variables $Q_{1/2}$ and $P_{1/2}$ are coupled bilinearly to a field at positions $\pm\mathbf{r}/2$, where g denotes the coupling constant. Although the notation suggests a three-dimensional setup, we will consider this model also in the one-dimensional case. Note that the masses of the oscillators have been set to unity.

Since the oscillators are coupled to the "velocity" of the scalar field, the positivity of the corresponding Hamiltonian is ensured,

$$
H = \frac{1}{2} \int d^3x \left(\dot{\phi}^2 + (\nabla\phi)^2 \right) + \frac{1}{2} \sum_{i=1,2} \left(\dot{Q}_i^2 + \Omega_0^2 Q_i^2 \right) .
\tag{6.35}
$$

The environmental field can be expanded according to

$$
\phi(\mathbf{x}) = \frac{1}{\mathcal{V}^{1/2}} \sum_{\mathbf{k}} \phi_{\mathbf{k}} e^{i\mathbf{k}\mathbf{x}} ,
\tag{6.36}
$$

where $\mathcal{V}$ is the quantization volume. We find

$$
L = L_{\text{sys}} + L_{\text{bath}} + L_{\text{int}}
\tag{6.37}
$$

with

$$
L_{\text{bath}} \;=\; \frac{1}{2} \sum_{\mathbf{k}} \left(\dot{\phi}_{\mathbf{k}} \dot{\phi}_{-\mathbf{k}} - \omega_k^2 \phi_{\mathbf{k}} \phi_{-\mathbf{k}} \right)
\tag{6.38}
$$

$$
L_{\text{sys}} \;=\; \frac{1}{2} \sum_{i=1,2} \left(\dot{Q}_i^2 - \Omega_0^2 Q_i^2 \right)
\tag{6.39}
$$

$$
L_{\text{int}} \;=\; \frac{g}{\mathcal{V}^{1/2}} \sum_{\mathbf{k}} \dot{\phi}_{\mathbf{k}} \left(e^{i\frac{\mathbf{k}\mathbf{r}}{2}} Q_1 + e^{-i\frac{\mathbf{k}\mathbf{r}}{2}} Q_2 \right) .
\tag{6.40}
$$

The field is assumed to be massless (photons), thus $\omega_k = k$. The delta function appearing in (6.34) leads to divergences in the bath correlators of the field ϕ. In

order to avoid these, we introduce a cutoff in the spectral densities. This corresponds to a smearing out of the delta function, that is

$$\delta(\mathbf{x}) \to f(\mathbf{x}) , \tag{6.41}$$

where the function f is peaked around the origin with a finite width δx. The position of the harmonic oscillators is measured by the field with an accuracy of δx which defines the cutoff for the field modes to be $\Omega_c \sim 1/\delta x$. Alternatively, we may state the interaction (6.40) in the form

$$L_{\text{int}} = \frac{1}{\mathcal{V}^{1/2}} \sum_{\mathbf{k}} g_k \dot{\phi}_{\mathbf{k}} \left(e^{i\frac{\mathbf{kr}}{2}} Q_1 + e^{-i\frac{\mathbf{kr}}{2}} Q_2 \right) \tag{6.42}$$

where we introduced a *mode dependent* coupling,

$$g_k = g \int d^3 x e^{i\mathbf{kx}} f(\mathbf{x}) \tag{6.43}$$

with $k = |\mathbf{k}|$. The g_k decrease exponentially around $\omega_k = \Omega_c$. This corresponds to the introduction of a spectral density $J(k)$ with a cutoff around $k \sim \Omega_c$. We will specify the shape of $J(k)$ below.

Applying a Legendre transformation to (6.37), we find the Hamiltonian

$$H = H_{\text{sys}} + H_{\text{bath}} + H_{\text{int}} + H_{\text{count}} \tag{6.44}$$

with

$$H_{\text{bath}} = \frac{1}{2} \sum_{\mathbf{k}} \left(\Pi_{\mathbf{k}} \Pi_{-\mathbf{k}} + \omega_k^2 \phi_{\mathbf{k}} \phi_{-\mathbf{k}} \right) , \tag{6.45}$$

$$H_{\text{sys}} = \frac{1}{2} \sum_{i=1,2} \left(P_i^2 + \Omega_0^2 Q_i^2 \right) , \tag{6.46}$$

$$H_{\text{int}} = -\frac{1}{\mathcal{V}^{1/2}} \sum_{\mathbf{k}} g_k \Pi_{\mathbf{k}} \left(e^{-i\frac{\mathbf{kr}}{2}} Q_1 + e^{i\frac{\mathbf{kr}}{2}} Q_2 \right) , \tag{6.47}$$

$$H_{\text{count}} = \frac{1}{2\mathcal{V}} \sum_{\mathbf{k}} g_k^2 \left(e^{-i\frac{\mathbf{kr}}{2}} Q_1 + e^{i\frac{\mathbf{kr}}{2}} Q_2 \right) \left(e^{i\frac{\mathbf{kr}}{2}} Q_1 + e^{-i\frac{\mathbf{kr}}{2}} Q_2 \right) . \tag{6.48}$$

The canonical momenta are given by

$$P_i = \dot{Q}_i \tag{6.49}$$

$$\Pi_{\mathbf{k}} = \dot{\phi}_{-\mathbf{k}} + \frac{g_k}{\mathcal{V}^{1/2}} \left(e^{i\frac{\mathbf{kr}}{2}} Q_1 + e^{-i\frac{\mathbf{kr}}{2}} Q_2 \right) , \tag{6.50}$$

where the counterterm H_{count} ensures the positive definiteness of the full Hamiltonian and avoids "runaway" solutions of the equations of motion. Without this counterterm,

direct couplings proportional to $Q_1(t)Q_2(t)$ would spoil the indirect coupling of the oscillators.

It is a straightforward task to derive the Heisenberg equations of motion for the environmental modes and the system oscillators

$$\ddot{\phi}_{\mathbf{k}}(t) + \omega_k^2 \phi_{\mathbf{k}}(t) + \frac{g_k}{\mathcal{V}^{1/2}} \left(e^{-i\frac{\mathbf{kr}}{2}} \dot{Q}_1(t) + e^{i\frac{\mathbf{kr}}{2}} \dot{Q}_2(t) \right) = 0 \,, \qquad (6.51)$$

$$\ddot{Q}_1(t) + \Omega_0^2 Q_1(t) - \frac{1}{\mathcal{V}^{1/2}} \sum_{\mathbf{k}} g_k \dot{\phi}_{\mathbf{k}}(t) e^{i\frac{\mathbf{kr}}{2}} = 0 \,, \qquad (6.52)$$

$$\ddot{Q}_2(t) + \Omega_0^2 Q_2(t) - \frac{1}{\mathcal{V}^{1/2}} \sum_{\mathbf{k}} g_k \dot{\phi}_{\mathbf{k}}(t) e^{-i\frac{\mathbf{kr}}{2}} = 0 \,. \qquad (6.53)$$

The differential equation (6.51) determines the temporal evolution of a particular field mode and has the solution

$$\phi_{\mathbf{k}}(t) = \phi_{\mathbf{k},\mathrm{hom}}(t) - \frac{1}{\mathcal{V}^{1/2}} \frac{g_k}{\omega_k} \int_0^t ds \sin(\omega_k(t-s)) \left(e^{-i\frac{\mathbf{kr}}{2}} \dot{Q}_1(s) + e^{i\frac{\mathbf{kr}}{2}} \dot{Q}_2(s) \right) \,, (6.54)$$

where $\phi_{\mathbf{k},\mathrm{hom}}(t)$ solves the homogeneous part of the equation.

Substituting the field variables in equations (6.52) and (6.53), we arrive at the quantum Langevin equations

$$\ddot{Q}_1(t) + \Omega_0^2 Q_1(t) = \frac{1}{\mathcal{V}^{1/2}} \sum_{\mathbf{k}} g_k \Pi_{\mathbf{k},\mathrm{hom}}(t) e^{-i\frac{\mathbf{kr}}{2}} \qquad (6.55)$$

$$- \frac{1}{\mathcal{V}} \sum_{\mathbf{k}} g_k^2 \frac{d}{dt} \int_0^t ds \cos(\omega_k(t-s)) \left(Q_1(s) + e^{i\mathbf{kr}} Q_2(s) \right)$$

and

$$\ddot{Q}_2(t) + \Omega_0^2 Q_2(t) = \frac{1}{\mathcal{V}^{1/2}} \sum_{\mathbf{k}} g_k \Pi_{\mathbf{k},\mathrm{hom}}(t) e^{i\frac{\mathbf{kr}}{2}} \qquad (6.56)$$

$$- \frac{1}{\mathcal{V}} \sum_{\mathbf{k}} g_k^2 \frac{d}{dt} \int_0^t ds \cos(\omega_k(t-s)) \left(e^{-i\mathbf{kr}} Q_1(s) + Q_2(s) \right) \,,$$

with the homogeneous field momenta

$$\Pi_{\mathbf{k},\mathrm{hom}}(t) = \dot{\phi}_{-\mathbf{k},\mathrm{hom}}(t) + \frac{1}{\mathcal{V}^{1/2}} g_k \cos(\omega_k t) \left[Q_1(0) e^{i\frac{\mathbf{kr}}{2}} + Q_2(0) e^{-i\frac{\mathbf{kr}}{2}} \right] \,. \qquad (6.57)$$

The specific form of $\Pi_{\mathbf{k},\mathrm{hom}}(t)$ can be derived from the following requirements. First, it has to coincide with the Schrödinger momenta $\Pi_{\mathbf{k}}$ for $t = 0$ since the inhomogeneous part of the Heisenberg momenta then vanishes. Second, it has to oscillate with the

frequency ω_k since it has to obey the same time dependence as $\phi_{\mathbf{k},\text{hom}}(t)$. Expressing the homogeneous field operators in terms of creation and annihilation operators leads to

$$\phi_{\mathbf{k},\text{hom}}(t) = \frac{1}{\sqrt{2\omega_k}}(a_{\mathbf{k}}e^{-i\omega_k t} + a_{-\mathbf{k}}^{\dagger}e^{i\omega_k t}) \tag{6.58}$$

$$\Pi_{\mathbf{k},\text{hom}}(t) = -i\sqrt{\frac{\omega_k}{2}}(a_{\mathbf{k}}e^{-i\omega_k t} - a_{-\mathbf{k}}^{\dagger}e^{i\omega_k t}). \tag{6.59}$$

The first terms on the right hand sides of equations (6.55) and (6.56) correspond to classical stochastic forces acting on the oscillators. The nonlocal memory terms contain the back-reaction of the oscillators on the bath and a bath-mediated retarded interaction which couples the oscillators to each other.

Before we state the formal solution of the quantum Langevin equations, we want to show that an equivalent set of integro–differential equations can be derived if one considers a bilinear coupling between the system oscillators and the *position* variables of the environmental field. This can be achieved by applying the canonical transformation $\phi_{\mathbf{k}} \to -\tilde{\Pi}_{-\mathbf{k}}/\omega_k$ and $\Pi_{\mathbf{k}} \to \tilde{\phi}_{-\mathbf{k}}\omega_k$ to the Hamiltonian (6.44). In the case of a one–dimensional setup, we find exactly the Hamiltonian which was presented in [154]. However, the counterterms (6.48) had to be assumed there in order to avoid a direct coupling of the oscillators. In contrast, the appearance of those terms is now justified by the field theoretic model (6.34).

The resulting equations of motion read, after the canonical transformation,

$$\ddot{Q}_1(t) + \Omega_0^2 Q_1(t) = \frac{1}{\mathcal{V}^{1/2}}\sum_{\mathbf{k}} g_k\omega_k\tilde{\phi}_{\mathbf{k},\text{hom}}(t)e^{i\frac{\mathbf{kr}}{2}} \tag{6.60}$$

$$-\frac{1}{\mathcal{V}}\sum_{\mathbf{k}} g_k^2\frac{d}{dt}\int_0^t ds\,\cos(\omega_k(t-s))\left(Q_1(s) + e^{i\mathbf{kr}}Q_2(s)\right)$$

and

$$\ddot{Q}_2(t) + \Omega_0^2 Q_2(t) = \frac{1}{\mathcal{V}^{1/2}}\sum_{\mathbf{k}} g_k\omega_k\tilde{\phi}_{\mathbf{k},\text{hom}}(t)e^{-i\frac{\mathbf{kr}}{2}} \tag{6.61}$$

$$-\frac{1}{\mathcal{V}}\sum_{\mathbf{k}} g_k^2\frac{d}{dt}\int_0^t ds\,\cos(\omega_k(t-s))\left(e^{-i\mathbf{kr}}Q_1(s) + Q_2(s)\right),$$

where the homogeneous fields $\tilde{\phi}_{\mathbf{k},\text{hom}}(t)$ and their corresponding momenta are given by expressions (6.58) and (6.59). Inverting the canonical transformation, $\tilde{\phi}_{\mathbf{k},\text{hom}}(t) \to \tilde{\Pi}_{-\mathbf{k},\text{hom}}(t)/\omega_k$, shows the equivalence to (6.55) and (6.56).

The quantum Langevin equations can be written in matrix form, i.e.

$$\dot{\mathbf{R}}(t) + \mathbf{Z}\mathbf{R}(t) + \frac{d}{dt}\int_0^t ds\,\mathbf{C}(t-s)\mathbf{R}(s) = \mathbf{B}(t), \tag{6.62}$$

where $\mathbf{R} = (Q_1, Q_2, P_1, P_2)$, $\mathbf{B} = (0, 0, B(\mathbf{r}/2, t), B(-\mathbf{r}/2, t))$. The matrices are defined as

$$
\mathbf{Z} = \begin{pmatrix} 0 & 0 & -1 & 0 \\ 0 & 0 & 0 & -1 \\ \Omega_0^2 & 0 & 0 & 0 \\ 0 & \Omega_0^2 & 0 & 0 \end{pmatrix}, \quad \mathbf{C}(t) = \begin{pmatrix} 0 & 0 & 0 & 0 \\ 0 & 0 & 0 & 0 \\ C(t,0) & C(t,r) & 0 & 0 \\ C(t,r) & C(t,0) & 0 & 0 \end{pmatrix}, \tag{6.63}
$$

with

$$
B(\mathbf{r}/2, t) = \frac{1}{\mathcal{V}^{1/2}} \sum_{\mathbf{k}} g_k \Pi_{\mathbf{k},\text{hom}}(t) e^{-i\frac{\mathbf{kr}}{2}} \tag{6.64}
$$

and

$$
C(t,r) = \frac{1}{\mathcal{V}} \sum_{\mathbf{k}} g_k^2 \cos(\omega_k t) e^{i\mathbf{kr}} . \tag{6.65}
$$

Then, the solution $\mathbf{R}(t)$ of equation (6.62) for initial $\mathbf{R}(0)$ and inhomogeneity $\mathbf{B}(t)$ is

$$
\mathbf{R}(t) = \mathbf{G}(t)\mathbf{R}(0) + \int_0^t ds \, \mathbf{G}(t-s)\mathbf{B}(s) , \tag{6.66}
$$

where the Green's function $\mathbf{G}(t)$ solves the homogeneous part of equation (6.62). Assuming that at $t = 0$ the total state factorizes in an initial oscillator state ρ_{sys} and a thermal state ρ_{bath} for the environment, the time evolution of the covariance matrix reads

$$
\mathbf{Cov}(t) = \mathbf{G}(t)\mathbf{Cov}(0)\mathbf{G}^\dagger(t) + \int_0^t ds \int_0^t ds' \, \mathbf{G}(t-s)\mathbf{K}(s-s')\mathbf{G}(t-s')^\dagger . \tag{6.67}
$$

The matrix $\mathbf{K}(t)$ contains the bath correlators and has the nonvanishing entries $K_{34}(t) = K_{43}(t) = K(r,t)$ and $K_{33}(t) = K_{44}(t) = K(0,t)$ which read, in the three–dimensional setting,

$$
K(r,t) = \langle \{B(\mathbf{r}/2, t), B(-\mathbf{r}/2, 0)\} \rangle_{\rho_{\text{bath}}} . \tag{6.68}
$$

In order to derive the model in one dimension, the quantization volume $\mathcal{V}$ has to be replaced by a quantization length $\mathcal{L}$ and $g_k \to h_k$ in all foregoing equations.

The explicit form of $C(t,r)$ and $K(r,t)$ for one and three dimensions will be derived using the one–dimensional spectral density

$$
J^{1D}(\omega) = \frac{1}{2\mathcal{L}} \sum_{k>0} h_k^2 \delta(\omega - \omega_k)\omega_k . \tag{6.69}
$$

The h_k can be related to the g_k by demanding that the overall coupling strength between oscillators and the field is the same, i.e.

$$\frac{1}{\mathcal{V}} \sum_{\mathbf{k}} g_k^2 = \frac{1}{\mathcal{L}} \sum_{k} h_k^2 \,. \tag{6.70}$$

Assuming that $g_k \propto \Theta(k - \Omega_c)$ and $h_k \propto \Theta(k - \Omega_c)$, we find

$$g_k^2 \approx \frac{6\pi}{\Omega_c^2} h_k^2 \,, \tag{6.71}$$

where the sums have been replaced by integrals according to

$$\sum_{k} \rightarrow \frac{\mathcal{L}}{2\pi} \int dk \quad \text{and} \quad \sum_{\mathbf{k}} \rightarrow \frac{\mathcal{V}}{(2\pi)^3} \int d^3k \,. \tag{6.72}$$

From here follow the bath correlators

$$K(r,t) = \begin{cases} 4 \int_0^\infty d\omega\, J^{1D}(\omega) \cos(\omega r) \cos(\omega t) \coth\left(\frac{\omega}{2T}\right) & \text{for D=1} \\ 4 \int_0^\infty d\omega\, J^{3D}(\omega) \frac{\sin(\omega r)}{\omega r} \cos(\omega t) \coth\left(\frac{\omega}{2T}\right) & \text{for D=3} \,, \end{cases}$$

with $J^{3D}(\omega) = 3 J^{1D}(\omega) \left(\frac{\omega}{\Omega_c}\right)^2$. The damping kernels have the form

$$C(r,t) = \begin{cases} 4 \int_0^\infty d\omega\, J^{1D}(\omega) \cos(\omega r) \cos(\omega t) & \text{for D=1} \\ 4 \int_0^\infty d\omega\, \frac{J^{3D}(\omega)}{\omega} \frac{\sin(r)}{\omega r} \cos(\omega t) & \text{for D=3} \,. \end{cases}$$

For a heat bath without boundary conditions we define the spectral density to be

$$J^{1D}(\omega) = \frac{1}{2\mathcal{L}} \sum_{k>0} h_k^2 \delta(\omega - \omega_k) \omega_k \equiv \frac{2\gamma}{\pi} \omega \left(\frac{\omega}{\Omega_c}\right)^{s-1} e^{-\frac{\omega}{\Omega_c}} \,, \tag{6.73}$$

where γ is the coupling strength with dimension of a mass and s is the spectral index.
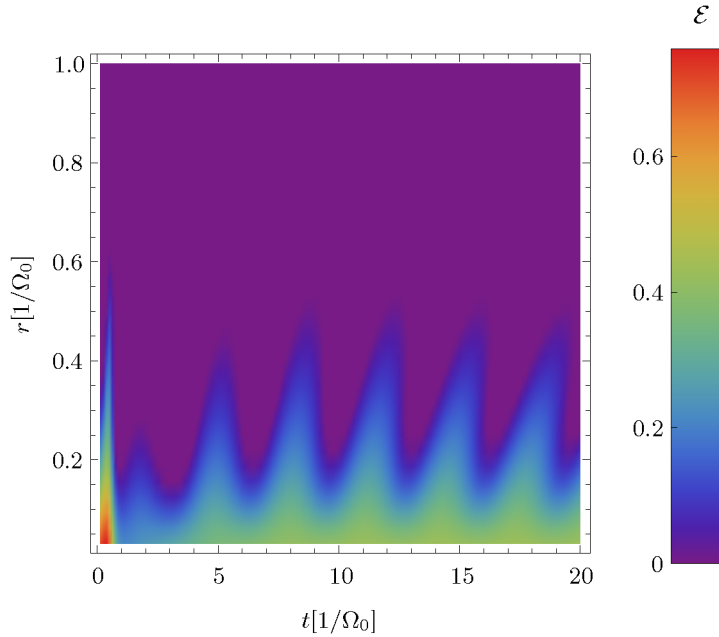
Figure 6.1: The generation of entanglement via a three–dimensional heat bath depends strongly on the distance. If the spatial separation exceeds a critical distance, the generated entanglement vanishes. We chose the parameters to be $\Omega_c = 10\,\Omega_0$, $\gamma = \Omega_0$, and $s = 1$. Initially, the system oscillators are in the ground state.

After applying numerical methods [155] one obtains the temporal evolution of entanglement. In fig. 6.1 we show the entanglement generation for a three–dimensional heat bath. The generated entanglement vanishes above a critical distance, i.e. entanglement generation via a bosonic heat bath is only viable for small spatial separations of the oscillators. For infinite times one observes below a critical distance nonvanishing asymptotic entanglement. In fig. 6.2 we depict the cutoff dependence of the critical distance where the heat bath is chosen to be one–dimensional. The critical distance decreases with increasing cutoff Ω_c which is usually of the order of the inverse size of the quantum systems. Since, when the Ω_c increases, more environmental modes contribute to decoherence and dissipation, the decrease of the critical distance is not surprising.

The appeareance of a critical distance which is roughly of the order of the inverse cutoff shows up in all numerical simulations. Thus, it seems to be very difficult to establish entanglement when the separation of the spins is larger than the inverse cutoff frequency $1/\Omega_c$.

However, as we will show in the following, the generation of entanglement can be enhanced significantly if the bath is subject to nontrivial boundary conditions.

Critical distance of the asymptotic entanglement
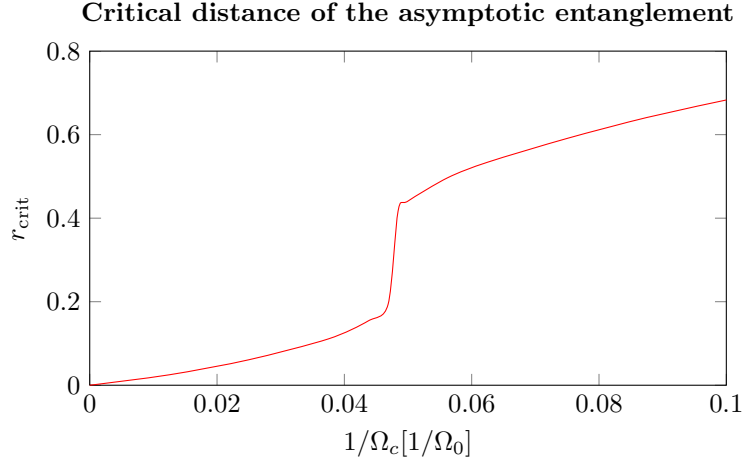
Figure 6.2: The critical distance of the asymptotic entanglement is roughly inverse proportional to the cutoff. We chose spectral index to be $s = 1$.

Van Hove Singularities

It has been shown by van Hove [156] that the spectral density of phonons in a crystal has analytic singularities. The nature of these singularities depends on the spatial geometry in determines the boundary conditions of the phonon bath.

As illustration, consider photons which are confined between two plates parallel to the $x - y$-plane. Due to the finite distance d between the plates, the standing wave-vectors are of the form $\mathbf{k} = k_x\mathbf{e}_x + k_y\mathbf{e}_y + (2\pi n/d)\mathbf{e}_z$. In contrast to k_x and k_y which can adopt all possible values, $k_z = 2\pi n/d$ can only adopt discrete values. This translates into singularities in the spectral density. For simplicity we assume that there is only a single van Hove singularity at frequency ω_0 which is determined by the largest possible wavelength. If the system is two–dimensional, the spectral density exhibits a logarithmic divergence around a frequency ω_0, whereas a one–dimensional system has a singularity of the form $1/\sqrt{\omega^2 - \omega_0^2}$.

We will show that these special spectral densities lead to an enhancement of entanglement compared to bath modes that are not subject to boundary conditions.

A one–dimensional system can be established if the environmental modes are trapped in a long hollow tube, whose diameter determines the position of the peak. We derive the one–dimensional van Hove spectral density from the continuum limit of the three–dimensional correlator $C(0,0)$, that is

$$C(0,0) = \frac{6}{\Omega_c^2} \int_0^\infty d\omega\, \omega J(\omega) = \frac{4\pi}{(2\pi)^3} \int_0^\infty dk k^2 g_k^2. \tag{6.74}$$

Now we impose boundary conditions on the bath modes. In the case of a hollow tube with length $\mathcal{L}$ and a quadratic cross section with side length a, we have $\mathcal{V} = a^2\mathcal{L}$.

We can decompose the vector $\mathbf{k}$ into the components

$$\mathbf{k} = k_{\mathcal{L}}\mathbf{e}_{\mathcal{L}} + k_x\mathbf{e}_x + k_y\mathbf{e}_y \,. \tag{6.75}$$

So we can write

$$C(0,0) = \frac{1}{(2\pi)^3} \lim_{k_{\max}\to\infty} \int_{-k_{\max}}^{k_{\max}} dk_{\mathcal{L}} \int_{-k_{\mathcal{L}}}^{k_{\mathcal{L}}} dk_x \int_{-\sqrt{k_{\mathcal{L}}^2-k_x^2}}^{\sqrt{k_{\mathcal{L}}^2-k_x^2}} dk_y g_k^2 \,. \tag{6.76}$$

Changing the integration variable $k_{\mathcal{L}}$ to $k = \sqrt{k_{\mathcal{L}}^2 + k_x^2 + k_y^2}$, we find

$$C(0,0) = \frac{1}{(2\pi)^3} \lim_{k_{\max}\to\infty} \int_{-k_{\max}}^{k_{\max}} dk \int_{-k}^{k} dk_x \int_{-\sqrt{k^2-k_x^2}}^{\sqrt{k^2-k_x^2}} \frac{dk_y\, k g_k^2}{\sqrt{k^2 - k_x^2 - k_y^2}} \,. \tag{6.77}$$

It is obvious that the expression (6.77) is equal to (6.74) in the limit of infinite a. However, due to the boundary conditions we have to replace the integral over k_x and k_y by a discrete sums,

$$C(0,0) = \frac{1}{2\pi a^2} \lim_{k_{\max}\to\infty} \int_{-k_{\max}}^{k_{\max}} dk \sum_{-\sigma_k \leq n_x}^{\sigma_k} \sum_{-\sqrt{\sigma_k^2-n_x^2}\leq n_y}^{\sqrt{\sigma_k^2-n_x^2}} \frac{g_k^2\Theta(1 - (\frac{n_x}{\sigma_k})^2 - (\frac{n_y}{\sigma_k})^2)}{\sqrt{1 - (\frac{n_x}{\sigma_k})^2 - (\frac{n_y}{\sigma_k})^2}} \tag{6.78}$$

with $\sigma_k = ka/(2\pi)$. Assuming that, at low temperatures, only the first peak is important and comparing with (6.3.1), we find

$$C_{\mathrm{vH}}(0,0) = \frac{6}{\Omega_c^2} \int_0^\infty d\omega\, \omega J_{\mathrm{vH}}(\omega) \,, \tag{6.79}$$

with

$$\begin{aligned} J_{\mathrm{vH}}(\omega) &= \frac{1}{\mathcal{L}} \sum_{k>\omega_0} \frac{\omega_0^2}{\sqrt{k^2 - \omega_0^2}} h_k^2 \delta(\omega - k) \\ &= \frac{2\gamma}{\pi}\Theta(\omega - \omega_0)\frac{\omega_0^2}{\sqrt{\omega^2 - \omega_0^2}} \left(\frac{\omega}{\Omega_c}\right)^{s-1} e^{-\frac{\omega}{\Omega_c}} \,, \end{aligned} \tag{6.80}$$

where we used $\omega_k = k$, $\omega_0 = 2\pi/a$ and absorbed constant factors of $\mathcal{O}(1)$ in the coupling strength γ. The spectral density (6.80) vanishes for $\omega < \omega_0$ and a significant fraction of the spectral weight is concentrated in the small region given by $\omega_0 < \omega < \omega_0 + \delta\omega$.

6.3.2 The Generic Toy Model

Due to the occurrence of a van Hove singularity in the spectral density (6.80) of an effectively *one–dimensional* system, we will obtain in the following an approximate solution of the model discussed in section 6.3. The tube model starting from the *three–dimensional* setup will be discussed in section 6.3.3.

In one dimension we can decompose the Hamiltonian (6.44) with respect to symmetric and antisymmetric modes of the environment and the system oscillators. Replacing $h_k \to h_k/2$ and using the variables

$$Q_S = \frac{(Q_1 + Q_2)}{\sqrt{2}}, \quad P_S = \frac{(P_1 + P_2)}{\sqrt{2}}, \tag{6.81}$$

$$Q_A = \frac{(Q_1 - Q_2)}{\sqrt{2}}, \quad P_S = \frac{(P_1 - P_2)}{\sqrt{2}}, \tag{6.82}$$

$$q_{k,S} = \frac{\phi_k + \phi_{-k}}{\sqrt{2}}, \quad p_{k,S} = \frac{\Pi_k + \Pi_{-k}}{\sqrt{2}}, \tag{6.83}$$

$$q_{k,A} = i\frac{\phi_k - \phi_{-k}}{\sqrt{2}}, \quad p_{k,A} = -i\frac{\Pi_k - \Pi_{-k}}{\sqrt{2}}, \tag{6.84}$$

we find the Hamiltonian

$$H = H_{\text{sys}} + \sum_{k>0} \left(H_{\text{bath},k} + H_{\text{int},k} + H_{\text{count},k} \right), \tag{6.85}$$

with

$$H_{\text{sys}} = \frac{1}{2} \left(P_S^2 + \Omega_0^2 Q_S^2 + P_A^2 + \Omega_0^2 Q_A^2 \right), \tag{6.86}$$

$$H_{\text{count},k} = \frac{h_k^2}{2\mathcal{L}} \cos^2\left(\frac{kr}{2}\right) Q_S^2 + \frac{h_k^2}{2\mathcal{L}} \sin^2\left(\frac{kr}{2}\right) Q_A^2, \tag{6.87}$$

$$H_{\text{bath},k} = \frac{1}{2} \left(p_{k,S}^2 + \omega_k^2 q_{k,S}^2 + p_{k,A}^2 + \omega_k^2 q_{k,A}^2 \right), \tag{6.88}$$

$$H_{\text{int},k} = -\frac{h_k}{\mathcal{L}^{1/2}} \cos\left(\frac{kr}{2}\right) p_{k,S} Q_S - \frac{h_k}{\mathcal{L}^{1/2}} \sin\left(\frac{kr}{2}\right) p_{k,A} Q_A. \tag{6.89}$$

We assume that the modes within the spectral peak can be approximated by two harmonic oscillators with frequency ω_0, one representing the symmetric modes within the peak and the other representing the antisymmetric ones. The justification for this approximation is as follows: the modes within the van Hove peak of the spectral density (6.80) are oscillating *coherently* at least for times $t < 1/\delta\omega$ and distances $r < 1/\delta\omega$, where $\delta\omega$ denotes the width of the peak. Therefore a substitution of those coherently oscillating modes with harmonic oscillators is viable within this

regime. For larger times and distances, the modes will oscillate incoherently and, consequently, the approximation is expected to break down.

The coupling oscillator representing the symmetric modes of the peak has the canonical variables $q_{\omega_0,S}$ and $p_{\omega_0,S}$ and couples to Q_S, whereas the coupling oscillator representing the antisymmetric modes of the peak has the canonical variables $q_{\omega_0,A}$ and $p_{\omega_0,A}$ and couples to Q_A. For the moment we consider g_{ω_0} to be independent from the spectral density. A relation between the two will be established in the course of the discussion of the tube model in section (6.3.3).

Since we treat the coupling oscillators separately, the Hamiltonian now reads

$$H \;=\; H_{0,S} + H_{0,A} + \sum_{k>0, k\neq\text{peak}} \left(H_{\text{bath},k} + H_{\text{int},k}\right) , \tag{6.90}$$

with

$$
\begin{aligned}
H_{0,S} &= \frac{1}{2}\left(P_S^2 + \Omega_S^2 Q_S^2\right) - g_{\omega_0}\cos\left(\frac{\omega_0 r}{2}\right) p_{\omega_0,S} Q_S \\
&\quad + \frac{1}{2}\left(p_{\omega_0,S}^2 + {\omega_0}^2 q_{\omega_0,S}^2\right) \\
H_{0,A} &= \frac{1}{2}\left(P_A^2 + \Omega_A^2 Q_A^2\right) - g_{\omega_0}\sin\left(\frac{\omega_0 r}{2}\right) p_{\omega_0,A} Q_A \\
&\quad + \frac{1}{2}\left(p_{\omega_0,A}^2 + {\omega_0}^2 q_{\omega_0,A}^2\right) .
\end{aligned}
\tag{6.91}
$$

Absorbing the counterterms, the frequencies of the symmetric and the antisymmetric mode of the system oscillators are renormalized according to

$$\Omega_S \;=\; \sqrt{\Omega_0^2 + \frac{1}{\mathcal{L}}\sum_{k>0} h_k^2 \cos^2\left(\frac{kr}{2}\right)} \tag{6.92}$$

$$\Omega_A \;=\; \sqrt{\Omega_0^2 + \frac{1}{\mathcal{L}}\sum_{k>0} h_k^2 \sin^2\left(\frac{kr}{2}\right)} . \tag{6.93}$$

The interaction between the system oscillators and the peak oscillators will be treated exactly, whereas the interaction between the bath modes and the system oscillators will be covered by a master equation [21, 120]. Restricting ourselves to a second–order master equation, we find that the evolution for the symmetric and antisymmetric modes are decoupled from each other. We conclude that the reduced density matrix is of the form

$$\rho_{\text{sys}} = \rho_A \otimes \rho_S , \tag{6.94}$$

where the index S refers to the symmetric modes and the index A to the antisymmetric ones. Since the calculation of ρ_S and ρ_A is completely analog, we will suppress the

indices. In order to diagonalize H_0 we introduce the canonical variables

$$
\begin{aligned}
\bar{P}_1 &= \frac{P + \xi\omega_0 q_{\omega_0}}{\sqrt{1+\xi^2}} \,, \\
\bar{P}_2 &= \frac{\bar{\Omega}_2(p_{\omega_0} + \xi\omega_0 Q)}{\omega_0\sqrt{1+\xi^2}} \,, \\
\bar{Q}_1 &= \frac{\omega_0 Q - \xi p_{\omega_0}}{\omega_0\sqrt{1+\xi^2}} \,, \\
\bar{Q}_2 &= \frac{\omega_0 q_{\omega_0} - \xi P}{\bar{\Omega}_2\sqrt{1+\xi^2}} \,.
\end{aligned}
\tag{6.95}
$$

The part of the Hamiltonian corresponding to the free evolution of system- and peak-oscillators has the diagonal form

$$
H_0 = \sum_{i=1,2} \frac{1}{2}\left(\bar{P}_i^2 + \bar{\Omega}_i^2\bar{Q}_i^2\right) \,.
\tag{6.96}
$$

The mixing-parameter ξ is given by

$$
\xi = \frac{1}{2\hat{g}\omega_0}\left(\omega_0^2 - \Omega^2 - \hat{g}^2 + \sqrt{(\Omega^2 + \hat{g}^2 - \omega_0^2)^2 + 4\hat{g}^2\omega_0^2}\right) \,,
\tag{6.97}
$$

and the eigenmodes read

$$
\begin{aligned}
\bar{\Omega}_1 &= \sqrt{\frac{1}{2}\left(\Omega^2 + \hat{g}^2 + \omega_0^2 + \sqrt{(\Omega^2 + \hat{g}^2 - \omega_0^2)^2 + 4\hat{g}^2\omega_0^2}\right)} \,, \\
\bar{\Omega}_2 &= \sqrt{\frac{1}{2}\left(\Omega^2 + \hat{g}^2 + \omega_0^2 - \sqrt{(\Omega^2 + \hat{g}^2 - \omega_0^2)^2 + 4\hat{g}^2\omega_0^2}\right)} \,.
\end{aligned}
$$

In this context, the coupling $\hat{g}$ denotes $g_{\omega_0}\cos(\omega_0 r/2)$ for the symmetric mode and $g_{\omega_0}\sin(\omega_0 r/2)$ for the antisymmetric mode, respectively.

Since we want to find an analytic approximation of the model, we treat the system–bath–interaction within a Born–Markov–approximation. The evolution equation of the reduced density matrix including the evolution of the two system oscillators and the peak oscillators reads

$$
\begin{aligned}
\dot{\rho} &= -i[H_0, \rho] - \int_0^\infty dt\, \nu(t, r)[Q, [Q(-t), \rho]] \\
&\quad + i\int_0^\infty dt\, \mu(t, r)[Q, \{Q(-t), \rho\}] \,,
\end{aligned}
\tag{6.98}
$$

with the real functions ν and μ defined by

$$
\begin{aligned}
\nu - i\mu &= \frac{1}{\mathcal{L}} \sum_{k>0} h_k^2 f(\omega_k) \langle p_k p_k(-t) \rangle \\
&= \frac{1}{2} \int_0^\infty d\omega J(\omega) f(\omega) \left(\coth\left(\frac{\omega}{2T}\right) \cos(\omega t) - i \sin(\omega t) \right) , \quad (6.99)
\end{aligned}
$$

where the spectral density, $J(\omega)$, is defined in equation (6.69) Furthermore the function f reads $f(\omega_k) = \cos^2(\omega_k r/2)$ for the symmetric bath modes and $f(\omega_k) = \sin^2(\omega_k r/2)$ for the antisymmetric ones, respectively. The first term on the right hand side of equation (6.98) describes the unitary evolution and is mainly responsible for the entanglement of the two system oscillators. The second and third term are dissipative contributions to the dynamics due to system–environment interaction. Note, that the system has been enlarged and includes the peak oscillators as well.

We restrict ourselves to Gaussian density matrices and work with a method for solving the differential equation (6.98) that has been used by Unruh and Zurek [29]. We transform the density matrix into the "$k - \Delta$"-representation according to

$$
\tilde{\rho}(\mathbf{k}, \boldsymbol{\Delta}) = \mathrm{tr}\left(\hat{\rho} e^{i\left(\mathbf{k}\hat{\mathbf{Q}} + \boldsymbol{\Delta}\hat{\mathbf{P}}\right)} \right) , \quad (6.100)
$$

with the vectors $\mathbf{k} = (k_1, k_2)$, $\boldsymbol{\Delta} = (\Delta_1, \Delta_2)$, $\hat{\mathbf{Q}} = (\hat{Q}_1, \hat{Q}_2)$ and $\hat{\mathbf{P}} = (\hat{P}_1, \hat{P}_2)$. This representation is related to the Wigner–distribution via a double Fourier transformation and has, in position representation, the form

$$
\tilde{\rho}(\mathbf{k}, \boldsymbol{\Delta}) = \int dx_1 dx_2 e^{i\mathbf{k}\mathbf{x}} \rho\left(\mathbf{x} + \frac{\boldsymbol{\Delta}}{2}, \mathbf{x} - \frac{\boldsymbol{\Delta}}{2} \right) , \quad (6.101)
$$

where $\mathbf{x} = (x_1, x_2)$. The x_i label the diagonal elements of the density matrix and the Δ_i determine the distance between diagonal and off–diagonal elements.

Using this particular representation we find that the master equation is *linear* in the derivatives with respect to k_i and Δ_i, whereas it would be quadratic in the derivatives with respect to the Q_i's. Although both representations are equivalent, the former makes it much easier to solve the differential equations.

With a Gaussian ansatz for the density matrix $\rho(\mathbf{k}, \boldsymbol{\Delta})$, we end up with a linear first order system of differential equations, which are given explicitly in the appendix (see (8.15 – 8.28)). The coefficients of the linear first order system (8.15 – 8.28) involve four different system–bath correlators α_i that depend on the energies $\bar{\Omega}_{1/2}$, the distance r and the spectral density $J(\omega)$.

Although the exact model exhibits a frequency gap, we assume $J(\omega)$ to be *nonvanishing* for all frequencies and given by the expression (6.3.1). Note, that the spectral density (6.3.1) follows from adding all van Hove–peaks and taking the limit $\omega_0 \to 0$.

In the exact model, the spectral weight of all modes $\omega < \omega_0$ is exactly zero, whereas, according to (6.3.1), we assume the spectral weight to be proportional to ω^s, which is valid if the spectral weight is negligible for $\omega_0 \ll \Omega_c$.

Before presenting our results, we comment on the physical interpretation of the bath correlators which is the same as in the Caldeira–Leggett model [21]. The system–bath correlator α_1 determines the decoherence rate and therefore the decay of interference terms. After singling out the α_1 term, the master equation reads in position basis

$$\dot{\rho}(Q,Q') = -\alpha_1(Q-Q')^2 \rho(Q,Q')\,. \tag{6.102}$$

The solution of (6.102) describes spatial localization of the oscillators, i.e.

$$\rho(Q,Q') \propto \exp(-\alpha_1(Q-Q')^2 t)\,, \tag{6.103}$$

which allows us to interpret $\alpha_1(Q-Q')^2$ as a decoherence rate. In Wigner representation, equation (6.102) has the form of a diffusion equation,

$$\frac{\partial}{\partial t}W(Q,P,t) = \alpha_1 \frac{\partial^2}{\partial P^2}W(Q,P,t)\,. \tag{6.104}$$

Thus, α_1 is also known as the normal–diffusion coefficient. The correlator α_2 is called anomalous-diffusion coefficient, since its contribution to the master equation, i.e.

$$\frac{\partial}{\partial t}W(X,P,t) = -\alpha_2 \frac{\partial}{\partial P}\frac{\partial}{\partial X}W(X,P,t)\,, \tag{6.105}$$

involves a mixed partial derivative. The correlator α_3 describes the Lamb shift and can therefore be added to the oscillator frequencies. Finally, α_4 determines dissipation due to the system–environment interaction, which leads to an exponential damping of the oscillator momenta,

$$\langle P\rangle(t) \propto e^{-2\alpha_4 t}\langle P\rangle(0). \tag{6.106}$$

Explicit expressions for the correlators are given in chapter 8 (see equations (8.64) – (8.71)). Note that α_1 and α_4 depend only on the value of the spectral density at the oscillator frequencies $\bar{\Omega}_{1/2}$.

In order to find explicit analytical solutions we need to decouple the system of differential equations. Since the dissipative part of equation (6.98) consists of sixteen different double commutators involving also higher order couplings between $\bar{Q}_{1/2}$ and $\bar{P}_{1/2}$ (see equation (8.3)), this cannot be done analytically. Neglecting terms $\mathcal{O}(\xi)$ in the *dissipative* part of equation (8.3) will remove the higher order couplings and we are left with the usual four double commutators known from the Caldeira-Leggett model. In this approximation we are able to decouple the system of differential

equations (8.15) – (8.28) analytically. The expectation values of the anticommutators, and therefore the negativity, can be expressed in terms of the solutions $c_i(t)$ of the differential equations, see equations (8.29) – (8.38).

We chose the system- and peak oscillators to be initially in a Gaussian state of the form

$$\rho = \frac{\sqrt{ab}}{2\pi} \exp\left(-\frac{q_{\omega_0}^2 a}{2} - \frac{Q^2 b}{2} \right) , \tag{6.107}$$

with the squeezing parameters a and b determining initial energies of the oscillators to be

$$E_{q_{\omega_0}} = \frac{a^2 + \omega_0^2}{4a} \tag{6.108}$$

$$E_Q = \frac{b^2 + \Omega_0^2}{4b} . \tag{6.109}$$

Only for $a = \omega_0$ and $b = \Omega_0$ the respective oscillators are in the ground state, otherwise they are in a superposition of (infinitely many) eigenstates.

From the approximate solutions, see (8.41) – (8.63), we find that the damping of the eigenmodes is solely determined by the dissipation-correlator α_4. The Lamb shift related to α_3 modifies the eigenmodes $\bar{\Omega}_{1/2}$. We found that, for small and intermediate times, the analytical expressions coincide very well with the numerical solutions found for the $c_i(t)$ from equations (8.15) – (8.28). However, the analytic solutions do not exhibit a damping of the peak oscillators which prevents us from defining a suitable asymptotic state in this case. Nevertheless, in section 6.3.2, we will give an analytic expression for the asymptotic entanglement which agrees, for small dissipative couplings γ, very well with the asymptotics obtained from the numerical solutions of equations (8.15) – (8.28).

Generation of Entanglement

In the following, we present the dependence of entanglement generation on the various model parameters. Although it is possible to give an approximate analytical formula for the entanglement using the solutions (8.41) – (8.63), it is a very lengthy expression which is difficult to interpret. Therefore, we elucidate the dependence of the entanglement generation by plotting the logarithmic negativity $\mathcal{E}$ for different sets of parameters. We will measure all quantities in units of the bare oscillator frequency Ω_0. For now, we consider couplings γ and g_{ω_0} to be *independent* from each other.

The starting point of the discussion is the dependence of the entanglement generation on the dissipative coupling γ for various initial states. Since we consider low

temperatures, it is sufficient to choose the initial state of the peak oscillators to be the ground state, i.e. $a = \omega_0$. If the system oscillators are prepared in their ground states, too, they have to evolve into an excited state in order to become entangled. In other words, the coupling to the bath changes the ground state of system and environment such that the system oscillators become excited. This effect is obviously only of order $g_{\omega_0}^2$. In fig. 4.11, we plotted the entanglement evolution in time for different dissipative couplings γ and spectral parameters $s = 1$ and $s = 3$. The damping of the logarithmic negativity increases with growing dissipative coupling strength γ. The decay rate of the entanglement is at least $\min[\alpha_{4,S}, \alpha_{4,A}]$, which can be deduced from the analytical solutions (8.41) – (8.63).

One can enhance the generation of entanglement if the system oscillators are initially prepared in a squeezed state, $b \neq \Omega_0$, which has energy greater than Ω_0, see equation (6.109). Thus they can release energy to the bath and evolve into an entangled state with lower energy. We depicted the entanglement generation for the squeezing parameters $b = 2\,\Omega_0$ and $b = 10\,\Omega_0$ in fig. 6.4 and 6.5. Compared to the case where the system oscillators were initially prepared in the ground state, the amount of generated entanglement increases by one and two orders of magnitude for the choices $b = 2\,\Omega_0$ and $b = 10\,\Omega_0$, respectively. Since the spectral density (6.3.1) contains a factor $1/\Omega_c^{s-1}$, the dissipation rate α_4 decreases with growing s which results in a weaker damping of the logarithmic negativity.

Entanglement can also be enhanced by increasing the coupling constant g_{ω_0}. Choosing $b = 10\,\Omega_0$, we find that, for $g_{\omega_0} = 0.1\,\Omega_0$, the maximal negativity is $\mathcal{E}_{max} \approx 0.8$, whereas for $g_{\omega_0} = \Omega_0$ we have $\mathcal{E}_{max} \approx 2$ (see fig. 6.6). In addition, the frequencies of the enveloping oscillations increase significantly with g_{ω_0}.

Next, we consider the influence of shifting the peak oscillator frequency ω_0 on the entanglement generation. In the limit $\gamma = 0$, any background effects due to dissipation effects are suppressed, see fig. 6.7. The entanglement is generated solely by the interaction with the peak oscillators. Although the maximal possible entanglement is not affected by the shift of ω_0, the negativity increases more slowly for large shifts. The periods of the enveloping oscillations of the negativity are increasing with $|\Omega_0 - \omega_0|$. Only if the system and peak oscillators are approximately in resonance, the negativity adopts a significant value after a short time.

For a nonvanishing dissipative coupling, one observes even in the limit of vanishing oscillator–peak coupling, that is $g_{\omega_0} \to 0$, the generation of a small amount of entanglement. This "background" effect is due to the dissipative effects: the symmetric mode and the antisymmetric mode are decaying on different time scales, which leads to entanglement of the system oscillators. In the first plot of fig. 6.8, we shifted the peak frequency ω_0 away from Ω_0, which results in a decrease of the negativity and a suppression of the oscillations. The remaining entanglement for frequencies ω_0 that are shifted far away from Ω_0 is solely due to the dissipative coupling. In the second

plot of fig. 6.8, we compared a large shift of ω_0 with vanishing coupling g_{ω_0}. From this plot it can be deduced that the entanglement due to the coupling constant g_{ω_0} is vanishing for $g_{\omega_0} \to 0$ as well as for $|\omega_0 - \Omega_0| \to \infty$. The remaining entanglement, however, is generated by the dissipative coupling γ and has at least a decay rate equal to $\min[\alpha_{4,S}, \alpha_{4,A}]$.

The generated entanglement decreases with increasing temperature since thermally excited bath modes contribute to the decoherence process. For the chosen parameters in fig. 6.9, the negativity depends only weakly on the temperature for $T < 0.2\,\Omega_0$.

Increasing the cutoff Ω_c lowers the generated entanglement, since also modes with small wavelengths contribute to the decoherence process, see fig. 6.10. It is well known that high–frequency modes are able to destroy coherences much faster than modes with low frequencies.

Here we treat the dissipative coupling strength γ and the coupling constant g_{ω_0} to be independent from the distance r. Hence the logarithmic negativity will not decrease with growing r. Due to the distance dependence of the bath correlators α_i and the couplings $g_{\omega_0,S} = g_{\omega_0} \cos(\omega_0 r/2)$ and $g_{\omega_0,A} = g_{\omega_0} \sin(\omega_0 r/2)$, we observe oscillations in the r–direction (see fig. 6.12) with a period π/ω_0. A special case is the limit $r \to 0$, where only the symmetric mode of the system oscillators is decaying. In contrast, the antisymmetric mode is not damped, since $\alpha_{4,A}(r = 0) = 0$. The environment is not able to resolve zero distance between the oscillators and the system does not thermalize, see fig. 6.11. In other words, vanishing distance leads to direct interaction between the oscillators which in turn leads inevitably to entanglement.
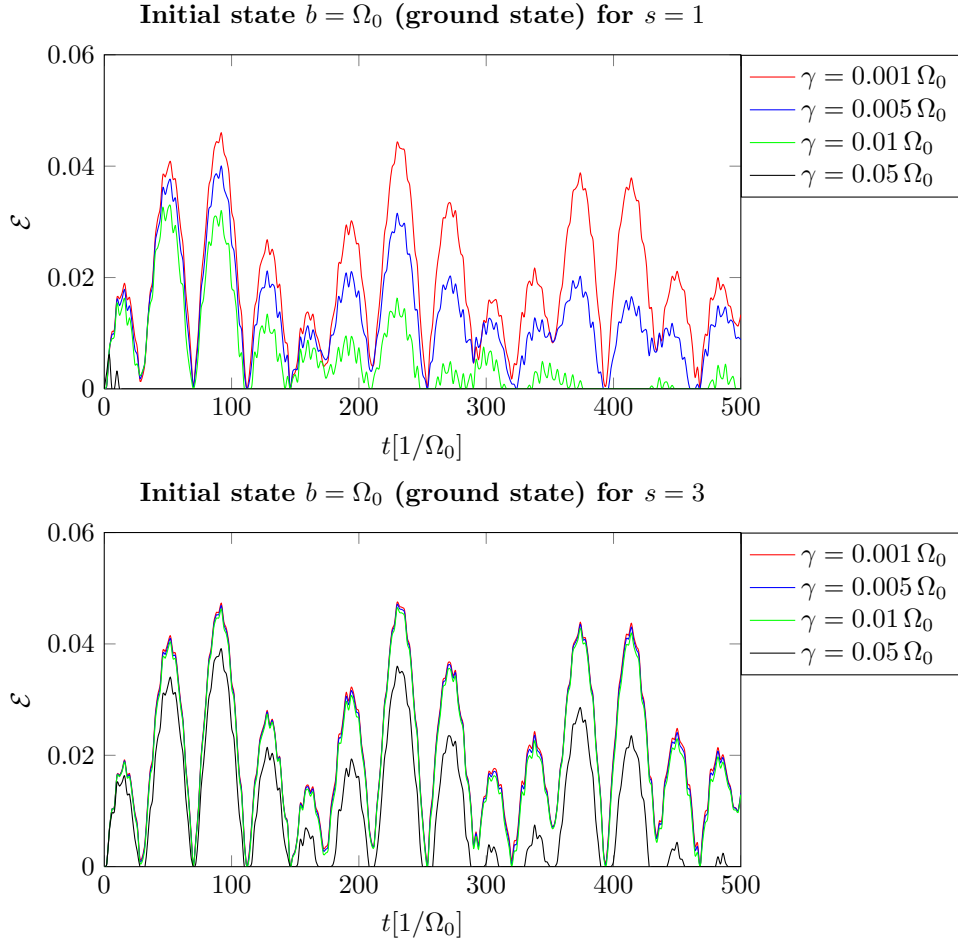
Figure 6.3: Since the system oscillators are initially prepared in their ground states, the amount of generated entanglement is small. We considered the spectral indices $s = 1$, which describes an ohmic bath, and $s = 3$, which refers to an electromagnetic field. The remaining parameters are $g_{\omega_0} = 0.1\,\Omega_0$, $T = 0.01\,\Omega_0$, $\Omega_c = 10\,\Omega_0$, $\omega_0 = \Omega_0$, $r = 1/\Omega_0$, and $a = \omega_0$.

Initial state $b = 2\,\Omega_0$ (weakly squeezed) for $s = 1$

Initial state $b = 2\,\Omega_0$ (weakly squeezed) for $s = 3$
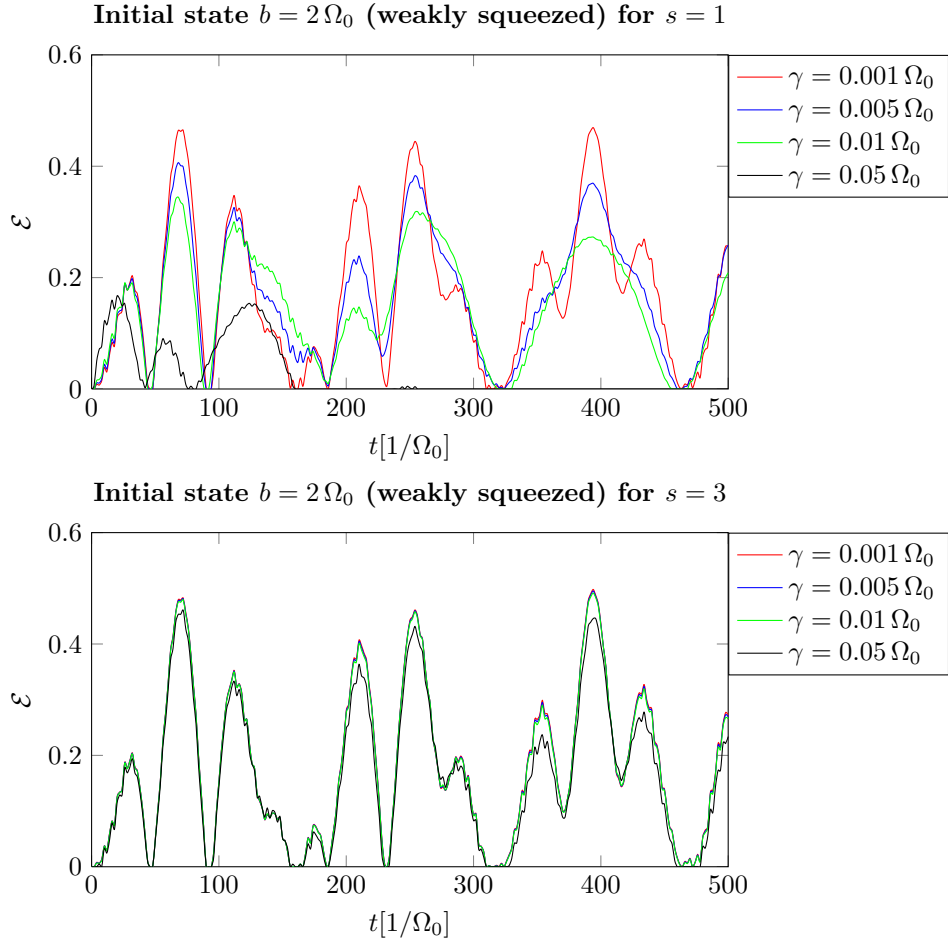
Figure 6.4: The initial preparation of the system oscillators in a squeezed state with the squeezing parameter $b = 2\,\Omega_0$ enhances the generation of entanglement by one order of magnitude compared to the case considered in fig. 6.3. The remaining parameters are $g_{\omega_0} = 0.1, \Omega_0$, $T = 0.01\,\Omega_0$, $\Omega_c = 10\,\Omega_0$, $\omega_0 = \Omega_0$, $r = 1/\Omega_0$, and $a = \omega_0$.

Initial state $b = 10\,\Omega_0$ (strongly squeezed) for $s = 1$

Initial state $b = 10\,\Omega_0$ (strongly squeezed) for $s = 3$
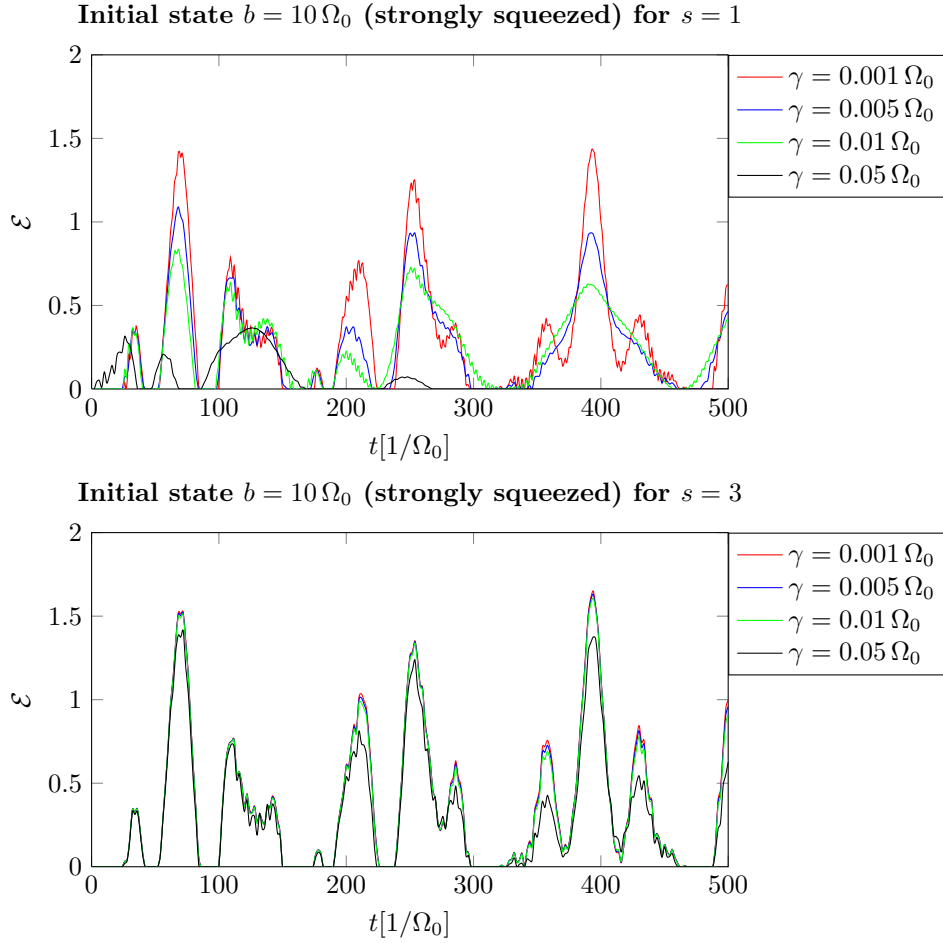
Figure 6.5: The initial preparation of the system oscillators in a squeezed state with the squeezing parameter $b = 10$ enhances the generation of entanglement by two orders of magnitude compared to the case considered in fig. 6.3. The remaining parameters are $g_{\omega_0} = 0.1\,\Omega_0$, $T = 0.01\,\Omega_0$, $\Omega_c = 10\,\Omega_0$, $\omega_0 = \Omega_0$, $r = 1/\Omega_0$, and $a = \omega_0$.

Dependence of the entanglement on the coupling constant g_{ω_0}
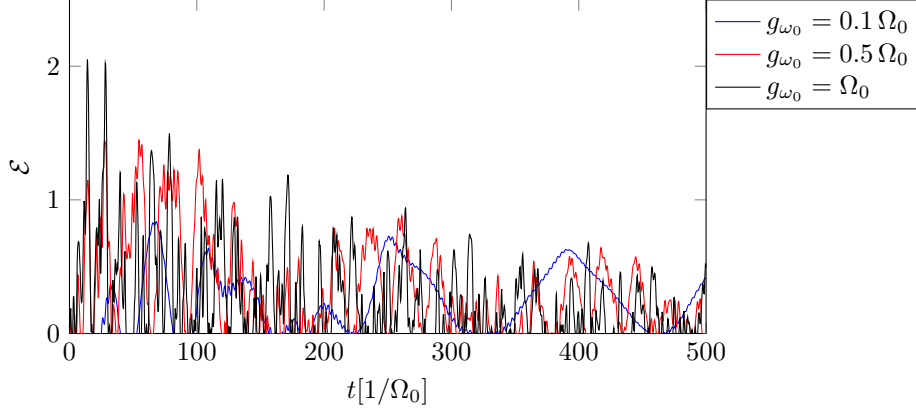
Figure 6.6: The maximal entanglement as well as the frequencies of the enveloping oscillations increase for growing g_{ω_0}. The remaining parameters are $\gamma = 0.01\,\Omega_0$, $T = 0.01\,\Omega_0$, $\Omega_c = 10\,\Omega_0$, $\omega_0 = \Omega_0$, $r = 1/\Omega_0$, $s = 1$, $a = \omega_0$, and $b = 10\,\Omega_0$.
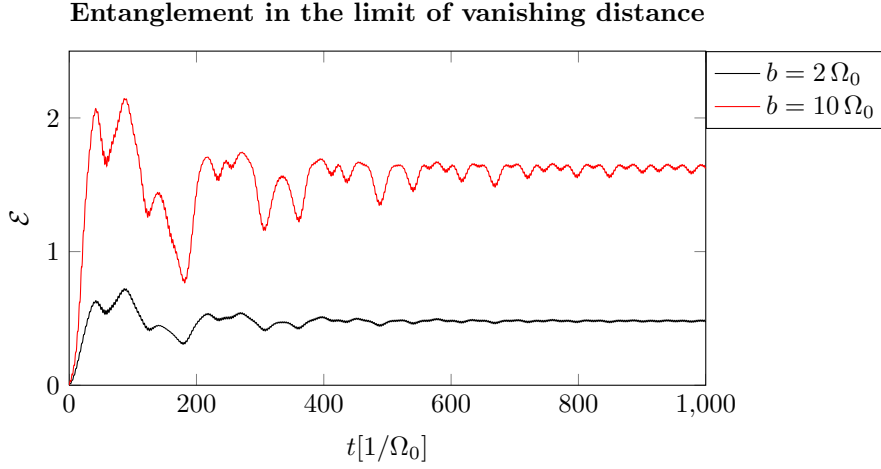
Dependence of the entanglement on ω_0 for $\gamma = 0$
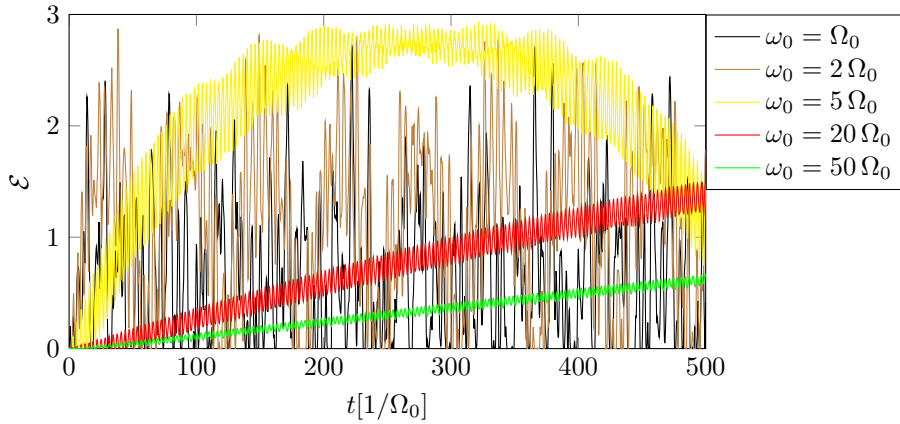
Figure 6.7: We depict the generation of entanglement for $\gamma = 0$ and different values of ω_0. Since, for $\gamma = 0$, the system evolves unitarily, the maximum value of $\mathcal{E}$ is not affected by the choice of ω_0. In contrast, the frequency of the enveloping oscillations decreases with growing ω_0. The remaining parameters are $\gamma = 0.01\,\Omega_0$, $T = 0.01\,\Omega_0$, $\Omega_c = 10\,\Omega_0$, $\omega_0 = \Omega_0$, $r = 1/\Omega_0$, $s = 1$, $a = \omega_0$, and $b = 10\,\Omega_0$.

Dependence of the entanglement on ω_0 for $\gamma = 0.01\,\Omega_0$
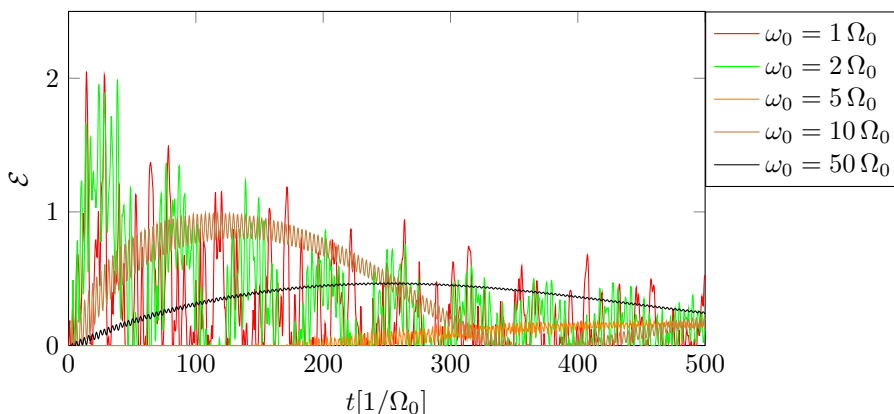
"Background" entanglement due to dissipative damping
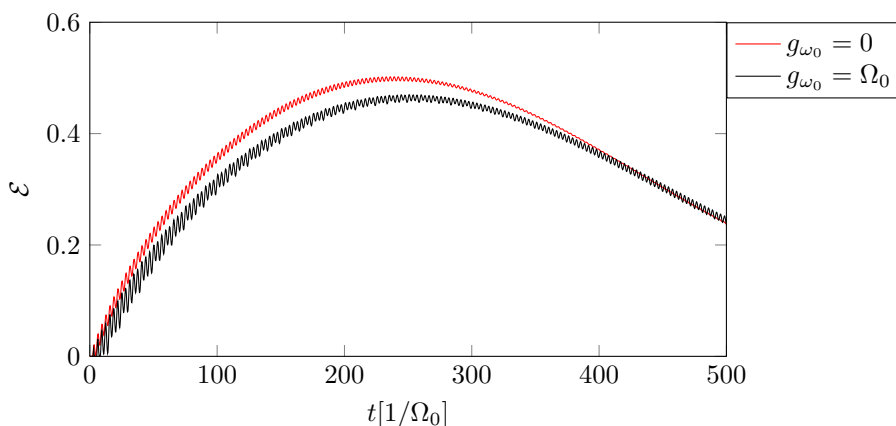
Figure 6.8: We depict, in the upper plot, the generation of entanglement for $\gamma = 0.01\,\Omega_0$ and different frequencies ω_0. The generated entanglement adopts its maximum value if the peak oscillators and the system oscillators are in resonance and decreases with the increasing shift of ω_0. In contrast to the case of $\gamma = 0$ (see fig. 6.7), we have nonvanishing entanglement for finite times in the limit $\omega_0 \to \infty$. Since the symmetric mode and the antisymmetric mode of the system oscillators are decaying at *different* rates ($\alpha_{4,S} \neq \alpha_{4,A}$), some entanglement is induced solely by the dissipative effects. As can be seen in the lower plot, the generated entanglement for large ω_0 approaches the "background" entanglement which can be obtained for $g_{\omega_0} \to 0$. The remaining parameters are $T = 0.01\,\Omega_0$, $\Omega_c = 10\,\Omega_0$, $\omega_0 = \Omega_0$, $r = 1/\Omega_0$, $s = 1$, $a = \omega_0$, and $b = 10\,\Omega_0$. In the upper plot we chose $g_{\omega_0} = \Omega_0$.

Dependence of the entanglement on the temperature T
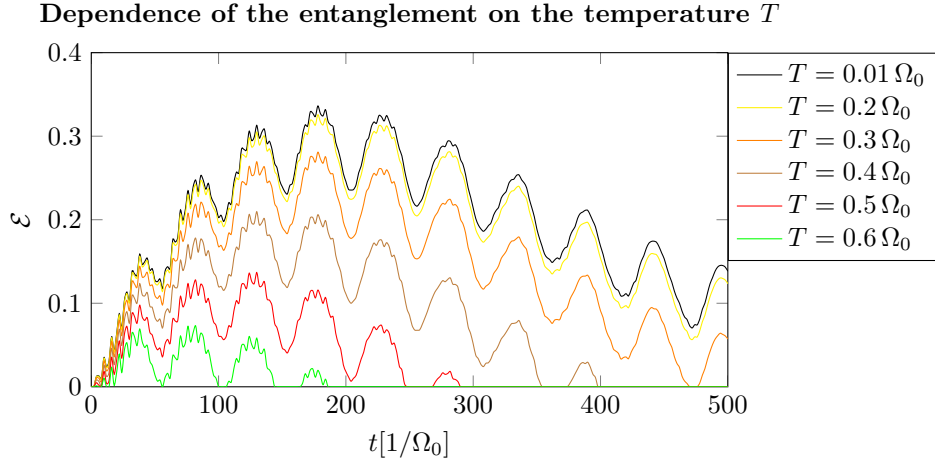
Figure 6.9: Since the decoherence rate increases with growing temperature, the generated entanglement decreases. Note that the temperature dependence of the entanglement is weak for $T < 0.2\,\Omega_0$. The remaining parameters are $g_{\omega_0} = 0.1\,\Omega_0$, $\gamma = 0.01\,\Omega_0$, $\Omega_c = 10\,\Omega_0$, $\omega_0 = 1.1\,\Omega_0$, $r = 1/\Omega_0$, $s = 1$, $a = \omega_0$, and $b = 2\,\Omega_0$.

Dependence of the entanglement on the cutoff frequency Ω_c
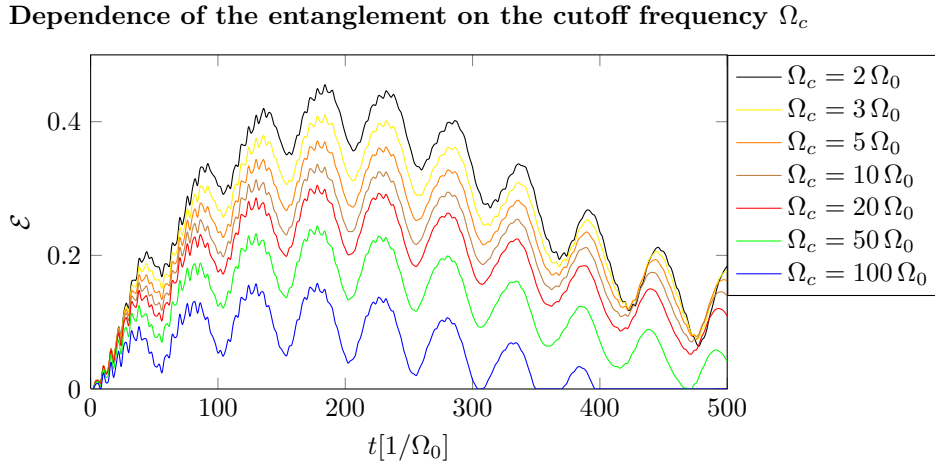
Figure 6.10: The generated negativity is lowered if the cutoff Ω_c increases, since environmental modes with large frequencies contribute to the decoherence process. The remaining parameters are $T = 0.01\,\Omega_0$, $g_{\omega_0} = 0.1\,\Omega_0$, $\gamma = 0.01\,\Omega_0$, $\omega_0 = 1.1\,\Omega_0$, $r = 1/\Omega_0$, $s = 1$, $a = \omega_0$, and $b = 2\,\Omega_0$.

Entanglement in the limit of vanishing distance

Figure 6.11: We plot the generation of entanglement in the limit $r = 0$ for an initial squeezing of $b = 2$ and $b = 10$. Since the antisymmetric mode is not decaying, the system does not thermalize and the negativity is oscillating around a nonzero value. The remaining parameters are $T = 0.01\,\Omega_0$, $g_{\omega_0} = 0.1\,\Omega_0$, $\gamma = 0.01\,\Omega_0$, $\Omega_c = 10\,\Omega_0$, $\omega_0 = 1.1\,\Omega_0$, $s = 1$, and $a = \omega_0$.

Asymptotic Entanglement

The exact asymptotic entanglement is given by the thermal expectation value of the covariance matrix with respect to the Hamiltonian (6.44). This is clearly not computable in an analytic way due the the bilinear system–bath interaction.

An approximate asymptotic state of the oscillators can be determined from the inhomogeneous parts of the differential equations (8.15) – (8.28), since the homogeneous parts of the solutions become damped due to dissipative effects and vanish in the limit $t \to \infty$. Note that the inhomogeneous parts, and thus the asymptotic state, do *not* depend on the initial conditions.

However, it is necessary to retain all higher order couplings of the master equation. In contrast, neglecting the terms $\mathcal{O}(\gamma\xi)$ in equations (8.15) – (8.28) would not lead to an asymptotically time–independent state since the peak oscillators remain undamped. In other words, the dissipative couplings $\mathcal{O}(\gamma\xi)$, which have been neglected in order to obtain the analytical solutions (8.41) – (8.63), are necessary for the thermalization of the peak oscillators.
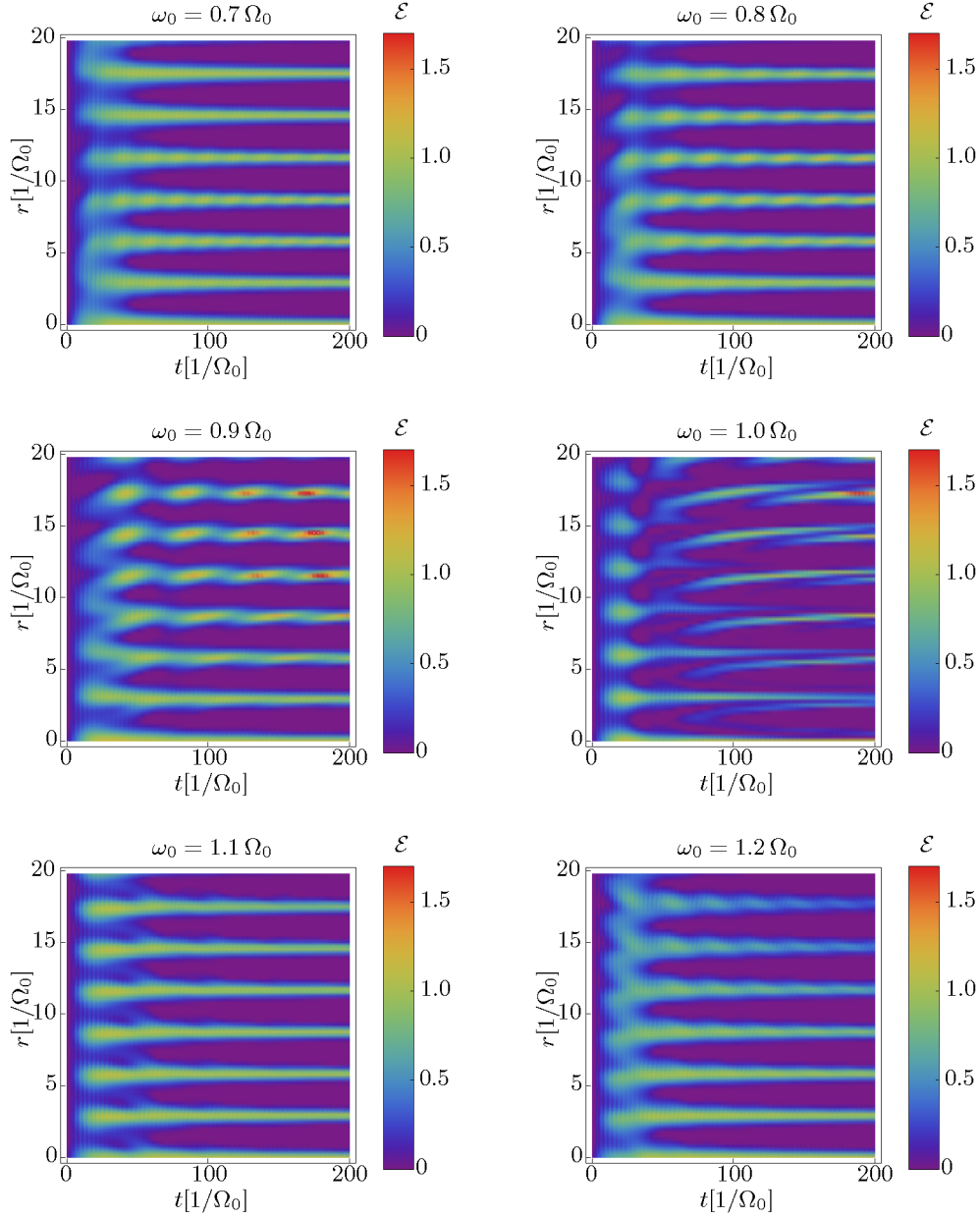
Figure 6.12: We depict the generation of entanglement for different values of ω_0. Due to the distance dependence of the couplings $g_{\omega_0,S/A}$, one observes oscillations in r–direction. We chose the parameters to be $\Omega_c = 5\,\Omega_0, T = 0.01\,\Omega_0, \omega_0 = \Omega_0, a = \omega_0, b = 5\,\Omega_0$ and $s = 1$.

We find that the lowest order of the asymptotic state is independent of the coupling strength γ since it involves only *ratios* of the bath correlators α_i. Thus, the approximate asymptotic state is of the form

$$|\Psi_{\text{asym}}\rangle = |\psi(\gamma^0)\rangle + |\psi(\mathcal{O}(\gamma^1))\rangle . \tag{6.110}$$

For small dissipative couplings, say $\gamma \to 0$, it is possible to obtain a simple analytic expression for the asymptotic logarithmic negativity. Therefore, we assume that the system oscillators as well as the peak oscillators thermalize for infinite times. Computing the thermal expectation value of the covariance matrix with respect to the Hamiltonian $H_0 = H_{0,S} + H_{0,A}$, whose parts are defined in (6.91) and (6.92), leads to the logarithmic negativity

$$\mathcal{E}_{\text{asym}} = -\log_2\left(\min\left[1, \lambda_1\right]\right) - \log_2\left(\min\left[1, \lambda_2\right]\right) , \tag{6.111}$$

where the symplectic eigenvalues are given by

$$\begin{aligned}
\lambda_1^2 &= \frac{1}{1+\xi_A^2}\left[\frac{\xi_A^2}{\bar{\Omega}_{A,2}}\coth\left(\frac{\bar{\Omega}_{A,2}}{2T}\right) + \frac{1}{\bar{\Omega}_{A,1}}\coth\left(\frac{\bar{\Omega}_{A,1}}{2T}\right)\right] \\
&\quad \times \frac{1}{1+\xi_S^2}\left[\bar{\Omega}_{S,1}\coth\left(\frac{\bar{\Omega}_{S,1}}{2T}\right) + \bar{\Omega}_{S,2}\xi_S^2\coth\left(\frac{\bar{\Omega}_{S,2}}{2T}\right)\right]
\end{aligned} \tag{6.112}$$

and

$$\begin{aligned}
\lambda_2^2 &= \frac{1}{1+\xi_S^2}\left[\frac{\xi_S^2}{\bar{\Omega}_{S,2}}\coth\left(\frac{\bar{\Omega}_{S,2}}{2T}\right) + \frac{1}{\bar{\Omega}_{S,1}}\coth\left(\frac{\bar{\Omega}_{S,1}}{2T}\right)\right] \\
&\quad \times \frac{1}{1+\xi_A^2}\left[\bar{\Omega}_{A,1}\coth\left(\frac{\bar{\Omega}_{A,1}}{2T}\right) + \bar{\Omega}_{A,2}\xi_A^2\coth\left(\frac{\bar{\Omega}_{A,2}}{2T}\right)\right] .
\end{aligned} \tag{6.113}$$

The indices S and A have been reintroduced for the symmetric and antisymmetric oscillator mode, respectively.

As can be seen from figs. 6.13–6.16, the expression (6.111) coincides with the negativity found from the inhomogeneous solutions of (8.15) – (8.28) for $\gamma/g_{\omega_0} \ll 1$. An increase of γ leads to a growing discrepancy, since the thermal state of four oscillators is different from the thermal state of a system which consists of four oscillators *and* a thermal bath. The master equations are able to resolve this difference when the dissipative coupling is not too strong.

The entanglement between the oscillators is mainly due to the coupling g_{ω_0} which determines the coupling of the system oscillators to the modes within the van Hove singularity. In fig. 6.17 we depict the g_{ω_0}–dependence of the asymptotic entanglement for various dissipative couplings γ. Depending on γ, the coupling g_{ω_0} has to exceed a minimum critical value such that the asymptotic entanglement is nonvanishing.

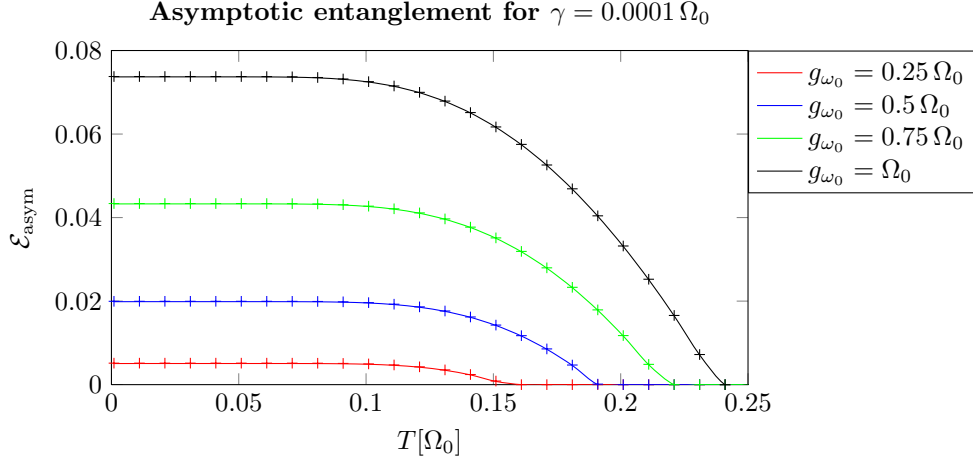**Asymptotic entanglement for** $\gamma = 0.0001\,\Omega_0$

Figure 6.13: The temperature dependence of the asymptotic logarithmic negativity is shown for a small dissipative coupling, $\gamma = 0.0001\,\Omega_0$. We chose various coupling constants g and found that the curves coincide with the thermal expectation values of the logarithmic negativity which have been obtained from expression (6.111) and which are depicted as colored marks. The remaining parameters have been chosen to be $\Omega_c = 3\,\Omega_0, \omega_0 = \Omega_0, r = 0$, and $s = 1$.

Asymptotic entanglement for $\gamma = 0.001\,\Omega_0$
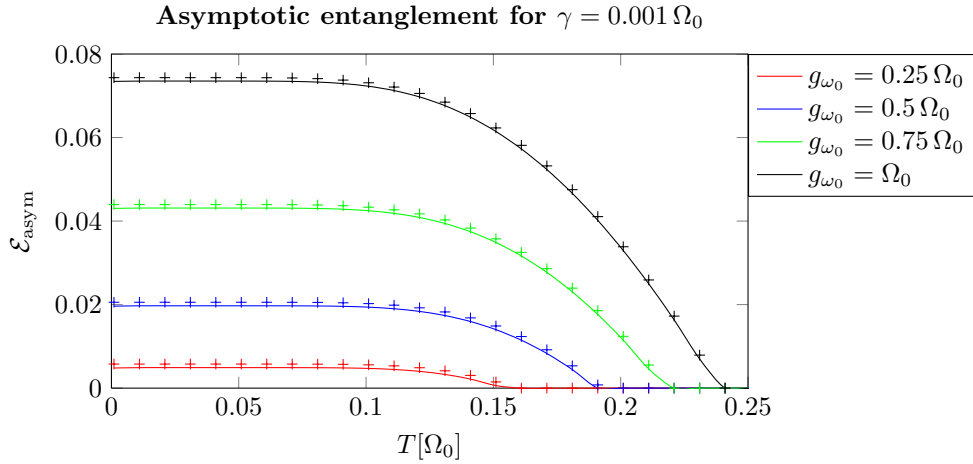
Figure 6.14: Here we chose the larger dissipative coupling $\gamma = 0.001\,\Omega_0$. Although the thermal expectation value is still a good approximation, terms $\mathcal{O}(\gamma\xi)$ lead to small corrections. The remaining parameters have been chosen to be $\Omega_c = 3\,\Omega_0, \omega_0 = \Omega_0, r = 0$, and $s = 1$.
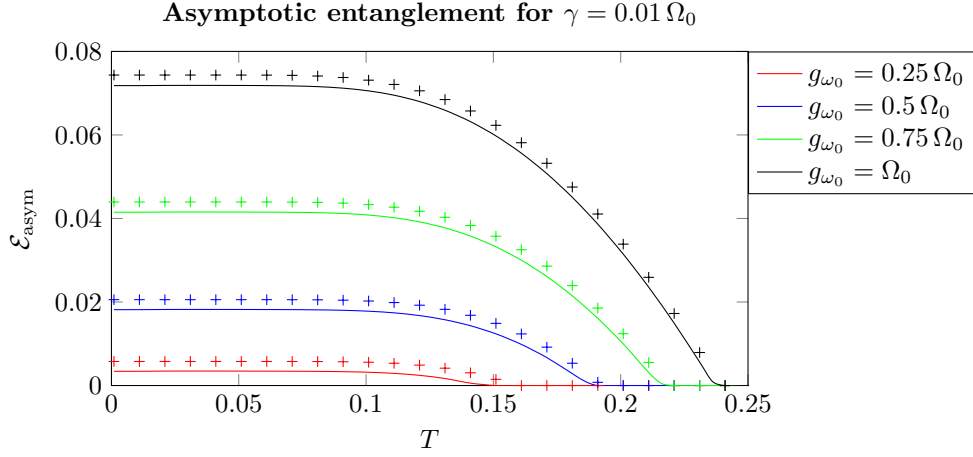
Figure 6.15: Here, we chose $\gamma = 0.01\,\Omega_0$; the correction terms from the asymptotics of equations (8.15 – 8.28) are increasing. The remaining parameters have been chosen to be $\Omega_c = 3\,\Omega_0, \omega_0 = \Omega_0, r = 0$, and $s = 1$.
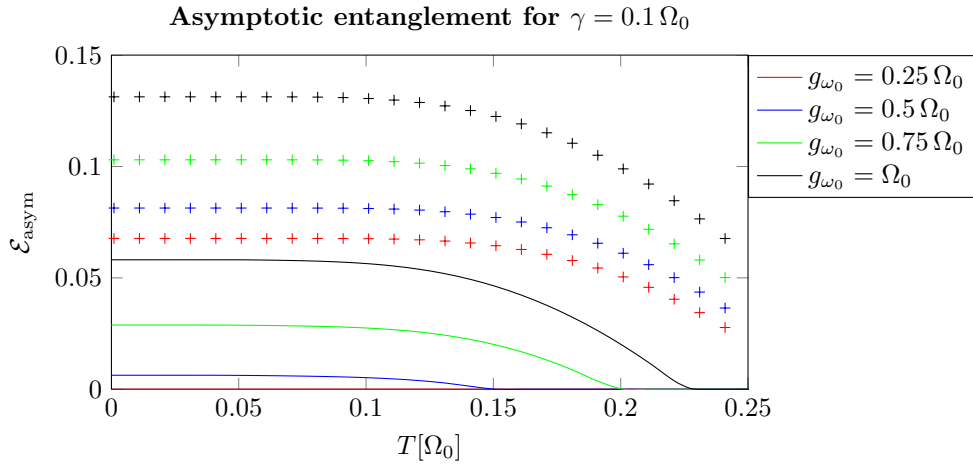
Figure 6.16: A large dissipative coupling $\gamma = 0.1\,\Omega_0$ leads to large corrections. This is due to the fact that the size of dissipative terms which have been neglected in equation 6.111 is of the same order of magnitude as the asymptotic entanglement. The remaining parameters have been chosen to be $\Omega_c = 3\,\Omega_0, \omega_0 = \Omega_0, r = 0$, and $s = 1$.

Dependence of the asymptotic entanglement on g_{ω_0}
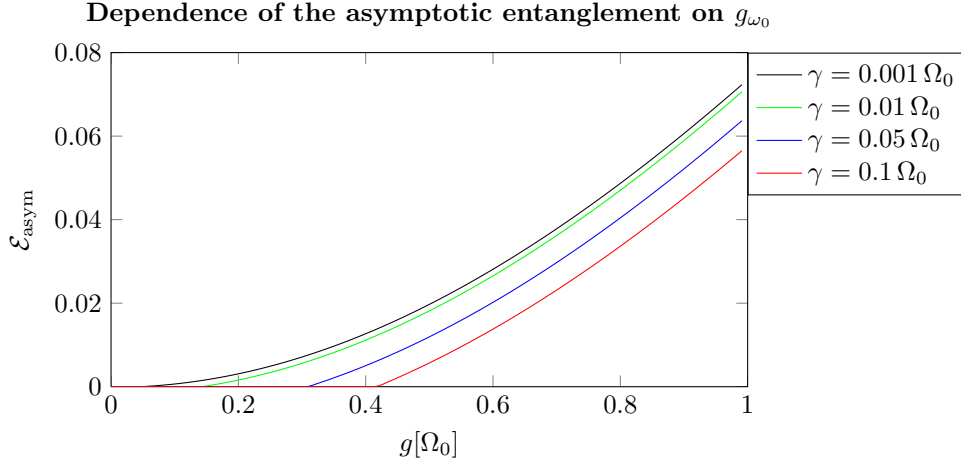
Figure 6.17: The minimal critical value for g, which is necessary in order to obtain nonvanishing asymptotic entanglement, increases with growing γ. In order to overcome the dissipative effects, the peak oscillators have to be coupled sufficiently strong to the system oscillators. The remaining parameters have been chosen to be $\Omega_c = 3\,\Omega_0, \omega_0 = \Omega_0, T = 0.01\,\Omega_0, r = 0$, and $s = 1$.

In general, one can say that the dissipative coupling leads to the localization of the oscillators which destroys any entanglement. In order to counterbalance this effect, the coupling g_{ω_0} has to be increased sufficiently.

Finally, we consider the distance dependence of the asymptotic entanglement in the limit of small γ. Since the coupling to the symmetric modes, $g_S = g_{\omega_0} \cos(\omega_0 r)$, and the coupling to the antisymmetric modes, $g_A = g_{\omega_0} \sin(\omega_0 r)$, are periodic in r, the distance dependence of the asymptotic entanglement is oscillating, too. As can be deduced from fig. 6.18, the characteristic period is π/ω_0 since the couplings appear quadratically in expression (6.111).

So far we have assumed that the bath correlators α_i are determined by the spectral density (6.3.1). Nevertheless, the correct van Hove spectral density (6.80) exhibits a frequency gap, that is the weight for modes below the van Hove singularity is exactly equal to zero. This implies that the system oscillators do not thermalize if their frequencies are located within the gap since the dissipative bath correlator α_4 vanishes then. Without a damping of the homogeneous solutions of the differential equations (8.15) – (8.28), an asymptotic time–independent state does not exist. In other words, the system oscillators are not able to exchange energy with the bath if there are no environmental modes that have the same energy as the oscillator modes. This result was also found via exact numerical simulations.

However, Gaussian states are solely determined by two–point–correlation functions.

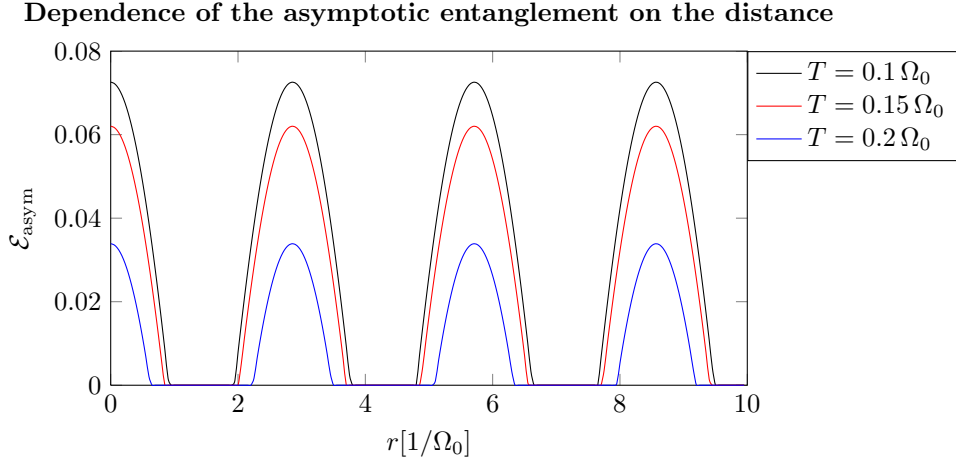**Dependence of the asymptotic entanglement on the distance**

Figure 6.18: The entanglement is oscillating with a characteristic period of π/ω_0 if the distance increases. The remaining parameters have been chosen to be $\Omega_c = 3\,\Omega_0, T = 0.01\,\Omega_0, \omega_0 = \Omega_0, r = 0$, and $s = 1$.

It is doubtful whether this idealizing assumption can be met in realistic physical situations. The van Hove spectral density may adopt nonzero values for modes below the singularity such that the bath correlator α_4 is nonvanishing.

In general, higher order correlation functions describing non–Gaussianities could lead to a thermalization of the system oscillators. For example, four–point–correlation functions would involve sums of the form

$$\sum_{p,q,t} f(\omega_p, \omega_q, \omega_t)\delta(\omega_p + \omega_q + \omega_t - \bar{\Omega})\,, \tag{6.114}$$

which are nonvanishing even if the oscillator mode $\bar{\Omega}$ is located within the gap.

6.3.3 Entanglement in a Tube

In the preceding sections, we discussed entanglement for a one–dimensional model. The singling out of two coupling oscillators, a symmetric and an antisymmetric one, was motivated with van Hove singularities, which have been discussed in section (6.3.1)

In the following we turn to a more realistic description of entanglement in a cylindical tube with radius ρ_0, i.e. we start from a three-dimensional model. We will see that the distance dependence of entanglement changes crucially.

Due to the cylindrical symmetry, we have to expand the field $\phi(\mathbf{x})$ in eigenfunctions

of the Laplacian in cylindrical coordinates,

$$\triangle = \frac{1}{\rho}\frac{\partial}{\partial\rho}\left(\rho\frac{\partial}{\partial\rho}\right) + \frac{1}{\rho^2}\frac{\partial^2}{\partial\varphi^2} + \frac{\partial^2}{\partial r^2}. \tag{6.115}$$

The eigenfunctions are determined by the boundary conditions of the field, i.e. $\phi(r, \rho_0, \varphi) = 0$ and $\phi(r, \rho, \varphi) = \phi(r, \rho, \varphi + 2\pi)$. For solving the eigenvalue equation $-\triangle u(\mathbf{x}) = \omega^2 u(\mathbf{x})$, we choose the ansatz

$$u(\mathbf{x}) = u_1(\rho)u_2(\varphi)u_3(r). \tag{6.116}$$

We find

$$u_1(\varphi) = e^{im\varphi}, \, m = 0, \pm 1. \pm 2, ..., \tag{6.117}$$

$$u_2(r) = e^{ik_\mathcal{L}r}, \tag{6.118}$$

$$u_3(\rho) = J_m(\kappa_{mn}\rho), \, n = 1, 2, ..., \tag{6.119}$$

where the J_m are Bessel functions of the first kind and $\kappa_{mn} = \lambda_{mn}/\rho_0$. λ_{mn} is the n-th zero of the function J_m. The eigenvalues of the Laplacian are therefore $\omega^2_{k_\mathcal{L}mn} = k_\mathcal{L}^2 + \kappa_{mn}^2$. Expanding the scalar field into the eigenfunctions leads with $\int dk_\mathcal{L} \to (2\pi/\mathcal{L})\sum_{k_\mathcal{L}}$ to the mode expansion

$$\phi(\mathbf{x}) = \frac{1}{\sqrt{\pi\rho_0^2\mathcal{L}}}\sum_{k_\mathcal{L},n,m}\frac{1}{J_{m+1}(\lambda_{mn})}\phi_{k_\mathcal{L},n,m}J_m(\kappa_{mn}\rho)e^{ik_\mathcal{L}r}e^{im\varphi} \tag{6.120}$$

$$= \sum_{k_\mathcal{L},n,m}\frac{1}{\mathcal{L}\rho_0 J_{m+1}(\lambda_{mn})\sqrt{\omega_{k_\mathcal{L}nm}}}J_m(\kappa_{mn}\rho)e^{ik_\mathcal{L}r}e^{im\varphi}a_{k_\mathcal{L},n,m} + h.c.,$$

$$\Pi(\mathbf{x}) = \frac{1}{\sqrt{\pi\rho_0^2\mathcal{L}}}\sum_{k_\mathcal{L},n,m}\frac{1}{J_{m+1}(\lambda_{mn})}\Pi_{k_\mathcal{L},n,m}J_m(\kappa_{mn}\rho)e^{ik_\mathcal{L}r}e^{im\varphi} \tag{6.121}$$

$$= -i\sum_{k_\mathcal{L},n,m}\frac{\sqrt{\omega_{k_\mathcal{L}nm}}}{\mathcal{L}\rho_0 J_{m+1}(\lambda_{mn})}J_m(\kappa_{mn}\rho)e^{ik_\mathcal{L}r}e^{im\varphi}a_{k_\mathcal{L},n,m} + h.c.,$$

where the normalization is determined through the canonical commutation relation $[\phi(\mathbf{x}), \Pi(\mathbf{y})] = i\delta(\mathbf{x} - \mathbf{y})$ and the orthonormality of the eigenfunctions,

$$\int dk_\mathcal{L}\sum_{n,m}\frac{1}{2\pi^2\rho_0^2[J_{m+1}(\lambda_{mn})]^2}J_m(\kappa_{mn}\rho)J_m(\kappa_{mn}\rho')e^{im(\varphi-\varphi')}e^{ik_\mathcal{L}(r-r')}$$

$$= \delta(\varphi - \varphi')\delta(r - r')\frac{\delta(\rho - \rho')}{\rho'}. \tag{6.122}$$

Decomposing into symmetric and antisymmetric oscillator variables leads to

$$
\begin{aligned}
q_{k_{\mathcal{L}},n,m,S} &= \frac{\phi_{k_{\mathcal{L}},n,m} + \phi_{-k_{\mathcal{L}},n,m}}{\sqrt{2}}, \\
p_{k_{\mathcal{L}},n,m,S} &= \frac{\Pi_{k_{\mathcal{L}},n,m} + \Pi_{-k_{\mathcal{L}},n,m}}{\sqrt{2}}, \\
q_{k_{\mathcal{L}},n,m,A} &= i\frac{\phi_{k_{\mathcal{L}},n,m} - \phi_{-k_{\mathcal{L}},n,m}}{\sqrt{2}}, \\
p_{k_{\mathcal{L}},n,m,A} &= -i\frac{\Pi_{k_{\mathcal{L}},n,m} - \Pi_{-k_{\mathcal{L}},n,m}}{\sqrt{2}} .
\end{aligned} \tag{6.123}
$$

With the system oscillator variables (6.81) and (6.82) we find the interaction

$$
H_{\text{int}} = -\sum_{k_{\mathcal{L}},m,n} \frac{g_{k_{\mathcal{L}}mn}}{\sqrt{\pi\rho_0^2\mathcal{L}}} \left(p_{k_{\mathcal{L}},n,m,S} Q_S \cos\left(\frac{k_{\mathcal{L}}r}{2}\right) + p_{k_{\mathcal{L}},n,m,A} Q_A \sin\left(\frac{k_{\mathcal{L}}r}{2}\right) \right), \tag{6.124}
$$

where the normalization factors have been absorbed in the couplings $g_{k_{\mathcal{L}}mn}$. We will consider, analogously to the procedure in section 6.3.2, the bath oscillators around the first van Hove peak as effective coupling oscillator, i.e. $\{p_{k_{\mathcal{L}},n=1,m=0,S}, k_{\mathcal{L}} \approx 0\} \rightarrow p_{\omega_0,S}$, $\{p_{k_{\mathcal{L}},n=1,m=0,A}, k_{\mathcal{L}} \approx 0\} \rightarrow p_{\omega_0,A}$, and $\{g_{k_{\mathcal{L}}10}/\sqrt{\pi\rho_0^2\mathcal{L}}, k_{\mathcal{L}} \approx 0\} \rightarrow g_{\omega_0}$. The peak frequency ω_0 has the value $\omega_0 = \lambda_{01}/\rho_0$ where $\lambda_{01} = 2.40483$ is the smallest eigenvalue of the cylindrical Laplacian. Singling out the Hamiltonian involving the system oscillators and the coupling oscillators, we have, analog to equations (6.91) and (6.92),

$$
\begin{aligned}
H_{0,S} &= \frac{1}{2}\left(P_S^2 + \Omega_S^2 Q_S^2\right) - g_{\omega_0} p_{\omega_0,S} Q_S + \frac{1}{2}\left(p_{\omega_0,S}^2 + \omega_0{}^2 q_{\omega_0,S}^2\right), \tag{6.125} \\
H_{0,A} &= \frac{1}{2}\left(P_A^2 + \Omega_A^2 Q_A^2\right) + \frac{1}{2}\left(p_{\omega_0,A}^2 + \omega_0{}^2 q_{\omega_0,A}^2\right), \tag{6.126}
\end{aligned}
$$

since $\cos(k_{\mathcal{L}}r)|_{k_{\mathcal{L}}\approx 0} \approx 1$ and $\sin(k_{\mathcal{L}}r)|_{k_{\mathcal{L}}\approx 0} \approx 0$. The frequencies Q_S and Q_A are renormalized through the counterterm, see below. We see that the entanglement is generated by the peak oscillator representing the symmetric peak modes, whereas the coupling oscillator representing the antisymmetric peak modes does not couple to Q_A and is therefore only a dummy variable. The Hamiltonian $H_{0,S}$ can be diagonalized using the variables (6.95) and $H_{0,A}$ already has diagonal form, that is $\xi_A = 0$, $\bar{\Omega}_{A,1} = \Omega_A$ and $\bar{\Omega}_{A,2} = \omega_0$.

For the computation of the bath correlators, we consider only the limit $\rho_0 \rightarrow \infty$, i.e. the boundary condition vanishes. We assume that this approximation resembles roughly the summation over all van Hove-singularities. In this limit, we will not use the variables (6.123) and consider instead the standard mode decomposition in

a large volume $\mathcal{V} = \mathcal{L}^3$, where we express the summation in terms of cylindrical coordinates, i.e. $\mathbf{k} = (k_\mathcal{L}, k_\rho, \varphi)$ with $\omega_k^2 = k^2 = \mathbf{k}^2 = k_\mathcal{L}^2 + k_\rho^2$. We have

$$\phi(\mathbf{x}) = \frac{1}{\mathcal{V}^{1/2}} \sum_{\mathbf{k}} \phi_{\mathbf{k}} e^{i\mathbf{kx}} = \frac{1}{\mathcal{V}^{1/2}} \sum_{k_\mathcal{L}, k_\rho, \varphi} \phi(k_\mathcal{L}, k_\rho, \varphi) e^{i\mathbf{kx}} . \tag{6.127}$$

Note that the fields $\phi(k_\mathcal{L}, k_\rho, \varphi)$ do *not* respect the cylindrical boundary conditions since we consider only the limit $\rho_0 \to \infty$. Decomposing the $\phi_{\mathbf{k}}$ and $\Pi_{\mathbf{k}}$ in this limit into symmetric and antisymmetric combinations leads to

$$\begin{aligned}
q_{\mathbf{k},S} &= \frac{\phi(k_\mathcal{L}, k_\rho, \varphi) + \phi(-k_\mathcal{L}, k_\rho, \varphi + \pi)}{\sqrt{2}}, \\
p_{\mathbf{k},S} &= \frac{\Pi(k_\mathcal{L}, k_\rho, \varphi) + \Pi(-k_\mathcal{L}, k_\rho, \varphi + \pi)}{\sqrt{2}}, \\
q_{\mathbf{k},A} &= i\frac{\phi(k_\mathcal{L}, k_\rho, \varphi) - \phi(-k_\mathcal{L}, k_\rho, \varphi + \pi)}{\sqrt{2}}, \\
p_{\mathbf{k},A} &= -i\frac{\Pi(k_\mathcal{L}, k_\rho, \varphi) - \Pi(-k_\mathcal{L}, k_\rho, \varphi + \pi)}{\sqrt{2}} .
\end{aligned} \tag{6.128}$$

Using this mode decomposition as well as the variables (6.81) and (6.82), we can express the Hamiltonian according to

$$H = H_{\text{sys}} + \sum_{k_\mathcal{L} > 0, k_\rho, \varphi} (H_{\text{bath},\mathbf{k}} + H_{\text{int},\mathbf{k}} + H_{\text{count},\mathbf{k}}) \tag{6.129}$$

with

$$\begin{aligned}
H_{\text{sys}} &= \frac{1}{2}(P_S^2 + \Omega_0^2 Q_S^2 + P_A^2 + \Omega_0^2 Q_A^2) \tag{6.130} \\
&\quad - g_{\omega_0} p_{\omega_0, S} Q_S + \frac{1}{2}\left(p_{\omega_0, S}^2 + \omega_0{}^2 q_{\omega_0, S}^2\right) + \frac{1}{2}\left(p_{\omega_0, A}^2 + \omega_0{}^2 q_{\omega_0, A}^2\right) , \\
H_{\text{count},\mathbf{k}} &= \frac{g_k^2}{2\mathcal{V}} \cos^2\left(\frac{k_\mathcal{L} r}{2}\right) Q_S^2 + \frac{g_k^2}{2\mathcal{V}} \sin^2\left(\frac{k_\mathcal{L} r}{2}\right) Q_A^2 , \tag{6.131} \\
H_{\text{bath},\mathbf{k}} &= \frac{1}{2}(p_{\mathbf{k},S}^2 + \omega_k^2 q_{\mathbf{k},S}^2 + p_{\mathbf{k},A}^2 + \omega_k^2 q_{\mathbf{k},A}^2) \tag{6.132} \\
H_{\text{int},\mathbf{k}} &= -\frac{g_k}{\mathcal{V}^{1/2}} \cos\left(\frac{k_\mathcal{L} r}{2}\right) p_{\mathbf{k},S} Q_S - \frac{g_k}{\mathcal{V}^{1/2}} \sin\left(\frac{k_\mathcal{L} r}{2}\right) p_{\mathbf{k},A} Q_A . \tag{6.133}
\end{aligned}$$

The couplings have been replaced according to $g_k \to g_k/2$. Absorbing the counterterms into the system Hamiltonian leads to

$$H_{\text{sys}} + \sum_{k_\mathcal{L} > 0, k_\rho, \varphi} H_{\text{count},\mathbf{k}} = H_{0,S} + H_{0,A} , \tag{6.134}$$

which defines the renormalized frequencies Ω_S and Ω_A.

The bath correlators of the evolution equation (6.98) involve mode sums which in the continuum limit read

$$
\sum_{k_{\mathcal{L}}>0,k_\rho,\varphi} \rightarrow \frac{\mathcal{V}}{(2\pi)^3} \lim_{k_{\max}\to\infty} \int_0^{2\pi} d\varphi \int_0^{k_{\max}} dk_{\mathcal{L}} \int_0^{\sqrt{k_{\max}^2-k_{\mathcal{L}}^2}} dk_\rho k_\rho
$$

$$
= \frac{\mathcal{V}}{(2\pi)^3} \int_0^\infty dk\,k \int_0^{2\pi} d\varphi \int_0^k dk_\rho k_\rho \frac{1}{\sqrt{k^2-k_\rho^2}}\,, \tag{6.135}
$$

where $k^2 = k_{\mathcal{L}}^2 + k_\rho^2$. For a finite radius ρ_0 the boundary conditions of the tube, the radial component of the wave vector k_ρ would only adopt discrete values which are determined by the diameter of the tube. Thus, we have

$$
\sum_{k_{\mathcal{L}}>0,k_\rho,\varphi} \rightarrow \frac{\mathcal{V}}{(2\pi)^3} \int_0^\infty dk\,k \int_0^{2\pi} d\varphi \sum_{n,m}^{\kappa_{mn}<k} \frac{\kappa_{mn}}{\rho_0\sqrt{k^2-\kappa_{mn}^2}}\,. \tag{6.136}
$$

However, in order to find analytical expressions for the energy shifts and bath correlators we consider, as stated above, only the continuum limit (6.135) and $\rho_0 \to \infty$. We find

$$
\Omega_{S/A} = \sqrt{\Omega_0^2 + \int_0^\infty d\omega \frac{J^{3D}(\omega)}{\omega}\left(1 \pm \frac{\sin(\omega r)}{\omega r}\right)}\,. \tag{6.137}
$$

The bath correlators read

$$
\alpha_{1,S/A} = \int_0^\infty dt\,\nu_{S/A}(r,t)\cos(\bar{\Omega}t) \tag{6.138}
$$

$$
= \frac{1}{2}\int_0^\infty dt \int_0^\infty d\omega\,J^{3D}(\omega)\left(1 \pm \frac{\sin(\omega r)}{\omega r}\right)\coth\left(\frac{\omega}{2T}\right)\cos(\omega t)\cos(\bar{\Omega}t)\,,
$$

$$
\alpha_{2,S/A} = -\int_0^\infty dt\,\nu_{S/A}(r,t)\frac{\sin(\bar{\Omega}t)}{\bar{\Omega}} \tag{6.139}
$$

$$
= -\frac{1}{2}\int_0^\infty dt \int_0^\infty d\omega\,J^{3D}(\omega)\left(1 \pm \frac{\sin(\omega r)}{\omega r}\right)\coth\left(\frac{\omega}{2T}\right)\cos(\omega t)\frac{\sin(\bar{\Omega}t)}{\bar{\Omega}}\,,
$$

$$
\alpha_{3,S/A} = -\int_0^\infty dt\,\mu_{S/A}(r,t)\cos(\bar{\Omega}t) \tag{6.140}
$$

$$
= -\frac{1}{2}\int_0^\infty dt \int_0^\infty d\omega\,J^{3D}(\omega)\left(1 \pm \frac{\sin(\omega r)}{\omega r}\right)\sin(\omega t)\cos(\bar{\Omega}t)\,,
$$

$$
\alpha_{4,S/A} = \int_0^\infty dt\,\mu_{S/A}(r,t)\frac{\sin(\bar{\Omega}t)}{\bar{\Omega}} \tag{6.141}
$$

$$
= \frac{1}{2}\int_0^\infty dt \int_0^\infty d\omega\,J^{3D}(\omega)\left(1 \pm \frac{\sin(\omega r)}{\omega r}\right)\sin(\omega t)\frac{\sin(\bar{\Omega}t)}{\bar{\Omega}}\,,
$$

where the functions $\mu_{S/A}$ and $\nu_{S/A}$ are defined by

$$\nu_{S/A} = \frac{1}{\mathcal{V}} \sum_{k_\mathcal{L}>0,k_\rho,\varphi} g_k^2 f_{S/A}(k_\mathcal{L}) \Re\langle p_{\mathbf{k},S/A} p_{\mathbf{k},S/A}(-t)\rangle \tag{6.142}$$

$$\mu_{S/A} = -\frac{1}{\mathcal{V}} \sum_{k_\mathcal{L}>0,k_\rho,\varphi} g_k^2 f_{S/A}(k_\mathcal{L}) \Im\langle p_{\mathbf{k},S/A} p_{\mathbf{k},S/A}(-t)\rangle . \tag{6.143}$$

with the functions $f_S(k_\mathcal{L}) = \cos^2(k_\mathcal{L}r/2)$ for the symmetric bath modes and $f_A(k_\mathcal{L}) = \sin^2(k_\mathcal{L}r/2)$ for the antisymmetric ones, respectively. We chose the spectral density to be

$$J^{3D}(\omega) = \frac{1}{4\pi\mathcal{L}} \sum_{k>0} g_k^2 \omega_k^3 \delta(\omega_k - \omega) = \frac{2\gamma}{\pi}\omega\left(\frac{\omega}{\Omega_c}\right)^{s-1} e^{-\frac{\omega}{\Omega_c}} . \tag{6.144}$$

Analytic expressions of the correlators are given in section 8.3.

Relation to the exact Model

So far we have treated the coupling constant g_{ω_0} and the coupling strength γ independently from each other. However, the peak oscillators are an effective description of the van Hove-singularity. Therefore, it should be possible to derive a relation between g_{ω_0} and γ. For a tube with finite radius we have, for $t = 0$

$$\begin{aligned}
\nu_S(r,0) &= \frac{1}{\mathcal{V}} \sum_{k_\mathcal{L}>0,k_\mathcal{R},\varphi} g_k^2 \langle p_{\mathbf{k},S}^2\rangle \\
&= \frac{1}{(2\pi)^3} \int_0^\infty dk\, k \int_0^{2\pi} d\phi \sum_{n>0}^{n<k/\omega_0} g_k^2 \frac{n\omega_0^2}{\sqrt{k^2 - n^2\omega_0^2}} \times \\
&\quad \times \cos^2\left(\sqrt{k^2 - n^2\omega_0^2}\, r\right) \frac{k}{2} \coth\left(\frac{k}{2T}\right) \\
&= \int_0^\infty d\omega \sum_{n>0}^{n<\omega/\omega_0} \frac{J^{3D}(\omega)}{\omega} \frac{n\omega_0^2}{\sqrt{\omega^2 - n^2\omega_0^2}} \times \\
&\quad \times \cos^2\left(\sqrt{\omega^2 - n^2\omega_0^2}\, r\right) \coth\left(\frac{\omega}{2T}\right) .
\end{aligned} \tag{6.145}$$

Including only the first van Hove peak in our considerations and confining the integration to the interval $(\omega_0, \omega_0 + \delta\omega)$, we find

$$\begin{aligned}
g_{\omega_0}^2 \langle p_{\omega_\mathbf{0},S}^2\rangle &= g_{\omega_0}^2 \frac{\omega_0}{2} \coth\left(\frac{\omega_0}{2T}\right) \\
&\approx J^{3D}(\omega_0)\sqrt{2\omega_0\delta\omega} \coth\left(\frac{\omega_0}{2T}\right) .
\end{aligned} \tag{6.146}$$

Thus, we have derived an effective coupling constant for the interaction between system and peak oscillators, g_{ω_0}. We know that the modes within the peak will oscillate coherently for distances $r < 1/\delta\omega$. Inserting this relation into (6.146) leads to an effective distance dependence of g_{ω_0}. Since g_{ω_0} would increase indefinitely for $r \to 0$, we need a natural cutoff for the smallest distance possible. The smallest distance which the bath modes are able to resolve is given by the inverse cutoff $1/\Omega_c$, therefore we assume

$$\delta\omega = \frac{1}{r + \frac{1}{\Omega_c}} \tag{6.147}$$

and obtain an effectively distance dependent coupling constant,

$$g_{\omega_0}^2(r) \approx \frac{4\sqrt{2}\gamma\omega_0}{\pi} \left(\frac{\omega_0}{\Omega_c}\right)^{s-1} \frac{e^{-\frac{\omega_0}{\Omega_c}}}{\sqrt{\omega_0 r + \frac{\omega_0}{\Omega_c}}} . \tag{6.148}$$

In the subsequent sections, we will investigate the distance dependence of entanglement generation using relation (6.148).

Generation of Entanglement

The negativity can now be evaluated for various parameters. Since we are interested especially in the time– and distance–dependence of the generated entanglement, we will use density plots in the following discussion.

In contrast to the one–dimensional model that was discussed in section 6.3.2, the coupling constant g_{ω_0} is not periodic in the distance parameter r but rather decreasing with growing separation of the system oscillators (see equation (6.148)). Thus, the generated entanglement will always decrease with growing r.

At first, we consider the dependence of negativity on the frequency of the coupling oscillator representing the symmetric modes within the spectral peak. We see from fig. 6.19 that the logarithmic negativity is maximal if the coupling oscillator and the system oscillators are approximately in resonance. For small distances, however, the value of ω_0 is less important.

An important ingredient for generating significant entanglement is the choice of the initial state. From fig. 6.20 we deduce that the initial state of the system oscillators should be far away from the ground state. If one chooses the ground state $(b = \Omega_0)$, the negativity is only of order γ, since the oscillators tend to stay in the ground state. The generation of entanglement can be enhanced significantly by choosing a strongly squeezed state since system oscillators then release energy to the bath and evolve into an entangled state.

Varying the coupling strength γ shows the following (see fig. 6.21): For small γ, the generation of entanglement takes longer than for large γ. Since the dissipation

rate depends on the coupling strength, the damping of the logarithmic negativity increases with γ.

The last dependence that we consider concerns the spectral index s. Since it appears in the spectral density (6.144) in the factor $(\omega/\Omega_c)^{s-1}$ we have to be careful. Increasing s by one introduces an additional factor of ω/Ω_c diminishes the effective coupling strength. Thus we will rescale the coupling according to $\gamma \to \gamma(\Omega_c/\Omega_0)^{s-1}$. We see in fig. 6.22 that the dependence of the entanglement on the spectral index is weak. Only for the large spectral index $s = 3$, the generation of entanglement is diminished.

We see that, due to the van Hove peak, entanglement can be generated over distances which are significantly larger that in the model without boundary conditions (see fig. 6.1).
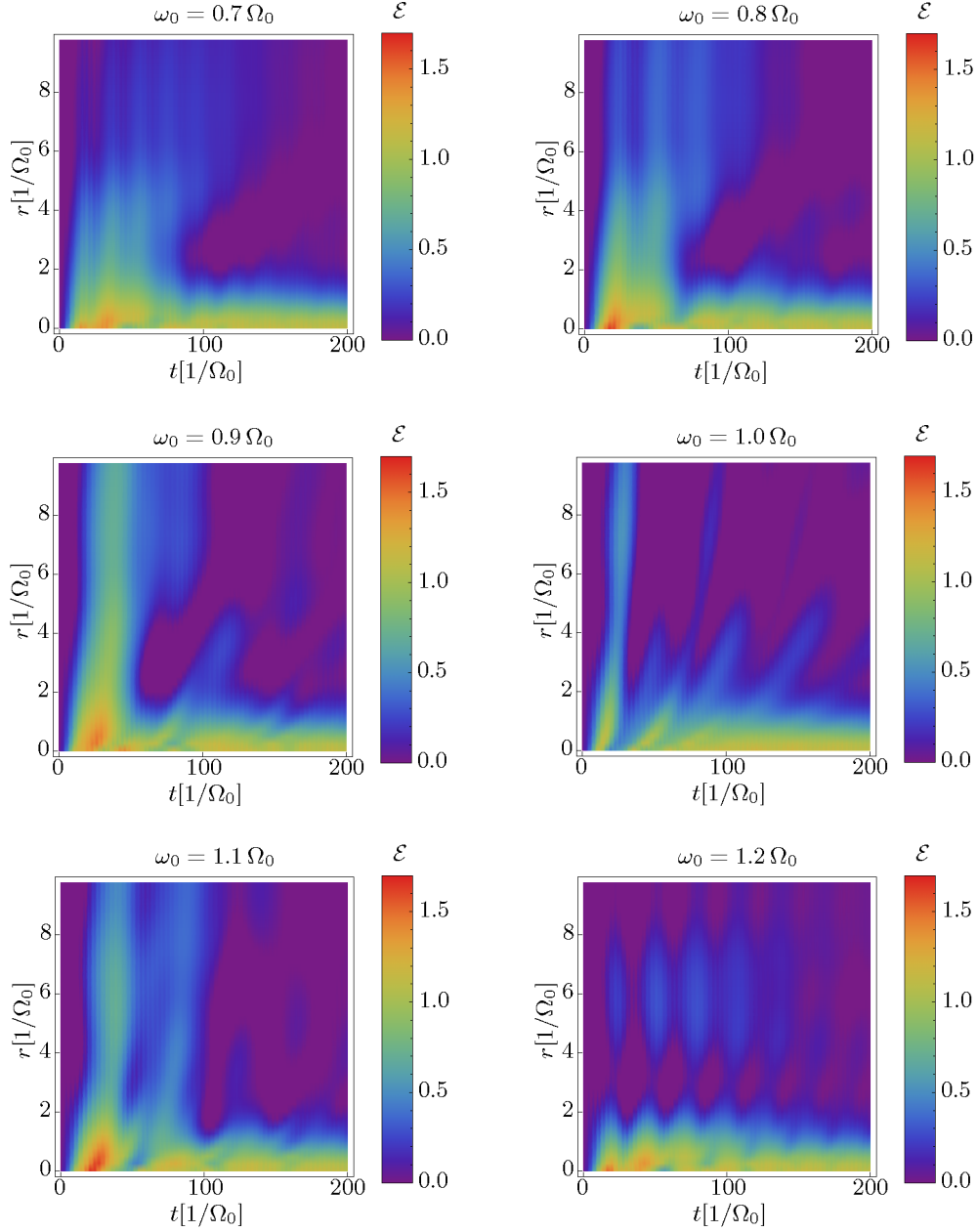
Figure 6.19: We plot the generation of entanglement for different frequencies ω_0 of the coupling oscillator. The maximal value of the negativity decreases with growing $|\omega_0 - \Omega_0|$, that is the peak oscillator and the system oscillator should be approximately in resonance. We chose the parameters to be $\gamma = 0.02\,\Omega_0, \Omega_c = 5\,\Omega_0, T = 0.01\,\Omega_0, b = 5\,\Omega_0, a = \omega_0$, and $s = 1$.
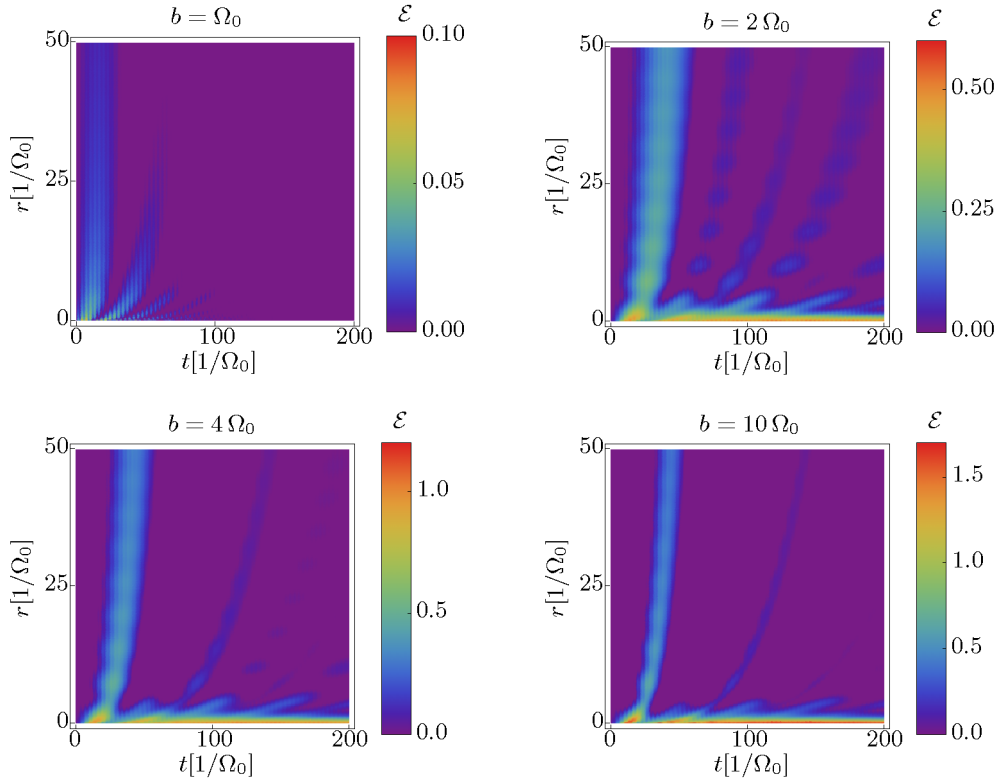
Figure 6.20: We depict the generation of entanglement for different initial states of the system oscillators. When the system oscillators are initially in the ground state ($b = \Omega_0$), the maximal negativity is of order 0.1 whereas this value increases by an order of magnitude for initially squeezed states. We chose the parameters to be $\gamma = 0.02\,\Omega_0, \Omega_c = 5\,\Omega_0, T = 0.01\,\Omega_0, \omega_0 = \Omega_0, a = \omega_0$, and $s = 1$.
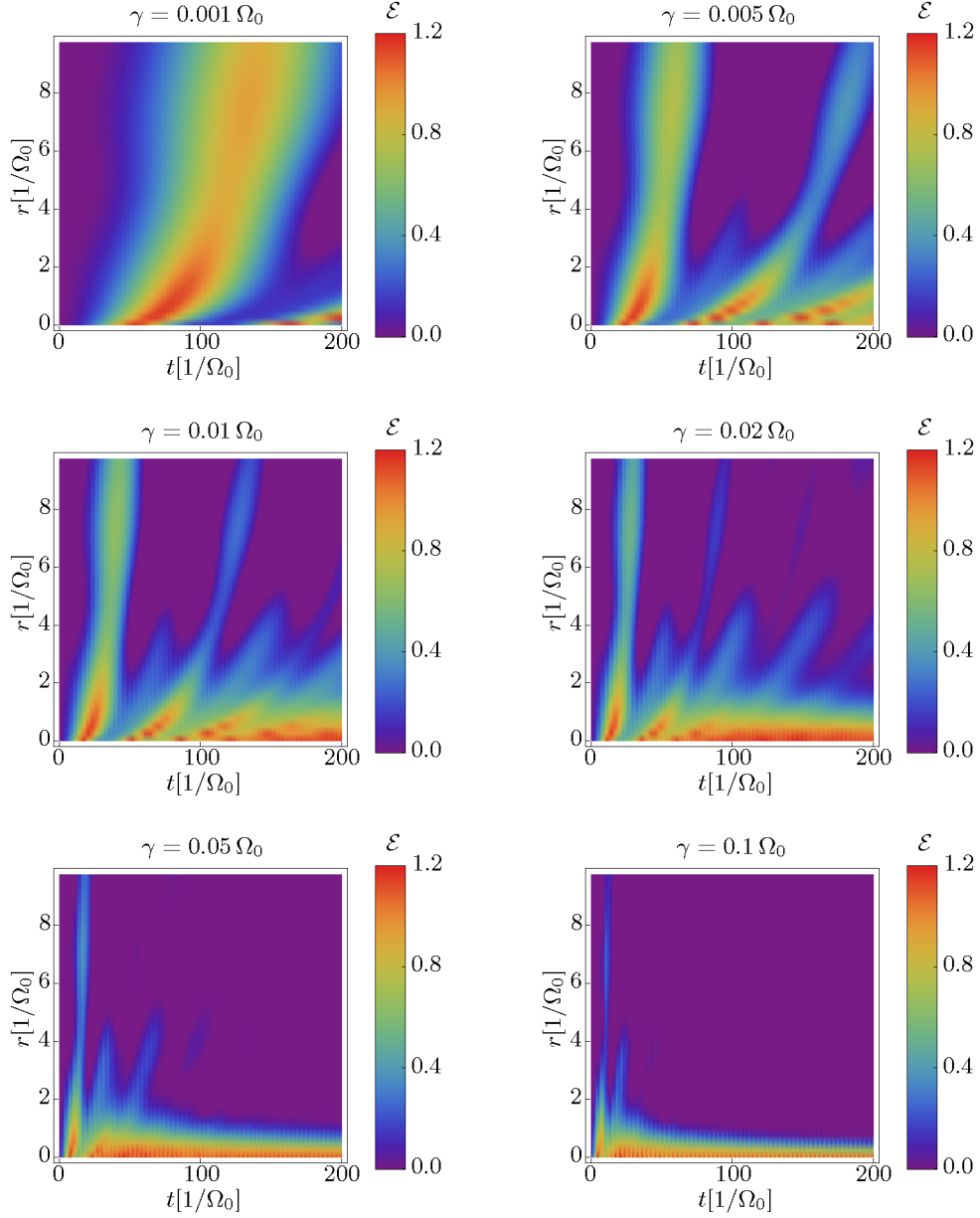
Figure 6.21: Here we show the generation of entanglement for different coupling strengths γ. For small $\gamma = 0.001\,\Omega_0$, the generation of entanglement takes longer than for $\gamma = 0.1\,\Omega_0$. However, the damping of entanglement increases with γ. We chose the parameters to be $b = 5\,\Omega_0, \Omega_c = 5\,\Omega_0, T = 0.01\,\Omega_0, \omega_0 = \Omega_0, a = \omega_0$, and $s = 1$.
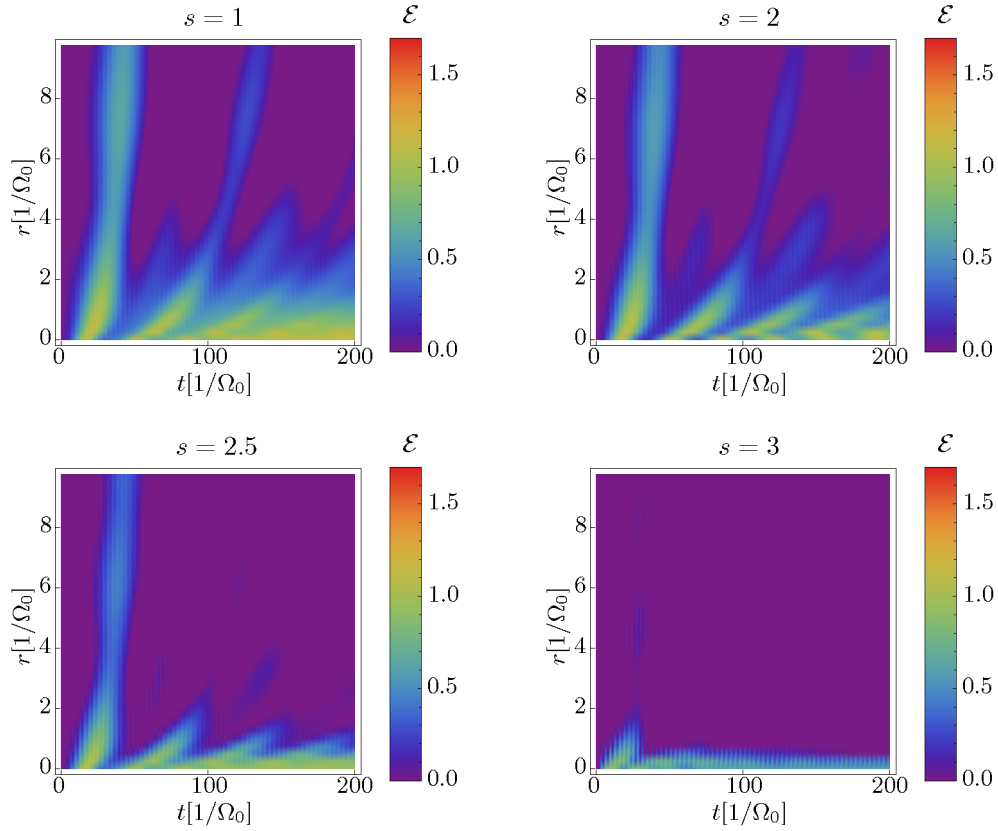
Figure 6.22: We show the dependence of entanglement generation for different spectral indices. The coupling strength has been rescaled according to $\gamma \to \gamma(\Omega_c/\Omega_0)^{s-1}$ and the parameters are $\gamma = 0.5\,\Omega_0$, $\Omega_c = 5\,\Omega_0$, $T = 0.01\,\Omega_0$, and $\omega_0 = \Omega_0$.

Asymptotic Entanglement

The asymptotic entanglement is given by the inhomogeneous solutions of the differential equations (8.15) – (8.28), since the homogeneous solutions become damped due to dissipative effects (see section 6.3.2). Retaining only terms of $\mathcal{O}(\gamma\xi)$ in the differential equations (as we did in order to find the approximate solutions 8.41) – (8.63) does not lead to a time–independent asymptotic state since the coupling oscillator does not thermalize within this approximation.

For a small coupling strength γ, it is possible to obtain a simple analytical expression by computing the thermal expectation value of the covariance matrix with respect to the Hamiltonian $H_0 = H_{0,S} + H_{0,A}$ whose parts are defined in (6.91) and (6.92). The result is

$$\mathcal{E}_{\mathrm{asym}} = -\log_2\left(\min\left[1, \lambda_1\right]\right) - \log_2\left(\min\left[1, \lambda_2\right]\right) , \tag{6.149}$$

where the symplectic eigenvalues are given by

$$\begin{aligned}
\lambda_1^2 &= \frac{1}{1+\xi^2}\frac{1}{\Omega_A}\coth\left(\frac{\Omega_A}{2T}\right) \times \\
&\quad \times \left[\bar{\Omega}_1\coth\left(\frac{\bar{\Omega}_1}{2T}\right) + \bar{\Omega}_2\xi^2\coth\left(\frac{\bar{\Omega}_2}{2T}\right)\right]
\end{aligned} \tag{6.150}$$

and

$$\begin{aligned}
\lambda_2^2 &= \frac{1}{1+\xi^2}\Omega_A\coth\left(\frac{\Omega_A}{2T}\right) \times \\
&\quad \times \left[\frac{\xi^2}{\bar{\Omega}_2}\coth\left(\frac{\bar{\Omega}_2}{2T}\right) + \frac{1}{\bar{\Omega}_1}\coth\left(\frac{\bar{\Omega}_1}{2T}\right)\right] .
\end{aligned} \tag{6.151}$$

In order to test expression (6.149), we have to make sure that the dissipative coupling strength γ is smaller than the peak coupling g_{ω_0}. Therefore, we will consider both parameters to be independent for the moment and ignore relation (6.148). We see from fig. 6.23 that the asymptotic entanglement given by the inhomogeneous solutions of (8.15) – (8.28) agrees with (6.149) only for $\gamma/g_{\omega_0} \ll 1$. For $\gamma/g_{\omega_0} = \mathcal{O}(1)$, the corrections due to the dissipative effects become important, although the qualitative shape of the curves remain unchanged.

In fig. 6.24 we used relation (6.148) and computed the temperature–dependence of the asymptotic entanglement for different values of γ. Obviously, $\mathcal{E}_{\mathrm{asym}}$ increases linearly with γ and is roughly of the same order as the coupling strength. This can be expected, since for low temperatures the asymptotic thermal state is approximately equal to the ground state of the total Hamiltonian. The *entangled* ground state (given here by the asymptotics of the solutions to the differential equations (8.15) –

(8.28)) differs from the *unentangled* ground state of $H_{0,S}|_{\gamma=0} + H_{0,A}|_{\gamma=0}$ only in order γ.

We show in fig. 6.25 the dependence of the asymptotic entanglement on the coupling strength γ. In order to obtain nonvanishing asymptotic entanglement, the coupling strength has to exceed a critical value that increases with the temperature.

In fig. 6.26 we depicted the cutoff–dependence for different temperatures. The asymptotic entanglement adopts a maximum value for an intermediate cutoff. From this intermediate cutoff, $\mathcal{E}_{asym}$ decreases with increasing Ω_c due to the growth of dissipation and decoherence. Furthermore, $\mathcal{E}_{asym}$ diminishes also with decreasing Ω_c, i.e. for a decreasing number of entanglement–generating environmental modes.

The distance–dependence of the asymptotic entanglement is shown in fig. 6.27. Clearly, $\mathcal{E}_{asym}$ decreases with increasing distance. This becomes also apparent from fig. 6.28 where we plot the citical distance, i.e. the distance above which the asymptotic entanglement vanishes, for different values of the cutoff and the temperature.
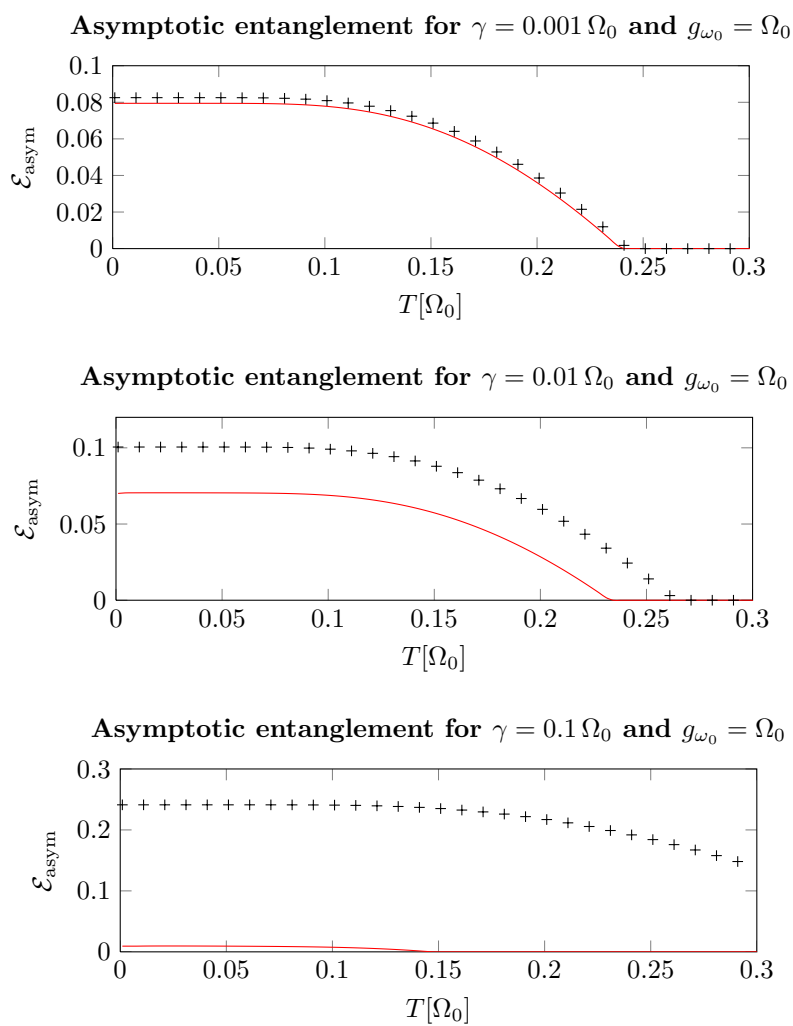
Figure 6.23: The marks denote the asymptotic entanglement given by the analytic expression (6.149), whereas the solid line is derived from the asymptotic solutions of (8.15) – (8.28). We chose the parameters to be $\Omega_c = 5\,\Omega_0, \omega_0 = \Omega_0, r = 0$, and $s = 1$.
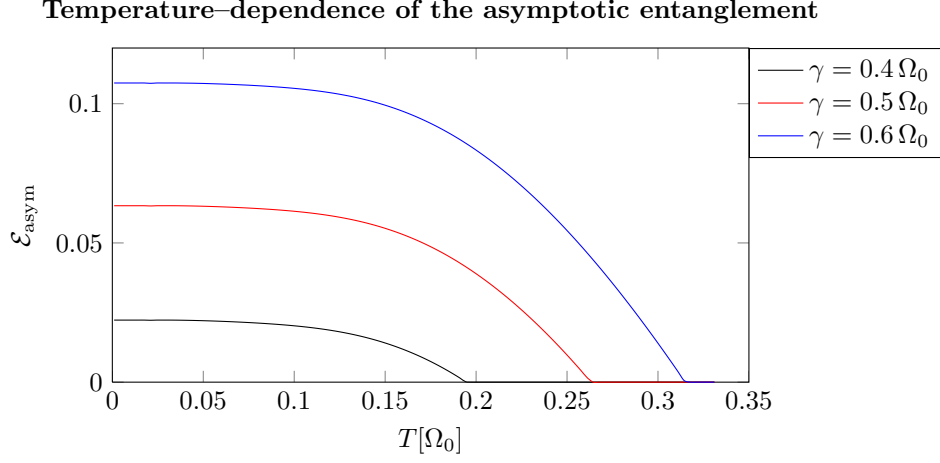
Temperature–dependence of the asymptotic entanglement

Figure 6.24: We depict the asymptotic logarithmic negativity for different values of γ. We chose the parameters to be $\Omega_c = 5\,\Omega_0, \omega_0 = \Omega_0, r = 0$, and $s = 1$.

Dependence of the asymptotic entanglement on γ
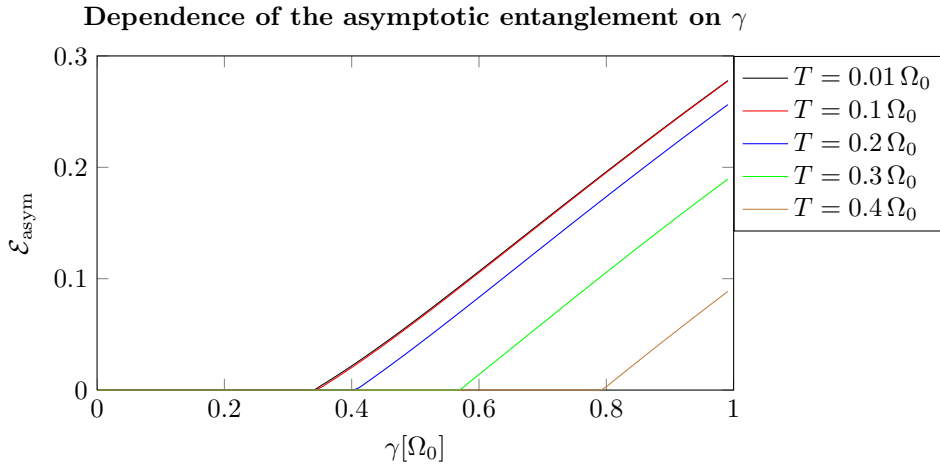
Figure 6.25: We plot the asymptotic logarithmic negativity for different values of T. The minimal value γ where $\mathcal{E}_{\mathrm{asym}} \neq 0$ increases with the temperature. The parameters were chosen to be $\Omega_c = 5\,\Omega_0, \omega_0 = \Omega_0, r = 0$, and $s = 1$.

Cutoff–dependence of the asymptotic entanglement
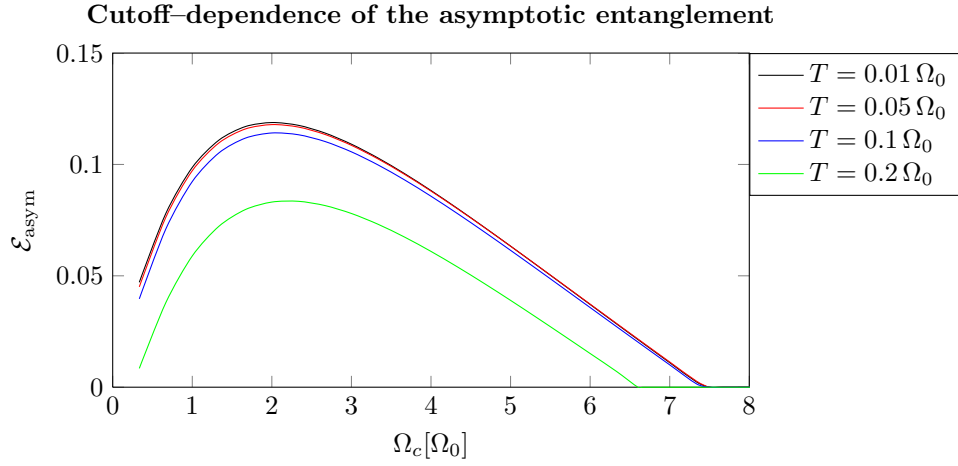
Figure 6.26: We depict the cutoff–dependence of $\mathcal{E}_{\mathrm{asym}}$ for different temperatures. The remaining parameters are $\gamma = 0.5\,\Omega_0, \omega_0 = \Omega_0, r = 0$, and $s = 1$.
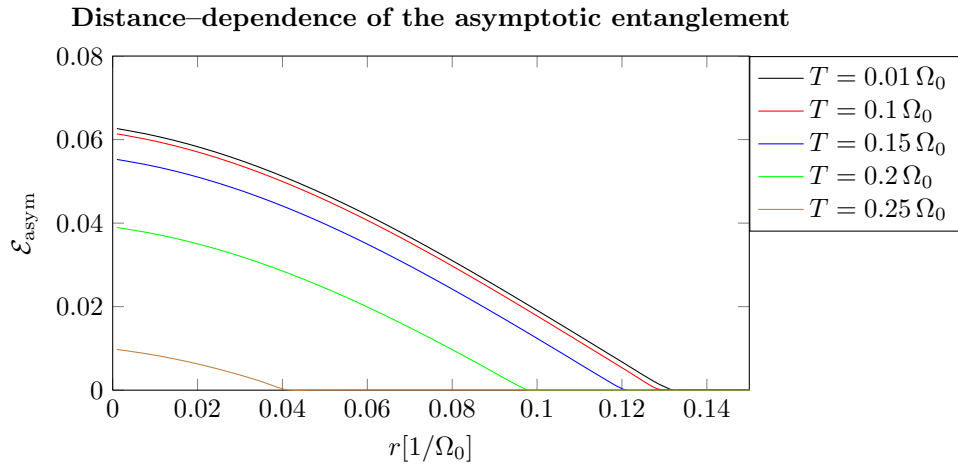
Distance–dependence of the asymptotic entanglement

Figure 6.27: We depict the distance–dependence of $\mathcal{E}_{\mathrm{asym}}$ for different temperatures. The remaining parameters are $\gamma = 0.5\,\Omega_0, \omega_0 = \Omega_0, \Omega_c = 5\,\Omega_0$, and $s = 1$.
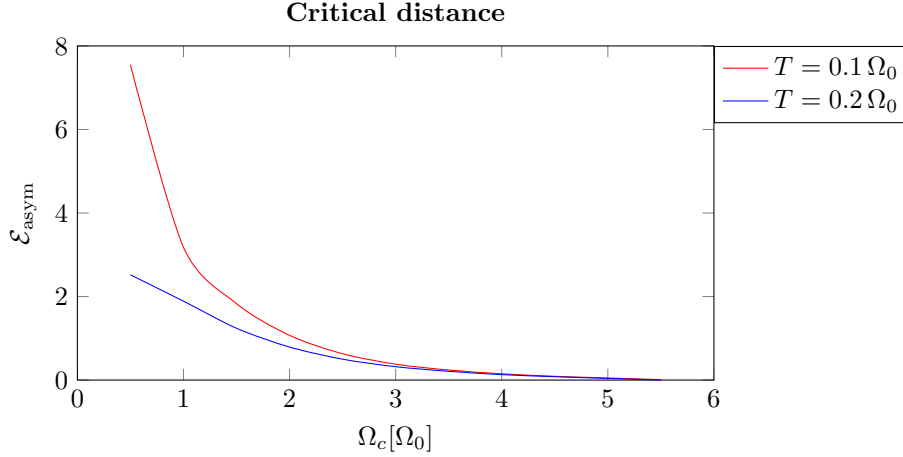
Critical distance

Figure 6.28: We depict the critical distance for different values of the temperature and the cutoff. The remaining parameters are $\gamma = 0.5\,\Omega_0, \omega_0 = \Omega_0, \gamma = 5\,\Omega_0$, and $s = 1$.

Decoherence Times

The question arises how this oscillator model may be related to a realistic situation, for instance the entanglement of atomic states.

An example would be the $6S_{1/2}$ hyperfine ground states $|F = 4, m_F = 0\rangle$ and $|F = 3, m_F = 0\rangle$ of cesium atoms [157]. The transition energy between these two states is $\omega_\epsilon/2\pi = 9.2$ GHz. An advantage of these hyperfine ground states is the long coherence time ~ 200 ms.

Although the transition between $|F = 4, m_F = 0\rangle$ and $|F = 3, m_F = 0\rangle$ could be described by spin dynamics, we want to relate this system to our oscillator model. Since for low temperatures only the ground state and the first excited state of an oscillator is significantly populated, we may replace the oscillators with spins via $Q \rightarrow (\sigma_+ + \sigma_-)/\sqrt{2\Omega_0}$ [153].

Restricting ourselves to the part of the master equation describing decoherence, it reads

$$\dot{\rho} = -\alpha_1(\Omega_0)[Q, [Q, \rho]]. \tag{6.152}$$

Thus, for low temperatures we have in the rotating wave approximation [120]

$$\dot{\rho}_{\mathrm{spin}} = -\frac{\alpha_1(\Omega_0)}{2\Omega_0}\left([\sigma_+, [\sigma_-, \rho_{\mathrm{spin}}]] + h.c.\right), \tag{6.153}$$

from which we deduce the decoherence time

$$t_{\mathrm{d}} \approx \frac{2\Omega_0}{\alpha_1(\Omega_0)}. \tag{6.154}$$

6.4 Entanglement of Spins via a Common Heat Bath

So far we haven chosen oscillators in order to study bath mediated entanglement. The advantage was that the oscillator model inhibited dissipative effects and could treated exactly up to the numerical solution of the Langevin equations (6.55) and (6.56).

However, in the original work of Braun [8, 130], the author discussed a dissipationless spin–boson–model which is known to be exactly solvable [78]. In contrast, the dissipative spin–boson–model is not exactly solvable, which makes it difficult to study the influence of dissipation on the generation of entanglement in this case. Applying the rotating wave approximation to the Hamiltonian will allow us to solve the dissipative spin–boson–model for a restricted set of initial conditions.

An analogous setup involving only a single spin has been considered by Garraway [158] in the context of atomic decay in a cavity [159].

We will see that it is possible to generate a significant amount of entanglement between the spins, even when they are separated from each other. However, we will argue that the amount of generated entanglement is too large and relies on the particular form of the Hamiltonian.

Let us describe the investigated model in more detail. The spins both have frequency ω_0 and are coupled to a three-dimensional heat bath consisting of harmonic modes of frequencies $\omega_k = k$. The spin splitting is given by $2\omega_0$ and σ_x^i, σ_y^i and σ_z^i denote the Pauli operators. It is convenient to define the raising and lowering operators

$$\sigma_+^i = \frac{1}{2}(\sigma_x^i + i\sigma_y^i) \quad \text{and} \quad \sigma_-^i = \frac{1}{2}(\sigma_x^i - i\sigma_y^i)\,. \tag{6.155}$$

The creation and annihilation operators for the bath modes are denoted by $b_{\mathbf{k}}^\dagger$ and $b_{\mathbf{k}}$. Placing the spins at the positions $\mathbf{r}_1$ and $\mathbf{r}_2$, we consider the Hamiltonian

$$H_0 \;=\; \sum_{i=1,2}\omega_0\sigma_z^i + \sum_{\mathbf{k}}\omega_k b_{\mathbf{k}}^\dagger b_{\mathbf{k}} + H_{\text{int}}\,, \tag{6.156}$$

with

$$H_{\text{int}} \;=\; \sum_{i=1,2}(\sigma_+^i + \sigma_-^i)\phi(\mathbf{r}_i)\,. \tag{6.157}$$

The environmental field ϕ can be decomposed according to

$$\phi(\mathbf{r}_i) = \sum_{\mathbf{k}}\left(\lambda_k b_{\mathbf{k}} e^{-i\mathbf{k}\mathbf{r}_i} + h.c.\right)\,. \tag{6.158}$$

Applying the rotating wave approximation, we have

$$H_{\text{int,rot}} = \sum_{i=1,2} \sum_{\mathbf{k}} (\sigma_+^i \lambda_k b_{\mathbf{k}} e^{-i\mathbf{k}\mathbf{r}_i} + h.c.) . \tag{6.159}$$

The coupling strengths λ_k are characterized by an ohmic spectral density

$$J(\omega) = 4\pi \int_0^\infty dk k^2 \lambda_k^2 \delta(k - \omega) = \lambda\,\omega \exp(-\omega/\Omega_c) \tag{6.160}$$

which coincides with the spectral density (6.3.1) for $s = 1$. We denote the cutoff with Ω_c and the coupling strength with λ.

The bilinear interaction (6.159) consists of combinations of creation operators for the spins and annihilation operators for the bath modes and vice versa. However, combinations of the form $\sigma_+^i b_{\mathbf{k}}^\dagger$ and $\sigma_-^i b_{\mathbf{k}}$ are missing which would appear in the usual spin boson model [78]. The absence of these terms guarantees an analytical solution for the model, since the interaction commutes with the generalized number operator

$$\hat{N} = \sum_{i=1,2} \sigma_+^i \sigma_-^i + \sum_{\mathbf{k}} b_{\mathbf{k}}^\dagger b_{\mathbf{k}} . \tag{6.161}$$

The disregard of the terms mentioned above is also known as the rotating wave approximation and is often used in the context of master equations in order to obtain an evolution equation of Lindblad form which guarantees the positive definiteness of the reduced density matrix (see [120] for a discussion of quantum master equations). It can be applied if the time scale of the intrinsic evolution, say $1/\omega_0$, is small compared to the relaxation time of the model. Roughly speaking, terms like $\sigma_+^i b_{\mathbf{k}}^\dagger$ and $\sigma_-^i b_{\mathbf{k}}$ are oscillating rapidly during the relaxation time in which the system changes appreciably. In the context of master equations, this approximation guarantees the positive definiteness of the reduced density matrix.

However, the generalized number operator (6.161) is obviously a *nonlocal* observable, since it involves terms defined at *different* positions, that is $\mathbf{r}_1$ and $\mathbf{r}_2$. We will show, in the following, that the time evolution pretends the generation of a significant amount of entanglement, which is due to the nonlocal observable.

The model (6.156) with the interaction (6.159) is exactly solvable for one–particle states $|\psi\rangle$ that are defined through $\langle\psi|\hat{N}|\psi\rangle = 1$. The general ansatz for such a state reads

$$\begin{aligned} |\psi(t)\rangle &= C_{10,0}(t)|10\rangle \otimes |0\rangle + C_{01,0}(t)|01\rangle \otimes |0\rangle + \\ &\quad + \sum_{\mathbf{k}} C_{00,\mathbf{k}}(t)|00\rangle \otimes |\mathbf{k}\rangle . \end{aligned} \tag{6.162}$$

From the Schrödinger equation involving the Hamiltonian (6.156), we find the differential equations

$$
\begin{aligned}
\dot{C}_{10,0}(t) &= -\sum_{\mathbf{k}} \int_0^t ds |\lambda_k|^2 e^{-i(k-\omega_0)(t-s)} \left[C_{10,0}(s) + C_{01,0}(s) e^{-i\mathbf{k}(\mathbf{r}_1-\mathbf{r}_2)} \right] \\
&\quad -i \sum_{\mathbf{k}} \lambda_k e^{-i\omega_0 t - i\mathbf{k}\mathbf{r}_1} C_{00,\mathbf{k}}(0)
\end{aligned}
\tag{6.163}
$$

and

$$
\begin{aligned}
\dot{C}_{01,0}(t) &= -\sum_{\mathbf{k}} \int_0^t ds |\lambda_k|^2 e^{-i(k-\omega_0)(t-s)} \left[C_{01,0}(s) + C_{10,0}(s) e^{-i\mathbf{k}(\mathbf{r}_2-\mathbf{r}_1)} \right] \\
&\quad -i \sum_{\mathbf{k}} \lambda_k e^{-i\omega_0 t - i\mathbf{k}\mathbf{r}_2} C_{00,\mathbf{k}}(0) \,.
\end{aligned}
\tag{6.164}
$$

Due to the special choice of initial states of the form (6.162), we are restricted in the choice of initial density matrices. Taking the bath modes to be in the ground state for $t = 0$, a possible separable initial state is

$$
\rho(t=0) = \frac{1}{2} \left(|0,1\rangle\langle 0,1| + |1,0\rangle\langle 1,0| \right) \otimes |0\rangle\langle 0| \,.
\tag{6.165}
$$

The time evolution of the reduced density matrix $\rho_{\text{sys}}(t) = \text{Tr}_{\text{bath}}\rho(t)$ can be expressed in terms of $C_{01,0}(t)$ and $C_{10,0}(t)$.

After a Laplace transformation $\mathcal{L}(C) = \tilde{C}$ of (6.163) and (6.164) with $C_{00,\mathbf{k}}(0) = 0$, we find

$$
\tilde{C}_{10,0}(q) = \frac{C_{10,0}(0)(q + F(q,0)) - C_{01,0}(0)F(q,r)}{(q + F(q,0))^2 - F^2(q,r)}
\tag{6.166}
$$

$$
\tilde{C}_{01,0}(q) = \frac{C_{01,0}(0)(q + F(q,0)) - C_{10,0}(0)F(q,r)}{(q + F(q,0))^2 - F^2(q,r)} \,,
\tag{6.167}
$$

with

$$
\begin{aligned}
F(q,r) &= \lambda \int_0^\infty d\omega \frac{\omega \exp(-\omega/\Omega)}{q + i(\omega - \omega_0)} \frac{\sin(\omega r)}{\omega r} \\
&= \frac{\lambda}{2r} \Bigg\{ e^{-\left(r+\frac{i}{\Omega_c}\right)(q-i\omega_0)} \left(\Gamma\left[0, -\left(r+\frac{i}{\Omega_c}\right)(q-i\omega_0)\right] \right. \\
&\quad \left. - \ln\left[\frac{1}{\Omega_c} - ir\right] + \ln\left[\frac{i}{q-i\omega_0}\right] + \ln\left[-\left(r+\frac{i}{\Omega_c}\right)(q-i\omega_0)\right] \right) \\
&\quad - e^{\left(r-\frac{i}{\Omega_c}\right)(q-i\omega_0)} \left(\Gamma\left[0, \left(r-\frac{i}{\Omega_c}\right)(q-i\omega_0)\right] \right. \\
&\quad \left. - \ln\left[\frac{1}{\Omega_c} + ir\right] + \ln\left[\frac{i}{q-i\omega_0}\right] + \ln\left[\left(r-\frac{i}{\Omega_c}\right)(q-i\omega_0)\right] \right) \Bigg\} \,,
\end{aligned}
\tag{6.168}
$$

where the spectral density (6.160) was used. The reduced density matrix reads explicitly

$$
\begin{aligned}
\rho_{\mathrm{sys}}(t) \;=\;& (1 - |C_{10,0}(t)|^2 - |C_{01,0}(t)|^2)|00\rangle\langle00| \\
&+ \frac{1}{2}(|C_{10,0}(t)|^2 + |C_{01,0}(t)|^2)(|01\rangle\langle01| + |10\rangle\langle10|) \\
&+ \Re(C_{10,0}(t)C_{01,0}^*(t))(|01\rangle\langle10| + |10\rangle\langle01|)\,,
\end{aligned}
\tag{6.169}
$$

where the coefficients $C_{10,0}(t)$ and $C_{01,0}(t)$ satisfy the differential equations (6.163) and (6.164) and the initial conditions $C_{10,0}(0) = 1$ and $C_{01,0}(0) = 0$, that is

$$
C_{10,0}(t) \;=\; \frac{1}{2}\mathcal{L}^{-1}\left(\frac{1}{q + F(q,0) - F(q,r)} + \frac{1}{q + F(q,0) + F(q,r)}\right)
\tag{6.170}
$$

and

$$
C_{01,0}(t) \;=\; \frac{1}{2}\mathcal{L}^{-1}\left(\frac{1}{q + F(q,0) + F(q,r)} - \frac{1}{q + F(q,0) - F(q,r)}\right),
\tag{6.171}
$$

where $\mathcal{L}^{-1}$ denotes the inverse Laplace transformation with respect to the variable q. In section 6.2.2 we defined the negativity $\mathcal{N}$ as measure for the entanglement for a bipartite system. For the reduced density matrix (6.169), we find

$$
\begin{aligned}
\mathcal{N} \;=\;& \frac{1 - |C_{10,0}(t)|^2 - |C_{01,0}(t)|^2}{2} \\
&- \sqrt{\left(\frac{1 - |C_{10,0}(t)|^2 - |C_{01,0}(t)|^2}{2}\right)^2 + \left[\Re(C_{10,0}(t)C_{01,0}^*(t))\right]^2}.
\end{aligned}
\tag{6.172}
$$

For the concurrence (6.31) we find with (6.169) and (6.32) the simple result

$$
\mathcal{C} = 2|\Re(C_{10,0}(t)C_{01,0}^*(t))|\,.
\tag{6.173}
$$

The negativity and the concurrence give different numerical values for the entanglement. However, we see that both are non-vanishing if and only if both $C_{10,0}$ and $C_{01,0}$ are different from zero. Since the analytical results are easier to express in terms of the concurrence than in terms of the negativity, we will use the former measure.

6.4.1 Entanglement Generation for Short Times

In the preceding section, we mentioned that, due to the non–local conserved quantity (6.161), the time evolution generates entanglement between the spins which would not be there without this symmetry. In the limit of small times, we are able to quantify this statement analytically. We compare the concurrence for short times,

which is due to the spin-bath interaction (6.159) with the concurrence generated by the interaction term (6.157). For the rotating wave interaction, we find the concurrence

$$\mathcal{C}(t) = \lambda \frac{\Omega^2 t^2}{1 + \Omega^2 r^2} \,, \tag{6.174}$$

which is only polynomially decreasing. Regardless of how far the spins are separated from each other, the spins become entangled as soon as the interaction is switched on. This is due to the fact that the events "switching on the interaction at position 1" and "switching on the interaction at position 2" are spatially separated. However, the weak polynomial decrease of the short time concurrence is due to the *nonlocal* conserved quantity 6.161.

In contrast, taking the bilinear interaction to be of the form (6.157) and computing the density matrix up to second order perturbation theory, we obtain

$$\begin{aligned}
\rho_{\text{sys}}(t) &= a(t)|00\rangle\langle 00| + (1/2 - b(t))(|01\rangle\langle 01| + |10\rangle\langle 10| \\
&\quad + (2b(t) - a(t))|11\rangle\langle 11| \\
&\quad - c(t)(|01\rangle\langle 10| + |10\rangle\langle 01|) \\
&\quad - d(t)(|00\rangle\langle 11| + |11\rangle\langle 00|) \,,
\end{aligned} \tag{6.175}$$

with the coefficients

$$\begin{aligned}
a(t) &= \int_0^t dt' \int_0^t dt'' e^{-i\omega_0(t'-t'')} B_0(t' - t'') \,, \\
b(t) &= 2\int_0^t dt' \int_0^{t'} dt'' \cos(\omega_0(t' - t'')) \Re(B_0(t' - t'')) \,, \\
c(t) &= 2\int_0^t dt' \int_0^{t'} dt'' \cos(\omega_0(t' - t'')) \Re(B_r(t' - t'')) \,, \\
d(t) &= \int_0^t dt' \int_0^t dt'' e^{-i\omega_0(t'+t'')} B_r(t' - t'') \,.
\end{aligned} \tag{6.176}$$

The bath correlation functions B_0 and B_r are defined as

$$\begin{aligned}
B_0 &= \langle 0|\phi(\mathbf{r_1})\phi(\mathbf{r_1})|0\rangle = \langle 0|\phi(\mathbf{r_2})\phi(\mathbf{r_2})|0\rangle \,, & (6.177) \\
B_r &= \langle 0|\phi(\mathbf{r_1})\phi(\mathbf{r_2})|0\rangle = \langle 0|\phi(\mathbf{r_2})\phi(\mathbf{r_1})|0\rangle \,. & (6.178)
\end{aligned}$$

The concurrence corresponding from the density matrix (6.175) reads

$$\mathcal{C} = \max\left\{0, 2|c(t)| - 2\sqrt{a(t)(2b(t) - a(t))}\right\} \,. \tag{6.179}$$

Put differently, there is nonvanishing entanglement if and only if the inequality

$$\int_0^\infty d\omega e^{-\frac{\omega}{\Omega}} \frac{\sin(\omega r)}{r} \left(\frac{1 - \cos[(\omega + \omega_0)t]}{(\omega + \omega_0)^2} + \frac{1 - \cos[(\omega - \omega_0)t]}{(\omega - \omega_0)^2} \right)$$
$$> \quad 2\sqrt{\int_0^\infty d\omega \omega e^{-\frac{\omega}{\Omega}} \frac{1 - \cos[(\omega + \omega_0)t]}{(\omega + \omega_0)^2}} \times$$
$$\times \sqrt{\int_0^\infty d\omega \omega e^{-\frac{\omega}{\Omega}} \frac{1 - \cos[(\omega - \omega_0)t]}{(\omega - \omega_0)^2}} \tag{6.180}$$

holds. This inequality is always violated which is due to the fact that $\frac{\sin(\omega r)}{\omega r} \le 1$. We find that there is no entanglement for short times when the rotating wave approximation is not applied and the observable (6.161) is not a conserved quantity. Under realistic conditions one would expect that the entanglement for short times is either exponentially small or vanishing if the separation of the spins exceeds a critical value. The polynomial decrease of the entanglement in equation (6.174) is an artifact of the rotating wave approximation.

6.4.2 Entanglement Generation for Finite Times

For the rotating wave interaction (6.159) we are able to compute the entanglement numerically for arbitrary times. In order to compute the inverse Laplace transform (6.170) and (6.171), we used a Mathematica package that includes the so called Durbin formula [160, 161]. The Laplace transform of a function $f(t)$ and its inverse formula are defined as

$$F(s) \quad = \quad \mathcal{L}[f(t)] = \int_0^\infty dt e^{-st} f(t), \tag{6.181}$$

$$f(t) \quad = \quad \mathcal{L}^{-1}[F(s)] = \frac{1}{2\pi i} \int_{v-i\infty}^{v+i\infty} ds e^{st} F(s), \tag{6.182}$$

where v is a real number which is greater than the real parts of all the singularities of the function $F(s)$, but otherwise arbitrary. According to Durbin [161], one can approximate the inverse Laplace transform in the interval $t \in [0, 2T]$ through the Fourier series

$$f_N(t) \quad = \quad \frac{e^{vt}}{T} \left(\frac{1}{2} \Re(F(v)) \right. \tag{6.183}$$
$$+ \quad \sum_{k=0}^N \left\{ \Re \left(F \left(v + i\frac{k\pi}{T} \right) \right) \cos \frac{k\pi t}{T} - \Im \left(F \left(v + i\frac{k\pi}{T} \right) \right) \sin \frac{k\pi t}{T} \right\} \right)$$

which coincides with $f(t)$ in the limit $v \to \infty$ and $N \to \infty$.

In fig. 6.29 we show the generation of entanglement for various distances. Immediately after switching on the system–bath interaction, one observes nonvanishing concurrence which increases to a maximum value that is roughly inversely proportional to r. If the bosons had enough time to travel between both spins, that is $t = r$, the slope of the curves increases as can be seen in fig. 6.30. From the density plots of fig. 6.31 we deduce that the entanglement for $t < r$ is small, the concurrence adopts its maximum value at $t \gtrsim r$ and decreases afterwards. The decrease of maximal concurrence depends only polynomially on the distance, which is again due to the conserved quantity (6.161). We conjecture that the generation of entanglement "close to perfect" over arbitrarily large distances in the model of Braun [130] has similar reasons. Since Braun's model is dissipationless the conserved quantity is given by

$$\Sigma = \sigma_{z,1}\sigma_{z,2} \,, \tag{6.184}$$

where the σ_z-Pauli matrices commute with the total Hamiltonian in [130]. In other words, remote quantum systems "know" about each other due to *nonlocal* conserved quantities. This in turn generates a significant amount of entanglement. However, it is doubtful whether (6.184) or (6.161) are viable conserved quantities in realistic physical settings.

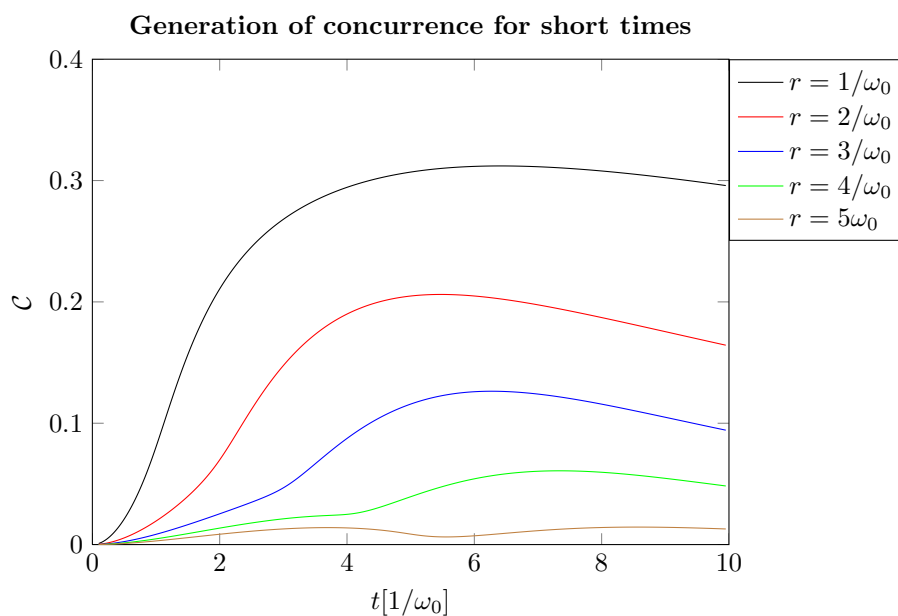**Generation of concurrence for short times**

Figure 6.29: Concurrence for different spin separations. The parameters were chosen to be $\lambda = 0.1\,\omega_0$ and $\Omega_c = 3\,\omega_0$.
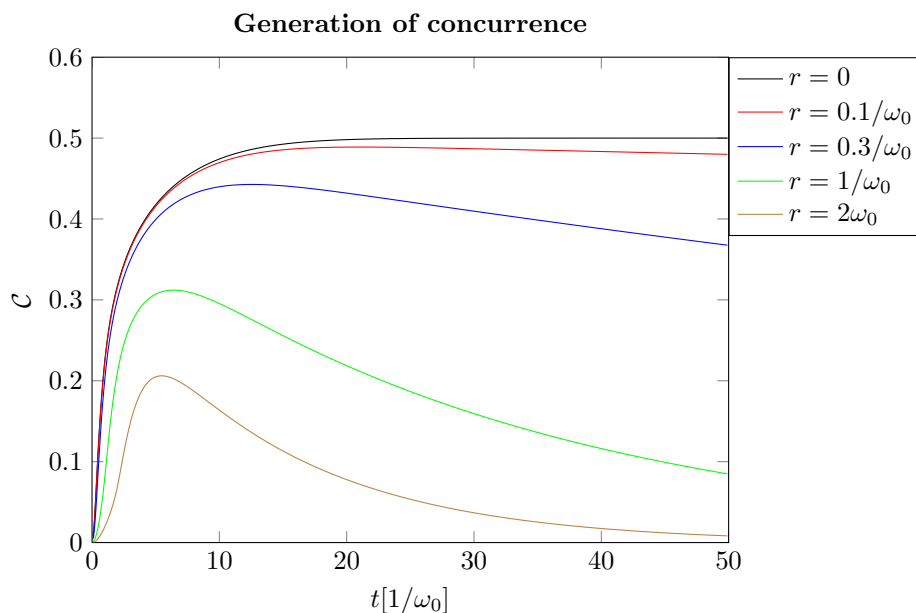
Generation of concurrence

Figure 6.30: As soon as the bosons had enough time to travel between the spins, the slope of the concurrence increases. The parameters were chosen to be $\lambda = 0.1\,\omega_0$ and $\Omega_c = 3\,\omega_0$.
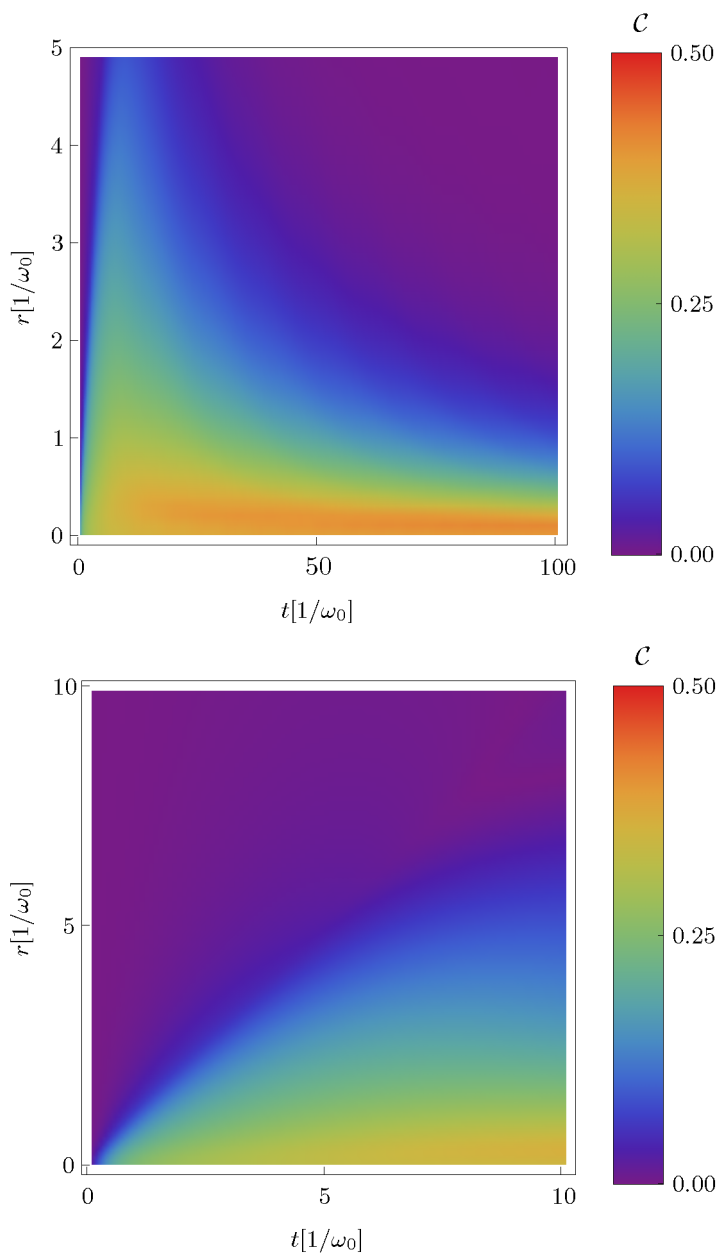
Figure 6.31: Maximum entanglement is generated at times $t \gtrsim r$ when the environmental bosons had enough time to bridge the spin separation at the speed of light. For large times, the concurrence decreases exponentially according to (6.185). The parameters were chosen to be $\lambda = 0.1\,\omega_0$ and $\Omega_c = 5\,\omega_0$.

6.4.3 Asymptotic Entanglement

For infinitely long times the inverse Laplace transformations (6.170) and (6.171) simplify drastically since one has to keep only the leading terms for $q \to 0$. We arrive at

$$\mathcal{C}(t) = \frac{1}{2} \left| e^{-2\kappa_- t} - e^{-2\kappa_+ t} \right| , \tag{6.185}$$

with

$$\kappa_\pm = \lambda \pi \omega_0 e^{-\frac{\omega_0}{\Omega}} \left(1 \pm \frac{\sin(\omega_0 r)}{\omega_0 r} \right) . \tag{6.186}$$

For $r \neq 0$ the entanglement vanishes always for infinite times. This is in agreement with the "thermal state" for vanishing temperature, that is the ground state.

Only in the limit $r = 0$, entanglement exists for $t \to \infty$ since vanishing distance corresponds to a direct interaction between the spins. We obtain the parameter-independent result

$$\lim_{t \to \infty} \lim_{r \to 0} \mathcal{C}(t) = \frac{1}{2} . \tag{6.187}$$

One may interpret this result in the following way: since a change in the coupling strength λ is a rescaling $t \to \lambda t$ for large times, the asymptotic expression should be independent of λ. Since the distance vanishes, the asymptotic expression can only depend on Ω_c/ω_0. But since the smallest resolvable distance $\sim 1/\Omega_c$ has no meaning for spins sitting on top of each other, a dependence on Ω_c is not viable.

6.5 Conclusions

We analyzed the generation of entanglement between remote quantum systems via an indirect system-bath interaction. In section 6.3 we focused on the entanglement of harmonic oscillators. For free environmental modes, a significant amount of entanglement can only be created for sufficiently small distances. The situation becomes better after imposing boundary conditions on the bath modes such that the spectral density exhibits so–called van Hove singularities. Thus we studied entanglement generation in a hollow tube. The environmental modes within the spectral peak are oscillating coherently for times and distances that are smaller than the inverse peak width. Thus, these modes can be interpreted as effective coupling oscillators which entangle the system oscillators. In order to generate a significant amount of entanglement, the system oscillators should initially be in a strongly squeezed state and their frequencies should be approximately in resonance with the peak modes.

In section 6.4 we analyzed a simplified two-spin-boson model without imposing boundary conditions on the bath modes. Due to the conservation of a nonlocal observable, the decrease of entanglement with growing distance is only polynomial. We believe that the existence of a nonlocal conserved quantity is also the reason for bath-induced entanglement in the model of Braun [130] over arbitrarily large distances.

7 Summary and Outlook

Within this thesis we have studied the impact of decoherence and dissipation on various quantum systems. In the first half of this work we focused on the phenomenon of localization and on the modification of tunneling rates through system-environment interaction. We investigated the emergence of a cosmological constant through decoherence and studied vacuum bubble nucleation. Nonetheless, there remain some open questions.

There exist various regularization methods for divergent quantities in flat and curved spacetime [80], mainly based on subtracting the divergent terms. These methods are known to be very useful in the context of closed systems but they may lead to unphysical results for open systems. For example, regularization can modify reduced density matrices such that they are not normalizable to unity [162]. Therefore, one may ask whether it is possible to find a sensible regularization of the infrared and ultraviolet divergences in the expressions for the reduced density matrix, obtained in section 4.4. A similar problem arises through ζ–function regularization method which has been used to compute the change of a tunneling rate, see section 4.5. The result differs drastically from the expression which would have been obtained by using a cutoff.

In section (5) we investigated the influence of nontrivial backgrounds on the tunneling rate. These considerations could be extended to the Kerr–spacetime. Since the corresponding metric is stationary it should be possible to obtain an integral representation for the tunneling amplitude. However, the nucleating vacuum bubble will not be spherical symmetric anymore.

The last part of this thesis, chapter 6, was dedicated to the bath mediated entanglement generation of remote quantum systems. We have seen that, due to the conservation of a nonlocal observable, more entanglement is generated than without this symmetry. We do not now to what extend this might be true in general. Therefore, given two systems coupled to a common heat bath and a nonlocal conserved quantity, what is the maximum entanglement that can be generated?

These open questions could be starting points for future research.

7 Summary and Outlook

8 Appendix I

8.1 Differential Equations

In order to avoid a cluttering of indices we will suppress the labels for the symmetric and antisymmetric modes.

The time evolution for the oscillator variables $\bar{Q}_{1/2}$ is given by

$$\bar{Q}_{1/2}(t) = \bar{Q}_{1/2} \cos(\bar{\Omega}_{1/2}t) + \frac{1}{\bar{\Omega}_{1/2}} \bar{P}_{1/2} \sin(\bar{\Omega}_{1/2}t) \,, \tag{8.1}$$

whereas for $\bar{P}_{1/2}$ we find

$$\bar{P}_{1/2}(t) = \bar{P}_{1/2} \cos(\bar{\Omega}_{1/2}t) - \bar{\Omega}_{1/2}\bar{Q}_{1/2} \sin(\bar{\Omega}_{1/2}t) \tag{8.2}$$

Using relations (6.95) we can decompose the differential equation (6.98) with respect to the (time-independent) operators $\bar{Q}_{1/2}$ and $\bar{P}_{1/2}$, that is

$$
\begin{aligned}
\dot{\rho} \;=\; & -i \sum_{i=1,2} \frac{1}{2} \left[\bar{P}_i^2 + \bar{\Omega}_i^2 \bar{Q}^2, \rho \right] \\[2mm]
& - \frac{\alpha_1(\bar{\Omega}_1)}{1+\xi^2} \left([\bar{Q}_1, [\bar{Q}_1, \rho]] + \frac{\xi}{\bar{\Omega}_2} [\bar{P}_2, [\bar{Q}_1, \rho]] \right) \\[2mm]
& - \frac{\alpha_2(\bar{\Omega}_1)}{1+\xi^2} \left([\bar{Q}_1, [\bar{P}_1, \rho]] + \frac{\xi}{\bar{\Omega}_2} [\bar{P}_2, [\bar{P}_1, \rho]] \right) \\[2mm]
& - \frac{\xi\,\alpha_1(\bar{\Omega}_2)}{(1+\xi^2)\bar{\Omega}_2^2} \left(\xi[\bar{P}_2, [\bar{P}_2, \rho]] + \bar{\Omega}_2[\bar{Q}_1, [\bar{P}_2, \rho]] \right) \\[2mm]
& + \frac{\xi\,\alpha_2(\bar{\Omega}_2)}{1+\xi^2} \left(\xi[\bar{P}_2, [\bar{Q}_2, \rho]] + \bar{\Omega}_2[\bar{Q}_1, [\bar{Q}_2, \rho]] \right) \\[2mm]
& - i\frac{\alpha_3(\bar{\Omega}_1)}{1+\xi^2} \left([\bar{Q}_1, \{\bar{Q}_1, \rho\}] + \frac{\xi}{\bar{\Omega}_2} [\bar{P}_2, \{\bar{Q}_1, \rho\}] \right) \\[2mm]
& - i\frac{\alpha_4(\bar{\Omega}_1)}{1+\xi^2} \left([\bar{Q}_1, \{\bar{P}_1, \rho\}] + \frac{\xi}{\bar{\Omega}_2} [\bar{P}_2, \{\bar{P}_1, \rho\}] \right) \\[2mm]
& - i\frac{\xi\,\alpha_3(\bar{\Omega}_2)}{(1+\xi^2)\bar{\Omega}_2^2} \left(\xi[\bar{P}_2, \{\bar{P}_2, \rho\}] + \bar{\Omega}_2[\bar{Q}_1, \{\bar{P}_2, \rho\}] \right) \\[2mm]
& + i\frac{\xi\,\alpha_4(\bar{\Omega}_2)}{1+\xi^2} \left(\xi[\bar{P}_2, \{\bar{Q}_2, \rho\}] + \bar{\Omega}_2[\bar{Q}_1, \{\bar{Q}_2, \rho\}] \right),
\end{aligned}
\tag{8.3}
$$

8 Appendix I

where ξ was defined in equation (6.97) and the α_i are correlation functions that are given explicitly in section 6.68.

The equations of motion in the "$k - \Delta$"-representation can be constructed by wrapping

$$\text{tr}\left(D...\right) = \text{tr}\left(e^{i\left(\mathbf{k}\hat{\mathbf{Q}}+\boldsymbol{\Delta}\hat{\mathbf{P}}\right)}...\right) \tag{8.4}$$

over equation (8.13). Using the relations

$$\begin{align}
\text{tr}(D[\bar{Q}_i, [\bar{Q}_j, \rho]]) &= \Delta_i \Delta_j \tilde{\rho} \tag{8.5}\\
\text{tr}(D[\bar{Q}_i, [\bar{P}_j, \rho]]) &= -\Delta_i k_j \tilde{\rho} \tag{8.6}\\
\text{tr}(D[\bar{P}_i, [\bar{Q}_j, \rho]]) &= -k_i \Delta_j \tilde{\rho} \tag{8.7}\\
\text{tr}(D[\bar{P}_i, [\bar{P}_j, \rho]]) &= k_i k_j \tilde{\rho} \tag{8.8}\\
\text{tr}(D[\bar{Q}_i, \{\bar{Q}_j, \rho\}]) &= -2i\Delta_i \partial_{k_j} \tilde{\rho} \tag{8.9}\\
\text{tr}(D[\bar{Q}_i, \{\bar{P}_j, \rho\}]) &= -2i\Delta_i \partial_{\Delta_j} \tilde{\rho} \tag{8.10}\\
\text{tr}(D[\bar{P}_i, \{\bar{Q}_j, \rho\}]) &= 2ik_i \partial_{k_j} \tilde{\rho} \tag{8.11}\\
\text{tr}(D[\bar{P}_i, \{\bar{P}_j, \rho\}]) &= 2ik_i \partial_{\Delta_j} \tilde{\rho}\,, \tag{8.12}
\end{align}$$

we arrive at

$$\begin{align}
\dot{\tilde{\rho}} = &\left(k_1 - \frac{2}{1+\xi^2}\alpha_4(\bar{\Omega}_1)\left(\Delta_1 - \frac{\xi}{\bar{\Omega}_2}k_2\right)\right)\partial_{\Delta_1}\tilde{\rho}\\
&+ \left(k_2 - \frac{2\xi}{(1+\xi^2)\bar{\Omega}_2^2}\alpha_3(\bar{\Omega}_2)(\bar{\Omega}_2\Delta_1 - \xi k_2)\right)\partial_{\Delta_2}\tilde{\rho}\\
&- \left(\bar{\Omega}_1^2\Delta_1 + \frac{2}{1+\xi^2}\alpha_3(\bar{\Omega}_1)\left(\Delta_1 - \frac{\xi k_2}{\bar{\Omega}_2}\right)\right)\partial_{k_1}\tilde{\rho}\\
&- \left(\bar{\Omega}_2^2\Delta_2 - \frac{2\xi}{1+\xi^2}\alpha_4(\bar{\Omega}_2)(\bar{\Omega}_2\Delta_1 - \xi k_2)\right)\partial_{k_2}\tilde{\rho}\\
&+ \frac{1}{1+\xi^2}\Bigg[-\alpha_1(\bar{\Omega}_1)\left(\Delta_1^2 - \frac{\xi}{\bar{\Omega}_2}k_2\Delta_1\right)\\
&\qquad +\alpha_2(\bar{\Omega}_1)\left(k_1\Delta_1 - \frac{\xi}{\bar{\Omega}_2}k_1 k_2\right)\\
&\qquad +\frac{\xi}{\bar{\Omega}_2^2}\alpha_1(\bar{\Omega}_2)(\bar{\Omega}_2 k_2\Delta_1 - \xi k_2^2)\\
&\qquad +\xi\,\alpha_2(\bar{\Omega}_2)(\bar{\Omega}_2\Delta_1\Delta_2 - \xi k_2\Delta_2)\Bigg]\tilde{\rho}\,. \tag{8.13}
\end{align}$$

With the gaussian ansatz

$$\begin{align}
\tilde{\rho}_{Qs,q} = &\exp\big(-c_1 k_1^2 - c_2 k_1\Delta_1 - c_3\Delta_1^2 - ic_4 k_1 - ic_5\Delta_1 - c_6 k_2^2 - c_7 k_2\Delta_2 - c_8\Delta_2^2\\
&-ic_9 k_2 - ic_{10}\Delta_2 - c_{11}k_1 k_2 - c_{12}k_1\Delta_2 - c_{13}k_2\Delta_1 - c_{14}\Delta_1\Delta_2\big) \tag{8.14}
\end{align}$$

we arrive at the first order system

$$\dot{c}_1 = c_2 \tag{8.15}$$

$$\dot{c}_2 = -\left(2\bar{\Omega}_1^2 + \frac{4}{1+\xi^2}\alpha_3(\bar{\Omega}_1)\right)c_1 + 2c_3$$
$$-\frac{1}{1+\xi^2}\left(2\alpha_4(\bar{\Omega}_1)c_2 - 2\xi\bar{\Omega}_2\alpha_4(\bar{\Omega}_2)c_{11} + \frac{2\xi}{\bar{\Omega}_2}\alpha_3(\bar{\Omega}_2)c_{12} + \alpha_2(\bar{\Omega}_1)\right) \tag{8.16}$$

$$\dot{c}_3 = -\left(\bar{\Omega}_1^2 + \frac{2}{1+\xi^2}\alpha_3(\bar{\Omega}_1)\right)c_2$$
$$-\frac{1}{1+\xi^2}\left(4\alpha_4(\bar{\Omega}_1)c_3 - 2\xi\bar{\Omega}_2\alpha_4(\bar{\Omega}_2)c_{13} + \frac{2\xi}{\bar{\Omega}_2}\alpha_3(\bar{\Omega}_2)c_{14} - \alpha_1(\bar{\Omega}_1)\right) \tag{8.17}$$

$$\dot{c}_4 = c_5 \tag{8.18}$$

$$\dot{c}_5 = -\left(\bar{\Omega}_1^2 + \frac{2}{1+\xi^2}\alpha_3(\bar{\Omega}_1)\right)c_4$$
$$-\frac{1}{1+\xi^2}\left(2\alpha_4(\bar{\Omega}_1)c_5 - 2\xi\bar{\Omega}_2\alpha_4(\bar{\Omega}_2)c_9 + \frac{2\xi}{\bar{\Omega}_2}\alpha_3(\bar{\Omega}_2)c_{10}\right) \tag{8.19}$$

$$\dot{c}_6 = -\frac{4\xi^2}{1+\xi^2}\alpha_4(\bar{\Omega}_2)c_6 + \left(1 + \frac{2\xi^2}{(1+\xi^2)\bar{\Omega}_2^2}\alpha_3(\bar{\Omega}_2)\right)c_7$$
$$+\frac{1}{1+\xi^2}\left(\frac{2\xi}{\bar{\Omega}_2}\alpha_3(\bar{\Omega}_1)c_{11} + \frac{2\xi}{\bar{\Omega}_2}\alpha_4(\bar{\Omega}_1)c_{13} + \frac{\xi^2}{\bar{\Omega}_2^2}\alpha_1(\bar{\Omega}_2)\right) \tag{8.20}$$

$$\dot{c}_7 = -2\bar{\Omega}_2^2 c_6 - \frac{2\xi^2}{1+\xi^2}\alpha_4(\bar{\Omega}_2)c_7 + \left(2 + \frac{4\xi^2}{(1+\xi^2)\bar{\Omega}_2^2}\alpha_3(\bar{\Omega}_2)\right)c_8$$
$$+\frac{1}{1+\xi^2}\left(\frac{2\xi}{\bar{\Omega}_2}\alpha_3(\bar{\Omega}_1)c_{12} + \frac{2\xi}{\bar{\Omega}_2}\alpha_4(\bar{\Omega}_1)c_{14} + \xi^2\alpha_2(\bar{\Omega}_2)\right) \tag{8.21}$$

$$\dot{c}_8 = -\bar{\Omega}_2^2 c_7 \tag{8.22}$$

$$\dot{c}_9 = c_{10} + \frac{1}{1+\xi^2}\left(\frac{2\xi}{\bar{\Omega}_2}\alpha_3(\bar{\Omega}_1)c_4 + \frac{2\xi}{\bar{\Omega}_2}\alpha_4(\bar{\Omega}_1)c_5\right.$$
$$\left. -2\xi^2\alpha_4(\bar{\Omega}_2)c_9 + \frac{2\xi^2}{\bar{\Omega}_2^2}\alpha_3(\bar{\Omega}_2)c_{10}\right) \tag{8.23}$$

$$\dot{c}_{10} = -\bar{\Omega}_2^2 c_9 \tag{8.24}$$

$$\dot{c}_{11} = \frac{1}{1+\xi^2}\left(\frac{4\xi}{\bar{\Omega}_2}\alpha_3(\bar{\Omega}_1)c_1 + \frac{2\xi}{\bar{\Omega}_2}\alpha_4(\bar{\Omega}_1)c_2\right) - \frac{2\xi^2}{1+\xi^2}\alpha_4(\bar{\Omega}_2)c_{11}$$
$$+\left(1 + \frac{2\xi^2}{\bar{\Omega}_2^2(1+\xi^2)}\right)c_{12} + c_{13} + \frac{\xi}{\bar{\Omega}_2(1+\xi^2)}\alpha_2(\bar{\Omega}_1) \tag{8.25}$$

$$\dot{c}_{12} = -\bar{\Omega}_2^2 c_{11} + c_{14} \tag{8.26}$$

$$\dot{c}_{13} = \frac{1}{1+\xi^2}\left(\frac{2\xi}{\bar{\Omega}_2}\alpha_3(\bar{\Omega}_1)c_2 + \frac{4\xi}{\bar{\Omega}_2}\alpha_4(\bar{\Omega}_1)c_3 + 4\xi\bar{\Omega}_2\alpha_4(\bar{\Omega}_2)c_6\right)$$

$$-\frac{2\xi}{(1+\xi^2)\bar{\Omega}_2}\alpha_3(\bar{\Omega}_2)c_7 - \left(\frac{2}{1+\xi^2}\alpha_3(\bar{\Omega}_1) + \bar{\Omega}_1^2\right)c_{11}$$

$$-\frac{2}{1+\xi^2}\left(\alpha_4(\bar{\Omega}_1) + \xi^2\alpha_4(\bar{\Omega}_2)\right)c_{13} + \left(1 + \frac{2\xi^2}{(1+\xi^2)\bar{\Omega}_2^2}\alpha_3(\bar{\Omega}_2)\right)c_{14}$$

$$-\frac{\xi}{(1+\xi^2)\bar{\Omega}_2}\left(\alpha_1(\bar{\Omega}_1) + \alpha_1(\bar{\Omega}_2)\right) \tag{8.27}$$

$$\dot{c}_{14} = \frac{1}{1+\xi^2}\left(2\xi\bar{\Omega}_2\alpha_4(\bar{\Omega}_2)c_7 - \frac{4\xi}{\bar{\Omega}_2}\alpha_3(\bar{\Omega}_2)c_8\right) - \left(\bar{\Omega}_1^2 + \frac{2}{1+\xi^2}\alpha_3(\bar{\Omega}_1)\right)c_{12} - \bar{\Omega}_2^2 c_{13}$$

$$-\frac{1}{1+\xi^2}\left(2\alpha_4(\bar{\Omega}_1)c_{14} + \xi\bar{\Omega}_2\alpha_2(\bar{\Omega}_2)\right) . \tag{8.28}$$

The expectation values of the anticommutators can be given in terms of the functions $c_i(t)$ according to

$$\langle\{\bar{Q}_1, \bar{Q}_1\}\rangle = 2(2c_1 + c_4^2) \tag{8.29}$$
$$\langle\{\bar{Q}_1, \bar{Q}_2\}\rangle = 2(c_{11} + c_4 c_9) \tag{8.30}$$
$$\langle\{\bar{Q}_2, \bar{Q}_2\}\rangle = 2(2c_6 + c_9^2) \tag{8.31}$$
$$\langle\{\bar{Q}_1, \bar{P}_1\}\rangle = 2(c_2 + c_4 c_5) \tag{8.32}$$
$$\langle\{\bar{Q}_2, \bar{P}_2\}\rangle = 2(c_7 + c_9 c_{10}) \tag{8.33}$$
$$\langle\{\bar{Q}_1, \bar{P}_2\}\rangle = 2(c_{12} + c_4 c_{10}) \tag{8.34}$$
$$\langle\{\bar{P}_1, \bar{P}_1\}\rangle = 2(2c_3 + c_5^2) \tag{8.35}$$
$$\langle\{\bar{P}_2, \bar{P}_2\}\rangle = 2(2c_8 + c_{10}^2) \tag{8.36}$$
$$\langle\{\bar{P}_1, \bar{P}_2\}\rangle = 2(c_{14} + c_5 c_{10}) \tag{8.37}$$
$$\langle\{\bar{Q}_2, \bar{P}_1\}\rangle = 2(c_{13} + c_5 c_9) . \tag{8.38}$$

8.2 Approximate Solutions of the Differential Equations

From the initial condition (6.107) we find that the functions c_4, c_5, c_9 and c_{10} are vanishing since they describe momentum and position displacements that are absent in symmetric gaussians. At $t = 0$, the nonvanishing anticommutators have the expectation values

$$\langle\{p_{\omega_0}, p_{\omega_0}\}\rangle = \frac{1}{\langle\{q_{\omega_0}, q_{\omega_0}\}\rangle} = a \tag{8.39}$$

$$\langle\{P, P\}\rangle = \frac{1}{\langle\{Q, Q\}\rangle} = b. \tag{8.40}$$

Neglecting terms of order $g^2\gamma$ in the differential equation, some of the equations (8.15) – (8.28) decouple from each other. For the coefficients concerning the oscillator with the variable $\bar{Q}_1$, we find

$$c_1 \;=\; \sum_{i=1}^{3} A_i e^{\lambda_i t} + \frac{\alpha_1(\bar{\Omega}_1) - 2\alpha_2(\bar{\Omega}_1)\alpha_4(\bar{\Omega}_1)}{4\alpha_4(\bar{\Omega}_1)(2\alpha_3(\bar{\Omega}_1) + \bar{\Omega}_1^2)} \tag{8.41}$$

$$c_2 \;=\; \sum_{i=1}^{3} A_i \lambda_i e^{\lambda_i t} \tag{8.42}$$

$$c_3 \;=\; \sum_{i=1}^{3} A_i \left(\frac{\lambda_i}{2} + \bar{\Omega}_1^2 + 2\alpha_3(\bar{\Omega}_1) + \alpha_4(\bar{\Omega}_1)\lambda_i \right) \lambda_i e^{\lambda_i t} + \frac{\alpha_1(\bar{\Omega}_1)}{4\alpha_4(\bar{\Omega}_1)}, \tag{8.43}$$

with the eigenmodes

$$\lambda_1 \;=\; -2\alpha_4(\bar{\Omega}_1) \tag{8.44}$$

$$\lambda_{2,3} \;=\; -2\left(\alpha_4(\bar{\Omega}_1) \pm i\sqrt{\bar{\Omega}_1^2 + 2\alpha_3(\bar{\Omega}_1) - \alpha_4^2(\bar{\Omega}_1)} \right). \tag{8.45}$$

The A_i are chosen such that

$$c_1(0) \;=\; \frac{\omega_0^2 + \xi^2\, ab}{4b\omega_0^2(1 + \xi^2)} \tag{8.46}$$

$$c_2(0) \;=\; 0 \tag{8.47}$$

$$c_3(0) \;=\; \frac{ab + \xi^2\omega_0^2}{4a(1 + \xi^2)}. \tag{8.48}$$

For the oscillator $\bar{Q}_2$ we find

$$c_6 \;=\; B_1 e^{2i\bar{\Omega}_2 t} + B_2 e^{-2i\bar{\Omega}_2 t} + B_3 \tag{8.49}$$

$$c_7 \;=\; 2i\bar{\Omega}_2 B_1 e^{2i\bar{\Omega}_2 t} - 2i\bar{\Omega}_2 B_2 e^{-2i\bar{\Omega}_2 t} \tag{8.50}$$

$$c_8 \;=\; -\bar{\Omega}_2^2(B_1 e^{2i\bar{\Omega}_2 t} + B_2 e^{-2i\bar{\Omega}_2 t} - B_3). \tag{8.51}$$

The B_i are chosen such that

$$c_6(0) \;=\; \frac{\omega_0^2 + \xi^2 ab}{4a\bar{\Omega}_2^2(1 + \xi^2)} \tag{8.52}$$

$$c_7(0) \;=\; 0 \tag{8.53}$$

$$c_8(0) \;=\; \frac{\bar{\Omega}_2^2(ab + \xi^2\omega_0^2)}{4b\omega_0^2(1 + \xi^2)} \tag{8.54}$$

The coupling between $\bar{Q}_1$ and $\bar{Q}_2$ is described by $c_{11}...c_{14}$, which read

$$c_{11} = \sum_{i=1}^{4} C_i e^{\kappa_i t} \tag{8.55}$$

$$c_{12} = -\sum_{i=1}^{4} C_i \frac{2\bar{\Omega}_2^2(\alpha_4(\bar{\Omega}_1) + \kappa_i)}{2\alpha_3(\bar{\Omega}_1) + \bar{\Omega}_1^2 - \bar{\Omega}_2^2 + 2\alpha_4(\bar{\Omega}_1)\kappa_i + \kappa_i^2} e^{\kappa_i t} \tag{8.56}$$

$$c_{13} = \sum_{i=1}^{4} C_i \kappa_i e^{\kappa_i t} + \sum_{i=1}^{4} C_i \frac{2\bar{\Omega}_2^2(\alpha_4(\bar{\Omega}_1) + \kappa_i)}{2\alpha_3(\bar{\Omega}_1) + \bar{\Omega}_1^2 - \bar{\Omega}_2^2 + 2\alpha_4(\bar{\Omega}_1)\kappa_i + \kappa_i^2} e^{\kappa_i t} \tag{8.57}$$

$$c_{14} = \sum_{i=1}^{4} C_i \frac{\bar{\Omega}_2^2(2\alpha_3(\bar{\Omega}_1) + \bar{\Omega}_1^2 - \bar{\Omega}_2^2 - \kappa_i^2)}{2\alpha_3(\bar{\Omega}_1) + \bar{\Omega}_1^2 - \bar{\Omega}_2^2 + 2\alpha_4(\bar{\Omega}_1)\kappa_i + \kappa_i^2} e^{\kappa_i t}, \tag{8.58}$$

with the eigenmodes

$$\kappa_{1,2,3,4} = -\alpha_4(\bar{\Omega}_1) \pm i \Big(2\alpha_3(\bar{\Omega}_1) - \alpha_4^2(\bar{\Omega}_1) + \bar{\Omega}_1^2 + \bar{\Omega}_2^2$$
$$\pm 2\bar{\Omega}_2 \sqrt{2\alpha_3(\bar{\Omega}_1) - \alpha_4^2(\bar{\Omega}_1) + \bar{\Omega}_1^2} \Big)^{1/2}. \tag{8.59}$$

The C_i are chosen such that

$$c_{11}(0) = 0 \tag{8.60}$$

$$c_{12}(0) = \frac{\xi \bar{\Omega}_2(\omega_0^2 - ab)}{2b\omega_0^2(1 + \xi^2)} \tag{8.61}$$

$$c_{13}(0) = \frac{\xi(\omega_0^2 - ab)}{2a\bar{\Omega}_2(1 + \xi^2)} \tag{8.62}$$

$$c_{14}(0) = 0. \tag{8.63}$$

8.3 Bath Correlators

8.3.1 Correlators of the Generic Toy Model

We define $f_S(\omega) = \cos^2(\omega r/2)$ for the symmetric modes and $f_A(\omega) = \sin^2(\omega r/2)$ for the antisymmetric modes. For $\bar{\Omega} > 0$ we find

$$\alpha_{1,S/A}(\bar{\Omega}) = \int_0^\infty dt\, \nu_{S/A}(r,t)\cos(\bar{\Omega}t) = \frac{\pi}{4}\coth\left(\frac{\bar{\Omega}}{2T}\right)J(\bar{\Omega})f_{S/A}(\bar{\Omega}) \tag{8.64}$$

and

$$\alpha_{4,S/A}(\bar{\Omega}) = \int_0^\infty dt\, \mu_{S/A}(r,t)\frac{\sin(\bar{\Omega}t)}{\bar{\Omega}} = \frac{\pi}{4\bar{\Omega}}J(\bar{\Omega})f_{S/A}(\bar{\Omega}). \tag{8.65}$$

The evaluation of the remaining correlators involve incomplete Γ-functions and an infinite sum. For $\bar\Omega > 0$ we find

$$
\begin{aligned}
\alpha_{2,S/A}(\bar\Omega) &= -\int_0^\infty dt\, \nu_{S/A}(r,t)\frac{\sin(\bar\Omega t)}{\bar\Omega} \\
&= -\frac{\gamma}{\Omega_c^{s-1}}\frac{T\Gamma(1+s)}{4\pi\bar\Omega}\sum_{n=-\infty}^{\infty}\frac{a_{|n|,S/A}(r,\bar\Omega,s)}{\nu_{|n|}^2+\bar\Omega^2}
\end{aligned}
\tag{8.66}
$$

and

$$
\begin{aligned}
\alpha_{3,S/A}(\bar\Omega) &= -\int_0^\infty dt\, \mu_{S/A}(r,t)\cos(\bar\Omega t) \\
&= \frac{\gamma}{\Omega_c^{s-1}}\frac{\Gamma(1+s)}{8\pi\bar\Omega}\frac{a_{0,S/A}(r,\bar\Omega,s+2)}{\bar\Omega^2}\,,
\end{aligned}
\tag{8.67}
$$

with $\nu_n = 2\pi nT$. If $n > 0$ the coefficients concerning the symmetric modes read

$$
\begin{aligned}
a_{n,S}(r,\bar\Omega,s) &= \\
&-2\bar\Omega^{1+s}e^{-\frac{\bar\Omega}{\Omega_c}}\left(\sin(\bar\Omega r)\sin(\pi s)+\cos(\pi s)\right)\Re\Gamma\left(-s,-\frac{\bar\Omega}{\Omega_c}\right) \\
&-2\bar\Omega^{1+s}e^{-\frac{\bar\Omega}{\Omega_c}}\left(\sin(\bar\Omega r)\cos(\pi s)-\sin(\pi s)\right)\Im\Gamma\left(-s,-\frac{\bar\Omega}{\Omega_c}\right) \\
&-2\bar\Omega^{1+s}e^{\frac{\bar\Omega}{\Omega_c}}\Gamma\left(-s,\frac{\bar\Omega}{\Omega_c}\right) \\
&+2\bar\Omega\nu_n^s\left[e^{\frac{i\nu_n}{\Omega_c}+\frac{i\pi s}{2}}\Gamma\left(-s,\frac{i\nu_n}{\Omega_c}\right)+c.c.\right] \\
&+\bar\Omega\nu_n^s\left[e^{\nu_n\left(\frac{i}{\Omega_c}-r\right)+\frac{i\pi s}{2}}\Gamma\left(-s,\nu_n\left(\frac{i}{\Omega_c}-r\right)\right)\right. \\
&\left.+e^{\nu_n\left(\frac{i}{\Omega_c}+r\right)+\frac{i\pi s}{2}}\Gamma\left(-s,\nu_n\left(\frac{i}{\Omega_c}+r\right)\right)+c.c.\right] \\
&-\bar\Omega^{s+1}\left[e^{-i\bar\Omega\left(\frac{i}{\Omega_c}+r\right)}\Gamma\left(-s,-i\bar\Omega\left(\frac{i}{\Omega_c}+r\right)\right)\right. \\
&\left.+e^{i\bar\Omega\left(\frac{i}{\Omega_c}+r\right)+i\pi s}\Gamma\left(-s,i\bar\Omega\left(\frac{i}{\Omega_c}+r\right)\right)+c.c.\right]\,,
\end{aligned}
\tag{8.68}
$$

8 Appendix I

and for $n = 0$ we find

$$
\begin{aligned}
a_{0,S}(r, \bar{\Omega}, s) \;=\; & \\
& -2\bar{\Omega}^{1+s} e^{-\frac{\bar{\Omega}}{\Omega_c}} \left(\sin(\bar{\Omega}r) \sin(\pi s) + \cos(\pi s) \right) \Re\Gamma\left(-s, -\frac{\bar{\Omega}}{\Omega_c} \right) \\
& -2\bar{\Omega}^{1+s} e^{-\frac{\bar{\Omega}}{\Omega_c}} \left(\sin(\bar{\Omega}r) \cos(\pi s) - \sin(\pi s) \right) \Im\Gamma\left(-s, -\frac{\bar{\Omega}}{\Omega_c} \right) \\
& -2\bar{\Omega}^{1+s} e^{\frac{\bar{\Omega}}{\Omega_c}} \Gamma\left(-s, \frac{\bar{\Omega}}{\Omega_c} \right) + \frac{2\bar{\Omega}}{s} \left[e^{\frac{i\pi s}{2}} \left(\frac{i}{\Omega_c} - r \right)^{-s} + c.c. \right] \\
& + \frac{4\Omega_c^s \bar{\Omega}}{s} - \bar{\Omega}^{s+1} \left[e^{-i\bar{\Omega}\left(\frac{i}{\Omega_c} + r \right)} \Gamma\left(-s, -i\bar{\Omega}\left(\frac{i}{\Omega_c} + r \right) \right) \right. \\
& \left. + e^{i\bar{\Omega}\left(\frac{i}{\Omega_c} + r \right) + i\pi s} \Gamma\left(-s, i\bar{\Omega}\left(\frac{i}{\Omega_c} + r \right) \right) + c.c. \right].
\end{aligned}
\tag{8.69}
$$

For the antisymmetric modes, the coefficients for $n > 0$ read

$$
\begin{aligned}
a_{n,A}(r, \bar{\Omega}, s) \;=\; & \\
& 2\bar{\Omega}^{1+s} e^{-\frac{\bar{\Omega}}{\Omega_c}} \left(\sin(\bar{\Omega}r) \sin(\pi s) - \cos(\pi s) \right) \Re\Gamma\left(-s, -\frac{\bar{\Omega}}{\Omega_c} \right) \\
& + 2\bar{\Omega}^{1+s} e^{-\frac{\bar{\Omega}}{\Omega_c}} \left(\sin(\bar{\Omega}r) \cos(\pi s) + \sin(\pi s) \right) \Im\Gamma\left(-s, -\frac{\bar{\Omega}}{\Omega_c} \right) \\
& - 2\bar{\Omega}^{1+s} e^{\frac{\bar{\Omega}}{\Omega_c}} \Gamma\left(-s, \frac{\bar{\Omega}}{\Omega_c} \right) \\
& + 2\bar{\Omega}\nu_n^s \left[e^{\frac{i\nu_n}{\Omega_c} + \frac{i\pi s}{2}} \Gamma\left(-s, \frac{i\nu_n}{\Omega_c} \right) + c.c. \right] \\
& - \bar{\Omega}\nu_n^s \left[e^{\nu_n\left(\frac{i}{\Omega_c} - r \right) + \frac{i\pi s}{2}} \Gamma\left(-s, \nu_n\left(\frac{i}{\Omega_c} - r \right) \right) \right. \\
& \left. + e^{\nu_n\left(\frac{i}{\Omega_c} + r \right) + \frac{i\pi s}{2}} \Gamma\left(-s, \nu_n\left(\frac{i}{\Omega_c} + r \right) \right) + c.c. \right] \\
& + \bar{\Omega}^{s+1} \left[e^{-i\bar{\Omega}\left(\frac{i}{\Omega_c} + r \right)} \Gamma\left(-s, -i\bar{\Omega}\left(\frac{i}{\Omega_c} + r \right) \right) \right. \\
& \left. + e^{i\bar{\Omega}\left(\frac{i}{\Omega_c} + r \right) + i\pi s} \Gamma\left(-s, i\bar{\Omega}\left(\frac{i}{\Omega_c} + r \right) \right) + c.c. \right].
\end{aligned}
\tag{8.70}
$$

and for $n = 0$ we find

$$
\begin{aligned}
a_{0,A}(r, \bar{\Omega}, s) \ = \ & \\
& 2\bar{\Omega}^{1+s}e^{-\frac{\bar{\Omega}}{\Omega_c}} \left(\sin(\bar{\Omega}r)\sin(\pi s) - \cos(\pi s)\right) \Re\Gamma\left(-s, -\frac{\bar{\Omega}}{\Omega_c}\right) \\
& +2\bar{\Omega}^{1+s}e^{-\frac{\bar{\Omega}}{\Omega_c}} \left(\sin(\bar{\Omega}r)\cos(\pi s) + \sin(\pi s)\right) \Im\Gamma\left(-s, -\frac{\bar{\Omega}}{\Omega_c}\right) \\
& -2\bar{\Omega}^{1+s}e^{\frac{\bar{\Omega}}{\Omega_c}}\Gamma\left(-s, \frac{\bar{\Omega}}{\Omega_c}\right) - \frac{2\bar{\Omega}}{s}\left[e^{\frac{i\pi s}{2}}\left(\frac{i}{\Omega_c} - r\right)^{-s} + c.c.\right] \\
& +\frac{4\Omega_c^s\bar{\Omega}}{s} + \bar{\Omega}^{s+1}\left[e^{-i\bar{\Omega}\left(\frac{i}{\Omega_c}+r\right)}\Gamma\left(-s, -i\bar{\Omega}\left(\frac{i}{\Omega_c} + r\right)\right)\right. \\
& \left. +e^{i\bar{\Omega}\left(\frac{i}{\Omega_c}+r\right)+i\pi s}\Gamma\left(-s, i\bar{\Omega}\left(\frac{i}{\Omega_c} + r\right)\right) + c.c.\right] .
\end{aligned}
\tag{8.71}
$$

8.3.2 Correlators of the Tube Model

For the decoherence rates we find

$$
\alpha_{1,S/A}(\bar{\Omega}) = \frac{\pi}{4}J^{3D}(\bar{\Omega})\left(1 \pm \frac{\sin(\bar{\Omega}r)}{\bar{\Omega}r}\right)\coth\left(\frac{\bar{\Omega}}{2T}\right) .
\tag{8.72}
$$

The dissipation correlators read

$$
\alpha_{4,S/A}(\bar{\Omega}) = \frac{\pi}{4}\frac{J^{3D}(\bar{\Omega})}{\bar{\Omega}}\left(1 \pm \frac{\sin(\bar{\Omega}r)}{\bar{\Omega}r}\right) .
\tag{8.73}
$$

8 Appendix I

The anomalous diffusion correlators have the form

$$
\begin{aligned}
\alpha_{2,S/A}(\bar{\Omega}) \;=\;& \frac{\gamma\Gamma(1+s)}{2\pi}\left(\frac{\bar{\Omega}}{\Omega_c}\right)^{s-1}\coth\left(\frac{\bar{\Omega}}{2T}\right)\times \\
& \times\left[e^{-\frac{\bar{\Omega}}{\Omega_c}}\left(\cos(\pi s)\Re\left\{\Gamma\left(-s,-\frac{\bar{\Omega}}{\Omega_c}\right)\right\}-\sin(\pi s)\Im\left\{\Gamma\left(-s,-\frac{\bar{\Omega}}{\Omega_c}\right)\right\}\right)\right. \\
& \left.+e^{\frac{\bar{\Omega}}{\Omega_c}}\Gamma\left(-s,\frac{\bar{\Omega}}{\Omega_c}\right)\right] \\
& -\frac{2T\gamma\Omega_c\Gamma(1+s)}{\pi}\left(\frac{1}{\bar{\Omega}^2 s}+\sum_{n=1}^{\infty}\left(\frac{2\pi nT}{\Omega_c}\right)^s\frac{c_n}{\bar{\Omega}^2+(2\pi nT)^2}\right) \\
& \pm\left\{-\frac{\gamma\Gamma(s-1)}{4\pi r\Omega_c}\left(\frac{\bar{\Omega}}{\Omega_c}\right)^{s-2}\coth\left(\frac{\bar{\Omega}}{2T}\right)\times\right. \\
& \times\left[2\cos(\bar{\Omega}r)e^{-\frac{\bar{\Omega}}{\Omega_c}}\left(\sin(\pi s)\Re\left\{\Gamma\left(-s+2,-\frac{\bar{\Omega}}{\Omega_c}\right)\right\}\right.\right. \\
& \left.+\cos(\pi s)\Im\left\{\Gamma\left(-s+2,-\frac{\bar{\Omega}}{\Omega_c}\right)\right\}\right) \\
& +ie^{\bar{\Omega}\left(\frac{1}{\Omega_c}+ir\right)}\Gamma\left(-s+2,\bar{\Omega}\left(\frac{1}{\Omega_c}+ir\right)\right) \\
& -ie^{\bar{\Omega}\left(\frac{1}{\Omega_c}-ir\right)}\Gamma\left(-s+2,\bar{\Omega}\left(\frac{1}{\Omega_c}-ir\right)\right) \\
& -ie^{-\bar{\Omega}\left(\frac{1}{\Omega_c}+ir\right)-i\pi s}\Gamma\left(-s+2,-\bar{\Omega}\left(\frac{1}{\Omega_c}+ir\right)\right) \\
& \left.+ie^{-\bar{\Omega}\left(\frac{1}{\Omega_c}-ir\right)+i\pi s}\Gamma\left(-s+2,-\bar{\Omega}\left(\frac{1}{\Omega_c}-ir\right)\right)\right] \\
& \left.+\frac{\gamma T\Gamma(s-1)}{\pi r}\sum_{n=1}^{\infty}\left(\frac{2\pi nT}{\Omega_c}\right)^{s-1}\frac{d_n}{\bar{\Omega}^2+(2\pi nT)^2}\right\}
\end{aligned}
\tag{8.74}
$$

with

$$
\begin{aligned}
c_n &= e^{-i\frac{2\pi nT}{\Omega_c} - i\frac{\pi s}{2}}\Gamma\left(-s, -i\frac{2\pi nT}{\Omega_c}\right) + e^{i\frac{2\pi nT}{\Omega_c} + i\frac{\pi s}{2}}\Gamma\left(-s, i\frac{2\pi nT}{\Omega_c}\right) ; \\
d_n &= e^{i2\pi nT\left(\frac{1}{\Omega_c} + ir\right) + i\frac{\pi s}{2}}\Gamma\left(-s+2, i2\pi nT\left(\frac{1}{\Omega_c} + ir\right)\right) \\
&\quad + e^{-i2\pi nT\left(\frac{1}{\Omega_c} - ir\right) - i\frac{\pi s}{2}}\Gamma\left(-s+2, -i2\pi nT\left(\frac{1}{\Omega_c} - ir\right)\right) \\
&\quad - e^{-i2\pi nT\left(\frac{1}{\Omega_c} + ir\right) - i\frac{\pi s}{2}}\Gamma\left(-s+2, -i2\pi nT\left(\frac{1}{\Omega_c} + ir\right)\right) \\
&\quad + e^{i2\pi nT\left(\frac{1}{\Omega_c} - ir\right) + i\frac{\pi s}{2}}\Gamma\left(-s+2, i2\pi nT\left(\frac{1}{\Omega_c} - ir\right)\right) .
\end{aligned}
\tag{8.75}
$$

The Lamb shifts due to the bath correlators are given by

$$
\begin{aligned}
\alpha_{3,S/A}(\bar{\Omega}) &= -\frac{\gamma\Gamma(3+s)\bar{\Omega}}{2\pi}\left(\frac{\bar{\Omega}}{\Omega_c}\right)^{s-1} \times \\
&\quad \times\left[e^{-\frac{\bar{\Omega}}{\Omega_c}}\left(\cos(\pi s)\Re\left\{\Gamma\left(-2-s, -\frac{\bar{\Omega}}{\Omega_c}\right)\right\} - \sin(\pi s)\Im\left\{\Gamma\left(-2-s, -\frac{\bar{\Omega}}{\Omega_c}\right)\right\}\right) \right. \\
&\quad \left. + e^{\frac{\bar{\Omega}}{\Omega_c}}\Gamma\left(-2-s, \frac{\bar{\Omega}}{\Omega_c}\right)\right] + \frac{\gamma\Omega_c^3\Gamma(3+s)}{\pi\bar{\Omega}^2(2+s)} \\
&\quad \pm \left\{\frac{\gamma\Gamma(1+s)}{4\pi r}\left(\frac{\bar{\Omega}}{\Omega_c}\right)^{s-1} \times \right. \\
&\quad \times\left[2\cos(\bar{\Omega}r)e^{-\frac{\bar{\Omega}}{\Omega_c}}\left(\sin(\pi s)\Re\left\{\Gamma\left(-s, -\frac{\bar{\Omega}}{\Omega_c}\right)\right\} + \cos(\pi s)\Im\left\{\Gamma\left(-s, -\frac{\bar{\Omega}}{\Omega_c}\right)\right\}\right)\right. \\
&\quad + ie^{\bar{\Omega}\left(\frac{1}{\Omega_c} + ir\right)}\Gamma\left(-s, \bar{\Omega}\left(\frac{1}{\Omega_c} + ir\right)\right) \\
&\quad - ie^{\bar{\Omega}\left(\frac{1}{\Omega_c} - ir\right)}\Gamma\left(-s, \bar{\Omega}\left(\frac{1}{\Omega_c} - ir\right)\right) \\
&\quad - ie^{-\bar{\Omega}\left(\frac{1}{\Omega_c} + ir\right) - i\pi s}\Gamma\left(-s, -\bar{\Omega}\left(\frac{1}{\Omega_c} + ir\right)\right) \\
&\quad \left.\left. + ie^{-\bar{\Omega}\left(\frac{1}{\Omega_c} - ir\right) + i\pi s}\Gamma\left(-s, -\bar{\Omega}\left(\frac{1}{\Omega_c} - ir\right)\right)\right]\right\} .
\end{aligned}
\tag{8.76}
$$

8 Appendix I

The Lamb shifts originating from the counter terms are determined by

$$
\int_0^\infty d\omega \frac{J^{3D}(\omega)}{\omega}\left(1 \pm \frac{\sin(\omega r)}{\omega r}\right) = \tag{8.77}
$$
$$
= \frac{2\gamma\Omega_c}{\pi}\left(\Gamma(s) \pm \frac{(1+\Omega_c^2 r^2)^{-\frac{s-1}{2}}\Gamma(s-1)\sin\left[(s-1)\arctan(\Omega_c r)\right]}{\Omega_c r}\right).
$$

9 Appendix II

In this section we shall give a short review of the ζ-function renormalization method as presented in [81]. The authors there considered the renormalization of a functional determinant defined by a second-order differential equation. Usually, neither the eigenvalues nor the eigenfunctions of the differential operator are known exactly. Moreover, even if all the eigenvalues are known, the determinant is an infinite product of eigenvalues, which is in general a divergent quantity.

To solve these problems, one represents the functional determinant via a generalized Riemann ζ-function. The determinant of an arbitrary differential operator $\mathcal{D}$ can be written as

$$(\mathrm{Det}\mathcal{D})^{1/2} = \exp\left(\frac{1}{2}\ln\prod_\lambda \lambda\right) = \exp\left(\frac{1}{2}\sum_\lambda \ln\lambda\right) = \exp(W)\,, \qquad (9.1)$$

where the eigenvalues of the operator are denoted by λ. We define the generalized ζ-function

$$\zeta(s) = \sum_\lambda \frac{1}{\lambda^s}\,, \qquad (9.2)$$

which is a convergent series for some $s > 0$ and can be continued analytically to $s = 0$. The exponent W in equation (9.1) can be obtained through

$$W = -\frac{1}{2}\frac{d}{ds}\zeta(s)\bigg|_{s=0}\,. \qquad (9.3)$$

Since the eigenvalues of $\mathcal{D}$ have the dimension of mass squared, this leads to a wrong dimensionality for W. Therefore we have to replace (9.3) by

$$W = -\frac{1}{2}\frac{d}{ds}\sum_\lambda \left(\frac{\mu^2}{\lambda}\right)^s\bigg|_{s=0} = -\frac{1}{2}\zeta'(0) - \frac{1}{2}\zeta(0)\ln\mu^2, \qquad (9.4)$$

where we have introduced a renormalization parameter μ with mass dimension one.

The differential operator corresponding to a single field mode may be labelled with n. In quantum mechanics we are confronted with a *finite* number of modes,

9 Appendix II

whereas in field theory we have to deal with an *infinite* number. For each fixed n, the eigenvalue equation reads

$$D_n u_n(-\lambda, t) = \lambda u_n(-\lambda, t) , \tag{9.5}$$

where λ is determined by the boundary condition

$$u_n(-\lambda, t_0) = 0 . \tag{9.6}$$

This boundary condition and a normalization determine the eigenfunctions uniquely. All the boundary conditions (9.6) can be collected in the equation

$$\mathrm{Det}\, u_n(-\lambda, t_0) = 0 , \tag{9.7}$$

where the determinant is taken with respect to all modes n and all eigenvalues λ. With the help of the Cauchy formula, the generalized ζ-function can be expressed as

$$\zeta(s) = \frac{1}{2\pi i} \int_C \frac{dz}{z^s} \frac{d}{dz} \sum_n \ln u_n(z, t_0) , \tag{9.8}$$

with the contour C encircling all roots of equation (9.7). Deforming the contour C to a contour $\tilde{C}$ which encircles the branch cut of the function z^{-s}, we find

$$\zeta(s) = \frac{\sin(\pi s)}{\pi} \int_0^\infty \frac{dM^2}{M^{2s}} \frac{d}{dM^2} \sum_n \ln u_n(M^2, t_0) . \tag{9.9}$$

First, we consider the regularization method for a quantum mechanical system. The necessary information for the regularization of a system with a finite number of modes is contained in the function

$$I(M^2) = \sum_n \ln u_n(M^2, t_0) . \tag{9.10}$$

Expanding this function for large M leads to

$$I(M^2 \to \infty) = \sum_{k=1}^N (I_k + \bar{I}_k \ln M^2) M^{2k} + (I^{\mathrm{R}})_{\ln} \ln M^2 + I^R(\infty) , \tag{9.11}$$

where $(I^{\mathrm{R}})_{\ln}$ is the coefficient of the logarithmic asymptotic term of $I(M^2)$, and $I^R(\infty)$ is the asymptotic value of the regular part of $I(M^2)$. According to [81], the ζ-function can be expanded according to

$$\zeta(s) = (I^{\mathrm{R}})_{\ln} + s[I^{\mathrm{R}}]_0^\infty + \mathcal{O}(s^2) , \tag{9.12}$$

where $[I^{\mathrm{R}}]_0^\infty = I^{\mathrm{R}}(\infty) - I^{\mathrm{R}}(0)$.

As a demonstration we will apply this method to the harmonic oscillator. The eigenvalue equation

$$\left(-\frac{d^2}{dt^2} + \omega^2\right) u(-\lambda, t) = \lambda u(-\lambda, t) \,, \quad u(-\lambda, t_0) = 0 \tag{9.13}$$

has a solution of the form

$$u(-\lambda, t) = Ae^{\sqrt{\omega^2 - \lambda}t} + Be^{-\sqrt{\omega^2 - \lambda}t} \,. \tag{9.14}$$

Performing the analytical continuation to the complex plane, $\lambda \to z$, the function u adopts on the negative real axis the form

$$u(M^2, t) = Ae^{\sqrt{\omega^2 + M^2}t} \,, \tag{9.15}$$

where we neglected the exponentially decreasing term. Using for convenience the normalization $u'(0) = 1$ leads to

$$I(M^2) = -\frac{1}{2}\ln(\omega^2 + M^2) + \sqrt{\omega^2 + M^2}t \,. \tag{9.16}$$

Since the term proportional to $\exp(-\sqrt{\omega^2 + M^2}t)$ has been neglected, the analytically continued eigenfunctions do not respect the boundary condition $u(-\lambda, t_0) = 0$.

From (9.16) we find $I^{\mathrm{R}}(0) = -\ln\omega + \omega t$, $(I^{\mathrm{R}})_{\ln} = -1/2$. Using equations (9.1), (9.4) and (9.12) we arrive at

$$\left(\mathrm{Det}\left[-\frac{d^2}{dt^2} + \omega^2\right]\right)^{-1/2} = \sqrt{\frac{\omega}{\mu}}e^{-\frac{\omega t}{2}} \tag{9.17}$$

which gives for large t the correct ground state energy of an harmonic oscillator.

In general, the exact shape of the eigenfunctions $u_n(-\lambda, t)$ is unknown and one approximates the u_n with a uniform asymptotic WKB-expansion. This asymptotic expansion has the property that

$$\ln u_n(M^2, t_0) = \phi_{\mathrm{WKB}}(n^2, M^2/n^2) \tag{9.18}$$

is uniform for $M^2/n^2 \to \infty$ and $M^2/n^2 \to 0$. In addition, it is also possible to use (9.18) for the regularization of functional determinants in field theory, that is, if the mode number n is not bounded. The expansion (9.18) has at most a *finite* power-law order growth in n [81, 163]. This fact allows us to use the parameter s to cure the divergences arising from the infinite number of modes. Changing the integration variable from $M^2 \to n^2 M^2$ leads to

$$\zeta(s) = \frac{\sin(\pi s)}{\pi}\int_0^\infty \frac{dM^2}{M^{2s}}\frac{d^2}{dM^2}I(M^2, s) \tag{9.19}$$

9 Appendix II

with

$$I(M^2, s) = \sum_n \frac{1}{n^{2s}} \ln u_n(M^2 n^2, t_0) \,. \tag{9.20}$$

For a finite parameter $s > 0$ the expression (9.19) is finite. Analytic continuation of the ζ-function from its convergence domain to $s = 0$ leads to [81]

$$
\begin{aligned}
\zeta(s) &= \frac{1}{s}(I^{\text{pole}})_{\ln} + (I^{\text{R}})_{\ln} + [I^{\text{pole}}]_0^\infty \\
&\quad + s \left\{ [I^{\text{R}}]_0^\infty - \int_0^\infty dM^2 \ln M^2 \frac{dI^{\text{pole}}(M^2)}{dM^2} \right\} + \mathcal{O}(s^2) \,.
\end{aligned} \tag{9.21}
$$

The coefficients $(I^{\text{pole}})_{\ln}$, $I^{\text{pole}}(\infty)$ and $I^{\text{R}}(\infty)$ are defined through the large M-expansion

$$
\begin{aligned}
I(M^2 \to \infty, s) &= \frac{(I^{\text{pole}})_{\ln} \ln M^2 + I^{\text{R}}(\infty)}{s} \\
&\quad + I^{\text{R}}(\infty) + (I^{\text{R}})_{\ln} \ln M^2 + \mathcal{O}(M^2)
\end{aligned} \tag{9.22}
$$

and the pole part $I^{\text{pole}}(M^2)$ is defined through

$$I(M^2, s) = \frac{I^{\text{pole}}(M^2)}{s} + \mathcal{O}(s^0) \,. \tag{9.23}$$

$I^{\text{pole}}(0)$ and $I^{\text{R}}(0)$ are determined by

$$I(M^2 \to 0, s) = \frac{I^{\text{pole}}(0)}{s} + I^{\text{R}}(0) + \mathcal{O}(s) \,. \tag{9.24}$$

It is also possible to apply the regularization method if the differential equation exhibits singular coefficients. According to Olver [163], the WKB expansion of a second-order differential equation

$$\frac{d^2 u(M^2, t)}{dt^2} = \omega(t)^2 u(M^2, t) = [f(t) + g(t)]u(M^2, t) \tag{9.25}$$

has the form

$$u(M^2, t) = C(M)(g(t))^{-1/4} \exp\left\{ \int_0^t dt' (g(t'))^{1/2} \right\} [1 + h(t)] \tag{9.26}$$

with $h(t) = \mathcal{O}(M^{-1})$. The function $h(t)$ can be expressed as Volterra integral

$$
\begin{aligned}
h(t) &= \frac{1}{2} \int_{t_0}^t \left(1 - \exp\left\{ 2 \int_0^{t'} g^{1/2}(t'')dt'' - 2 \int_0^t g^{1/2}(t')dt' \right\} \right) \times \\
&\quad \times \psi(t')[1 + h(t')]dt'
\end{aligned} \tag{9.27}
$$

with

$$\psi(t) = \frac{f(t)}{g^{1/2}(t)} - \frac{1}{g^{1/4}(t)} \frac{d^2}{dt^2} \frac{1}{g^{1/4}(t)} \;. \tag{9.28}$$

Therefore the WKB expansion only makes sense if the kernel of (9.27) is bounded. This leads to the condition

$$\Psi(t) = \int_{t_0}^t dt' |\psi(t')| < \infty \;. \tag{9.29}$$

Here, t_0 and t are the boundaries of the interval under consideration. The split of $\omega(t)^2$, see (9.25), is chosen such that singular coefficients like $1/t$ in the differential equation do not destroy the WKB expansion. This is the reason for the $1/4$–trick in the paper [81].

As already mentioned above, the evaluation of $I(M^2, s)$ involves an important approximation. In order to fulfill the boundary condition (9.6), two linearly independent solutions of the corresponding differential equation are required. After analytical continuation, the solutions are of the form $u \sim \exp(Mt)$ and $u \sim \exp(-Mt)$. The second solution is exponentially decreasing and will therefore be discarded. This implies that the analytically continued functions $u(M^2, t_0)$ *do not* respect the boundary condition (9.6). The choice of μ corresponds to a choice of the path integral normalization. In order to coincide with Schrödinger evolution, one needs to choose $\mu = \pi$.

9 Appendix II

Bibliography

[1] H. D. Zeh. *On the interpretation of measurement in quantum theory.* Found. Phys., **1**(1):69, (1970).

[2] W. H. Zurek. *Pointer basis of quantum apparatus: Into what mixture does the wave packet collapse?* Phys. Rev. D, **24**(6):1516, (1981).

[3] W. H. Zurek. *Environment-induced superselection rules.* Phys. Rev. D, **26**(8):1862, (1982).

[4] E. Joos. *Elements of environmental decoherence.* in P. Blanchard, D. Giulini, E. Joos, C. Kiefer, I.-O. Stamatescu, *Decoherence: Theoretical, Experimental, and Conceptual Problems*, Springer, Berlin. (2000).

[5] Leonard Susskind. The anthropic landscape of string theory. 2003.

[6] S. Coleman. *Fate of the false vacuum: Semiclassical theory.* Phys. Rev. D, **15**(10):2929, (1977).

[7] S. Coleman and F. De Luccia. *Gravitational effects on and of vacuum decay.* Phys. Rev. D, **21**(12):3305, (1980).

[8] D. Braun. *Creation of Entanglement by Interaction with a Common Heat Bath.* Phys. Rev. Lett., **89**(27):277901, (2002).

[9] F. Benatti, R. Floreanini, and M. Piani. *Environment Induced Entanglement in Markovian Dissipative Dynamics.* Phys. Rev. Lett., **91**(7):070402, (2003).

[10] E. Fick. *Einführung in die Grundlagen der Quantentheorie.* Aula-Verlag Wiesbaden. (1988).

[11] F. Schwabl. *Quantenmechanik.* Springer. (2008).

[12] W. Nolting. *Grundkurs Theoretische Physik 5/1. Quantenmechanik.* Springer. (2000).

[13] W. Greiner. *Quantenmechanik: Einführung.* Verlag Harry Deutsch. (2005).

Bibliography

[14] W. Heisenberg. *Über den anschaulichen Inhalt der quantentheoretischen Kinematik und Mechanik.* Z. Phys, **43**(3-4):172, (1927).

[15] N. Bohr. *The quantum postulate and the recent development of atomic theory.* Nature, **121**:580, (1928).

[16] M. Jammer. *The Philosophy of Quantum Mechanics*. John Wiley & Sons, New York. (1974).

[17] W. K. Wootters and W. H. Zurek. *Complementarity in the double-slit experiment: Quantum nonseparability and a quantitative statement of Bohr's principle.* Phys. Rev. D, **19**(2):473, (1979).

[18] M. O. Scully and K. Drühl. *Quantum eraser: A proposed photon correlation experiment concerning observation and "delayed choice" in quantum mechanics.* Phys. Rev. A, **25**(4):2208, (1982).

[19] N. Bohr. *Can Quantum-Mechanical Description of Physical Reality be Considered Complete?* Phys. Rev., **48**(8):696, (1935).

[20] C. Kiefer. *On the interpretation of quantum theory - from Copenhagen to the present day.* quant-ph/0210152, (2002).

[21] M. Schlosshauer. *Decoherence and the Quantum-to-Classical Transition*. Springer, Berlin. (2007).

[22] J. von Neumann. *Mathematische Grundlagen der Quantenmechanik*. Springer, Berlin, (1932).

[23] W. H. Zurek. *Decoherence and the transition from quantum to classical.* Phys. Today, **44**(10):36, 1991.

[24] E. Joos and H. D. Zeh. *The Emergence of classical properties through interaction with the environment.* Z. Phys., **B 59**(2):223, (1985).

[25] E. Joos, H. D. Zeh, C. Kiefer, D. Giulini, J. Kupsch, and I-O. Stamatescu. *Decoherence and the Appearance of a Classical World in Quantum Theory*. Springer, Berlin. (2003).

[26] H. D. Zeh. *Toward a quantum theory of observation.* Found. Phys., **3**(1):109, (1973).

[27] W. H. Zurek. *Preferred States, Predictability, Classicality and the Environment-Induced Decoherence.* Prog. Theor. Phys., **89**(281), (1993).

[28] J. P. Paz and W. H. Zurek. *Quantum Limit of Decoherence: Environment Induced Superselection of Energy Eigenstates.* Phys. Rev. Lett., **82**(26):5181, (1999).

[29] W. G. Unruh and W. H. Zurek. *Reduction of a wave packet in quantum Brownian motion.* Phys. Rev. D, **40**(4):1071, (1989).

[30] H. Everett. *"Relative State" Formulation of Quantum Mechanics.* Rev. Mod. Phys., **29**(3):454, (1957).

[31] B. S. DeWitt. *Quantum mechanics and reality.* Phys. Today, **23**(9), (1970).

[32] D. Deutsch. *Quantum Theory as a Universal Physical Theory.* Int. J. Theor. Phys., **24**(1):1, (1985).

[33] W. H. Zurek. *Decoherence, einselection and the existential interpretation (the rough guide).* Phil. Trans. R. Soc. Lond. A, **356**(1743):1793, (1998).

[34] M. Schlosshauer. *Decoherence, the measurement problem, and interpretations of quantum mechanics.* Rev. Mod. Phys., **76**(4):1267, (2005).

[35] M. Tegmark. *Apparent Wave Function Collapse Caused by Scattering.* Found. Phys. Lett., **6**(6):571, (1993).

[36] M. Brune, E. Hagley, J. Dreyer, X. Maître, A. Maali, C. Wunderlich, J. M. Raimond, and S. Haroche. *Observing the Progressive Decoherence of the "Meter" in a Quantum Measurement.* Phys. Rev. Lett., **77**(24):4887, (1996).

[37] M. Arndt, O. Nairz, J. Vos-Andreae, C. Keller, G. van der Zouw, and A. Zeilinger. *Wave-particle duality of C60 molecules.* Nature, **401**:680, (1999).

[38] I. Chiorescu, Y. Nakamura, C. J. P. M. Harmans, and J. E. Mooij. *Coherent Quantum Dynamics of a Superconducting Flux Qubit.* Science, **299**(5614):1869, (2003).

[39] C. Kiefer. *Decoherence in quantum electrodynamics and quantum gravity.* Phys. Rev. D, **46**(4):1658, (1992).

[40] C. Kiefer. *Quantum Gravity, Second edition.* Oxford University Press, Oxford. (2007).

[41] C. Kiefer. *Continuous Measurement of Minisuperspace Variables by Higher Multipoles.* Class. Quant. Grav., **4**(5):1369, (1987).

Bibliography

[42] V. Sahni and A. A. Starobinsky. *The Case for a Positive Cosmological Lambda-term.* Int. J. Mod. Phys. D, **9**(4):373, (2000).

[43] T. Padmanabhan. *Cosmological Constant - the Weight of the Vacuum.* Phys. Rep., **380**(5-6):235, (2003).

[44] P. J. E. Peebles and B. Ratra. *The cosmological constant and dark energy.* Rev. Mod. Phys., **75**(2):559, (2003).

[45] J. Frieman, M. Turner, and D. Huterer. *Dark Energy and the Accelerating Universe.* Ann. Rev. Astron. Astrophys., **46**:385, (2008).

[46] A. R. Liddle and D. H. Lyth. *Cosmological Inflation and Large-Scale Structure.* Cambridge University Press, Cambridge. (1998).

[47] M. Spradlin, A. Strominger, and A. Volovich. *Les Houches Lectures on De Sitter Space.* hep-th/0110007, (2001).

[48] E. Schrödinger. *Expanding Universes.* Cambridge University Press, Cambridge. (1950).

[49] N. et al. Jarosik. *Seven-Year Wilkinson Microwave Anisotropy Probe (WMAP) Observations: Sky Maps, Systematic Errors, and Basic Results.* (2010).

[50] A. D. Dolgov. *The Very Early Universe.* Cambridge University Press, Cambridge. (1983).

[51] S. Weinberg. *The cosmological constant problem.* Rev. Mod. Phys., **61**(1):1, (1989).

[52] S. M. Barr. *Attempt at a classical cancellation of the cosmological constant.* Phys. Rev. D, **36**(6):1691, (1987).

[53] V. Sahni and S. Habib. *Does Inflationary Particle Production Suggest $\Omega_m < 1$?* Phys. Rev. Lett., **81**(9):1766, (1998).

[54] P. J. E. Peebles and B. Ratra. *Cosmology with a time-variable cosmological 'constant'.* Astrophys. J., **325**:L17, (1988).

[55] A. Yu. Kamenshchik, U. Moschella, and V. Pasquier. *An alternative to quintessence.* Phys. Lett. B, **511**(2-4):265, (2001).

[56] R. R. Caldwell. *A phantom menace? Cosmological consequences of a dark energy component with super-negative equation of state.* Phys. Lett. B, **545**(1-2):23, (2002).

[57] R. R. Caldwell, M. Kamionkowski, and N. N. Weinberg. *Phantom Energy: Dark Energy with w < 1 Causes a Cosmic Doomsday.* Phys. Rev. Lett., **91**(7):071301, (2003).

[58] S. Weinberg. *Anthropic Bound on the Cosmological Constant.* Phys. Rev. Lett., **59**(22):2607, (1987).

[59] H. Martel, P. R. Shapiro, and S. Weinberg. *Likely Values of the Cosmological Constant.* Astrophys. J., **492**(1):29, (1998).

[60] M. R. Douglas. *The statistics of string/M theory vacua.* JHEP, **05**:046, (2003).

[61] F. Denef and M. R. Douglas. *Distributions of flux vacua.* JHEP, **05**:072, (2004).

[62] M. R. Douglas and S. Kachru. *Flux compactification.* Rev. Mod. Phys., **79**(2):733, (2007).

[63] F. Denef, M. R. Douglas, and S. Kachru. *Physics of string flux compactifications.* Ann. Rev. Nucl. Part. Sci., **57**:119, (2007).

[64] S. Ashok and M. R. Douglas. *Counting flux vacua.* JHEP, **01**:060, (2004).

[65] R. Blumenhagen, B. Körs, Dieter Lüst, and Stephan Stieberger. *Four-dimensional string compactifications with D-branes, orientifolds and fluxes.* Phys. Rep., **445**(1-6):1, (2007).

[66] M. Grana. *Flux compactifications in string theory: A comprehensive review.* Phys. Rep., **423**(3):91, (2006).

[67] L. A. Kofman, N. Y. Gnedin, and N. A. Bahcall. *Cosmological constant, COBE cosmic microwave background anisotropy, and large scale clustering.* Astrophys. J., **413**(1):1, (1993).

[68] J. P. Ostriker and Paul J. Steinhardt. *The Observational case for a low density universe with a nonzero cosmological constant.* Nature, **377**:600, (1995).

[69] S. et al. Perlmutter. *Discovery of a Supernova Explosion at Half the Age of the Universe and its Cosmological Implications.* Nature, **391**:51, (1998).

[70] Adam G. et al. Riess. *Observational Evidence from Supernovae for an Accelerating Universe and a Cosmological Constant.* Astron. J., **116**:1009, (1998).

[71] J. Yokoyama. *Cosmological Constant From Degenerate Vacua.* Phys. Rev. Lett., **88**(15):151302, (2002).

Bibliography

[72] G. L. Kane, M. J. Perry, and A. N. Zytkow. *A possible mechanism for generating a small positive cosmological constant.* hep-th/0311152, (2003).

[73] A. O. Caldeira and A. J. Leggett. *Quantum tunnelling in a dissipative system.* Ann. Phys. (N.Y.), **149**(2):374, (1983).

[74] S. Coleman. *Aspects of Symmetry.* Cambridge University Press, Cambridge. (1988).

[75] C. G. Callan and S. Coleman. *Fate of the false vacuum. II. First quantum corrections.* Phys. Rev. D, **16**(6):1762, (1977).

[76] A. O. Caldeira and A. J. Leggett. *Path integral approach to quantum Brownian motion.* Physica A, **121**(3):587, (1983).

[77] V. Mukhanov. *Physical Foundations of Cosmology.* Cambridge University Press, Cambridge. (2005).

[78] A. J. Leggett, S. Chakravarty, A. T. Dorsey, M. P. A. Fisher, A. Garg, and W. Zwerger. *Dynamics of the dissipative two-state system.* Rev. Mod. Phys., **59**(1):1, (1987).

[79] K. Kuchar. *Ground state functional of the linearized gravitational field.* J. Math. Phys., **11**(12):3322, (1970).

[80] L. Parker and D. Toms. *Quantum Field Theory in Curved Spacetime.* Cambridge University Press, Cambridge. (2009).

[81] A. O. Barvinsky, A. Yu. Kamenshchik, and I. P. Karmazin. *One loop quantum cosmology: Zeta function technique for the Hartle-Hawking wave function of the universe.* Annals Phys., **219**(2):201, (1992).

[82] M. A. Evgrafov. *Analytic Functions.* Dover, New York. (1978).

[83] V. V. Nesterenko, G. Lambiase, and G. Scarpetta. *Calculation of the Casimir energy at zero and finite temperature: Some recent results.* Riv. Nuovo Cim., **27N6**:1, (2004).

[84] H. B. G. Casimir. *On the Attraction Between Two Perfectly Conducting Plates.* Proc. Kon. Nederland. Akad. Wetensch., **B51**:61, (1948).

[85] B. Carr. *Universe or Multiverse?* Cambridge University Press, Cambridge. (2007).

[86] K. Lee and E. J. Weinberg. *Decay of the true vacuum in curved space-time.* Phys. Rev. D, **36**(4):1088, (1987).

[87] T. Clifton, A. D. Linde, and N. Sivanandam. *Islands in the landscape.* JHEP, **02**:024, (2007).

[88] S. Kachru, R. Kallosh, A. Linde, and S. P. Trivedi. *de Sitter vacua in string theory.* Phys. Rev. D, **68**(4):046005, (2003).

[89] D. I. Podolsky, J. Majumder, and N. Jokela. *Disorder on the landscape.* JCAP, **05**:024, (2008).

[90] S. H. H. Tye, D. Wohns, and Y. Zhang. *Coleman-de Luccia Tunneling and the Gibbons-Hawking Temperature.* Int. J. Mod. Phys. A, **25**(5):1019, (2010).

[91] S. W. Hawking and I. L. Moss. *Supercooled phase transitions in the very early universe.* Phys. Lett. B, **110**(1):35, (1982).

[92] G. W. Gibbons and S. W. Hawking. *Cosmological event horizons, thermodynamics, and particle creation.* Phys. Rev. D, **15**(10):2738, (1977).

[93] S. Sarangi, G. Shiu, and B. Shlaer. *Rapid Tunneling and Percolation in the Landscape.* Int. J. Mod. Phys. A, **24**(4):741, (2009).

[94] H. S. H. Tye. *A new view of the cosmic landscape.* hep-th/0611148.

[95] E. J. Copeland, A. Padilla, and P. M. Saffin. *No resonant tunneling in standard scalar quantum field theory.* JHEP, **01**:066, (2008).

[96] M. Schechter and P. C. E. Stamp. *What are the interactions in quantum glasses?* J. Phys.: Condens. Matter, **20**(24):244136, (2008).

[97] W. H. Louisell. *Quantum Statistical Properties of Radiation.* John Wiley & Sons, New York. (1973).

[98] N. G. van Kampen. *Stochasic Processes in Physics and Chemistry.* North-Holland Publishing Company. (1981).

[99] M. B. Voloshin, I. Yu. Kobzarev, and L. B. Okun'. *Bubbles in Metastable Vacuum.* Sov. L Nucl. Phys, **20**:644, (1975).

[100] S. K. Blau, E. I. Guendelman, and A. H. Guth. *Dynamics of false-vacuum bubbles.* Phys. Rev. D, **35**(6):1747, (1987).

[101] V. A. Berezin, V. A. Kuzmin, and I. I. Tkachev. *Dynamics of bubbles in general relativity.* Phys. Rev. D, **36**(10):2919, (1987).

Bibliography

[102] W. Fischler, C. Krishnan, S. Paban, and M. Zanic. *Vacuum bubble in an inhomogeneous cosmology.* JHEP, **05**:041, (2008).

[103] A. D. Linde. *Decay of the false vacuum at finite temperature.* Nucl. Phys. B., **216**(2):421, (1983).

[104] A. D. Linde. *A new inflationary universe scenario: A possible solution of the horizon, flatness, homogeneity, isotropy and primordial monopole problems.* Phys. Lett. B, **108**(6):389, (1982).

[105] A. Vilenkin. *Birth of inflationary universes.* Phys. Rev. D, **27**(12):2848, (1983).

[106] J. B. Hartle and S. W. Hawking. *Wave function of the Universe.* Phys. Rev. D, **28**(12):2960, (1983).

[107] A. Vilenkin. *Creation of universes from nothing.* Phys. Lett. B, **117**:25, (1982).

[108] S. W. Hawking and I. G. Moss. *Supercooled phase transitions in the very early universe.* Phys. Lett. B, **110**(1):35, (1982).

[109] R. Basu, A. H. Guth, and A. Vilenkin. *Quantum creation of topological defects during inflation.* Phys. Rev. D, **44**(2):340, (1991).

[110] J. Garriga. *Nucleation rates in flat and curved space.* Phys. Rev. D, **49**(12):6327, (1994).

[111] L. Susskind. *The anthropic landscape of string theory.* hep-th/0302219, (2003).

[112] M. R. Douglas and S. Kachru. *Flux compactification.* Rev. Mod. Phys., **79**(2):733, (2007).

[113] E. Keski-Vakkuri and P. Kraus. *Tunneling in a time-dependent setting.* Phys. Rev. D, **54**(12):7407, (1996).

[114] G. Hinshaw et al. *Five-Year Wilkinson Microwave Anisotropy Probe (WMAP) Observations: Data Processing, Sky Maps, and Basic Results.* Astrophys. J. Suppl., **180**(2):225, (2009).

[115] S. Parke. *Gravity and the decay of the false vacuum.* Phys. Lett. B, **121**(5):313, (1983).

[116] D. Simon, J. Adamek, A. Rakic, and J. C. Niemeyer. *Tunneling and propagation of vacuum bubbles on dynamical backgrounds.* JCAP, **11**:008, (2009).

[117] L. Brink, P. di Vecchia, and P. Howe. *A locally supersymmetric and reparametrization invariant action for the spinning string.* Phys. Lett. B, **65**(5):471, (1976).

[118] C. Kiefer, F. Queisser, and A. A. Starobinsky. *Cosmological Constant from Decoherence?* in preparation.

[119] C. Kiefer, F. Queisser, and A. A. Starobinsky. *Cosmological Constant from Decoherence?* Proceedings of the 12th Marcel Grossmann Meeting (Paris).

[120] H. P. Breuer and F. Petruccione. *The theory of open quantum systems.* Oxford University Press, Oxford. (2002).

[121] P. Feynman and A. Hibbs. *Quantum Mechanics and Path Integrals.* McGraw-Hill, New York. (1965).

[122] L. K. Grover. *Quantum Mechanics Helps in Searching for a Needle in a Haystack.* Phys. Rev. Lett., **79**(2):325, (1997).

[123] P. W. Shor. *Polynomial-Time Algorithms for Prime Factorization and Discrete Logarithms on a Quantum Computer.* SIAM J. Comput., **26**(5):1484, (1997).

[124] L. M. K. Vandersypen et al. *Experimental realization of Shor's quantum factoring algorithm using nuclear magnetic resonance.* Nature, **414**:883, (2001).

[125] M. A. Nielsen and I. L. Chuang. *Quantum Computation and Quantum Information.* Cambridge University Press, Cambridge. (2000).

[126] A. K. Ekert. *Quantum cryptography based on Bell's theorem.* Phys. Rev. Lett., **67**(6):661, (1991).

[127] *World Premiere: Bank Transfer via Quantum Cryptography Based on Entangled Photons.*

[128] C. H. Bennett, G. Brassard, C. Crépeau, R. Jozsa, A. Peres, and W. K. Wootters. *Teleporting an unknown quantum state via dual classical and Einstein-Podolsky-Rosen channels.* Phys. Rev. Lett., **70**(13):1895, (1993).

[129] W. K. Wootters and W. H. Zurek. *A single quantum cannot be cloned.* Nature, **299**:802, 1882.

[130] D. Braun. *Entanglement from thermal blackbody radiation.* Phys. Rev. A, **72**(6):062324, (2005).

Bibliography

[131] F. Benatti and R. Floreanini. *Entangling oscillators through environment noise.* J. Phys. A, **39**(11):2689, (2006).

[132] S. Oh and J. Kim. *Entanglement between qubits induced by a common environment with a gap.* Phys. Rev. A, **73**(6):062306, (2006).

[133] D. Solenov, D. Tolkunov, and V. Privman. *Exchange interaction, entanglement, and quantum noise due to a thermal bosonic field.* Phys. Rev. B, **75**(3):035134, (2007).

[134] D. Solenov, D. Tolkunov, and V. Privman. *Coherent interaction of spins induced by thermal bosonic environment.* Phys. Lett. A, **359**(2):81, (2006).

[135] J. S. Prauzner-Bechcicki. *Two-mode squeezed vacuum state coupled to the common thermal reservoir.* J. Phys. A, **37**(15):L173, (2004).

[136] J.-H. An and W.-M. Zhang. *Non-Markovian entanglement dynamics of noisy continuous-variable quantum channels.* Phys. Rev. A, **76**(4):042127, (2007).

[137] C.-H. Chou, T. Yu, and B. L. Hu. *Exact master equation and quantum decoherence of two coupled harmonic oscillators in a general environment.* Phys. Rev. E, **77**(1):011112, (2008).

[138] K.-L. Liu and H.-S. Goan. *Non-Markovian entanglement dynamics of quantum continuous variable systems in thermal environments.* Phys. Rev. A, **76**(2):022312, (2007).

[139] C. Hörhammer and H. Büttner. *Environment-induced two-mode entanglement in quantum Brownian motion.* Phys. Rev. A, **77**(4):042305, (2008).

[140] J. P. Paz and A. J. Roncaglia. *Dynamics of the Entanglement between Two Oscillators in the Same Environment.* Phys. Rev. Lett., **100**(22):220401, (2008).

[141] R. Horodecki, P. Horodecki, M. Horodecki, and K. Horodecki. *Quantum entanglement.* Rev. Mod. Phys., **81**(2):865, (2009).

[142] R. F. Werner. *Quantum states with Einstein-Podolsky-Rosen correlations admitting a hidden-variable model.* Phys. Rev. A, **40**(8):4277, (1989).

[143] A. Peres. *Separability Criterion for Density Matrices.* Phys. Rev. Lett., **77**(8):1413, (1996).

[144] M. Horodecki, P. Horodecki, and R. Horodecki. *Separability of mixed states: necessary and sufficient conditions.* Phys. Lett. A, **223**(1), (1996).

[145] G. Vidal and R. F. Werner. *Computable measure of entanglement.* Phys. Rev. A, **65**(3):032314, (2002).

[146] R. Simon. *Peres-Horodecki Separability Criterion for Continuous Variable Systems.* Phys. Rev. Lett., **84**(12):2726, (2000).

[147] R. Simon, N. Mukunda, and B. Dutta. *Quantum-noise matrix for multimode systems: U(n) invariance, squeezing, and normal forms.* Phys. Rev. A, **49**(3).

[148] R. Simon, E. C. G. Sudarshan, and N. Mukunda. *Gaussian pure states in quantum mechanics and the symplectic group.* Phys. Rev. A, **37**(8):3028, (1988).

[149] J. Williamson. *On the Algebraic Problem Concerning the Normal Forms of Linear Dynamical Systems.* Am. J. Math., **58**(1):141, (1936).

[150] V. I. Arnold. *Mathematical Methods of Classical Mechanics.* Springer, New York, (1978).

[151] W. K. Wootters. *Entanglement of Formation of an Arbitrary State of Two Qubits.* Phys. Rev. Lett., **80**(10):2245, (1998).

[152] C. H. Bennett, D. P. DiVincenzo, J. A. Smolin, and W. K. Wootters. *Mixed-state entanglement and quantum error correction.* Phys. Rev. A, **54**(5):3824, (1996).

[153] K. Shiokawa and B. L. Hu. *Qubit decoherence and non-Markovian dynamics at low temperatures via an effective spin-boson model.* Phys. Rev. A, **70**(6):062106, (2004).

[154] T. Zell, F. Queisser, and R. Klesse. *Distance Dependence of Entanglement Generation via a Bosonic Heat Bath.* Phys. Rev. Lett., **102**:160501, (2009).

[155]

[156] L. van Hove. *The Occurrence of Singularities in the Elastic Frequency Distribution of a Crystal.* Phys. Rev., **89**(6):1189, (1953).

[157] S. et al. Kuhr. *Coherence Properties and Quantum State Transportation in an Optical Conveyor Belt.* Phys. Rev. Lett., **91**(21):213002, (2003).

[158] B. M. Garraway. *Nonperturbative decay of an atomic system in a cavity.* Phys. Rev. A, **55**(3):2290, (1997).

[159] V. Weisskopf and W. Wigner. *Berechnung der natürlichen Linienbreite auf Grund der Diracschen Lichttheorie.* Z. Phys., **63**(1-2):54, (1930).

Bibliography

[160] P. Durbin and J. Abate. *Numerical inversion of Laplace transforms and the Finite Fourier Transforms.* Comp. J, **17**:371, (1974).

[161] P. Robert and R. Huysmans. *Algorithm 619: automatic numerical inversion of the Laplace transform [D5].* ACM Trans. Math. Softw., **10**(3):348, (1984).

[162] A. O. Barvinsky, A. Yu. Kamenshchik, C. Kiefer, and I. V. Mishakov. *Decoherence in quantum cosmology at the onset of inflation.* Nucl. Phys. B, **551**:374, 1999.

[163] F. W. J. Olver. *Asymptotics and Special Functions.* Academic Press, New York and London. (1974).

Erklärung

Ich versichere, dass ich die von mir vorgelegte Dissertation selbständig angefertigt, die benutzten Quellen und Hilfsmittel vollständig angegeben und die Stellen der Arbeit – einschließlich Tabellen, Karten und Abbildungen –, die anderen Werken im Wortlaut oder dem Sinn nach entnommen sind, in jedem Einzelfall als Entlehnung kenntlich gemacht habe; dass diese Dissertation noch keiner anderen Fakultät oder Universität zur Prüfung vorgelegen hat; dass sie – abgesehen von unten angegebenen Teilpublikationen – noch nicht veröffentlicht worden ist sowie, dass ich eine solche Veröffentlichung vor Abschluss des Promotionsverfahrens nicht vornehmen werde. Die Bestimmungen der Promotionsordnung sind mir bekannt. Die von mir vorgelegte Dissertation ist von Herrn Prof. Dr. Claus Kiefer betreut worden.

Köln, den 27. September 2010

_____

Friedemann Queisser

Teilpublikationen

[1] T. Zell, F.Q. and R. Klesse: *Distance dependence of entanglement generation via a bosonic heat bath.* Physical Review Letters, **102**(16):160501, 2009.

[2] C. Kiefer, F.Q. and A. A. Starobinsky: *Cosmological Constant from Decoherence?* in preparation.

[3] C. Kiefer, F.Q. and A. A. Starobinsky: *Cosmological Constant from Decoherence?* Proceedings of the 12th Marcel Grossmann Meeting (Paris).

[4] F.Q. *Influence of nontrivial backgrounds and decoherence on vacuum decay.* arXiv: 1004.2921 [gr-qc], 2010

[5] F.Q. *Book Review: "DID TIME BEGIN? WILL TIME END? Maybe the Big Bang Never Occurred", Paul H. Frampton* Annalen der Physik **522**(8):608, 2010.

Acknowledgments

Lebenslauf

Persönliche Daten

Name:	Friedemann Queißer
Nationalität:	deutsch
Geburtsdatum:	30. August 1980
Geburtsort:	Radebeul
Adresse:	Dürener Strasse 349
	50935 Köln
Telefon:	(0049)1787782439
Email:	fsq@thp.uni-koeln.de

Bildungsweg

1987 - 1992	Lößnitz–Grundschule Radebeul
1992 - 1999	Gymnasium Luisenstift Radebeul
1999 - 2000	Studium der Physik, TU Dresden
2000 - 2001	Zivildienst
2001 - 2003	Studium der Physik, TU Dresden
2003 - 2004	Auslandaufenthalt, Duke University, (Durham, North Carolina)
2004 - 2005	Studium der Physik, TU Dresden
2005 - 2006	Diplomarbeit in der Arbeitsgruppe von Dr. Ralf Schützhold
2006 - 2010	Doktorand in der Arbeitsgruppe von Prof. Dr. Claus Kiefer